

**Physical and Chemical Analysis of Pig Carcass
Decomposition in a Fine Sand**

by

Melina Larizza

A Thesis Submitted in Partial Fulfillment
of the Requirements for the Degree of

Masters of Applied Bioscience

in

The Faculty of Science

University of Ontario Institute of Technology

August 2010

©Melina Larizza, 2010

Certification of Approval

Copyright Agreement

Abstract

The development and improvement of methods used for the estimation of the postmortem interval (PMI) is a common area of research in forensic science. This research was conducted to physically and chemically analyze pig carcass decomposition on a soil surface using conventional and newly developed methods for the potential use in estimating the PMI. Photographs of pig carcasses decomposing on forested and open land were scored using a decomposition scoring system and decomposition scores were related to accumulated degree days (ADD). Overall, the ADD values were significantly different for the two groups of carcasses; however, the ADD values for the onset of each score demonstrated more similarity between groups. Decomposition scoring results also indicated that refinements must be made to the calculation of ADD to allow for a meaningful comparison of pig and human decomposition. The decomposition of pig carcasses altered the water content, pH and fatty acid content of soil. The fatty acids, myristic, palmitic, palmitoleic, stearic and oleic acids were successfully extracted and analyzed from decomposition soil. Palmitic, stearic and oleic acids were the most abundant fatty acids detected whilst the levels of myristic and palmitoleic acids were negligible in comparison. A three peak fatty acid cycle was also observed for each fatty acid. Variations in soil pH and fatty acid content of decomposition soil have the potential to indicate the presence of a decomposition site. Furthermore, a nonlinear diffusion model was developed to predict the development of the cadaver decomposition island (CDI) in soil over time. The simulation of the model indicated that the diffusion model has the potential to generate PMI estimations for early stages of decomposition by corresponding the effective radius of the CDI to a particular time point. The general findings of this research indicate that more accurate methods for PMI estimations can potentially be developed with further research.

Keywords: Decomposition, Diffusion model, Postmortem Interval, Soil, Taphonomy

Acknowledgements

This research has truly been a collaborative project and I feel privileged to have worked with such dedicated and enthusiastic researchers. I would like to thank my supervisor Dr. Shari Forbes for her mentorship, guidance and passion for forensic research. I would also like to thank Dr. C. Sean Bohun for his relentless work on the diffusion model and nonparametric statistics, Sgt. Diane Cockle for introducing me to Dr. Forbes and for her valuable contribution to the scoring of decomposition photographs and Dean William Smith for his helpful advice and support. I would like to extend my appreciation to the Royal Canadian Mounted Police for providing the research facility and sharing their resources.

I would like to express my sincere gratitude to Dr. Christopher O'Brien for his invaluable mentorship and endless support with statistical analysis and editing. Furthermore, I would like to express my gratitude to Sonja Stadler and Amanda Lowe for their continuous support, assistance, insightful discussions and laughter. The past two years would not have been possible without the endless help, support, guidance and patience of Michael Accardi. I would like to thank Laura Benninger, Galiena Tse and all other members of the Forbes lab for their assistance and guidance. I would also like to thank all Applied Bioscience graduate students and members of the Faculty of Science at UOIT for their assistance, friendship and support throughout this project.

To my family and friends, your endless love, support and encouragement means the world to me. *Cara Nonna, ci manchi tanto.*

Table of Contents

Certification of Approval	ii
Copyright Agreement	iii
Abstract.....	iv
Acknowledgements	v
Table of Contents.....	vi
List of Tables	x
List of Figures	xi
List of Appendices	xv
List of Abbreviations	xvi
<i>Chapter 1 – Introduction</i>	1
1.1 <i>Forensic Taphonomy.....</i>	2
1.2 <i>Postmortem Interval.....</i>	2
1.3 <i>Decomposition</i>	4
1.3.1 <i>Central Metabolism and Adenosine Triphosphate</i>	4
1.3.2 <i>Autolysis</i>	5
1.3.3 <i>Autolysis: Postmortem Changes.....</i>	6
1.3.4 <i>Putrefaction</i>	7
1.3.5 <i>Putrefaction: Postmortem Changes.....</i>	8
1.3.6 <i>Skeletonization.....</i>	9
1.4 <i>Factors Affecting the Decomposition Process.....</i>	9
1.4.1 <i>Climatic Factors</i>	9
1.4.2 <i>Physical Factors</i>	11
1.5 <i>Soil Decomposition</i>	12
1.5.1 <i>Cadaver Decomposition Island</i>	13
1.6 <i>Lipid Degradation.....</i>	15
1.6.1 <i>Fatty acid analysis.....</i>	16
1.7 <i>Diffusion Model.....</i>	17
1.8 <i>Research Aims and Objectives.....</i>	19

Chapter 2 – Materials and Methods	20
2.1 <i>Research Site</i>	21
2.2 <i>Research Trial 1 – Summer 2008</i>	21
2.3 <i>Research Trial 2 – Summer 2009</i>	24
2.4 <i>Scoring of Photographs for Decomposition</i>	26
2.4.1 <i>Decomposition Stages</i>	26
2.4.2 <i>Baseline Decomposition</i>	27
2.4.3 <i>Insect and Scavenging Activity</i>	28
2.4.4 <i>Environmentally Dependent States</i>	29
2.4.5 <i>Decomposition Scoring</i>	29
2.4.6 <i>Statistical Analysis</i>	30
2.5 <i>Soil Analysis</i>	30
2.5.1 <i>Gravimetric water content of soil</i>	30
2.5.2 <i>Soil pH</i>	30
2.5.3 <i>Soil characterization</i>	31
2.6 <i>Fatty Acid Analysis</i>	31
2.6.1 <i>Reagents</i>	31
2.6.2 <i>Standards</i>	31
2.6.3 <i>Method Optimization I: Solvents and Derivatizing Agents</i>	32
2.6.4 <i>Method Optimization II: Fatty Acid Extraction Method and Recovery</i>	34
2.6.5 <i>Sample Processing</i>	38
2.6.6 <i>GC-MS Analysis</i>	38
2.6.7 <i>Detection Parameters and Reproducibility</i>	39
2.6.8 <i>Statistical Analysis</i>	40
2.7 <i>Diffusion Model</i>	40
2.7.1 <i>Diffusion Model Test</i>	40
2.7.2 <i>Derivation of the Diffusion Model</i>	40
 Chapter 3 – Decomposition Scoring	 46
3.1 <i>Climatic Conditions</i>	47
3.2 <i>Decomposition Stages</i>	50

3.2.1 Summer 2008 Trial – Shaded Pig Carcasses	50
3.2.2 Summer 2008 Trial – Sun Exposed Pig Carcasses.....	51
3.2.3 Summer 2009 Trial – Sun Exposed Pig Carcasses.....	53
3.3 Decomposition Scoring	56
3.3.1 Comparison of Shaded and Sun Exposed Pig Carcasses	56
3.3.2 Comparison of Pig and Human Decomposition.....	59
3.4 Discussion.....	64
3.4.1 Decomposition Stages.....	64
3.4.2 Decomposition Scoring: Shaded and Sun Exposed Carcasses	66
3.4.3 Decomposition Scoring: Pig Carcasses and Human Remains	67
3.5 Limitations	68
3.6 Relevance to Forensic Science.....	68
Chapter 4 – Soil Analysis.....	70
4.1 Physicochemical Properties of Soil	71
4.2 Gravimetric Water Content of Soil	73
4.2.1 Results	73
4.2.2 Discussion	76
4.3 Soil pH.....	79
4.3.1 Results	79
4.3.2 Discussion	82
4.4 Fatty Acid Analysis	84
4.4.1 2008 Summer Trial	86
4.4.2 2009 Summer Trial	97
4.4.3 Discussion	111
4.5 Limitations	121
4.6 Relevance to Forensic Science.....	122
Chapter 5 – Diffusion Model	123
5.1 Results.....	124
5.1.1 Diffusion Model Test.....	124

5.1.2 <i>Simulation of the Diffusion Model</i>	124
5.2 <i>Discussion</i>	126
5.3 <i>Limitations</i>	129
5.4 <i>Relevance to Forensic Science</i>	130
Chapter 6 – <i>Conclusions and Future Considerations</i>	131
6.1 <i>Conclusions</i>	132
6.2 <i>Future Considerations</i>	133
Chapter 7 – <i>References</i>	136
Chapter 8 – <i>Appendices</i>	146
<i>Appendix A – Tissue Decomposition Classification System</i>	147
<i>Appendix B – Myristic Acid Content of Soil Samples by Distance</i>	149
<i>Appendix C – Palmitic Acid Content of Soil Samples by Distance</i>	156
<i>Appendix D – Palmitoleic Acid Content of Soil Samples by Distance</i>	163
<i>Appendix E – Stearic Acid Content of Soil Samples by Distance</i>	170
<i>Appendix F – Oleic Acid Content of Soil Samples by Distance</i>	177

List of Tables

Table 1. Percent concentration of fatty acids recovered from spiked soil samples	37
Table 2. Summary of characteristic parameters of the diffusion model.....	44
Table 3. Physicochemical properties of soil collected at the research site	72
Table 4. Relative percent (%) composition of fatty acids detected in the 2008 trial	96
Table 5. Relative percent (%) composition of fatty acids detected at each distance from the carcasses in the 2009 trial.....	109
Table 6. Perimeter measurements of the cadaver decomposition island (CDI).....	110

List of Figures

Figure 1. Research site: Technical and Protective Operations Facility, Royal Canadian Mounted Police, Ottawa, Ontario, Canada.	23
Figure 2. Open land at research site: Technical and Protective Operations Facility, Royal Canadian Mounted Police, Ottawa, Ontario, Canada.	25
Figure 3. Schematic of soil structure	41
Figure 4. The capillary pressure, P_C , as a function of the moisture content, θ	42
Figure 5. Schematic of fluid flow through the boundaries of the control volume with respect to the moisture content at a point.	43
Figure 6. Average daily temperatures and precipitation amounts for the forested land of the summer 2008 trial.	47
Figure 7. Average daily temperatures and precipitation amounts for the open land of the summer 2008 trial.....	48
Figure 8. Average daily temperatures and precipitation amounts for the open land of the summer 2009 trial.....	49
Figure 9. Representative photographs of pig carcasses in various decomposition stages taken in the forested land at the Technical and Protective Operations Facility in Ottawa, Ontario, Canada during the 2008 summer trial.....	51
Figure 10. Representative photographs of pig carcasses in various decomposition stages taken in the open land at the Technical and Protective Operations Facility in Ottawa, Ontario, Canada during the 2008 summer trial.....	53
Figure 11. Representative photographs of pig carcasses in various decomposition stages taken in the open land at the Technical and Protective Operations Facility in Ottawa, Ontario, Canada during the 2009 summer trial.....	55
Figure 12. Median ADD values with the range for decomposition scores observed in shaded and sun exposed pig carcasses of the 2008 and 2009 summer trials	57

Figure 13. Median ADD value for the onset of decomposition scores observed in shaded and sun exposed pig carcasses of the 2008 and 2009 summer trials.....	59
Figure 14. Decomposition score as a function of ADD for shaded pig carcasses of the 2008 trial	60
Figure 15. Decomposition score as a function of ADD for sun exposed pig carcasses of the 2008 trial	61
Figure 16. Decomposition score as a function of ADD for sun exposed pig carcasses of the 2009 trial	62
Figure 17. Decomposition score as a function of ADD for shaded and sun exposed pig carcasses of the 2008 and 2009 trials and for human remains.....	63
Figure 18. Gravimetric water content of control and experimental soil collected within the cadaver decomposition island at the Technical and Protective Operations Facility in Ottawa, Ontario, Canada during the 2008 summer trial.....	74
Figure 19. Gravimetric water content of control and experimental soil collected within the cadaver decomposition island at the Technical and Protective Operations Facility in Ottawa, Ontario, Canada during the 2009 summer trial.....	75
Figure 20. Soil pH of control and experimental soil collected within the cadaver decomposition island at the Technical and Protective Operations Facility in Ottawa, Ontario, Canada during the 2008 summer trial.....	80
Figure 21. Soil pH of control and experimental soil collected within the cadaver decomposition island at the Technical and Protective Operations Facility in Ottawa, Ontario, Canada during the 2009 summer trial.....	81
Figure 22. Sample chromatogram of an experimental soil sample collected at 123.0 ADD of the 2008 trial within the cadaver decomposition island at the Technical and Protective Operations Facility in Ottawa, Ontario, Canada.	85
Figure 23. Myristic acid content of control and experimental soil collected within the cadaver decomposition island at the Technical and Protective Operations Facility in Ottawa, Ontario, Canada during the 2008 summer trial.....	87

Figure 24. Palmitic acid content of control and experimental soil collected within the cadaver decomposition island at the Technical and Protective Operations Facility in Ottawa, Ontario, Canada during the 2008 summer trial	88
Figure 25. Palmitoleic acid content of control and experimental soil collected within the cadaver decomposition island at the Technical and Protective Operations Facility in Ottawa, Ontario, Canada during the 2008 summer trial	90
Figure 26. Stearic acid content of control and experimental soil collected within the cadaver decomposition island at the Technical and Protective Operations Facility in Ottawa, Ontario, Canada during the 2008 summer trial	91
Figure 27. Oleic acid content of control and experimental soil collected within the cadaver decomposition island at the Technical and Protective Operations Facility in Ottawa, Ontario, Canada during the 2008 summer trial	93
Figure 28. Fatty acid content of experimental soil collected within the cadaver decomposition island at the Technical and Protective Operations Facility in Ottawa, Ontario, Canada during the 2008 summer trial	95
Figure 29. Myristic acid content of experimental soil collected 0 cm, 10 cm, 20 cm, 30 cm, 40 cm and 50 cm away from the pig carcasses at the Technical and Protective Operations Facility in Ottawa, Ontario, Canada during the 2009 summer trial	98
Figure 30. Palmitic acid content of experimental soil collected 0 cm, 10 cm, 20 cm, 30 cm, 40 cm and 50 cm away from the pig carcasses at the Technical and Protective Operations Facility in Ottawa, Ontario, Canada during the 2009 summer trial	99
Figure 31. Palmitoleic acid content of experimental soil collected 0 cm, 10 cm, 20 cm, 30 cm, 40 cm and 50 cm away from the pig carcasses at the Technical and Protective Operations Facility in Ottawa, Ontario, Canada during the 2009 summer trial	101
Figure 32. Stearic acid content of experimental soil collected 0 cm, 10 cm, 20 cm, 30 cm, 40 cm and 50 cm away from the pig carcasses at the Technical and Protective Operations Facility in Ottawa, Ontario, Canada during the 2009 summer trial	102
Figure 33. Oleic acid content of experimental soil collected 0 cm, 10 cm, 20 cm, 30 cm, 40 cm and 50 cm away from the pig carcasses at the Technical and Protective Operations Facility in Ottawa, Ontario, Canada during the 2009 summer trial	104

Figure 34. Fatty acid content of experimental soil collected within the cadaver decomposition island at the Technical and Protective Operations Facility in Ottawa, Ontario, Canada during the 2009 summer trial.....	106
Figure 35. Relative fatty acid content with respect to the distances at which experimental soil samples were collected within the cadaver decomposition island at the Technical and Protective Operations Facility in Ottawa, Ontario, Canada during the 2009 summer trial.....	108
Figure 36. The behaviour of moisture content, representative of decomposition fluid, as a function of radius, r , and time, T , for Rubicon sandy loam soil	125
Figure 37. Evolution of the liquid front in Rubicon sandy loam and Isere sand.	126

List of Appendices

Appendix A – Tissue Decomposition Classification System	147
Appendix B – Myristic Acid Content of Soil Samples by Distance	149
Appendix C – Palmitic Acid Content of Soil Samples by Distance.....	156
Appendix D – Palmitoleic Acid Content of Soil Samples by Distance.....	163
Appendix E – Stearic Acid Content of Soil Samples by Distance.....	170
Appendix F – Oleic Acid Content of Soil Samples by Distance	177

List of Abbreviations

ADD	Accumulated degree days
ADP	Adenosine diphosphate
ATP	Adenosine triphosphate
ANOVA	Analysis of variance
BSTFA	<i>N,O</i> -bis(trimethylsilyl)trifluoroacetamide
CDI	Cadaver decomposition island
CPC	Canadian Police College
CV	Coefficient of variation
r^2	Correlation coefficient
ETC	Electron transport chain
FAMEs	Fatty acid methyl esters
Fe ³⁺	Ferric ions
GC	Gas Chromatograph
GC-MS	Gas Chromatography-Mass Spectrometry
GI	Gastrointestinal
HMDS	Hexamethyldisilazane
H ₂ S	Hydrogen sulfide gas
IFIS	Integrated Forensic Identification Services
IS	Internal standard
LOD	Limit of detection
LOQ	Limit of quantitation
LOS	Limit of saturation
m/z	Mass to charge ratio
C14:0	Myristic acid

C19:0	Nonadecanoic acid
C18:1	Oleic acid
C16:0	Palmitic acid
C16:1	Palmitoleic acid
Pa	Pascal
PAR	Peak area ratio
PMI	Postmortem interval
RPM	Revolutions per minute
RCMP	Royal Canadian Mounted Police
SD	Standard deviation
s.e.	Standard error
SOP	Standard Operating Procedure
C18:0	Stearic acid
TPOF	Technical and Protective Operations Facility
TBS	Total body score
TIC	Total ion count
TMCS	Trimethylchlorosilane
TMS	Trimethylsilyl
C ₂	Two carbon unit

Chapter 1 – Introduction

1.1 Forensic Taphonomy

Taphonomy can be defined as the study of the postmortem period as it relates to the degradation, burial and fossilization of dead organisms (Haglund and Sorg, 1997a; Forbes, 2008b). It was developed to comprehend the ecology of a decomposition site i.e. how the site affects and is affected by the presence of decomposing remains, either plant or animal (Carter and Tibbett, 2008). Taphonomy was initially described as a branch of palaeontology (Efremov, 1940). Today, taphonomy takes on a multidisciplinary approach involving the disciplines of archaeology, paleoanthropology and microbiology (Haglund and Sorg, 1997a). The application of taphonomy to forensic science necessitated the inclusion of other disciplines namely, anthropology, mycology, botany and entomology (Forbes, 2008b). Forensic taphonomy is concerned with the use of scientific approaches to ascertain the time of death, recreate perimortem and postmortem events, differentiate human activities from natural occurrences and assist in the determination of the cause and manner of death (Haglund and Sorg, 1997b; Forbes, 2008b).

1.2 Postmortem Interval

Estimating the postmortem interval (PMI) is essential in forensic investigations. PMI estimates can narrow the time range of death of an individual, potentially aiding in the identification of the deceased and focusing the number of suspects in homicide investigations (Catts, 1992; Megyesi et al., 2005). Up to 72 hours after death, PMI estimations are based on the visual examination of the body and determining gastric contents (Vass et al., 2002). During this initial period the most accurate method for estimating the PMI is determining the potassium content of the vitreous humour of the eye (James et al., 1997). A revised formula was developed to more accurately estimate the PMI based on the potassium content of vitreous humour (Munoz et al., 2001). Munoz et al. (2001) asserted that almost 30% of the error associated with previous formulae is reduced in the revised formula. Furthermore, Vass et al. (1992) demonstrated that volatile fatty acids extracted from soil collected beneath decomposing human remains

can be used for estimating the PMI. Additional research concluded that the PMI could also be estimated by analyzing the rate of DNA degradation in the human rib bone (Perry et al., 1988) and the cellular changes of leukocytes (Babapulle and Jayasundera, 1993) in the time range of weeks and 36-84 hours after death, respectively.

The inaccuracy of PMI estimates increases with more advanced stages of decomposition (Prieto et al., 2004; Swann et al., 2010a). Following the onset of putrefaction (approximately 72 hours after death in a temperate environment) methods used in forensic entomology are the most accurate for estimating the PMI in cases where entomological activity is observed (Amendt et al., 2004). Forensic entomology is the study of insects in relation to criminal investigations. Blow flies (family Calliphoridae) are the initial and main consumers of carrion (Shean et al., 1993) and are therefore responsible for increasing the rate of soft tissue removal from bone structures. As such, they are the most important entomological specimens used for estimating the PMI (Shean et al., 1993). PMI estimates based on entomological data are generated by relating the developmental stage of immature flies to the amount of heat required to reach the particular stage through the use of temperature data (Catts and Goff, 1992). Catts (1992) identified several factors that may greatly affect the natural succession and/or development of insects associated with decomposing remains, thus skewing the accuracy of PMI estimations. These factors include the effects of antemortem alcohol consumption and drug abuse, the cause and time (i.e. day or night) of death of the deceased and the treatment and location of the remains (Catts, 1992).

Scavenging behaviours can also affect the rate of soft tissue removal and ultimately the estimation of the PMI (O'Brien et al., 2007). Mammalian scavengers are capable of consuming extensive amounts of soft tissue as well as destroying and displacing bones (Bass, 1997; O'Brien et al., 2007) thereby impinging on PMI estimations. It is also possible that cadavers are consumed *ex situ* further interfering with PMI estimations and the criminal investigation (Bass, 1997; Carter et al., 2007).

It has been emphasized that estimating the time of death will always be burdened with great uncertainty due to the lack of information regarding the perimortem period (Simonsen et al., 1977).

1.3 Decomposition

Decomposition is the process whereby the tissue of dead organisms is degraded through the chemical and biological degradation of tissue to simpler forms of matter and the physical removal of soft tissue by arthropods and scavengers (Clark et al., 1997).

1.3.1 Central Metabolism and Adenosine Triphosphate

Central metabolism is the set of cellular biochemical processes that sustain life in living organisms and is responsible for directing the material and energy resources of the cell (Campbell and Reece, 2002b). Living cells release the energy stored in the covalent bonds of carbohydrates to drive the biosynthesis of macromolecules i.e. lipids, proteins, carbohydrates and nucleic acids (Gill-King, 1997). These macromolecules are required for the synthesis, repair and replacement of organelles, cellular membrane and cell products as well as for cell growth and cell division (Gill-King, 1997).

Adenosine triphosphate (ATP) is a fundamental carrier of chemical energy in cells as energy is stored in the phosphate bonds of ATP (Campbell and Reece, 2002b). It can be transported throughout the cell and coupled to various metabolic reactions (Gill-King, 1997). The greatest source of ATP is generated by a process known as oxidative phosphorylation. In mammalian cells, the electron transport chain (ETC) is a series of electron carrier proteins embedded in the inner mitochondrial membrane that partake in sequential reduction-oxidation reactions in which electrons (removed from hydrogen) are shuttled to and from each carrier protein (Campbell and Reece, 2002d). Oxygen is used as the final electron acceptor and is subsequently reduced to water (Gill-King, 1997). As the electrons move, the free energy released drives the remaining hydrogen ions (protons) across the membrane and into the intermembrane space of the mitochondrion, producing a proton gradient (Gill-King, 1997). Protons move down the gradient and back across the membrane through the protein complex ATP synthase, which uses the free energy of the moving proton to form a phosphate bond between adenosine diphosphate (ADP) and inorganic phosphate, generating a molecule of ATP (Campbell and Reece, 2002d). The disruption of oxidative phosphorylation may be caused by anoxia or damage to the membrane or any part of the ETC (Gill-King, 1997).

1.3.2 *Autolysis*

At death, circulation is halted leading to the intercellular decline of pH in plasma and tissue as buffer systems fail (Gill-King, 1997). Buffers are substances that enable biological fluids to resist changes in pH when acidic or basic substances are introduced (Campbell and Reece, 2002a). Furthermore, there is an intracellular decline in pH as the central metabolic pathway is shifted to a fermentative one (Gill-King, 1997), in which carbohydrates are partially degraded without the use of oxygen (Campbell and Reece, 2002d). The decline in pH is caused by the anaerobic conversion of pyruvic acid to lactic acid (Gill-King, 1997). This pathway produces a small amount of ATP, however, it is insufficient to sustain typical levels of biosynthesis, repair and replacement of cellular membrane, organelles and molecules (Gill-King, 1997).

The loss of membrane structure and function is one of the initial consequences of decreased ATP production and biosynthesis (Gill-King, 1997). The fatty acid tails of phospholipid molecules within the plasma membrane surrounding the cell and organelles are promptly oxidized and are not replaced (Gill-King, 1997). Moreover, transport proteins, responsible for pumping various ions and molecules against their concentration gradients and for maintaining membrane selectivity (Campbell and Reece, 2002c), and proteins of the ETC are not replaced (Gill-King, 1997). As membrane selectivity is lost the cytoplasm and organelles swell. Hydrolytic enzymes once compartmentalized in lysosomes are expelled into the cytoplasm where they are activated by the declining pH and begin to digest proteins, carbohydrates and residual membrane, while fats are affected to a lesser extent (Clark et al., 1997; Janaway et al., 2009). Intercellular cell junctions are eventually denatured, causing cells to detach and leading to what is grossly observed as irreversible tissue necrosis (Gill-King, 1997). The process of enzymatic self-digestion resulting in cellular destruction is known as autolysis. Autolysis is the precursor to putrefaction.

1.3.3 Autolysis: Postmortem Changes

Defining features are apparent throughout the decomposition process. Postmortem changes alter the physical nature and appearance of the body as decomposition proceeds and have been used for estimating the PMI (Goff, 2009).

Algor mortis, livor mortis and rigor mortis are postmortem changes that typically occur two hours after death (Clark et al., 1997; Goff, 2009; Janaway et al., 2009). At death, the body loses the ability to regulate internal temperature (Goff, 2009). Algor mortis is the cooling of the body to the ambient temperature as body heat is lost to the surrounding environment (Clark et al., 1997; Janaway et al., 2009). If death occurs in extreme heat, the body temperature may rise after death (Clark et al., 1997). Goff (2009) contends that ambient temperatures can be reached in 18 to 20 hours.

The cessation of circulation initiates the physical process of livor mortis (also known as lividity or postmortem hypostasis) (Goff, 2009). As blood is no longer circulated by the heart at death, blood settles to dependent areas of the body, resulting in discolouration (Goff, 2009). The dependent areas undergo a colour change from red to purple as oxygen dissociates from the hemoglobin in erythrocytes; deoxyhemoglobin is purple in colour (Clark et al., 1997; Janaway et al., 2009). Deoxyhemoglobin is also formed in blood vessels. Marbling is the delineation of superficial blood vessels by deoxyhemoglobin (Clark et al., 1997). In general, the full development of livor mortis is complete two to four hours after death (Goff, 2009). At this time, blood is fluid and can be displaced by applying pressure to the area (blanching) (Goff, 2009). Once the pressure is removed the blood will quickly refill the area (Clark et al., 1997; Goff, 2009). As algor mortis ensues, the fat tissue in the dermis enveloping the capillaries solidifies thereby pinching them and fixing the blood in place; this phenomenon is known as the fixation of lividity (Clark et al., 1997) and typically occurs eight to twelve hours after death depending on temperature and age of the deceased, among other factors (Goff, 2009; Janaway et al., 2009).

Rigor mortis is characterized by the stiffening of muscles approximately two to six hours after death (Goff, 2009). Muscle cells become more permeable to calcium ions

as their membranes lose integrity (Gill-King, 1997). The influx of calcium ions causes the end-to-end joining of sarcomeres, known as a muscle contraction. ATP-dependent pumps that are responsible for pumping calcium ions out of the cell, thereby releasing muscles from the contracted state, are non-functional after death due to the cessation of ATP synthesis (Gill-King, 1997). The entire body will be rigid approximately 24 hours after death (Clark et al., 1997) and will relax only when the muscle cells themselves begin to decompose (Gill-King, 1997).

The hydrolytic enzymes released and activated at the dermal-epidermal junction during autolysis can loosen the epidermis from the underlying dermal layer (Clark et al., 1997). Fluid can build up within this junction forming epidermal bullae (Cockle, 2008) and the epidermis can be easily separated from the dermis resulting in skin slippage (Clark et al., 1997).

1.3.4 Putrefaction

Putrefaction is an anaerobic phase of decomposition whereby soft tissue becomes liquefied (Cockle, 2008). At end-stage autolysis, an almost completely anaerobic environment is developed within the body which is conducive to the growth of endogenous anaerobic bacteria (Gill-King, 1997). Microorganisms of the gastrointestinal (GI) tract invade neighbouring tissues through the vascular and lymphatic systems (Janaway et al., 2009). The bacteria can utilize the breakdown products from the autolytic process as nutrients to stimulate their growth (Clark et al., 1997; Janaway et al., 2009). Soft tissue is degraded by the activity of the microorganisms through the breakdown of protein, carbohydrate and fat components into diverse acids, gases, liquids and simple molecules (Gill-King, 1997; Vass et al., 2002; Dent et al., 2004). These by-products are the basis of colour changes, odours and bloating characteristic of putrefaction. Anaerobic organisms that have been implicated in the putrefactive process are species of the genus *Clostridium*, in particular *Clostridium perfringens* and species of the genus *Bacteroides* and *Streptococcus*; Enterobacteria have also been implicated in the process (Janaway et al., 2009). Throughout the decomposition process the endogenous microbiota may intermingle with environmental microorganisms such as soil bacteria,

fungi and amoebas; these organisms can also participate in the degradation process (Janaway et al., 2009).

1.3.5 Putrefaction: Postmortem Changes

The degradation of macromolecules by microorganisms during the putrefactive process leads to the accumulation of by-products such as, acids, gases and simple molecules, that produce distinct features of putrefaction (Gill-King, 1997). Bloating is the accumulation of gases causing the distension of the body, particularly in the abdomen and in areas of livor mortis (Clark et al., 1997). Providing no injuries vent the gases, this effect substantially distorts the contour of the body (Clark et al., 1997).

Another prominent feature of putrefaction is colour changes. Protein breakdown products (i.e. amino acids) are transported into bacterial cells where endogenous enzymes cleave amine and carboxyl groups via deamination and decarboxylation (Gill-King, 1997). Sulfur-containing amino acids are further broken down by desulfhydration to produce hydrogen sulfide gas (H_2S) (Gill-King, 1997). H_2S can readily diffuse through tissues (Clark et al., 1997) and react with iron to yield the black precipitate ferrous sulfide (Gill-King, 1997) or hemoglobin to form sulfhemoglobin, a green pigment (Clark et al., 1997). Furthermore, Gill-King (1997) asserts that phenylpyruvic acid, a breakdown product of the amino acid phenylalanine, reacts with ferric ions (Fe^{3+}) to produce a green complex. The accumulation of these molecules and complexes leads to the distinct colour changes observed throughout decomposition, typically from red to purple to green to brown then to black.

Adipocere formation is the process whereby adipose tissue is converted to a solid white, soap-like substance (Forbes et al., 2005c). Adipocere is mainly composed of saturated fatty acids (i.e. myristic, palmitic and stearic acids), however, may also contain unsaturated fatty acids (i.e. palmitoleic and oleic acids) as well as hydroxy fatty acids and salts of fatty acids (Forbes et al., 2003). Furthermore, Takatori (1996) demonstrated the presence of oxo fatty acids in adipocere. It is formed through the activity of putrefactive bacteria in anaerobic environments where sufficient moisture is present (Forbes et al., 2005d). The formation of adipocere preserves soft tissues as the presence of fatty acids

decreases the pH of the environment and increases dehydration thus inhibiting the growth of microorganisms (Clark et al., 1997; Pinheiro, 2006). The mummification of soft tissue also has a preservative effect as desiccated tissue inhibits degradation by microorganisms (Forbes et al., 2005d).

1.3.6 *Skeletonization*

Skeletonization is the removal of all soft tissue from bone structures (Clark et al., 1997; Pinheiro, 2006). Complete or partial skeletonization of remains is possible (Clark et al., 1997; Pinheiro, 2006). The degree of skeletonization is dictated by the environmental conditions to which the remains are exposed (Pinheiro, 2006).

1.4 *Factors Affecting the Decomposition Process*

The rate of decomposition is affected by several factors. These factors may accelerate or delay the decomposition process. The complexity of the interactions amid the various factors is not well known as the effects of each are most often described and researched independently from the other factors. Nevertheless, each factor plays a vital role in the decomposition process and individual effects need to be understood in order to study and explain the effects of complex interactions.

1.4.1 *Climatic Factors*

Temperature is the major factor affecting decomposition (Mann et al., 1990; Bass, 1997; Gill-King, 1997; Vass et al., 2002). In general, the reaction rate of chemical processes increases with an increase in temperature (Gill-King, 1997). Providing cellular enzymes remain intact, cell metabolism can be slowed or accelerated by affecting the enzyme systems that control reactions through temperature change (Gill-King, 1997). The hydrolytic enzymes responsible for the chemical degradation of cellular constituents operate more efficiently at higher ambient temperatures. The microorganisms responsible for the chemical breakdown of tissue are, also, greatly affected by temperature (Campobasso et al., 2001). Particularly low or high temperatures will inhibit microbial proliferation thus delaying tissue breakdown (Campobasso et al., 2001). The

rate of decomposition generally increases with an increase in temperature and decreases with a decrease in temperature.

Water is essential for the biochemical reactions responsible for tissue degradation (Gill-King, 1997). Hydrolysis is a chemical reaction in which molecules are broken down to simpler forms by reaction with water. (Harris, 2003). Hydrolytic enzymes released into the cytoplasm during autolysis degrade molecules through hydrolysis reactions (Gill-King, 1997). Furthermore, moisture promotes the growth of microorganisms. The body is an important source of water for the microorganisms that invade and degrade tissues after death (Gill-King, 1997).

The water content of the atmosphere can, also, greatly affect decomposition. Humidity and aridity affect the extent of water loss of exposed tissue, in particular at the skin surface (Mann et al., 1990; Aturaliya and Lukasewycz, 1999). The rate at which water is removed from the skin surface is an important determinant of the effect on decomposition of underlying tissues as well as the skin (Aturaliya and Lukasewycz, 1999). Excessive evaporation of water from the skin surface into the surrounding environment may lead to the mummification of underlying tissues (Aturaliya and Lukasewycz, 1999).

In arid climates or in circumstances of extremely high temperatures dehydration of the skin occurs rapidly producing a hard and leathery covering, impermeable to the transfer of water from underlying tissues to the surface (Galloway, 1997; Aturaliya and Lukasewycz, 1999). The mummified skin covering retains moisture within the visceral tissues thereby providing an environment for continued tissue degradation (Aturaliya and Lukasewycz, 1999). Mummification has a preservative effect and mummified tissue can remain intact for several years (Mann et al., 1990).

Precipitation introduces water into the environment. It prevents the soil surrounding the decomposing remains as well as the remains from drying (Archer, 2004). Moreover, a moist environment encourages the growth of microorganisms; of importance are those responsible for tissue degradation (Archer, 2004). Precipitation can, also, rehydrate dried remains allowing for continued tissue degradation (Archer, 2004).

1.4.2 *Physical Factors*

The most influential physical factor affecting the rate of soft tissue removal is access of the body to arthropods. Bass (1997) described insect activity as the major factor responsible for accelerating the rate of soft tissue removal. Providing the carrion is exposed to the environment and the conditions are favourable, insects are typically the first to discover a decomposing body (Catts and Goff, 1992; Amendt et al., 2004). Forensically important arthropods are species of the order Diptera (flies) and Coleoptera (beetles) (Amendt et al., 2004). Blow flies (Calliphoridae) are among the first colonizers and are major consumers of carrion (Amendt et al., 2004). Adult flies are known to oviposit on decomposing remains within a few hours after death (Catts and Goff, 1992). In a study carried out by Shean et al. (1993) examining differential decomposition of sun exposed and shaded pig carrion, blowflies were attracted to the pig carcasses within 20 minutes after death and oviposition was observed two to three hours later in natural orifices. The blow fly larvae are necrophagous, meaning they feed on decomposing tissue (Goff, 2009), and can reduce a cadaver to a complete skeleton in two weeks (Bass, 1997). Other necrophagous dipteran species such as flesh flies (Sarcophagidae) and various necrophagous beetle species (e.g. Silphidae, Dermestidae) contribute to the consumption and thereby removal of soft tissue from decomposing organisms (Goff, 2009).

Vertebrate scavengers are also known for physically removing soft tissue from decomposing remains (Clark et al., 1997) and modifying bone structures of skeletonized remains (O'Brien et al., 2007). The alteration of soft and hard tissues can be mistaken for perimortem trauma during forensic investigations (O'Brien et al., 2007). Furthermore, the removal of soft tissue can greatly affect the rate of decomposition and thus PMI estimations (O'Brien et al., 2007). The behaviour of scavengers can vary with geographical location and season, further affecting the decomposition process and estimation of the PMI (O'Brien et al., 2007).

Vertebrate scavengers typically include various types of birds (e.g. vultures and crows), rodents, mammalian carnivores (Rodriguez, 1997) and domestic pets (Clark et al., 1997). The pecking and tearing feeding activities of birds creates small strips of

tissue having a fibrous appearance (Rodriguez, 1997). Rodents tend to feed on the face, scalp and finger tips early in the decomposition process (Rodriguez, 1997). They are also known for their ability to gnaw (Haglund, 1997b), particularly on bone, often resembling cut marks produced by a knife or sharp tool (Rodriguez, 1997). Carnivores will feed directly on the soft tissue of decomposing remains (O'Brien et al., 2010). Coyotes and domestic dogs are often cited as the canines responsible for scavenging cadavers (Haglund, 1997a). These large animals can cause extensive damage to soft tissue and are notorious for scattering skeletal remains over large areas (up to a 16.1 km radius for coyotes in open landscapes) (Mann et al., 1990; Rodriguez, 1997).

1.5 Soil Decomposition

Soil is a complex matrix consisting of mineral particles of varying sizes (i.e. gravel, sand, silt and clay) and organic material (Fitzpatrick, 2008). The complexity of the matrix is amplified by dynamic biological, chemical, physical and mineralogical properties (Fitzpatrick, 2008). Traditionally in forensics, soil is analyzed for the purpose of comparison of soil material related to a crime scene (Benninger et al., 2008; Carter and Tibbett, 2008; Fitzpatrick, 2008). Evidence marked with soil can be analyzed to determine whether it was associated with a particular location, usually the crime scene (Fitzpatrick, 2008). However, Carter and Tibbett (2008) assert that in this context soil is viewed as a passive medium, when in fact it is a dynamic medium that is rapidly influenced by environmental change. In particular, soil properties can be used to provide information about decomposing remains.

The effect of the properties of soil on the decomposition process is most often studied with respect to buried remains (Forbes et al., 2005c; Forbes et al., 2005d; Carter et al., 2010). It has been demonstrated that soil pH, temperature, moisture and oxygen content (Forbes et al., 2005c) and particle size of the soil (Forbes et al., 2005b) can affect the rate and degree of adipocere formation in buried remains. Soil properties may also affect the microbial community present (Carter et al., 2007), which can directly participate in the decomposition process (Pfeiffer et al., 1998).

The effect of soil on remains decomposing on a soil surface is currently unknown. However, it can be speculated that the soil microbial community as well as the soil properties (e.g. moisture content and soil pH) can impact the area of the remains that is in direct contact with the soil surface. The soil environment may also dictate which microbial species inhabit the area potentially affecting the rate of decomposition (Carter and Tibbett, 2008).

Increasingly, studies are being conducted on the interaction of soil and the decomposition of human and animal remains to aid in the estimation of the PMI (Vass et al., 1992; Benninger et al., 2008). Vass et al. (1992) analyzed volatile fatty acids, anions and cations in soil solutions produced from soft tissue and bone decomposition of human cadavers to aid in PMI estimations. Propionic, butyric and valeric volatile fatty acids were detected in specific ratios in soil solutions in a temperature dependent manner and thus can be used in PMI estimations (Vass et al., 1992). It was also demonstrated that decomposing remains will yield particular ratios of ions namely, sodium, chloride, ammonium, potassium, calcium, magnesium and sulphate, which can be used for estimating the PMI (Vass et al., 1992).

A study was conducted to determine the potential for using a soil-based approach for PMI estimates (Benninger et al., 2008). Soil samples collected beneath pig carcasses were analyzed for moisture content, soil pH, total carbon, total nitrogen, soil-extractable phosphorus and lipid-phosphorous (Benninger et al., 2008). Significant increases in the concentration of lipid-phosphorous, total nitrogen and soil-extractable phosphorous were detected in soil containing decomposition fluid 43, 72 and 100 days postmortem, respectively (Benninger et al., 2008). Benninger et al. (2008) alleged that these soil properties can potentially be used for estimating the PMI upon further research.

1.5.1 *Cadaver Decomposition Island*

The decomposing remains of a human or animal are greatly affected by the environment in which they are found and vice versa. Cadaveric material can be quickly introduced into the surrounding environment through putrefaction or insect activity forming a cadaver decomposition island (CDI) (Carter et al., 2007). The CDI forms as

decomposition fluid leaches from decomposing remains into the surrounding environment; it is apparent as a darkened stain around the remains and death of nearby vegetation (Carter et al., 2007). It provides a localized pulse of concentrated nutrients into the soil (Benninger et al., 2008), having the potential to positively or adversely affect biological communities (e.g. microorganisms) depending on the specific energy requirements of the community (Carter et al., 2007). CDIs are generally associated with a proliferation in microbial biomass and activity as they are hubs for carbon and nutrient flow (Carter et al., 2007). Benninger et al. (2008) state that nitrogen-, phosphorous- and carbon-based by-products generated throughout the putrefactive process may be retained in the soil environment. Furthermore, decomposition fluid can supply the soil with an abundance of organic matter as well as inorganic compounds such as, ammonium, calcium, potassium, sulphate, magnesium, sodium, sulfur and manganese (Carter et al., 2007).

The chemical analysis of decomposition fluid may provide more detail regarding the degradative pathway of proteins, lipids and carbohydrates by elucidating some of the intermediate and end-point products. Swann et al. (2010a; 2010b) conducted chemical analyses on decomposition fluid collected from pork rashers, stillborn piglets and adult pig carcasses. Volatile fatty acids (acetic, propionic, isobutyric, butyric, isovaleric and valeric acids) and long chain fatty acids (myristic, palmitic, palmitoleic, stearic, oleic and linoleic acids) were detected in decomposition fluid by Gas Chromatography-Mass Spectrometry (GC-MS) (Swann et al., 2010a; Swann et al., 2010b). However, long chain fatty acids were not detected in the decomposition fluid of stillborn piglets. It was determined that the fat content of a piglet is 1% (Widdowson, 1950). As such, the lack of long chain fatty acids is conceivable in that these fatty acids are associated with the degradation of adipose tissue (Swann et al., 2010b). Moreover, benzeneacetic acid, benzenepropionic acid, 2-piperidone and isocaproic acid were previously unreported compounds identified in decomposition fluid (Swann et al., 2010a). These compounds, however, have been implicated in protein breakdown (Swann et al., 2010a). Furthermore, a comparative analysis of the lipid content of decomposition fluid and adipocere was conducted (Cabirol et al., 1998). The researchers determined that the adipocere samples contained a greater concentration of fatty acids than the decomposition

fluid, indicating a decrease in the decomposition rate of adipocere (Cabirol et al., 1998). The resistance of adipocere to degradation is well documented (Pfeiffer et al., 1998; Forbes et al., 2005c; Janaway et al., 2009).

1.6 Lipid Degradation

Human adipose tissue is typically composed of 5-30% water, 2-3% proteins and 60-85% lipids or fats, by weight (Dent et al., 2004). Triglycerides (neutral fat) comprise 90-99% of the lipids in adipose tissue (Dent et al., 2004). The constituents of a triglyceride molecule are a glycerol molecule bound to three free fatty acids (Fiedler and Graw, 2003; Dent et al., 2004). Monounsaturated oleic acid (C18:1) is cited as the most abundant fatty acid in adipose tissue, followed by polyunsaturated linoleic acid (C18:2), monounsaturated palmitoleic acid (C16:1) and the saturated palmitic acid (C16:0) (Pfeiffer et al., 1998; Dent et al., 2004; Janaway et al., 2009).

At death, neutral fats are hydrolyzed by intrinsic lipases to yield glycerol and free fatty acids (Fiedler and Graw, 2003; Dent et al., 2004; Notter et al., 2009), yielding a mixture of unsaturated and saturated fatty acids (Forbes et al., 2004). Microorganisms can also possess lipolytic activity. *Clostridium perfringens*, for example, is a Gram-positive anaerobe most often associated with the degradation of fat (Janaway et al., 2009). It originates in the GI tract and possesses efficient lipolytic enzymes (Janaway et al., 2009). The soil microbial community beneath a decomposing pig carcass was characterized to enumerate the lipolytic and proteolytic bacteria associated with decomposition (Howard et al., 2010). Results indicated that lipid-degrading Gram-negative bacteria (e.g. *Acinetobacter* spp.) were more prominent in the soil microbial community throughout decomposition than proteolytic bacteria (Howard et al., 2010). The researchers deduced that the lipid constituents of the carcass supplied more nutrients to the soil community than the protein content (Howard et al., 2010). Pfeiffer et al. (1998) also highlighted the importance of Gram-negative bacteria in the degradation of lipids.

Subsequent to the hydrolysis of lipids, unsaturated fatty acids can undergo oxidative degradation to form aldehydes and ketones in aerobic conditions (Dent et al., 2004) or can be converted to saturated fatty acids via hydrogenation in anaerobic conditions (Bereuter et al., 1996; Fiedler and Graw, 2003; Dent et al., 2004). Both processes are carried out by microorganisms associated with the decomposition process. The hydrogenation of oleic and linoleic acids and palmitoleic acid will produce stearic acid and palmitic acid, respectively (Forbes et al., 2004; Notter et al., 2009). In addition, the hydrogenation theory postulated by Bereuter et al. (1996) indicates that microorganisms can cleave a two carbon unit (C_2) from fatty acid chains via a one step β -oxidation.

1.6.1 Fatty acid analysis

The process of fatty acid analysis involves the extraction of fatty acids from soil or tissue, derivatization and detection. Fatty acids can be extracted using solvent or solid-phase extraction procedures (Forbes et al., 2003; Notter et al., 2008). GC-MS is commonly used for the analysis of fatty acids (Forbes et al., 2003; Vane and Trick, 2005; Forbes et al., 2005c; Notter et al., 2008). Specifically, these studies examined the fatty acid content of adipocere, which encompasses much of the fatty acid research in decomposition. In order to perform GC-MS analysis target compounds must be sufficiently stable and volatile (Halket and Zaikin, 2003). Derivatization, or chemical transformation, can improve the physico-chemical properties of compounds for efficient detection by GC-MS (Halket and Zaikin, 2003). Trimethylsilyl (TMS) derivatives are regularly used for GC-MS analysis to enhance the volatility and stability of organic compounds containing a hydrogen donor (Little, 1999). Bereuter et al. (1996) highlighted the requirement for the derivatization of fatty acids prior to analysis. The polarity of the carboxylic end of the fatty acid chain is reduced by replacing the active hydrogen with a TMS group, thus increasing the volatility and stability of the molecule (Halket and Zaikin, 2003). The resultant TMS fatty acid ester provides good chromatographic resolution and improves mass spectral characteristics (Halket and Zaikin, 2003).

Forbes et al. (2003) developed a method for the extraction and detection of free fatty acids from adipocere in gravesoils. Fatty acids were extracted from soil using chloroform, converted to TMS fatty acid esters and subsequently analyzed by GC-MS. This method proved efficient for the detection of trace levels of fatty acids in gravesoil from a 12 year old burial site (Forbes et al., 2003). The saturated fatty acids known to comprise adipocere were detected (e.g. myristic, palmitic and stearic acids). Oleic acid and 10-hydroxy stearic acid were also identified (Forbes et al., 2003). Palmitic acid was the most abundant fatty acid identified in all gravesoil samples. Notter et al. (2008) developed a solid phase extraction method in conjunction with an adaptation of the GC-MS method developed by Forbes et al. (2003) to quantify free fatty acids in adipocere. Fatty acids were also derivatized to TMS fatty acid esters for GC-MS analysis. The aforementioned fatty acids were also detected in adipocere samples; however, palmitoleic acid and traces of lauric and arachidic acids were also identified (Notter et al., 2008). Several other studies have successfully detected fatty acids by TMS derivatization and GC-MS analysis (Bereuter et al., 1996; Vane and Trick, 2005; Forbes et al., 2005b; Forbes et al., 2005c; Forbes et al., 2005d; Notter et al., 2009).

Vass et al. (2002) stated that more accurate PMI estimates can be obtained by identifying biomarkers of decomposition. The development of fatty acid profiles over the course of the decomposition process has the potential to assist in PMI estimations and elucidate key aspects of the lipid degradation pathway.

1.7 Diffusion Model

Diffusion models are used to simulate the random movement of a material through a given medium. The Gaussian plume model is perhaps the most renowned modern example and is widely used in pollution models (Tirabassi, 1989). It is used to predict the movement of pollutants in the air assuming constant temperature, wind velocity and direction (Shieh et al., 1972). Diffusion models are also used to model the transport of heat through various media or objects (Wang and Daniels, 2006). Interestingly, Wang and Daniels (2006) developed a mathematical paradigm to be used in

forensic computer network analysis. Specifically, they used a form of heat diffusion model and graph spectral methods to identify important components, patterns and spread of a cyber attack (Wang and Daniels, 2006).

Mathematical simulations have been performed to model the diffusion of pollutants, typically pesticides, in soil (Cosoli et al., 2010; Shaw et al., 2010). These techniques allow for the consideration of environmentally-related problems such as adsorption or diffusion of pollutants in porous or layered media (Cosoli et al., 2010). Cosoli et al. (2010) affirmed that molecular simulation techniques provide opportunities for systems to be examined at varying conditions. Soil mineralogy and particle size distribution are properties that affect the binding, diffusion and adsorption of pesticides in soil systems (Cosoli et al., 2010). Cosoli et al. (2010) used these same techniques to identify important parameters for the diffusion and adhesion of atrazine in a saturated sand matrix. Furthermore, Ptashnyk et al. (2010) developed a dual-porosity model to represent the diffusion of solutes in soil. The model considers the effect of micro-scale concentration gradients on macro-scale gradients (Ptashnyk et al., 2010).

The movement of fluid through a porous medium can be modelled by a diffusion model based on particular aspects of the fluid and medium (Bear and Bachmat, 1990). The continuum approach assumes that matter is continuous throughout the area it occupies. This approach is practical for solving problems related to single phases (i.e. solid, liquid or gas), but can be expanded to include multiphase systems (Bear and Bachmat, 1990). The advantages of using the continuum model of a porous medium are: the requirement to identify the precise configuration of the interphase boundaries is eliminated, processes occurring in the medium can be described in terms of 'differentiable quantities' facilitating problem solving through mathematical analysis and the quantities are measurable and thus useful for practical applications (Bear and Bachmat, 1990). Soil is a porous medium and is composed of a solid matrix and pore space i.e. space that is void. This void can be filled with fluid or gas. Saturated soils are characterized by all of the voids being fluid. Soils that are not saturated are considered unsaturated. The flow of fluid can occur through the material via the interconnected pores and voids.

A diffusion model can also be used to predict the development of the CDI as decomposition fluid leaches from the decomposing remains into the surrounding environment. The diffusion model holds the potential to relate to PMI or specific decomposition stages. Parameters such as the porosity and permeability of soil and the point source of the fluid should be considered for the model. Soil permeability is the capacity of the soil to transmit fluid through pore spaces and porosity is the volume fraction of the pores between the particles of soil (Bear and Bachmat, 1990). Upon development of the diffusion model, it may be possible to estimate the PMI based on values determined for parameters in the model.

1.8 Research Aims and Objectives

This research was conducted to physically and chemically analyze pig carcass decomposition using conventional and newly developed methods for potential use in PMI estimations and to better understand decomposition given intrinsic and extrinsic factors in Southeastern Ontario. The objectives of this study were to determine a relationship of visible attributes of human and pig decomposition using a decomposition scoring system, generate a fatty acid profile from decomposition fluid in soil using GC-MS analysis and develop a diffusion model to predict the development of the CDI in soil over time by accounting for soil and fluid parameters. Each objective was examined for its usefulness in estimating the PMI.

Chapter 2 – Materials and Methods

2.1 Research Site

This research was conducted in collaboration with Sergeant Diane Cockle of the Integrated Forensic Identification Services (IFIS) program support, Royal Canadian Mounted Police (RCMP). Research trials were carried out at the Technical and Protective Operations Facility (TPOF), an RCMP facility in Ottawa, Ontario. TPOF is enclosed by barbed wire fencing, thereby limiting the number of animal species present, with the exception of mainly herbivore species such as deer (*Odocoileus virginianus* Zimmermann 1780) and porcupines (*Erethizon dorsatum* Linnaeus 1758). The facility measures approximately 3.5 km² and the taphonomic experimental area within TPOF is approximately 0.004 km² (1 acre) of forested land and open land lacking the presence of trees and shrubs. Ottawa is part of the Great Lakes-St. Lawrence Forest, which encompasses a mix of coniferous and deciduous trees (Ontario Ministry of Natural Resources, 2008) and is located at latitude 45° 22' north and longitude 75° 43' west and is 114 m above sea level (City of Ottawa, 2008). The average monthly temperatures and rainfall for the Ottawa region in June, July and August are 18.4°C and 91 mm, 21.0°C and 88.9 mm and 19.7°C and 87.6 mm, respectively (Environment Canada, 2004). Two research trials were conducted during the summer months of 2008 and 2009.

2.2 Research Trial 1 – Summer 2008

This study involved the analysis of the decomposition of domestic pig carcasses (*Sus scrofa* Linnaeus 1758) on soil surface vegetation. The use of human bodies is ideal for conducting decomposition studies. However, due to practical and ethical restrictions, the use of animals carcasses is required (Anderson and VanLaerhoven, 1996). A variety of animal carcasses have been used as human proxies in decomposition studies worldwide (Anderson and VanLaerhoven, 1996). Catts and Goff (1992) emphasize that in order to extrapolate from these studies to the human condition the animal model must meet specific requirements. For instance, the decomposition pattern of the animal model must approximate that of human decomposition (Catts and Goff, 1992). Furthermore, the animal model must be easy to obtain, inexpensive and unlikely to provoke public

opposition (Catts and Goff, 1992). Catts and Goff (1992) cite the use of domestic pigs as appropriate models for human decomposition. Domestic pig carcasses are considered appropriate models due to the fact that their internal anatomy, fat distribution, skin and general lack of hair is comparable to that of humans (Anderson and VanLaerhoven, 1996; Schoenly et al., 2006). Moreover, pigs and humans are omnivorous and it is suggested they share a similar gut flora (Anderson and VanLaerhoven, 1996).

The research area was divided into two different environments: the forested land and the open land. Photographs of the research site, including both the forested land and open land, were taken using a Nikon D100 SLR digital camera (Figure 1). Medium format, high resolution photographs were taken. An Onset HOBO[®] Pro V2 External Temperature and Relative Humidity Data Logger was placed in each area along with a precipitation gauge. The data logger was programmed to record the ambient temperature and relative humidity every hour for the duration of the study and the amount of rainfall was recorded using a standard rain gauge each sampling day. The data logger sensor was placed in a radiation shield prior to placement in the open land to eliminate the effect of solar radiation on the ambient temperature readings. Data was retrieved from the data logger using HOBOWare[®] Pro Data Logging Software Version 2.X. A reference soil sample was collected with a scupula in a 20 mL glass vial from the area on which each pig was deposited (experimental site). A control site, an area on the soil surface lacking the presence of a pig carcass, was established two metres away from each carcass. The site possessed similar topographic features to those of the surface on which each corresponding pig was deposited.



Figure 1. Research site: Technical and Protective Operations Facility, Royal Canadian Mounted Police, Ottawa, Ontario, Canada. (A) Forested land (B) Open land.

For the 2008 trial a total of six pigs carcasses were used; three were placed in each environment. Three 30 kg, antibiotic-free pigs were obtained from the Experimental Farm in Ottawa, Ontario. They were killed by means of a barbiturate overdose at approximately 8:00 AM on May 30, 2008. To prevent scavenging, the carcasses were wrapped in chicken wire with a mesh size of 2 cm. The carcasses were deposited on the soil surface vegetation approximately 20 m apart in the forested land between 11:00 AM and 12:00 PM on the same day as their death. These carcasses were protected from direct sun exposure due to the presence of trees and shrubs (shaded carcasses). Three additional pigs, raised and killed under the same aforementioned conditions, were deposited on the soil surface approximately 20 m apart in the open land between 11:00 AM and 12:00 PM on June 13, 2008. These pigs were exposed to full sun (sun exposed carcasses). The sun exposed carcasses were deposited on the soil surface vegetation approximately two weeks after the deposition of the first set of carcasses (May 30, 2008). Both sets of carcasses were being utilized during a Forensic Identification field exercise organized by the Canadian Police College (CPC) and deposition was required two weeks apart to allow for the manifestation of entomological specimens in various developmental stages.

In order to standardize the photographs, four reference stakes numbered one to four were placed in the soil around each of the carcasses. The stakes marked the locations where the photographs were to be taken and the numbers corresponded to the

order in which they were taken. Each carcass was photographed on each sampling day in the forested land and open land.

Soil samples were also collected on each sampling day. Samples were collected daily from the day of deposition of the carcasses (0.0 accumulated degree days (ADD)) until the removal of soft tissue was almost complete; at which point samples were collected once a week until the carcass was reduced to a complete skeleton and only desiccated tissue and bones remained. Samples were collected beneath the pig carcass by lifting the chicken wire that encased the carcass or within the cadaver decomposition island (CDI) if it was present. A control soil sample was also collected for each experimental site each sampling day. A scupula was used to collect the soil and transfer it into glass vials. The scupula was rinsed with isopropyl alcohol between sample collections to remove soil traces from the previous sample collection. All soil samples were stored in a -10°C freezer until transportation to a -20°C freezer in the Forbes laboratory at the University of Ontario Institute of Technology upon completion of the research trial, pending further analysis.

2.3 Research Trial 2 – Summer 2009

The second research trial was conducted in the open land only. Photographs of the research site were taken (Figure 2). The data logger, with attached radiation shield, and precipitation gauge were placed in the open land. The data logger was programmed to record ambient temperature and relative humidity every hour for the duration of the study and the amount of rainfall was recorded each sampling day. The data was retrieved upon completion of the study.



Figure 2. Open land at research site: Technical and Protective Operations Facility, Royal Canadian Mounted Police, Ottawa, Ontario, Canada.

Soil samples were collected using a stainless steel soil core sampler with an internal diameter of 2 cm. Soil samples were collected in Ziploc[®] Brand Snack Bags. A control site was established 2 m away from each pig carcass and possessed similar topographic features to the surface on which the corresponding pig was placed. A reference and a control core soil sample that extended 5 cm into the soil were collected for each experimental and control site prior to the commencement of the trial. Three samples of relatively undisturbed soil (one for each experimental site) were collected in Ziploc[®] Brand Containers using a trowel. The undisturbed soil was collected within 2 m of each experimental site. These samples were collected again on June 18, 2009 and on July 8, 2009. The undisturbed soil was used to determine the rate at which fluid diffused through the soil (refer to 2.7.1 *Diffusion Model Test*).

Three 50 kg, antibiotic-free pigs were acquired from the Experimental Farm. They were killed by means of a barbiturate overdose at approximately 9:00 AM on June 10, 2009. Each carcass was wrapped in chicken wire with a mesh size of 2 cm and placed on the soil surface vegetation approximately 20 m apart in the open land at the research area between 10:00 AM and 11:00 AM. All pigs were exposed to full sun.

Photographs of the carcasses were taken (no standardization) and soil samples were collected each sampling day. Core soil samples, that extended 5 cm into the soil commencing at the soil-carcass boundary (0 cm) and every 10 cm from the carcass up to 50 cm, were collected for each carcass each sampling day. This sampling method was aimed at characterizing the CDI at regular intervals throughout the decomposition process and at determining if the perimeter of the CDI could be detected through fatty acid analysis. The top 2 cm of the core soil sample was separated from the bottom 3 to 5 cm and placed in separate bags. The separation of the soil layers allowed for the independent characterization of each layer. Soil from an undisturbed area (no previous sampling) was collected each sampling day and areas that appeared to contain decomposition fluid were chosen for sampling. The 'Observed CDI Perimeter' was measured using a metre stick. It was made visible by the decomposition fluid that leached into the soil environment thereby forming a darkened area; the perimeter of the darkened area was defined as the 'Observed CDI Perimeter'. A core soil sample was also collected from the control site of each carcass. Samples were collected daily from the commencement of the study (day of deposition of carcasses) until the removal of soft tissue was almost complete. Subsequently, samples were collected three times a week for two weeks. Samples were stored in a freezer at -10°C until they were transported to a -20°C freezer in the Forbes laboratory upon completion of the study, pending further analysis.

2.4 Scoring of Photographs for Decomposition

2.4.1 Decomposition Stages

The process of decomposition can be divided into stages based on gross tissue changes, time intervals but, more frequently, a combination of both. Autolysis and putrefaction are cellular decomposition processes that lead to the development of distinct decomposition stages. Payne (1965) described six stages of decomposition for pig carcasses: fresh, bloated, active decay, advanced decay, dry and remains stages. These stages are often cited in decomposition studies (Sharanowski et al., 2008; Goff, 2009;

Matuszewski et al., 2010). However, the decomposition stages referred to herein were developed by Cockle (2008) as a classification system for human decomposition. In this study, the system was used to classify decomposition stages in photographs of human remains as well as pig carcasses. These stages separated the chemical and biological degradation of soft tissue from the physical removal of soft tissue by arthropods and scavengers. Moreover, environmentally dependent states such as, mummification, wet and dry moulding and adipocere formation were considered.

2.4.2 *Baseline Decomposition*

Baseline decomposition stages were used to describe the degradation of soft tissue by cellular decomposition processes (Cockle, 2008). These stages excluded the consumption of soft tissue by arthropods and scavengers. Each stage was assigned a number, in square brackets, to allow for the scoring of photographs using the decomposition scoring system. Baseline decomposition was divided into three categories: autolysis, putrefaction and skeletonization. Each category was further subdivided into stages. The initial stage of autolysis was identified shortly after death when there were ‘no visible changes’ [0] to the carcass. The ‘first visible change’ [1] stage was characterized by the appearance of livor mortis and/or rigor mortis. The final stage of autolysis was ‘first tissue change’ [2]. This stage was characterized by the manifestation of fluid blisters or epidermal bullae and skin slippage as the separation of the epidermal and dermal layers allowed for fluid to accumulate between the layers. Marbling of superficial blood vessels and browning of exposed tissue was also a feature of this stage.

Putrefaction was depicted as the biological process of tissue liquefaction via microbial degradation (Cockle, 2008). It was also subdivided into three stages: ‘first colour change’ [3], ‘full bloat’ [4] and ‘post bloat’ [5]. ‘First colour change’ [3] referred to the colour changes associated with putrefactive decay: blood transformed into a green colour and tissue was converted to a greenish-blue colour. The onset of abdominal swelling was also visible during this stage. ‘Full bloat’ [4] was characterized by the complete distension of the abdomen in combination with colour changes associated with blood and tissue e.g. green, purple and black. The release of gases caused the abdomen

to collapse and thus initiated the 'post bloat' [5] stage. At this stage the blood and tissue were brown to black in colour.

Skeletonization was described as the process whereby the liquefaction of tissue by autolysis and putrefaction exposed bone (Cockle, 2008). The stages of skeletonization were based on the level of bone exposure. In the 'first sign of bone' [6] stage, less than half of the total bone was exposed. Features of putrefactive decay were still apparent; however, bones were exposed in the extremities and/or areas of shallow tissue depth. The consecutive stage was characterized by the exposure of more than half of the skeleton ('more than half of bone exposed' [7] stage) with at least 5% of tissue remaining. In 'total skeletonization' [8], a small amount of tissue remained on the skeleton (under 5%), consisting of dry tissue or tendons.

2.4.3 Insect and Scavenging Activity

The effect of insect and scavenging activity on the removal of soft tissue was represented by the level of activity. Five stages were included in the level of insect activity: oviposition, 'minimal maggot activity', 'moderate maggot activity', 'extreme maggot activity' and beetles. Oviposition occurred when adult flies laid eggs in moist areas (typically orifices) on the carcass. The extent of maggot coverage on the carcass was described in terms of 'minimal', 'moderate' and 'extreme maggot activity'. The beetle stage simply indicated the presence of beetles.

Three stages were included in the level of scavenging activity: scavenging, 'moderate scavenging' and 'extreme scavenging'. Scavenging was used to describe any small scale scavenging such as rodent activity. 'Moderate scavenging' and 'extreme scavenging' were characterized by the consumption of up to 50% and more than 50% of soft tissue, respectively.

2.4.4 *Environmentally Dependent States*

Variations in environmental factors, such as temperature, humidity, acidity and fungal or bacterial activity, can alter the typical course of baseline decomposition (Cockle, 2008). These variations can trigger the development of one or more environmentally dependent states namely, mummification, wet and dry moulding and adipocere formation. The development of these states on the remains were described in terms of the extent of formation on the remains (Cockle, 2008).

2.4.5 *Decomposition Scoring*

The Tissue Decomposition Classification System developed by Cockle (2008) was used to score the level of pig and human decomposition from photographs based on the physical attributes of decomposition (refer to Appendix A). Photographs of pig decomposition were taken each sampling day at the research site during the 2008 and 2009 summer research trials. Photographs of human decomposition were obtained from solved homicide cases in the Ottawa region from Sgt. Diane Cockle. Pig photographs were scored by the primary researcher and human photographs were scored by Sgt. Diane Cockle. It is important to note that assigning decomposition stages to a particular carcass was performed by the researcher and a level of subjectivity was required. Decomposition scores were related to accumulated degree days (ADD). ADD is the sum of the average daily temperature for a given time period. It corresponds to heat energy units required for the progression of a biological process, such as decomposition (Megyesi et al., 2005). It is a temporal measurement without the use of time and facilitates comparison of studies across geographical regions and seasons (Adlam and Simmons, 2007). ADD is a measure of accumulated temperature and does not account for other factors that affect decomposition including humidity, rainfall, presence or absence of clothing and perimortem trauma or postmortem artefacts (Megyesi et al., 2005). The use of ADD allows for a quantitative approach and thus, may provide more information regarding the relationship between decomposition and the PMI (Megyesi et al., 2005). For the human remains cases ADD was calculated using temperature data obtained from Canada's National Climate and Weather Data Archive whereas the ADD corresponding to this research was calculated using temperature data collected over the duration of the trials.

The ADD values obtained for human decomposition were visually compared to the distribution of the ADD values for the shaded and sun exposed carcasses.

2.4.6 Statistical Analysis

A Wilcoxon Rank-Sum Test was conducted to compare the range of ADD values obtained for each decomposition score and to compare the ADD values for the onset of each score for the shaded and sun exposed pig carcasses.

2.5 Soil Analysis

Due to time constraints, soil analysis was not performed on soil samples collected from shaded pig carcasses in the summer 2008 trial.

2.5.1 Gravimetric water content of soil

The gravimetric water content of soil was determined for all soil samples collected in the open land during the 2008 and 2009 summer trials. Soil samples were removed from the freezer and thawed. In the case where sufficient soil was available, only a portion of the sample was used for analysis. The remaining soil was returned to the freezer for later use, as required. Aluminum containers were weighed (M_C) prior to the addition of the wet soil samples. Subsequently, the mass of the wet soil sample and container were weighed (M_{WC}). Soil samples were dried in an oven overnight at 80°C and reweighed (dry soil sample and container) (M_{DC}). Samples were then ground with a pestle, sieved to remove small stones and plant material and stored in glass vials, pending further analysis. The gravimetric water content of the soil samples was calculated using the following equation:

$$\text{Gravimetric water content (\%)} = (M_{WC} - M_{DC}) / (M_{DC} - M_C) \times 100.$$

2.5.2 Soil pH

Soil pH was measured using the Mettler Toledo SevenEasy pH Instrument. The instrument was calibrated with solutions of pH four, seven and ten. Distilled water was

added to dried soil samples (refer to 2.5.1 *Gravimetric Water Content of Soil* for drying procedure) in disposable culture tubes in a ratio of one to five, soil to water. Samples were mixed rigorously using a vortex for 10 seconds and allowed to settle for at least five minutes. Subsequently, the pH of the soil was measured by completely immersing the pH probe into the solution, while ensuring the probe did not come into contact with the soil settled at the bottom of the tube. The instrument was allowed to stabilize before recording the pH value. All pH measurements were recorded in triplicate at 22°C.

2.5.3 Soil characterization

Three representative soil samples (10 g of control soil per research site for the forested and open land in 2008 and the open land in 2009) were dried in an aluminum container in an oven at 80°C overnight and stored in a glass vial. The samples were sent to the Agriculture and Food Laboratory at the University of Guelph in Guelph, Ontario, where soil characterization tests were performed to determine the relative amounts of gravel, sand, silt and clay in the soil, identify the soil texture and determine the electrical conductivity of the soil.

2.6 Fatty Acid Analysis

2.6.1 Reagents

The solvents N-hexane (GC Grade) and chloroform (HPLC Grade) were obtained from Fisher Scientific (Ottawa, Canada). The derivatizing agents hexamethyldisilazane (HMDS) and *N,O*-bis(trimethylsilyl)trifluoroacetamide (BSTFA) with 1% trimethylchlorosilane (TMCS), both GC Grade, were obtained from Fluka Analytical (Seelze, Germany). Trimethylchlorosilane (TMCS), also GC Grade, was obtained from Aldrich Chemistry (Steinheim, Germany).

2.6.2 Standards

Myristic acid (C14:0), Sigma Grade 99-100%, and palmitic acid (C16:0), minimum 99%, were obtained from Sigma-Aldrich (St. Louis, USA). Palmitoleic acid

(C16:1), standard for GC, was obtained from Fluka Analytical (Seelze, Germany). Stearic acid (C18:0), Grade I, ~99% capillary GC, and oleic acid (C18:1), reagent grade ~99%, were acquired from Sigma-Aldrich (St. Louis, USA). Nonadecanoic acid (C19:0), standard for GC, was obtained from Fluka Analytical (Seelze, Germany).

2.6.3 Method Optimization I: Solvents and Derivatizing Agents

Soil samples collected from the open land during the 2008 and 2009 summer trials were analyzed for fatty acid content. The methodology developed for fatty acid analysis of decomposition soil (soil samples containing decomposition fluid) was an adaptation of the methodology developed by Forbes et al. (2003) and Notter et al. (2008).

A mixed fatty acid standard was prepared containing five fatty acids presumed to be present in decomposition soil. The fatty acids used to make the fatty acid standard were myristic acid (C14:0), palmitic acid (C16:0), palmitoleic acid (C16:1), stearic acid (C18:0) and oleic acid (C18:1). Stock solutions of 1000 $\mu\text{g/mL}$ were made for each of the fatty acids. As the saturated fatty acids C14:0, C16:0 and C18:0 were obtained in powder form, 25 mg of each fatty acid was measured using a Mettler Toledo AB204-S Analytical Balance, added to a 25 mL volumetric flask and made up to volume in hexane (1 mg/mL = 1000 $\mu\text{g/mL}$). The unsaturated fatty acids C16:1 and C18:1 obtained were in liquid form at room temperature. The volume required to make a 1000 $\mu\text{g/mL}$ stock solution of the fatty acids was calculated using the required mass (25 mg) and known density of the liquids. The density of C16:1 and C18:1 is 894.0 mg/mL and 895.0 mg/mL, respectively. The following calculation was performed to determine the volume of each fatty acid required:

$$\text{Volume} = \text{Mass} / \text{Density}.$$

Therefore, 28.0 μL and 27.9 μL of C16:1 and C18:1 were added to a 25 mL volumetric flask, respectively, and made up to volume with hexane.

A ten times dilution was performed for each fatty acid and combined to make a mixed fatty acid standard with a concentration of 100 $\mu\text{g/mL}$ of each fatty acid. Appropriate dilutions were also carried out to make a series of standards ranging from

10 µg/mL to 0.001 µg/mL. One millilitre of each mixed standard (10 µg/mL to 0.001 µg/mL) was placed into a disposable screw top culture tube and 0.75 mL of hexane and 0.25 mL of HMDS were added. Samples were incubated in a Fisher Scientific Isotemp[®] Heat Block at 70°C for 15 minutes and transferred to a GC-MS vial upon cooling, followed by GC-MS analysis. A standard curve was generated; however, a ten-fold decrease in signal on the gas chromatogram was not observed (as expected) for each successive standard.

HMDS is known to be a relatively weak silylating agent and should be used with the addition of a catalyst to improve the silylation of target compounds (Little, 1999). Trimethylchlorosilane (TMCS) is a catalyst commonly added to silylating agents (Little, 1999; Halket and Zaikin, 2003). TMCS was added to HMDS (HMDS+TMCS) in a ratio of three to one HMDS to TMCS. The range of mixed standards was processed using the abovementioned procedure using HMDS+TMCS as the derivatizing agent. The fatty acids were derivatized more efficiently; however, a quantitative decrease in signal was still not observed. Consequently, the ratio of hexane and derivatizing agent were modified in an attempt to achieve optimal derivatization of the fatty acids. The amount of fatty acid standard used remained unchanged (1 mL). The original volumes of hexane and HMDS+TMCS were 0.75 mL and 0.25 mL, respectively. The volumes were altered to 0.5 mL each and to 0.25 mL hexane and 0.75 mL HMDS+TMCS. The volumes of 0.5 mL each of hexane and HMDS+TMCS yielded the greatest increase in signal with respect to the original volumes. Nevertheless, when a standard curve was generated for the standards a quantitative decrease in signal was not observed. HMDS+TMCS was, therefore, deemed an inadequate derivatizing agent for the analysis of fatty acids in hexane.

Of the common commercial reagents, BSTFA is one of the strongest silylating agents (Little, 1999). The silylating power of BSTFA is also enhanced with the addition of one to ten percent TMCS (Little, 1999). Notter et al. (2008) used BSTFA as the derivatizing agent in place of HMDS. As such, BSTFA was tested as the derivatizing agent for the analysis of fatty acids in decomposition soil. Initially, 1 mL of the 10 µg/mL fatty acid standard, 0.5 mL hexane and 0.5 mL BSTFA were tested to

determine the appropriate amount of BSTFA to add to the reaction. The initial test indicated that an excessive amount of BSTFA was being used and the volume of BSTFA was reduced to 0.2 mL per reaction; the volume of hexane was increased to 0.8 mL to compensate. This volume of BSTFA proved adequate for the derivatization of fatty acids in a 2 mL reaction. In some cases the levels of fatty acids detected were two times greater when BSTFA was used as the derivatizing agent as compared to HMDS+TMCS. However, when a standard curve was generated for the range of fatty acid standards, a quantitative decrease in signal was not observed.

Due to the inability to generate suitable standard curves the use of a different organic solvent was sought. Forbes et al. (2003) used chloroform as the organic solvent for the analysis of fatty acids in gravesoil and, therefore, was tested for use as the organic solvent in this study.

A new concentration range of fatty acid standards was prepared to better mimic the levels of fatty acids present in the decomposition soil samples as indicated by preliminary results. The following concentrations of fatty acid standards containing all five fatty acids (C14:0, C16:0, C16:1, C18:0 and C18:1) were prepared: 20 µg/mL, 10 µg/mL, 5 µg/mL, 1 µg/mL and 0.1 µg/mL. One millilitre of each fatty acid standard was added to a disposable screw top culture tube along with 0.8 mL chloroform and 0.2 mL BSTFA. The standards were incubated at 70°C for 15 minutes, allowed to cool and transferred to vials for GC-MS analysis. The standard curve that was generated yielded a quantitative decrease in signal. The correlation coefficient (r^2) values obtained for each fatty acid were greater than 0.990. Hereafter, the analysis of fatty acids was conducted using chloroform as the organic solvent and BSTFA as the derivatizing agent.

2.6.4 Method Optimization II: Fatty Acid Extraction Method and Recovery

Fatty acids contained within soil samples must be extracted prior to analysis. The fatty acid extraction procedure developed by Forbes et al. (2003) was carried out to determine the percent recovery of the method for the soil type found at the research site. Two hundred milligrams of dried control soil from one of the control sites (not containing decomposition fluid) was placed into each of five disposable screw top culture tubes.

The soil samples were spiked with 1.0 mL of the known concentrations of the mixed fatty acid standards (20 µg/mL, 10 µg/mL, 5 µg/mL, 1 µg/mL and 0.1 µg/mL) and placed in an oven at 80°C to allow the chloroform layer to evaporate. Subsequently, the fatty acids were re-suspended in 1.8 mL of chloroform and sonicated in a Fisher Scientific FS110D Ultrasonic Cleaner at room temperature for 15 minutes. Samples were centrifuged using a Fisher Scientific Centrifuge at 8,000 RPM for five minutes. The chloroform layer was drawn off and transferred to another disposable culture tube. A volume of 0.2 mL of BSTFA was added to the tubes followed by incubation in a heat block at 70°C for 15 minutes. Upon cooling, samples were analyzed by GC-MS. This method was inadequate for the extraction of fatty acids in soil from the research site as extraction efficiencies were below 10% for each fatty acid.

Three different extraction procedures were carried out to establish a method for the efficient extraction of fatty acids from the soil type used in this study. Two hundred milligrams of dried control soil was placed into five disposable screw top culture tubes and spiked with 1.0 mL of each concentration of fatty acid standard (50 µg/mL, 40 µg/mL, 30 µg/mL, 20 µg/mL, 10 µg/mL, 5 µg/mL, 1 µg/mL and 0.1 µg/mL). The tubes were placed in an oven at 80°C to allow the chloroform to evaporate. Subsequently, the fatty acids were re-suspended in 1.8 mL of chloroform. To extract the fatty acids, one set of samples was incubated in a heat block at 70°C for one hour and mixed by pulse vortexing every 15 minutes. The other two sets were either sonicated at room temperature for one hour and mixed by pulse vortexing every 30 minutes or sonicated at 55°C for one hour and mixed by pulse vortexing every 30 minutes. All samples were centrifuged at 8,000 RPM for five minutes. The chloroform layer was drawn off and transferred to another disposable culture tube followed by the addition of 0.2 mL of BSTFA. Samples were incubated at 70°C for 15 minutes in a heat block. Upon cooling, samples were analyzed by GC-MS. Samples sonicated at 55°C for one hour demonstrated the most efficient extraction of fatty acids, yielding percent recoveries of 95.0-115.2% for soil samples spiked with 10-50 µg/mL fatty acid standard (Table 1). For soil spiked with 0.1-5 µg/mL fatty acid standard, percent recoveries were substantially variable. However, this method was able to extract lower levels of fatty acids when compared to the other

methods. Therefore, this method was used to process the soil samples obtained over the course of the research study.

Table 1. Percent concentration of fatty acids recovered from spiked soil samples.

Standard ($\mu\text{g/mL}$)	% Recovery of free fatty acid standard														
	C14:0			C16:0			C16:1			C18:0			C18:1		
	Mean \pm SD	CV		Mean \pm SD	CV		Mean \pm SD	CV		Mean \pm SD	CV		Mean \pm SD	CV	
50	95.3 \pm 3.3	3.4		105.8 \pm 4.5	4.3		95.0 \pm 21.0	22.1		112.2 \pm 2.4	2.1		109.3 \pm 3.6	3.3	
40	96.4 \pm 2.6	2.7		101.5 \pm 2.5	2.5		108.2 \pm 3.1	2.9		110.0 \pm 4.9	4.5		112.6 \pm 1.1	1.0	
30	101.0 \pm 1.6	1.6		110.1 \pm 5.8	5.3		113.2 \pm 5.8	5.1		109.8 \pm 8.3	7.6		112.2 \pm 1.7	1.5	
20	112.3 \pm 1.3	1.2		112.0 \pm 4.6	4.1		110.4 \pm 7.6	6.9		115.2 \pm 6.0	5.2		110.9 \pm 4.6	4.1	
10	98.4 \pm 5.6	5.7		113.1 \pm 9.2	8.2		111.2 \pm 4.1	3.7		108.1 \pm 7.5	7.0		108.8 \pm 10.0	9.2	
5	28.6 \pm 11.4	39.8		62.5 \pm 28.5	45.5		51.7 \pm 6.5	12.6		65.4 \pm 35.1	53.7		65.6 \pm 9.7	14.8	
1	-	-		39.7 \pm 66.2	166.9		-	-		88.1 \pm 74.1	84.1		25.0 \pm 15.3	61.0	

§C14:0 = myristic acid, C16:0 = palmitic acid, C16:1 = palmitoleic acid, C18:0 = stearic acid, C18:1 = oleic acid;

§§SD = standard deviation; CV = coefficient of variation

2.6.5 Sample Processing

Fatty acid analysis of soil was performed on soil samples collected during the 2008 and 2009 summer research trials. However, due to time constraints only samples collected from the open land (sun exposed carcasses) were analyzed. The following procedure was carried out for each soil sample. Two hundred milligrams of dried soil was placed into a disposable screw top culture tube and 1.75 mL of chloroform was added to the tube. Samples were mixed by pulse vortexing. Samples were sonicated at 55°C for one hour then mixed by pulse vortexing at 30 minutes. Subsequently, samples were centrifuged at 8,000 RPM for five minutes. The chloroform layer was drawn off and transferred to another disposable culture tube. Prior to transfer, appropriate dilutions were performed, as necessary, based on the colour of the chloroform layer. Preliminary studies indicated high levels of fatty acids in samples in which the chloroform layer possessed a yellow to dark brown colour. Samples that required dilution were typically diluted 10, 100 or 1000 times. Subsequently, 0.050 mL (50 µL) of 100 µg/mL internal standard (C19:0) and 0.200 mL (200 µL) of BSTFA were added to the samples and incubated at 70°C for 15 minutes. Upon cooling, samples were transferred to GC-MS vials and either immediately analyzed by GC-MS or stored in a -20°C freezer pending analysis by GC-MS. If GC-MS results indicated that samples were too concentrated, the samples were re-extracted, diluted appropriately and re-analyzed. Soil samples from the 2008 research trial were processed in triplicate. Due to the number of samples collected in the 2009 research trial, samples were processed only once.

2.6.6 GC-MS Analysis

All analyses were performed on a Varian 450-GC Gas Chromatograph coupled with a Varian 240-MS Ion Trap Mass Spectrometer. Samples were injected into the gas chromatograph with a Varian PAL Autosampler. A 1 µL aliquot of the sample was analyzed on a VF-23ms (Varian Inc. Canada, Mississauga, Canada) high polarity fused silica capillary column (30 m x 0.25 mm x 0.25 µm). The carrier gas used was helium at a constant column flow of 1.0 mL/minute. The initial column temperature was 50°C where it was held for two minutes. The temperature was then increased at a rate of 15°C/minute to 150°C and held for one minute. Subsequently, the temperature was

increased at a rate of 10°C/minute to 220°C where it was held for 3.33 minutes. The total run time was 20 minutes. All samples were injected in the splitless mode. The analysis was carried out in total ion count (TIC) mode. The ion trap mass spectrometer employed electron ionization. It was held at 250°C and activated at six minutes from the commencement of the run to circumvent the detection of the solvent and excess derivatizing agent. The target TIC was 20,000 counts and the scan time was 0.50 seconds/scan. The scan range analyzed was 50 to 450 mass to charge ratio (m/z). Peaks corresponding to trimethylsilyl (TMS) fatty acid esters were identified based on comparison of their retention time to the fatty acid standards and mass spectra against the NIST MS Search 2.0 Library. The GC-MS output provides the peak area for the compound of interest, a measure of the abundance of the compound. The peak area ratio (PAR) was calculated by dividing the peak area of the fatty acid of interest by the peak area of the internal standard (Area/IS Area). The internal standard used in this study was nonadecanoic acid (C19:0). The PAR was used as a measure of the relative abundance of the fatty acids extracted from the soil to allow for statistical analysis. Furthermore, the 'Detected CDI Perimeter' was determined based on the furthest distance from the carcasses at which fatty acids were detected above basal levels in the soil.

2.6.7 Detection Parameters and Reproducibility

A range of mixed fatty acid standards were prepared in order to determine the detection limits of the GC-MS: 100 µg/mL, 50 µg/mL, 40 µg/mL, 30 µg/mL, 20 µg/mL, 10 µg/mL, 5 µg/mL, 1 µg/mL, 0.1 µg/mL and 0.01 µg/mL. Standards were processed using the procedure outlined above (2.6.4 *Method Optimization II: Fatty Acid Extraction Method and Recovery*). The limit of detection (LOD), limit of quantitation (LOQ) and limit of saturation (LOS) were determined to be 0.1 µg/mL, 1.0 µg/mL and 50 µg/mL, respectively.

The reproducibility of the GC-MS instrument was measured by injecting the same sample (one of the extracted experimental soil samples) into the GC-MS ten times. The samples were analyzed under the same conditions and on the same day. The coefficient of variation (CV) was determined to be 11.0%.

2.6.8 Statistical Analysis

Statistical analyses were performed using VSN International Genstat 12th Edition. Two-way Analysis of Variance (ANOVA) tests were performed on the data.

2.7 Diffusion Model

2.7.1 Diffusion Model Test

A diffusion model test was carried out on undisturbed soil collected from the research site (refer to 2.3 *Research Trial 2 – Summer 2009* for procedure) to determine if soil properties required for the diffusion model could be established; this was achieved by determining the rate at which a fixed amount of fluid diffused through the soil. A cylindrical polypropylene tube with an internal diameter of 1.5 cm was opened at both ends and placed firmly on the soil surface. Five millilitres of Ward's Drip and Projected Blood (Rochester, USA) (used to mimic blood for blood spatter analysis) was injected into the top end of the tube onto the soil surface using a repeater pipette. The imitation blood was used in this test to mimic decomposition fluid. The time required for the 5 mL of transfer blood to diffuse through the soil and thus out of the tube was recorded. A cross-section of the soil was subsequently photographed and the path measured in order to provide more detail about the passage of the transfer blood through the soil.

The gravimetric water content of soil was measured for the soil used in the diffusion model test (refer to 2.5.1 *Gravimetric Water Content of Soil* for procedure). As liquid was introduced into the soil environment during the test, the water content of the soil was measured from an area in close proximity to the area tested.

2.7.2 Derivation of the Diffusion Model

A diffusion model was developed to predict the development of the cadaver decomposition island (CDI) in soil over time and was developed in conjunction with Dr. C. Sean Bohun (University of Ontario Institute of Technology). As decomposition fluid leaches from decomposing remains into the surrounding soil environment a CDI is

formed, characterized by a dark stain surrounding the remains. For this model, the soil was considered to be a matrix of solids with voids that can contain either gas (e.g. air) or fluid (e.g. water). The structure of the soil can be described in terms of the moisture content, the porosity or the saturation. All of these are functions of the radius, r , depth, z , and possibly time, t . Moisture content, θ , is the volume of fluid in a reference volume of soil divided by the reference volume whereas porosity, ϕ , is the volume of voids in the soil divided by the reference volume. Saturation, S , is defined as the volume of fluid divided by the volume of voids in the soil. To clarify these concepts refer to Figure 3.

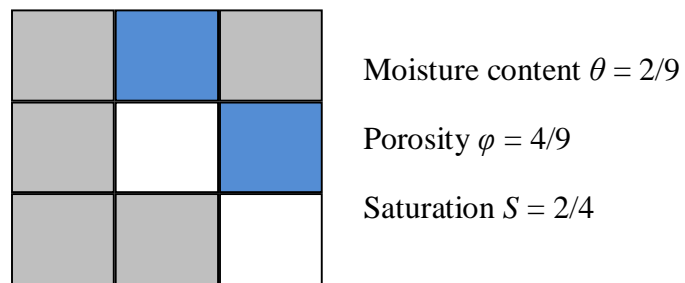


Figure 3. Schematic of soil structure. Grey boxes indicate the soil matrix, blue boxes indicate void space occupied by fluid and white boxes indicate empty void space.

Several features were considered when developing the model (personal communication with Dr. C. Sean Bohun). The first major structural assumption was the soil matrix does not deform when fluid passes through it. Also, the decomposition fluid was considered to be similar to water with respect to viscosity (i.e. same order of magnitude). Viscosity, μ , is measured in Poise (1 Poise = 0.1 Pa·s) and the viscosity of water (μ_{H_2O}) is equal to 10^{-3} Pa·s at standard temperature and pressure. The permeability of the soil was also considered for the model. The permeability of soil is the capacity of soil to transmit fluid through pore spaces (Bear and Bachmat, 1990). It can be viewed as the effective cross-sectional area of a typical conduit (channel) through the material. In lay terms, permeability can be described as the ease at which fluid can be driven through a given material. The typical units of permeability are the darcy (1 darcy = 9.87×10^{-13} m²). Soil permeability, κ , is a strong function of moisture content, θ , of the soil and for the ease of computation it was assumed that

$$\kappa(\theta) = \kappa_0 \left(\frac{\theta}{\theta_0}\right)^m \quad (2.1)$$

where κ_0 , θ_0 and m are characteristic values for a given soil type. The characteristic soil permeability was assumed to be approximately $\kappa_0 = 10^{-12} \text{ m}^2$. Another component considered for the model was the capillary pressure, P_C , which is also a function of the moisture content of the soil. This pressure reflects the ability of soil to retain moisture due to adhesion (attraction of fluid molecules to the walls of the pores or soil matrix) and cohesion (intermolecular attraction of fluid molecules). Figure 4 illustrates the behaviour of P_C with moisture content, θ . For the purposes of this work, it was assumed that the model remains in the plateau region or cadaver regime (highlighted in red in Figure 4) and therefore,

$$P_C(\theta) = \alpha \left(\frac{\theta - \theta_0}{\theta_0}\right) + \beta \quad (2.2)$$

where α and β are constants that depend on the soil type.

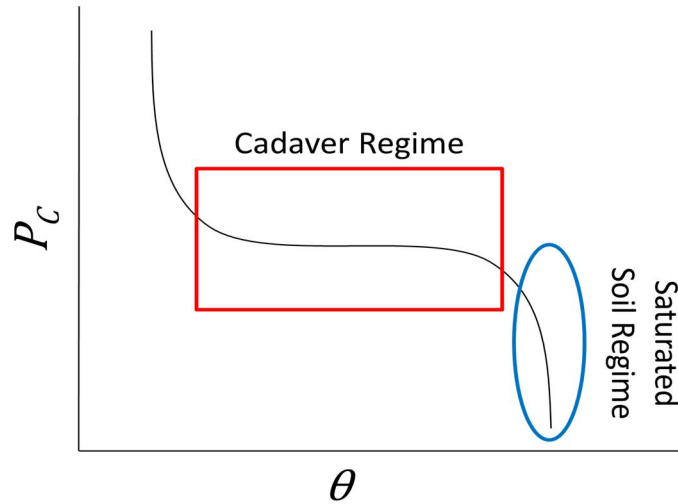


Figure 4. The capillary pressure, P_C , as a function of the moisture content, θ . The cadaver regime is highlighted in red and the saturated soil regime is highlighted in blue.

As seen in Figure 4, the capillary pressure is high in soils with low moisture content and decreases sigmoidally with increasing soil moisture content. Capillary pressure declines rapidly in saturated soils.

The derivation of the diffusion model began with the conservation of fluid for a porous medium

$$\frac{\partial \theta}{\partial t} + \nabla \cdot \left(\frac{\vec{Q}}{A} \right) = 0. \quad (2.3)$$

Since the right hand side of the equation is zero it was presumed that all of the decomposition fluid leaches into the surrounding soil and is not affected by evaporation or precipitation. This equation stipulates that the time rate of change of the moisture content at a point is governed solely by the flow of fluid through the boundaries of the control volume (Figure 5).

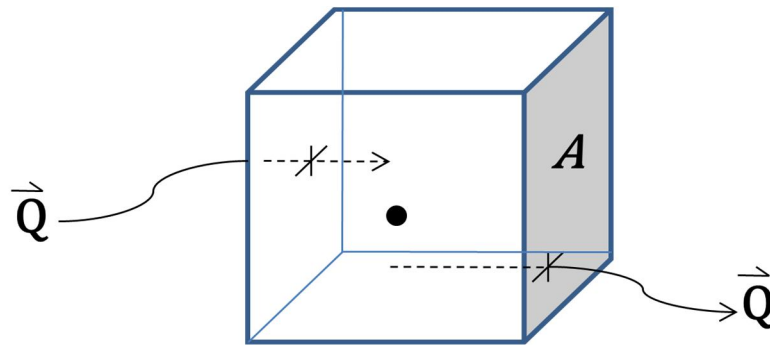


Figure 5. Schematic of fluid flow through the boundaries of the control volume with respect to the moisture content at a point.

The flux of fluid per area (volume per time per area) was assumed to be driven by differences in pressure and gravitational forces. Because of this, the flux was assumed to be

$$\frac{\vec{Q}}{A} = -\frac{\kappa}{\mu} (\nabla P - \rho_f g \hat{k}) \quad (2.4)$$

where the pressure

$$P = \rho_s g z - P_c(\theta) \quad (2.5)$$

is a combination of the pressure due to the weight of the soil above a point and the capillary pressure at a point.

Putting all of these factors together gives the following porous medium equation used to simulate the diffusion model

$$\frac{\partial \theta}{\partial t} - Am\theta^{m-1} \frac{\partial \theta}{\partial z} - B\nabla \cdot (\theta^m \nabla \theta) = 0 \quad (2.6)$$

where,

$$A = \frac{g\kappa_0}{\mu\theta_0} (\rho_s - \rho_f) \frac{T}{L}, \quad B = \frac{\alpha\kappa_0}{\mu\theta_0} \frac{T}{L^2}$$

and L and T are a characteristic length and time, respectively. The first term in the equation, $\frac{\partial \theta}{\partial t}$, is used to describe the time rate of change of the moisture content at a point. Advection, the bulk motion of fluid, is described by the second term, $-Am\theta^{m-1} \frac{\partial \theta}{\partial z}$, while the diffusion of fluid through the soil is described by the third term in the equation, $-B\nabla \cdot (\theta^m \nabla \theta)$.

Table 2. Summary of characteristic parameters of the diffusion model. The value for κ_0 ¹ was taken from (Tzimopoulos and Sakellarios-Makrantonaki, 1996) and θ_0 , α and β were taken from (Assouline and Tartakovsky, 2001).

Property	Symbol	Value
Standard gravity	g	9.81 m·s ⁻²
Permeability	κ_0	2.21x10 ⁻¹³ m ²
Soil density	ρ_s	1,500 kg·m ⁻³
Fluid density	ρ_f	1,000 kg·m ⁻³
Viscosity	μ	10 ⁻³ Pa·s
Moisture content	θ_0	0.38
Capillary pressure parameters	α	21,000 Pa
	β	6,900 Pa

¹

$$\kappa_s = \left(\frac{0.78 \text{ cm}}{\text{hr}} \right) \text{ so that, } \kappa_0 = \left(\frac{0.78 \text{ cm}}{\text{hr}} \right) \left(\frac{1 \text{ m}}{100 \text{ cm}} \right) \left(\frac{1 \text{ hr}}{3,600 \text{ s}} \right) \left(\frac{\mu}{\rho_f g} \right) = 2.21 \times 10^{-13} \text{ m}^2.$$

Advection can be neglected if A is much smaller than B ($A \ll B$) which corresponds to

$$L \ll \frac{\alpha}{g(\rho_s - \rho_f)} = \frac{21\,000 \text{ Pa}}{(9.81 \text{ ms}^{-2})(1500 \text{ kg} \cdot \text{m}^{-3} - 1000 \text{ kg} \cdot \text{m}^{-3})} = 4.3 \text{ m}$$

which is true as per the CDI measurements taken at the research site during the 2009 trial (refer to Table 6). Therefore, advection can be neglected.

T was chosen to be 23 hours so that $B = 1$. Therefore, for the time and length scales of this process the advection term can be ignored, leaving the porous medium equation

$$\frac{\partial \theta}{\partial t} - \nabla \cdot (\theta^m \nabla \theta) = 0. \quad (2.7)$$

This equation was used to simulate the development of the CDI in soil over time. Note that $T = 1$ corresponds to 23 hours and distances of one correspond to 1 m. Soil type is characterized by the quantity m (refer to Tzimopoulos and Sakellarios-Makrantonaki, 1996 for typical values).

Chapter 3 – Decomposition Scoring

3.1 Climatic Conditions

The temperature, relative humidity and precipitation were measured at each research area for the duration of each trial. Figure 6 displays the average daily temperatures and precipitation amounts for the forested land for each experimental day of the 2008 summer trial. The average daily temperature during the trial was 18.5°C. The average maximum and minimum temperatures were 23.4°C and 14.5°C, respectively. A total of 227.0 mm of rain fell over the course of the trial. In addition, the average relative humidity was 84.4%.

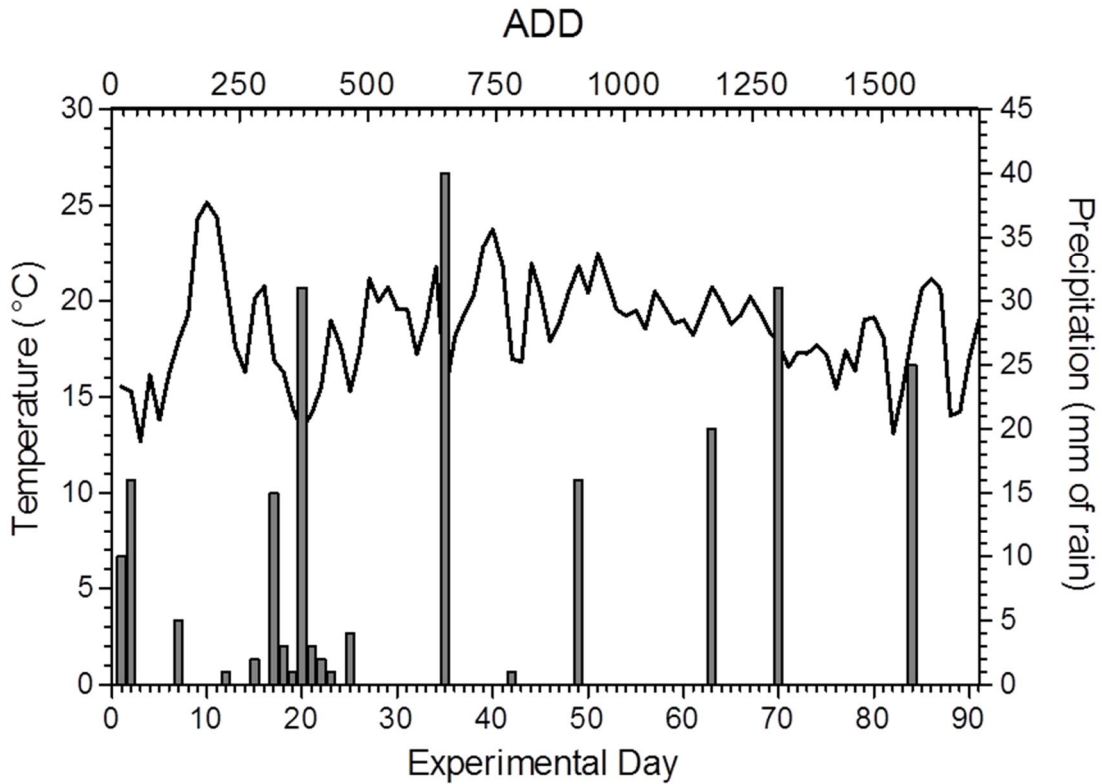


Figure 6. Average daily temperatures and precipitation amounts for the forested land of the summer 2008 trial. Line represents temperature and bars represent precipitation.

The average daily temperatures and precipitation amounts for the open land of the summer 2008 trial are shown for each experimental day in Figure 7. The average daily temperature was 20.0°C, with an average daily maximum and minimum of 26.8°C and 14.7°C, respectively. The total precipitation was 201.5 mm of rain and the average relative humidity was 83.5%.

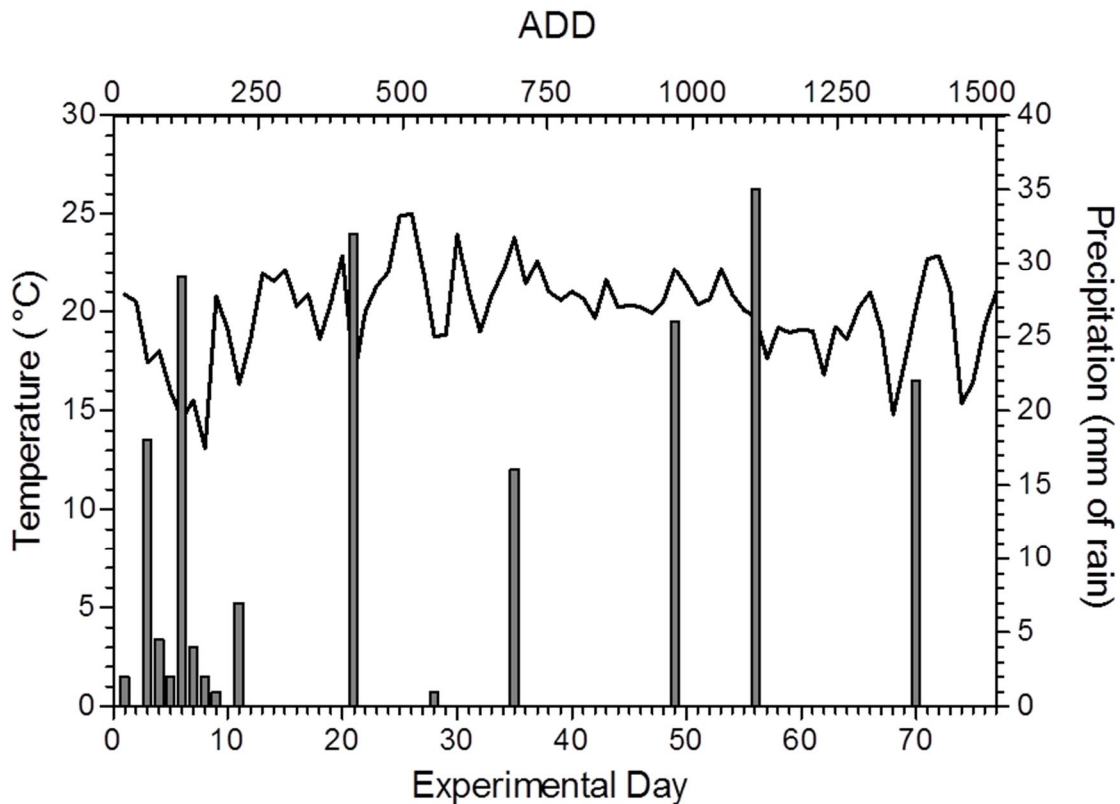


Figure 7. Average daily temperatures and precipitation amounts for the open land of the summer 2008 trial. Line represents temperature and bars represent precipitation.

The average daily temperatures and precipitation amounts for the open land of the summer 2009 trial are illustrated for each experimental day (Figure 8). The average daily temperature was measured to be 20.5°C. The average daily maximum temperature was 28.0°C whilst the average daily minimum temperature was 15.1°C. The amount of precipitation that fell over the course of the study was 79.5 mm of rain; however, the majority of precipitation fell during the second half of the trial. Furthermore, the average relative humidity was 80.1%.

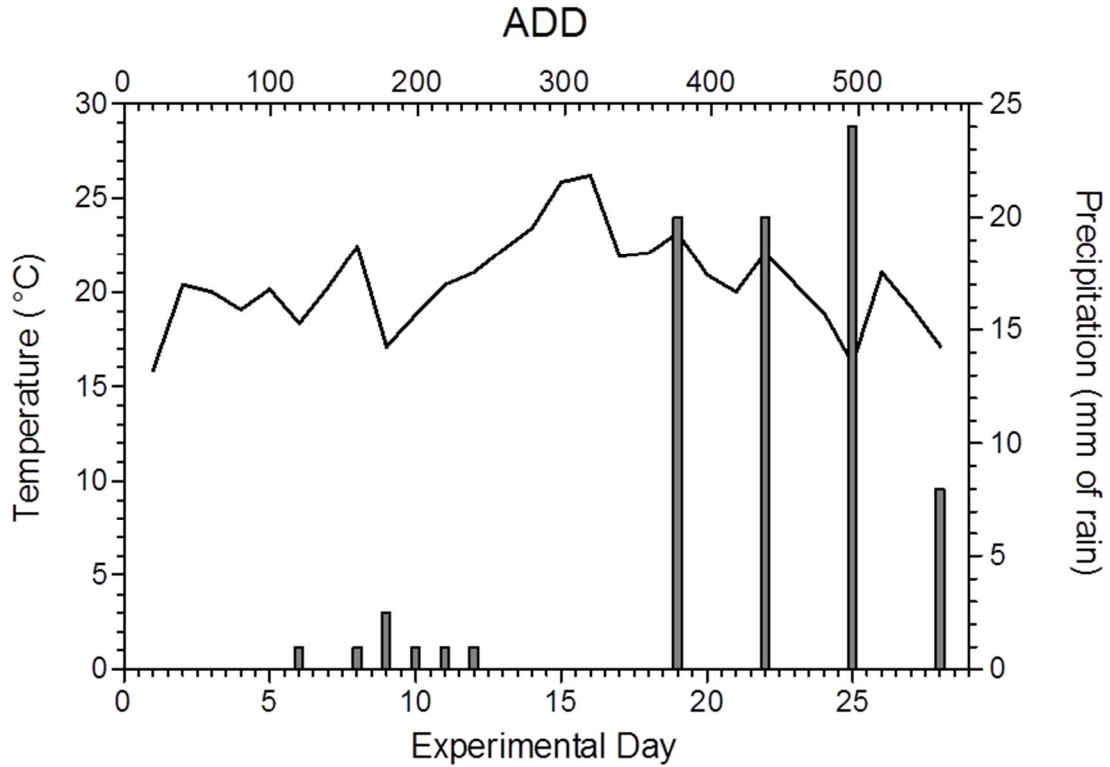


Figure 8. Average daily temperatures and precipitation amounts for the open land of the summer 2009 trial. Line represents temperature and bars represent precipitation.

Overall, the average daily temperature was comparable for the open land of both summer trials. Conversely, the average daily temperature was approximately 2.0°C lower for the forested land during the 2008 trial. The open land of the 2009 trial exhibited the highest average maximum temperature; specifically, it was 4.6°C above the average maximum temperature of the 2008 forested land trial. The average minimum temperatures and relative humidity were similar for each experimental site. In general, less rain fell during the 2009 trial compared to the 2008 trial.

3.2 Decomposition Stages

Decomposition stages are described in terms of the Tissue Decomposition Classification System (refer to Appendix A) and each stage observed is referred to in square brackets.

3.2.1 Summer 2008 Trial – Shaded Pig Carcasses

At the commencement of the study (0.0 ADD) a purple discolouration was present on the abdomen of each pig carcass (Figure 9a). This area was identified as livor mortis and was indicative of the ‘first visible change’ [1]. Furthermore, rigor mortis was not observed. The ‘first colour change’ [3] was observed by 30.9 ADD. A green area was visible on the abdomen (Figure 9b). Oviposition by arthropods (Order: Diptera) was initially observed in the mouth and eyes of each pig carcass at 107.6 ADD. By 126.9 ADD, beetles (Order: Coleoptera) were observed in these same areas; further oviposition was seen along the dorsal side of each carcass. ‘Minimal’ to ‘moderate maggot activity’ was noted from 151.2 ADD up to and including 200.7 ADD. ‘Full bloat’ [4] was reached by 151.2 ADD in one carcass and 176.3 ADD in another. Figure 9c is representative of the complete distension of a carcass; however, the putrefactive colour changes typically associated with the bloat stage in humans were not apparent. The ‘post bloat’ [5] stage was seen in only one carcass at 239.3 ADD. At 176.3 ADD the ‘first sign of bone’ [6] was observed in one of the three carcasses at the same time that the full bloat [4] stage was reached (Figure 9d). The other two carcasses reached stage [6] by 275.7 and 239.3 ADD. Bone was first exposed in the head region of each carcass. ‘Extreme maggot activity’ was most evident during this stage as large maggot masses covered the ventral side of the carcasses (Figure 9e). Browning tissue is also illustrated on the hip of the carcass in Figure 9e. It was also during this stage that much of the decomposition fluid leached from the carcasses into the surrounding soil. Total desiccation of skin and tissue occurred by 275.7 ADD in each carcass. The ‘more than half of bone exposed’ [7] stage was reached by 371.5, 387.1 and 456.3 ADD in the carcasses. Mummified skin and tissue concealed bones of the vertebral column in the carcasses (Figure 9f). The ‘no visible changes’ [0], ‘first tissue change’ [2] and ‘total skeletonization’ [8] stages were

not observed for the shaded carcasses in this trial. Due to the presence of leaf litter on the soil surface the CDI was not clearly defined for these carcasses.

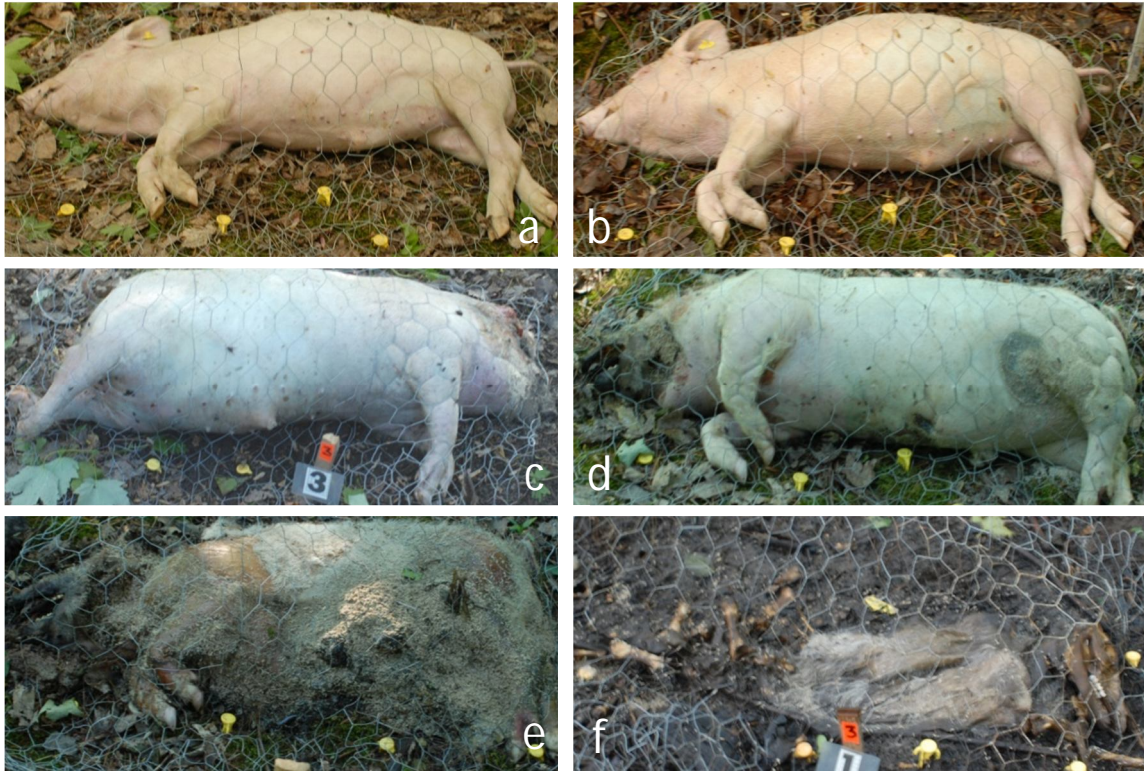


Figure 9a-f. Representative photographs of pig carcasses taken in the forested land at the Technical and Protective Operations Facility in Ottawa, Ontario, Canada during the 2008 summer trial. (a) first visible change (b) first colour change (c) full bloat (d) first sign of bone (e) extreme maggot activity (f) more than half of bone exposed.

3.2.2 Summer 2008 Trial – Sun Exposed Pig Carcasses

‘No visible changes’ [0] were observed at 0.0 ADD and the carcasses had not cooled to ambient temperature (Figure 10a). A small amount of feces were protruding from the anus of each carcass. At 20.9 ADD the ‘first colour change’ [3] and onset of abdominal swelling were evident; blackened areas were visible in the abdomen (Figure 10b). Oviposition was also observed in the mouth and anus of each carcass. The ‘full bloat’ [4] stage was characterized by the complete distension of the carcasses and a greenish-black hue in the abdominal region (Figure 10c). These features were visible at

58.9 ADD in two of the three carcasses and at 76.9 ADD in the other carcass. 'Minimal' to 'moderate maggot activity' was noted from 41.4 ADD up to and including 123.0 ADD. The 'first sign of bone' [6] was also observed at 123.0 ADD. Furthermore, the mummification of tissue surrounding the head region and the leaching of decomposition fluid from the carcasses into the surrounding environment were apparent (Figure 10d). The leaching of decomposition fluid into the surrounding environment and 'extreme maggot activity' were most prominent during this stage. In Figure 10e, maggot masses covered the entire carcass and frothing produced by the maggot activity was visible in the area surrounding the carcass, forming the CDI. The onset of stage [7] ('more than half of bone exposed') occurred at 176.0 ADD in one carcass and at 192.4 ADD in the other two carcasses. The bones of the skull and extremities were completely exposed whilst those of the core region were partially covered by dried skin, tissue and bristles (Figure 10f). Moreover, scavenging was suspected as elements of a skull were located a few metres away from one of the carcasses. The stages of 'first visible change' [1], 'first tissue change' [2], 'post bloat' [5] and 'total skeletonization' [8] were not observed in any of the carcasses on the sampling days.

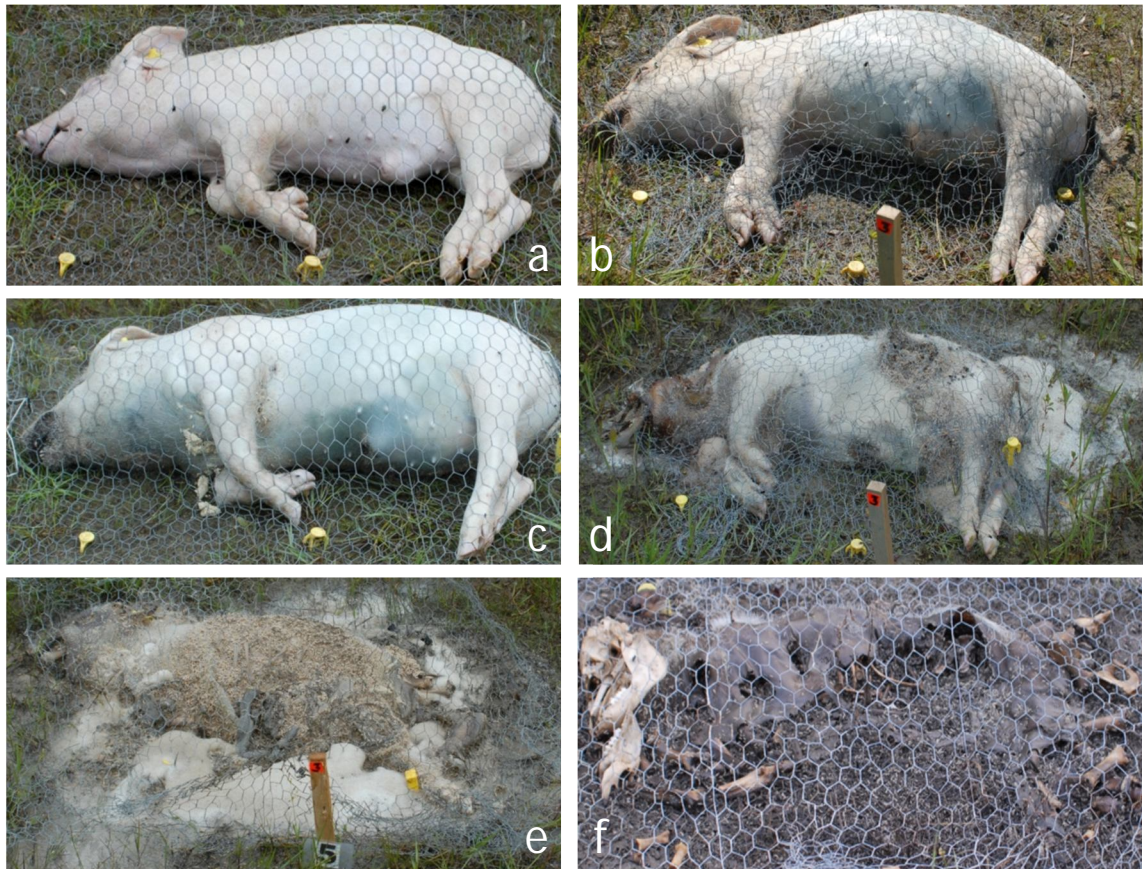


Figure 10a-f. Representative photographs of pig carcasses taken in the open land at the Technical and Protective Operations Facility in Ottawa, Ontario, Canada during the 2008 summer trial. (a) no visible change (b) first colour change (c) full bloat (d) first sign of bone (e) extreme maggot activity (f) more than half of bone exposed.

3.2.3 Summer 2009 Trial – Sun Exposed Pig Carcasses

At the commencement of the trial (0.0 ADD) ‘no visible changes’ [0] were observed and the carcasses had not cooled to ambient temperature (Figure 11a). However, contusions were visible on the ears of each carcass (Figure 11a inset). It was not determined whether the contusions were caused by antemortem or perimortem trauma. By 15.9 ADD, livor mortis, a characteristic seen in stage [1], was visible in the abdominal area and neck region of the carcasses (Figure 11b). Furthermore, oviposition was noted in the mouth and anus of each carcass. The browning of tissue in the abdomen and extremities and the onset of abdominal bloating (‘first colour change’ [3] stage) were observed at 36.3 ADD (Figure 11c). Two of the three carcasses were in ‘full bloat’ [4] at

56.3 ADD and the other carcass was in 'full bloat' [4] at 75.3 ADD. Scavenging was suspected as puncture lesions were observed primarily in the abdominal region (Figure 11d). Small strips of tissue (most likely intestines) were located adjacent to one of the carcasses (Figure 11d white arrow). Blackening of the abdominal tissue was also apparent. In another carcass, the accumulation of gases during this stage caused the expulsion of the intestines from the abdomen (Figure 11e). 'Minimal' to 'moderate maggot activity' was observed from 36.3 ADD up to and including 134.0 ADD. The 'first sign of bone' [6] appeared in two of the carcasses at 113.8 ADD and in the other at 95.5 ADD. Several rib bones and bones of the skull and extremities are exposed in Figure 11f. During stage [6], 'extreme maggot activity' and the leaching of decomposition fluid were extensive in each carcass (Figure 11f). The 'more than half of bone exposed' [7] stage was apparent in two of the three carcasses; the onset occurred by 461.6 ADD in one carcass and at 517.2 ADD in the other. 'Total skeletonization' [8] was observed in the remaining carcass by 517.2 ADD. The entire skeleton was exposed and the CDI was apparent in the surrounding soil (Figure 11g). First tissue change [2] and post bloat [5] stages were not observed in this research trial.

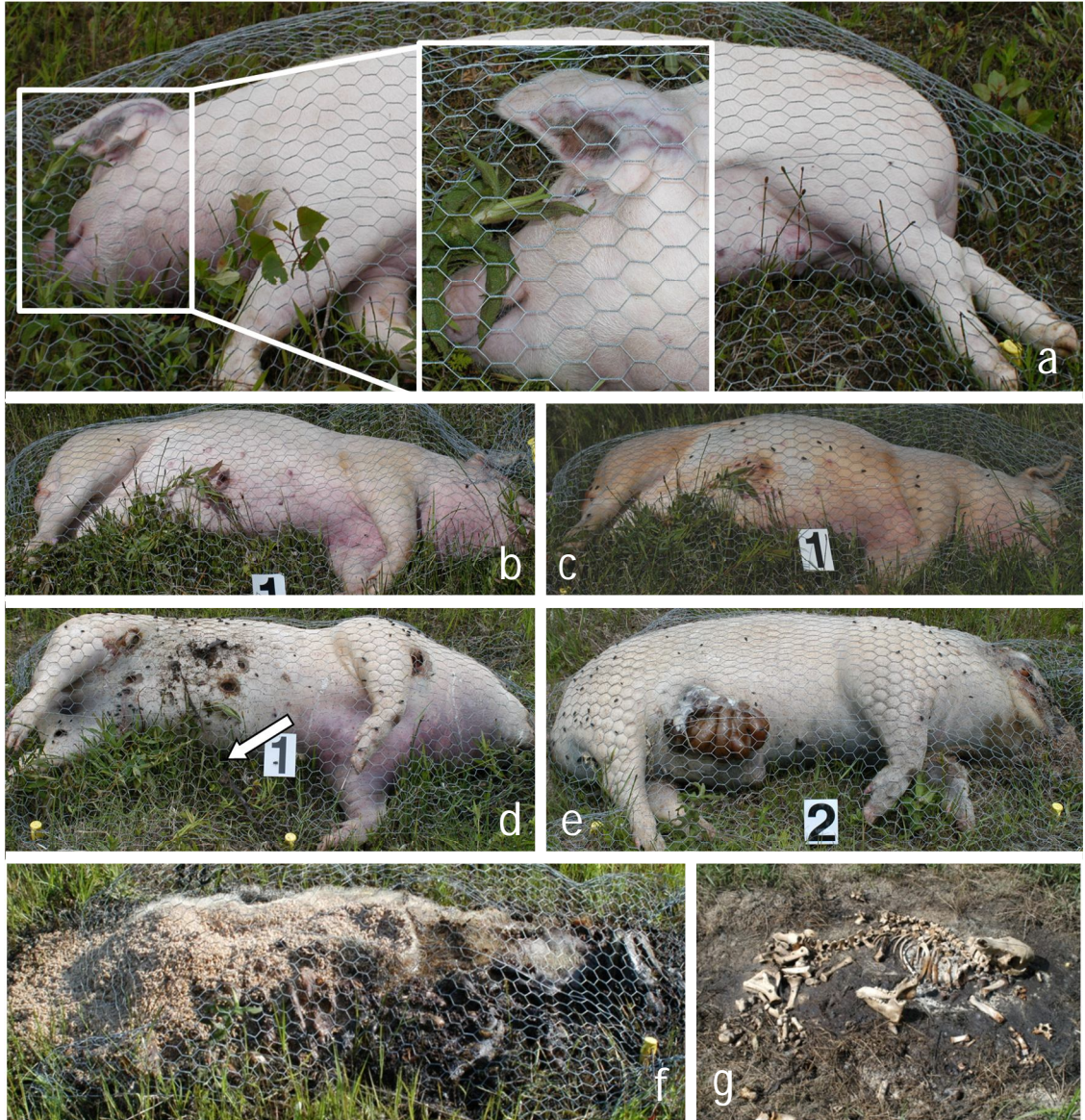


Figure 11a-g. Representative photographs of pig carcasses taken in the open land at the Technical and Protective Operations Facility in Ottawa, Ontario, Canada during the 2009 summer trial. (a) no visible change. Inset: contusion on ear (b) first visible change (c) first colour change (d) puncture lesions on carcass. White arrow: strip of tissue (e) expulsion of intestine from abdomen (f) first sign of bone (g) total skeletonization and CDI.

3.3 Decomposition Scoring

Photographs of pig carcasses decomposing in the forested land (shaded pig carcasses) and open land (sun exposed pig carcasses) at the research site during the 2008 and 2009 studies were scored using the Tissue Decomposition Classification System (refer to Appendix A). Photographs of human remains from solved homicide cases were also scored using the scoring system to determine the relationship of visible attributes of human and pig decomposition. Due to the quantitative nature of this study the decomposition stages of the classification system will be referred to as the decomposition score; however, the terms stage and score are interchangeable.

3.3.1 Comparison of Shaded and Sun Exposed Pig Carcasses

The median ADD values obtained for the shaded and sun exposed pig carcasses for each decomposition score were compared to determine if there was a significant difference. Figure 12 illustrates the median ADD values with the range for each decomposition score observed for both sets of carcasses. A Wilcoxon Rank-Sum (Mann-Whitney) Test was conducted on the unpaired, nonparametric data to compare the median ADD values for each score of the shaded and sun exposed carcasses. A comparison of ADD values was carried out only for decomposition scores (representative of decomposition stages) which were observed in both shaded and sun exposed carcasses. Hence, a comparison was not conducted on decomposition scores [0], [2], [5] and [8] due to a lack of data.

The median tendencies for decomposition score [1] for shaded and sun exposed pigs carcasses were 7.8 and 15.9 ADD, respectively; the distributions in the two groups were significantly different (Mann-Whitney $U = 0$, $n_{Shade} = 6$, $n_{Sun} = 3$, $p = 0.012$). For decomposition score [3] the median tendencies were 73.5 and 36.3 ADD for shaded and sun exposed carcasses, respectively. Due to the fact that the sample size for both sets of carcasses is greater than eight ($n_{Shade} = 23$ and $n_{Sun} = 11$), the data has approximately a standard normal distribution (Zwillinger and Kokoska, 2000) where $Z = -3.55$ and $p = 0.0004$, thus indicating that the medians were different in the two groups. The median tendencies for decomposition score [4] were 200.7 and 76.9 ADD for shaded and

sun exposed carcasses, respectively. There is evidence to suggest the distributions in the two groups were significantly different (Mann-Whitney $U = 0$, $n_{Shade} = 7$, $n_{Sun} = 18$, $p < 0.001$). For shaded and sun exposed carcasses with a decomposition score of [6] the median tendencies were 313.4 and 176.0 ADD, respectively. The data approximates a standard normal distribution due to the sample sizes ($n_{Shade} = 31$ and $n_{Sun} = 47$) where $Z = 4.48$ and $p = 7.57 \times 10^{-6}$. There is strong evidence to suggest the medians were different. For decomposition score [7] the median tendencies were 773.7 and 574.6 ADD for shaded and sun exposed pig carcasses, respectively. The data approximates a standard normal distribution as the samples sizes were $n_{Shade} = 45$ and $n_{Sun} = 45$, where $Z = 1.90$ and $p = 0.057$; thus, indicating that the medians were not significantly different. This result is contrary to all other decomposition score datasets compared.

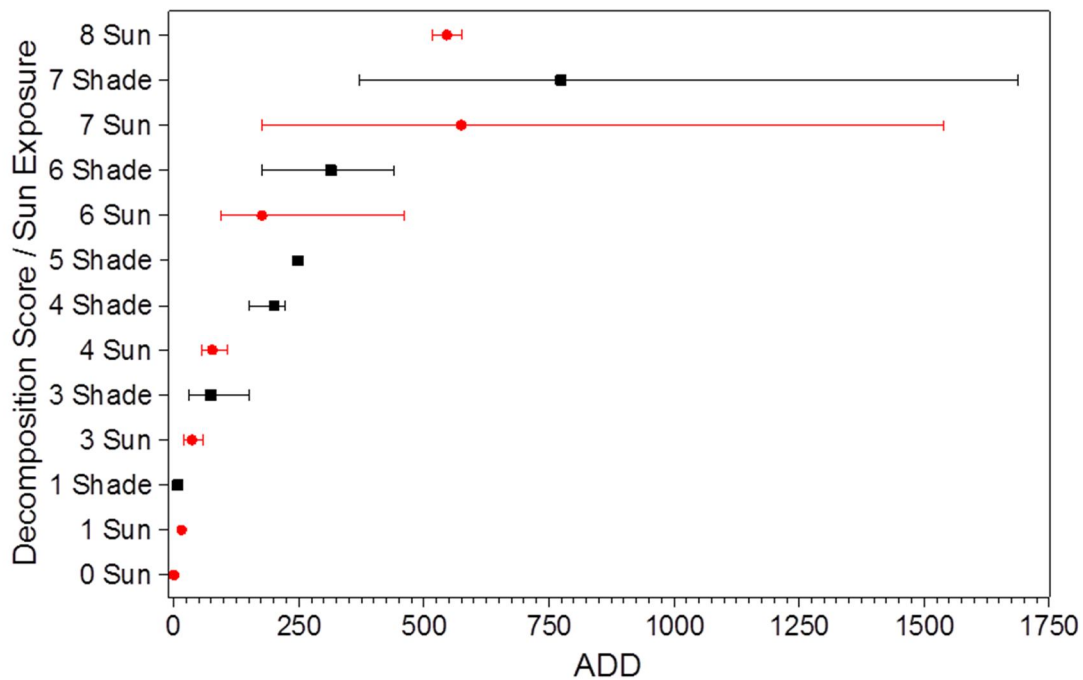


Figure 12. Median ADD values with the range for decomposition scores observed in shaded (■) and sun exposed (●) pig carcasses of the 2008 and 2009 summer trials.

Figure 13 portrays the median ADD value for the onset of decomposition scores observed in the shaded and sun exposed pig carcasses of both trials. Again, a comparison of the decomposition scores [0], [2], [5] and [8] for the shaded and sun exposed pig

carcasses was not conducted. For the onset of decomposition score [1] the median tendencies for shaded and sun exposed carcasses were 0.0 and 15.9 ADD, respectively. There is little evidence to suggest the medians were different (Mann-Whitney $U = 0$, $n_{Shade} = 3$, $n_{Sun} = 3$, $p = 0.050$). The median tendencies for the onset of decomposition score [3] for shaded and sun exposed carcasses were 30.9 and 28.6 ADD, respectively. There was no significant difference between the medians of the two groups (Mann-Whitney $U = 9$, $n_{Shade} = 3$, $n_{Sun} = 6$, $p = 0.548$). For the onset of decomposition score [4] the median tendencies were 163.7 and 58.9 ADD for the shaded and sun exposed pig carcasses. The medians were significantly different for the two groups (Mann-Whitney $U = 0$, $n_{Shade} = 2$, $n_{Sun} = 6$, $p = 0.036$). The median tendencies for the onset of decomposition score [6] for shaded and sun exposed carcasses were 239.3 and 118.4 ADD, respectively. There is evidence to suggest the medians were different (Mann-Whitney $U = 0$, $n_{Shade} = 3$, $n_{Sun} = 6$, $p = 0.012$). For the onset of decomposition score [7] the median tendencies were 387.1 and 192.4 ADD, respectively. There was no significant difference between the medians of the two groups (Mann-Whitney $U = 6$, $n_{Shade} = 3$, $n_{Sun} = 5$, $p = 0.393$).

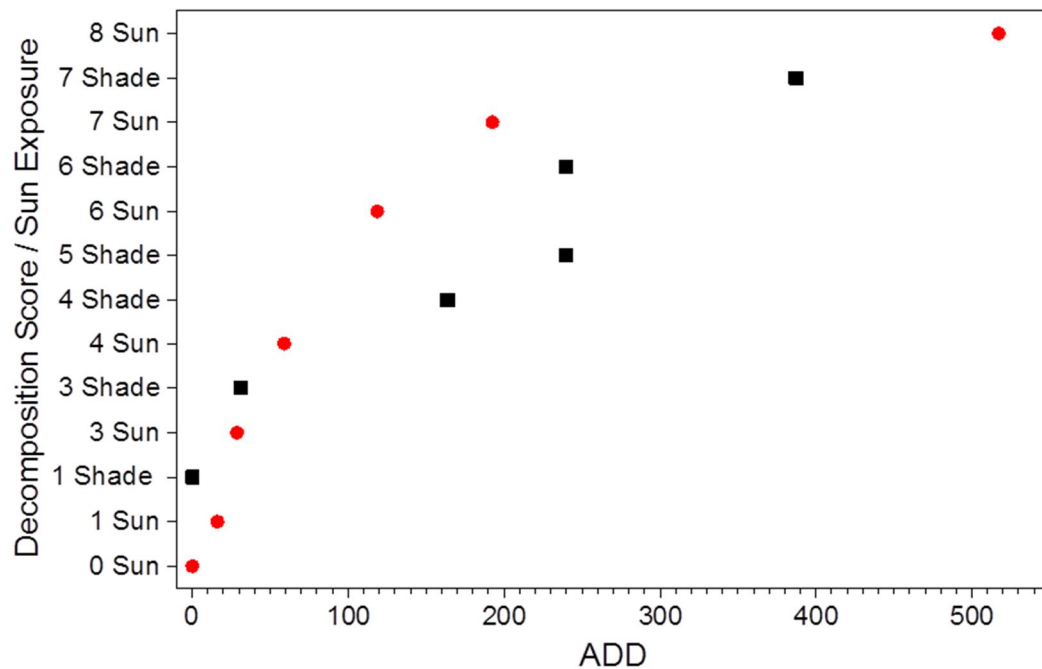


Figure 13. Median ADD value for the onset of decomposition scores observed in shaded (■) and sun exposed (●) pig carcasses of the 2008 and 2009 summer trials.

3.3.2 Comparison of Pig and Human Decomposition

Figure 14 depicts the decomposition score as a function of ADD for shaded pig carcasses of the 2008 trial. The progression of decomposition is relatively consistent between the three pig carcasses with most of the decomposition occurring in the first 400 ADD. The corresponding data for the decomposition score as a function of ADD for sun exposed pig carcasses of the 2008 and 2009 trials are portrayed in Figure 15 and Figure 16, respectively. Again, the progression of decomposition is relatively consistent for each set of carcasses. Each dataset provides comparable decomposition profiles, however, the time development is significantly different. Consider, for example, the first onset of decomposition score [6] which is 230.4 ± 50.3 ADD ($n = 3$) for shaded carcasses of the 2008 trial, 123.0 ± 0.0 ADD ($n = 3$) for sun exposed carcasses of the 2008 trial and 107.7 ± 10.6 ADD ($n = 3$) for sun exposed carcasses of the 2009 trial.

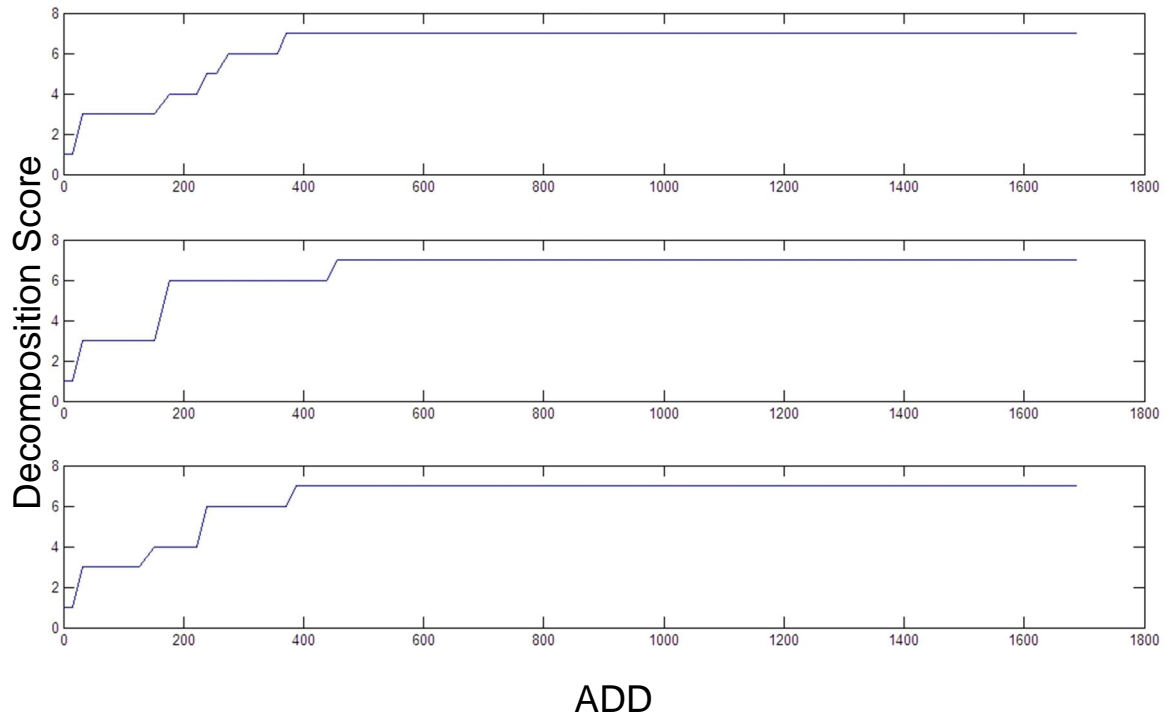


Figure 14. Decomposition score as a function of ADD for shaded pig carcasses of the 2008 trial. Each figure is representative of the distribution for an individual pig carcass.

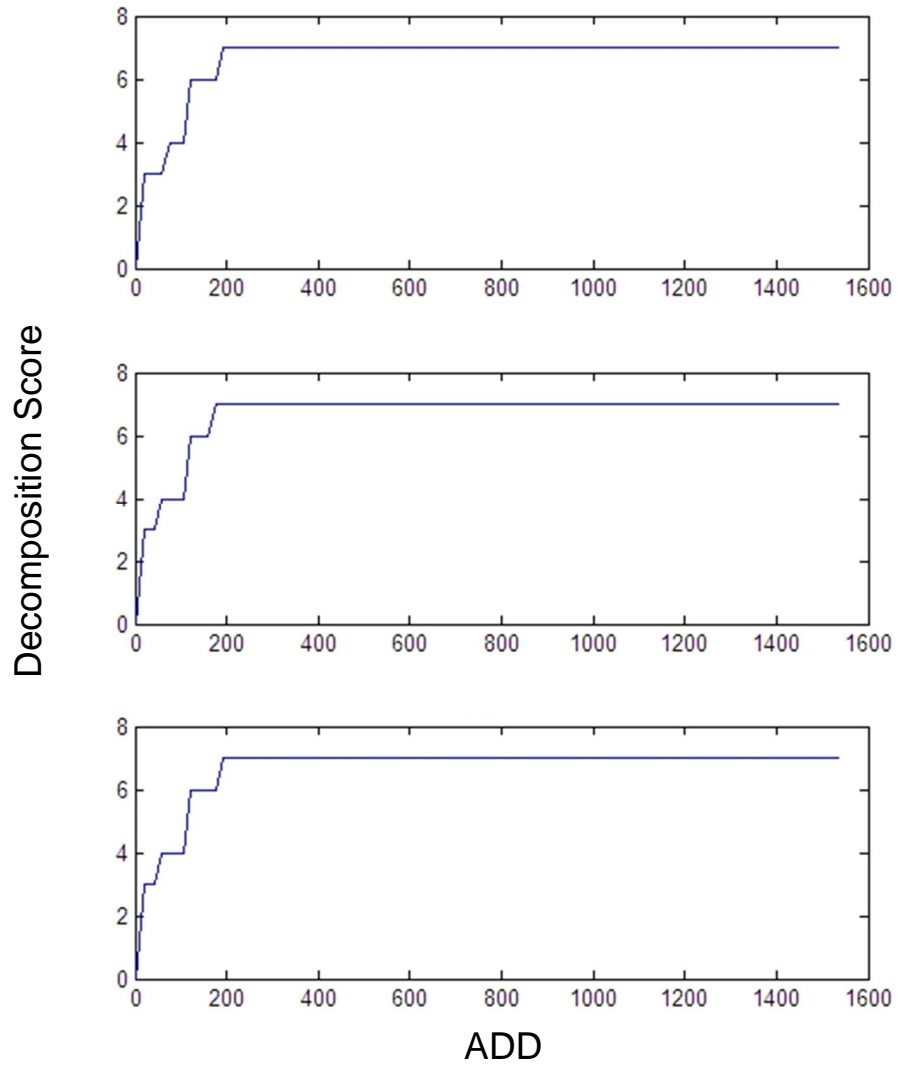


Figure 15. Decomposition score as a function of ADD for sun exposed pig carcasses of the 2008 trial. Each figure is representative of the distribution for an individual pig carcass.

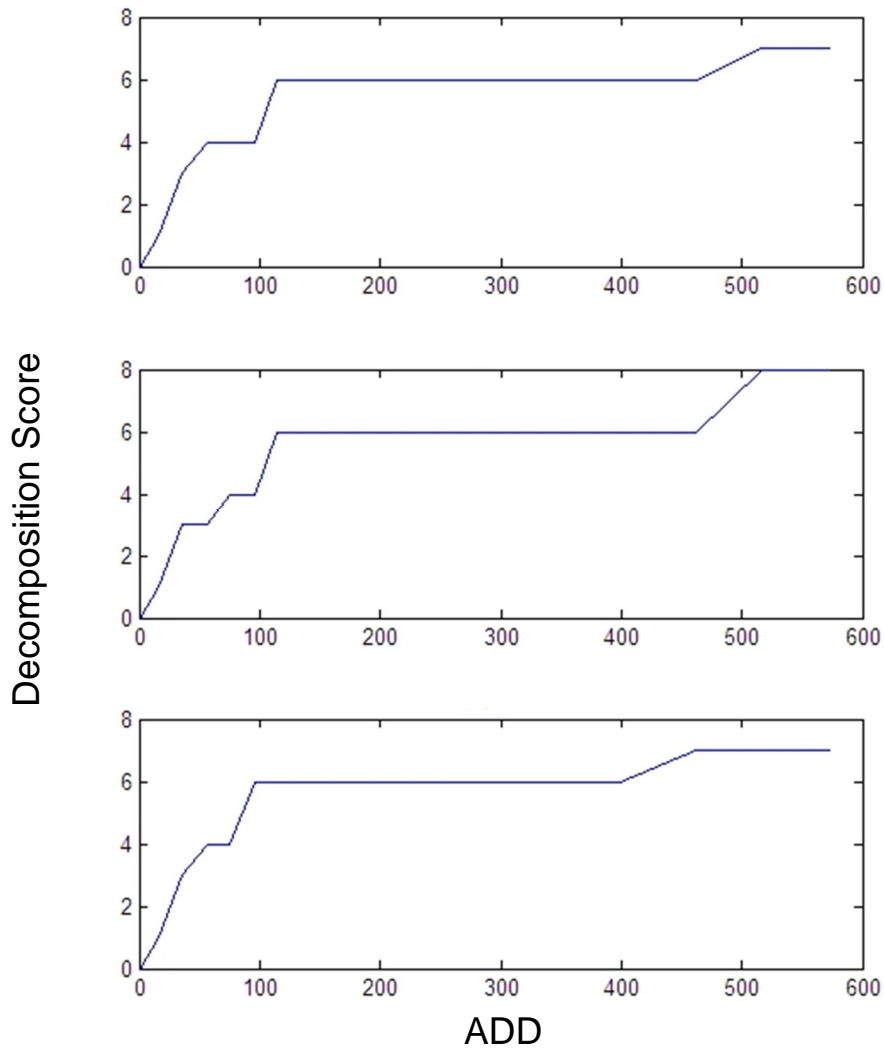


Figure 16. Decomposition score as a function of ADD for sun exposed pig carcasses of the 2009 trial. Each figure is representative of the distribution for an individual pig carcass.

Figure 17 is a compilation of all decomposition profiles onto a single graph. It is apparent that using ADD as the independent variable results in increasing the variance when comparing multiple datasets. Also included in this figure are eleven samples of human data separated into no sun (shaded remains), partial sun and full sun (sun exposed remains). The variability of the human remains data is consistent with the pig carcass data.

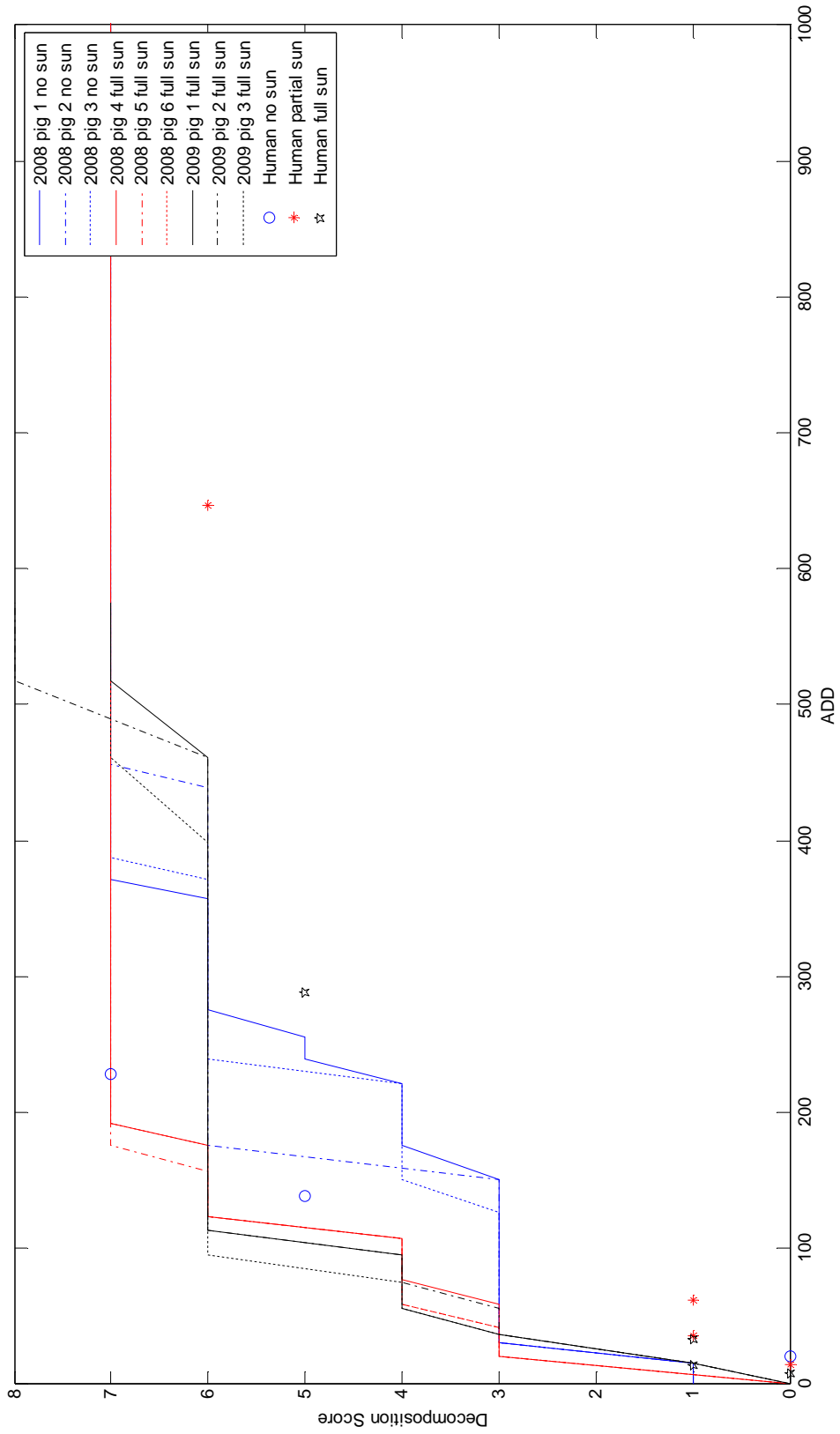


Figure 17. Decomposition score as a function of ADD for shaded and sun exposed pig carcasses of the 2008 and 2009 trials and for human remains.

3.4 Discussion

3.4.1 Decomposition Stages

The process of decomposition can be divided into distinct stages based on gross tissue changes, time intervals and often a combination of both (Payne, 1965; Bass, 1997; Clark et al., 1997; Gill-King, 1997; Goff, 2009). A study conducted by Payne (1965) was one of the earliest references to decomposition stages. Six stages of pig carcass decomposition were described: fresh, bloated, active decay, advanced decay, dry and remains stages (Payne, 1965). Each stage was described in terms of the physical appearance of the pig carcasses and the arthropod species associated with the remains. The number of days required to reach each stage was also indicated. Furthermore, a physical description of decomposition categories was provided by Clark et al. (1997). The categories described were putrid, bloating, destruction and skeleton (Clark et al., 1997). Each category was further subdivided into stages based on the physical attributes of human decomposition (Clark et al., 1997). The authors indicated, however, that an absolute time interval cannot be allocated to any of the stages due to the varying environmental conditions, differences in body type and the manner and cause of death (Clark et al., 1997). Gill-King (1997) offered a unique view on the decomposition process by describing the chemical and biological changes that occur in the body after death and how these changes lead to the distinct features observed throughout decomposition. The author also provided a time range during which some of the changes occur.

The Tissue Decomposition Classification System (refer to Appendix A) was originally developed by Cockle (2008) as a system to score photographs of human remains based on the physical attributes of decomposition due to chemical and biological changes. Cockle (2008) presented a unique interpretation of decomposition suggesting that the chemical and biological degradation of tissue should be differentiated from the physical removal of soft tissue by arthropods and scavengers. The stages for baseline decomposition (i.e. the chemical and biological degradation of tissue) were established based on the typical progression of decomposition as observed in human bodies and were assigned a point value (Cockle, 2008). In cases where differential decomposition is

observed (i.e. when an area on the body is in a different stage of decomposition than another (Wilson et al., 2007)), photographs are scored based on the most advanced stage of decomposition observed. Stages for insect and scavenger activity as well as the development of environmentally dependent states (i.e. mummification, wet and dry moulding and adipocere formation) were also described (Cockle, 2008). The scoring of decomposition photographs provides a quantitative approach that may allow for more accurate PMI estimations (Megyesi et al., 2005; Cockle, 2008). Although time intervals were not provided for the stages, it has been speculated that each baseline decomposition stage can be related to accumulated degree days (ADD) as a means of estimating the PMI given a particular environment and set of circumstances (personal communication with Sgt. Cockle, 2008).

Physical descriptions of decomposition stages are important in order to portray the decomposition process using the amalgamation of all factors involved (i.e. chemical, biological and physical processes) whereas chemical descriptions can be more important early in the decomposition process when the activity of arthropods have yet to have a substantial effect (Gill-King, 1997). The separation of chemical and physical processes becomes important, particularly with respect to human decomposition, in cases where arthropod activity is not observed even at advanced stages of decomposition (personal communication with Sgt. Cockle, 2008). Furthermore, a quantitative approach to estimating PMI facilitates statistical analysis and has the potential to provide more accurate PMI estimations.

This classification system was used in this study to score photographs of pig carcass decomposition taken at the research site in the forested and open areas during the 2008 and 2009 studies. Certain decomposition stages were not observed during the research trials. For example, the 'post bloat' [5] stage was not observed in the pig carcasses placed in the open area in both the 2008 and 2009 trials. This discrepancy was due to the occurrence of differential decomposition in the carcasses. The skull of the carcasses in each of the trials was typically skeletonized prior to the onset of the 'post bloat' [5] stage. The photographs were designated as stage [6] ('first sign of bone') and as a result stage [5] was not used. With the omission of stage [5], the leaching of

decomposition fluid from the carcasses occurred during the ‘first sign of bone’ [6] stage according to the classification system; however, this finding is misleading as the leaching of decomposition fluid is typically associated with the putrefactive process e.g. stage [5] (Gill-King, 1997; Vass et al., 2002; Dent et al., 2004). These results indicate that the classification system should be revised to better represent the decomposition process of pig carcasses. A possible solution is to develop a scoring system for different regions of the carcass. Detailed decomposition stages were outlined and assigned a point value in a study by Megyesi et al. (2005) for three regions of the human body: head and neck, trunk and limbs. Photographs of human decomposition were given a score for each region of the body and a total body score (TBS) was calculated (Megyesi et al., 2005). A regression equation was generated to predict the ADD from the TBS and ultimately the date of death of the individual from the predicted ADD (Megyesi et al., 2005). However, this scoring system requires that the entire cadaver remain intact and therefore cannot be used if remains have been scattered or removed by scavengers. Scoring systems must therefore be developed for human cadavers and pig carcasses that account for the differential decomposition of remains as well as the possibility of recovering partial remains.

3.4.2 Decomposition Scoring: Shaded and Sun Exposed Carcasses

In the comparison of the median ADD values obtained for the shaded and sun exposed pig carcasses of the 2008 and 2009 studies, it was determined that the medians were similar for decomposition score [7] only. The medians for decomposition scores [1], [3], [4] and [6] were found to be significantly different for the two groups of carcasses. The use of ADD facilitates comparisons across varying environmental conditions (Adlam and Simmons, 2007) as it accounts for the accumulation of temperature as a measure of the heat energy units required to propagate a biological process, such as decomposition (Megyesi et al., 2005). It can be hypothesized, therefore, that the range of ADD values obtained for each decomposition score in the shaded and sun exposed pig carcasses should be similar. However, a similarity in ADD values between the two groups was observed for decomposition score [7] only. The median ADD values were typically higher in the shaded carcasses ultimately indicating that

higher temperatures are required for the pig carcasses to progress through decomposition in the shade. This result is in support of a study conducted by Shean et al. (1993) in which sun exposed pig carcasses decomposed at a faster rate than shaded carcasses due to the increased rate of calliphorid larval development which was related to increased ambient air temperatures. This may indicate that ADD does not in fact facilitate inter-environmental comparisons. However, in this study a radiation shield was placed on the data logger sensor so as to reduce the effect of solar radiation on the ambient temperature readings. It is possible that the sun exposed carcasses were exposed to higher temperatures than those recorded by the data logger instrument. Thus, it appears that the ADD values for the decomposition scores for the shaded and sun exposed carcasses are significantly different when in fact the ADD values for the sun exposed carcasses may have been underestimated. Further studies are required to test this hypothesis.

For the onset of decomposition scores [1], [3] and [7] the median ADD values were similar for the two groups; however, there was a significant difference between the median ADD values for the onset of the decomposition scores [4] and [6]. There is more similarity between the median ADD values for the onset of decomposition scores for the two sets of carcasses than the median ADD values obtained for each decomposition score overall. This discrepancy may be attributed to the method by which decomposition photographs are scored. The onset of each decomposition score is characterized by particular physical attributes of decomposition; when scoring multiple carcasses there is a higher probability of the onset being detected correctly. Conversely, there are no physical attributes that are used to characterize the end of a particular score; the end of each score is determined by the commencement of the following score. Further characterization of the decomposition scores may be required to resolve this discrepancy.

3.4.3 *Decomposition Scoring: Pig Carcasses and Human Remains*

The comparison of decomposition score as a function of ADD for shaded and sun exposed pig carcasses of the 2008 and 2009 trials indicated that using ADD as the independent variable results in increasing the variance when comparing multiple sets. It appears that ADD is not sufficient to compensate for the decomposition rate for the data being considered. The problem is exacerbated with considerable changes in ADD. For

example, if the ADD for shaded carcasses was 12 ADD and 15 ADD for sun exposed carcasses a large effect would not be expected. However, nonlinear relationships could develop if the sun exposed carcasses possessed an ADD of 30, for instance, thus increasing the variance observed. Although the variability of the human data is consistent with the pig data, refinements must be made to the calculation of ADD before a meaningful comparison between pig and human data can be attempted.

3.5 Limitations

An important limitation to this study was that the effect of solar radiation on the sun exposed pig carcasses was not accounted for. Solar radiation may have had a direct effect on the temperatures to which the carcasses were exposed and thus an effect on the extent of heat loading on the carcasses. The increased temperatures due to solar radiation were not measured in this study. Furthermore, solar radiation may have had an indirect effect by increasing the rate at which the fly larvae (maggots) were developing, thus increasing the rate of decomposition. The effect of the ambient temperature and solar radiation should be considered when studying the decomposition of sun exposed remains. The temperature differences associated with solar radiation should also be considered in the calculation of ADD.

3.6 Relevance to Forensic Science

Decomposition has been characterized in many ways: physically (Payne, 1965; Clark et al., 1997), chemically (Gill-King, 1997) and quantitatively (Megyesi et al., 2005; Cockle, 2008; Fitzgerald and Oxenham, 2009). Characterizing decomposition is important in forensic science as distinct features observed or detected throughout the process can be related to time intervals under particular conditions and thus may aid in estimating the PMI. Quantitative approaches, such as decomposition scoring, have the ability to facilitate statistical analysis potentially providing more accurate PMI estimations. Decomposition photographs taken at a crime scene can be scored using the

decomposition scoring system. This study demonstrated that the use of ADD as a time scale for which to relate to decomposition scores holds the potential to aid in estimating the PMI with further research.

It may be taken for granted by some researchers that pig decomposition can be used as a model for human decomposition. It has been cited that pig carcasses can be used as analogues for human decomposition due to their similarities with an adult human torso (Anderson and VanLaerhoven, 1996; Schoenly et al., 2006). This study indicated that refinements must be made to the calculation of ADD before a meaningful comparison between pig and human data can be attempted. The variability of the ADD values obtained for the decomposition scores of the pig carcasses must be decreased to facilitate comparison of the datasets. Decreasing the variability would confirm the usefulness of relating ADD to the decomposition of pig carcasses and could then be compared to the decomposition of human remains. Further research may reveal whether pig carcasses can be used as proxies to model human decomposition.

Chapter 4 – Soil Analysis

4.1 Physicochemical Properties of Soil

Soil characterization tests were conducted by the Agriculture and Food Laboratory at the University of Guelph in Guelph, Ontario, to determine the physicochemical properties of the soil at the research site. One sample from each research area from the 2008 and 2009 summer trials was analyzed (Table 3). The composition of gravel and sand and the electrical conductivity of the soil were similar for each site. The soil texture for each site was determined to be fine sand.

Table 3. Physicochemical properties of soil collected at the research site.

Experimental Site	Trial	Composition (%)							Texture	Electrical Conductivity (mS/cm)	
		Gravel	Sand					Clay			
			Very fine	Fine	Medium	Coarse	Very coarse				
Forested land	Summer 2008	0.0	27.4	60.5	1.6	0.2	0.0	6.2	3.5	Fine sand	0.100
Open land	Summer 2008	0.0	29.6	58.0	1.9	0.1	0.0	6.5	3.5	Fine sand	0.189
Open land	Summer 2009	0.0	25.9	64.1	1.8	0.3	0.0	5.3	2.6	Fine sand	0.199

4.2 Gravimetric Water Content of Soil

4.2.1 Results

The gravimetric water content of soil was determined for control and experimental soil samples of the sun exposed pig carcasses of the 2008 and 2009 summer trials. Overall, the gravimetric water content of experimental soil was significantly greater ($p < 0.05$) than control soil for the 2008 trial (Figure 18). However, there was no distinct pattern as the water content varied across ADD. The water content was significantly higher in experimental samples at 92.8, 156.8, 176.0, 211.0 and 396.6 ADD. In particular, the 'first sign of bone' [6] stage was observed in the carcasses at 156.8 and 176.0 ADD whereupon decomposition fluid leached from the carcasses into the surrounding soil environment. In the 2009 trial, the water content was significantly higher in experimental samples than control samples across all ADD except at 0.0 ADD and from 233.8 ADD up to and including 305.3 ADD (Figure 19). Conversely, at 256.0 and 305.3 ADD the water content was significantly lower in experimental samples.

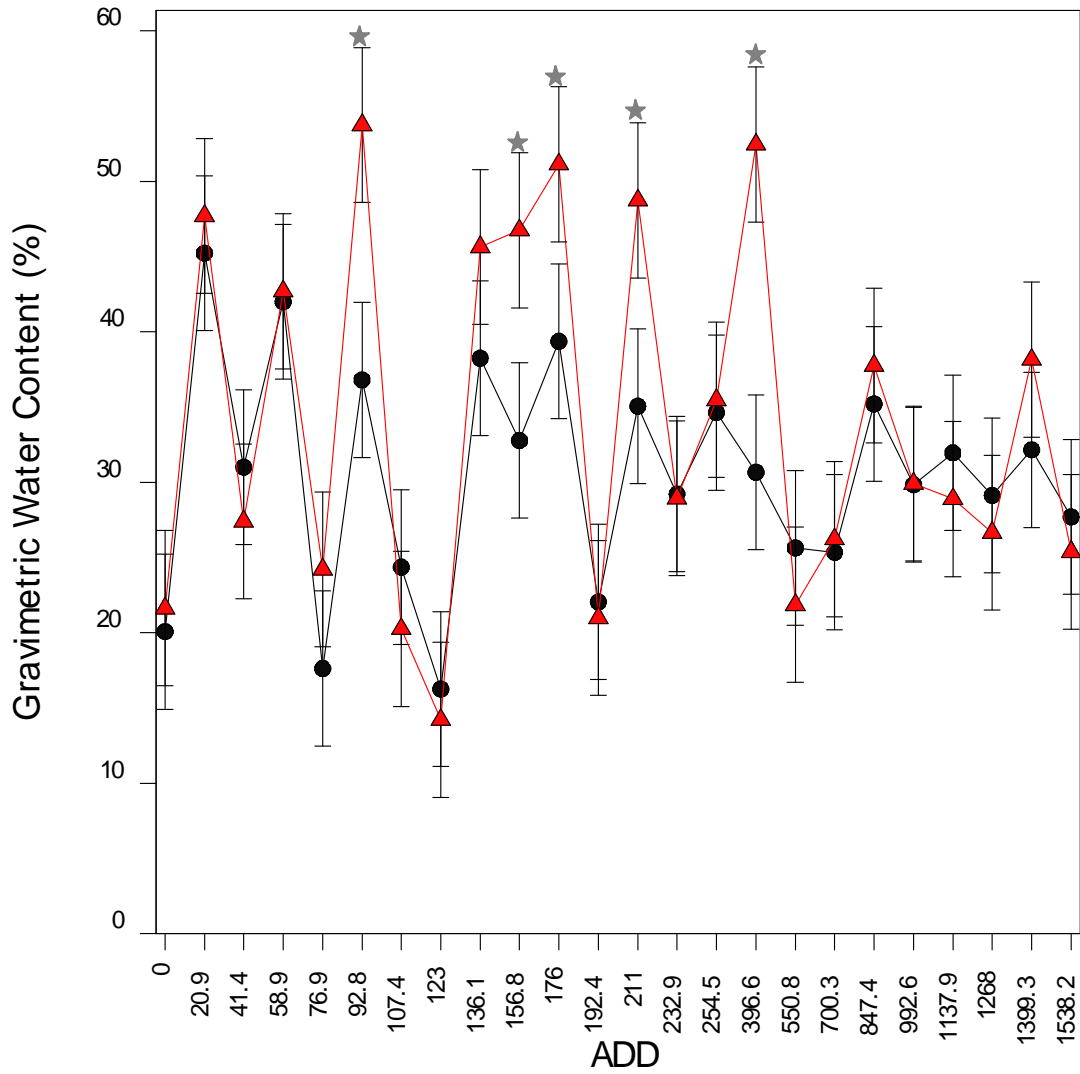


Figure 18. Gravimetric water content of control (●) and experimental (▲) soil collected within the cadaver decomposition island at the Technical and Protective Operations Facility in Ottawa, Ontario, Canada during the 2008 summer trial. ★ = significant difference $p < 0.05$ (ANOVA, $F_{\text{Treatment}(1, 96)} = 5.61$, $p = 0.020$, $F_{\text{ADD}(23, 96)} = 6.43$, $p < 0.001$, $F_{\text{Int}(23, 96)} = 0.99$, $p = 0.487$, bars = s.e. of differences of means).

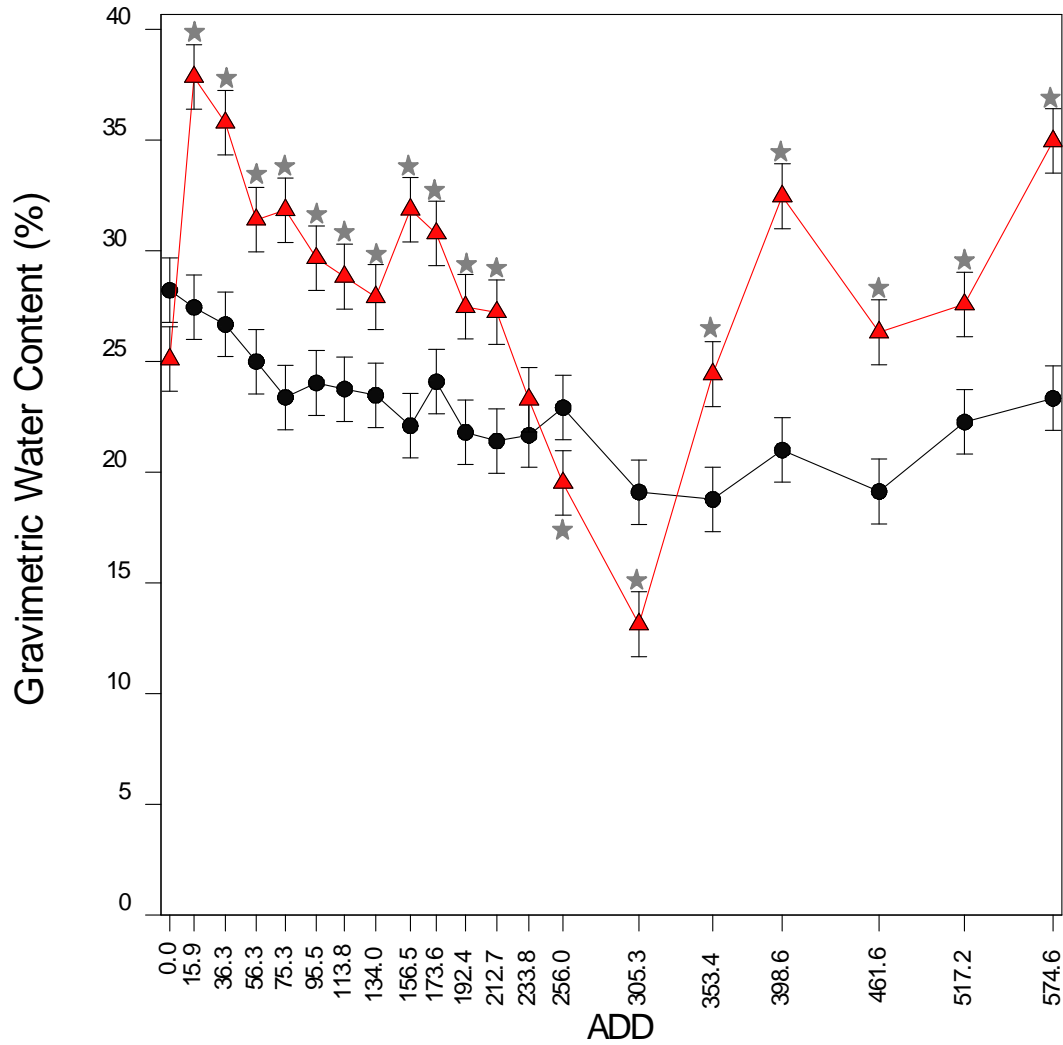


Figure 19. Gravimetric water content of control (●) and experimental (▲) soil collected within the cadaver decomposition island at the Technical and Protective Operations Facility in Ottawa, Ontario, Canada during the 2009 summer trial. ★ = significant difference $p < 0.05$ (ANOVA, $F_{\text{Treatment}(1, 680)} = 136.89$, $p < 0.001$, $F_{\text{ADD}(19, 680)} = 12.91$, $p < 0.001$, $F_{\text{Int}(19, 680)} = 5.50$, $p < 0.001$, bars = s.e. of differences of means).

4.2.2 Discussion

The decomposition of pig (*Sus scrofa*) carcasses on a soil surface was found to alter the chemical properties and composition of the underlying soil. The process of decomposition provides localized nutrient enrichment in the surrounding environment (Carter et al., 2007; Benninger et al., 2008; Dadour and Harvery, 2008). The release of decomposition fluid from decomposing remains into the soil creates a microenvironment with increased soil microbial biomass and activity (Carter et al., 2007; Benninger et al., 2008). Furthermore, decomposition fluid is composed of the degradative products of autolysis and putrefaction which can be identified and analyzed through soil analysis to determine their usefulness in estimating the postmortem interval (PMI) (Benninger et al., 2008).

In decomposition studies, the effect of the water content of soil is most often studied with regards to its effect on the decomposition process of buried remains (Wilson et al., 2007; Carter and Tibbett, 2008; Carter et al., 2010). Carter and Tibbett (2008) indicated that soil moisture can influence the metabolism of microorganisms that participate in the decomposition process. Furthermore, the soil texture can affect the decomposition of buried remains depending on water content of the soil by promoting the desiccation or degradation of tissue (Carter et al., 2010). Conversely, Wilson et al. (2007) and Benninger et al. (2008) highlight the effect of the decomposition process on the water content of the surrounding burial and soil surface environment, respectively. The gravimetric water content of experimental soil samples collected within the cadaver decomposition island (CDI) of this research was determined to be significantly higher than the water content of control soil samples in the 2008 and 2009 summer trials. Although there was no distinct pattern in the 2008 trial, the significantly higher water content at 156.8 and 176.0 ADD could be attributed to the leaching of decomposition fluid into the surrounding soil (refer to Figure 18). Similarly, Wilson et al. (2007) determined that the soil surrounding decomposing pig carcasses was wetter than soils lacking the presence of pig carcasses. Conversely, Benninger et al. (2008) concluded that there was no significant difference between the water content of gravesoil (decomposition soil) beneath decomposing pig carcasses and control soil. The difference

in results obtained in this study could be due to differences in the sampling regime. In the study conducted by Benninger et al. (2008) soil was collected at a more profound depth where decomposition fluid may not have reached. Drier soil may have been collected as a result leading to the outcome of no observed differences between control soil and gravesoil. The water content of soil is also affected by the amount of precipitation (Fleetwood and Larsson, 1968; Taylor and Seastedt, 1994; Lay et al., 2008). Fleetwood and Larsson (1968) determined that the water content increased 18-22% after a heavy rainfall in a sandy soil. Large amounts of precipitation most likely have a greater effect on the water content of soil than the leaching of decomposition fluid in the soil and could potentially mask the effects of leaching on the water content of soil; however, no known literature has been found on the subject. The substantial levels of precipitation that fell during the first 10 days (approximately 62.5 mm of rain by 176.0 ADD) of the 2008 trial (refer to Figure 7) may have masked the effect of decomposition fluid on the water content of the soil. Moreover, the variation of water content between experimental and control samples could be attributed to the sampling method. Soil samples were collected using a scupula with no particular standardization i.e. the depth and amount of soil collected may have varied with each sampling day. However, the effect of the lack of standardization of sampling on the water content of soil is unknown and has not been cited in the literature.

In the 2009 trial, the gravimetric water content of experimental soil was significantly higher than the water content of control soil, except at 0.0 and 233.8 ADD where there was no significant difference and at 256.0 and 305.3 ADD where the water content was significantly lower in experimental soil (refer to Figure 19). The increased water content of experimental samples could be attributed to the leaching of decomposition fluid into the soil environment. The amount of precipitation that fell during the first half of the trial was minimal compared to the second half (refer to Figure 8). It was during the first half of the trial that the majority of decomposition fluid leached from the carcasses into the surrounding soil. Thus, the amount of precipitation that fell during the first half of the trial would not have masked the effect of leaching decomposition fluid on the water content of the soil. Furthermore, the pattern observed was relatively consistent over the course of the trial and may be associated with the

sampling regime. In contrast to 2008 samples, the sample collection procedure for 2009 samples was highly standardized. Moreover, the decreased water content of experimental samples at 256.0 and 305.3 ADD could be attributed to the lack of vegetation within the CDI. The CDI is characterized by the death of underlying and neighbouring vegetation potentially due to nitrogen toxicity, smothering by the remains or decomposition fluid, secretion of antibiotics by maggots and/or other unidentified factors (Carter et al., 2007). During this period the soil of the CDI was dry due to the lack of precipitation and lack of decomposition fluid leaching into the soil (leaching of decomposition fluid had ceased). Plant cover can act as a canopy that retains moisture thus reducing the rate of evaporation in the soil (Ritchie, 1981). As the control sites were partially covered by vegetation it is possible that a higher level of moisture was retained in the control soil samples as compared to experimental soil samples.

Benninger (2008) determined that soil-based methods have the potential to act as a tool for estimating the PMI. However, the authors determined that there was no significant difference between the water content of experimental and control soil samples and therefore the water content of soil cannot be used to estimate the PMI. In this study, it was also determined that the gravimetric water content of soil is not useful for efficiently estimating the PMI due to the lack of a distinct pattern observed throughout the decomposition process. Confounding variables, such as the sampling method, amount of precipitation and effects of evaporation, may be the basis for the lack of a distinct pattern.

4.3 Soil pH

4.3.1 Results

The soil pH was measured for control and experimental samples of the 2008 and 2009 summer research trials. In general, the pH of experimental soil samples was significantly less ($p < 0.05$) than the pH of control soil samples of the 2008 (Figure 20) and 2009 (Figure 21) trials. In the 2008 trial, the pH of experimental samples was significantly lower than control samples from 76.9 ADD up to and including 700.3 ADD. The soil pH decreased from a pH of 7.5 to 5.4 from 58.9 to 136.1 ADD. Thereafter, pH values continuously increased, approaching pH values of control samples by 847.4 ADD. The lowest pH values were measured from 123.0 ADD up to and including 254.5 ADD; values ranged from pH 5.4 to 6.0. This period coincided with the leaching of decomposition fluid from the carcasses into the soil. Moreover, the pH of experimental samples was significantly less than control samples across all ADD except 0.0 ADD in the 2009 trial. The pH of experimental samples remained relatively constant over the course of the trial with pH values ranging from 6.0 to 6.9.

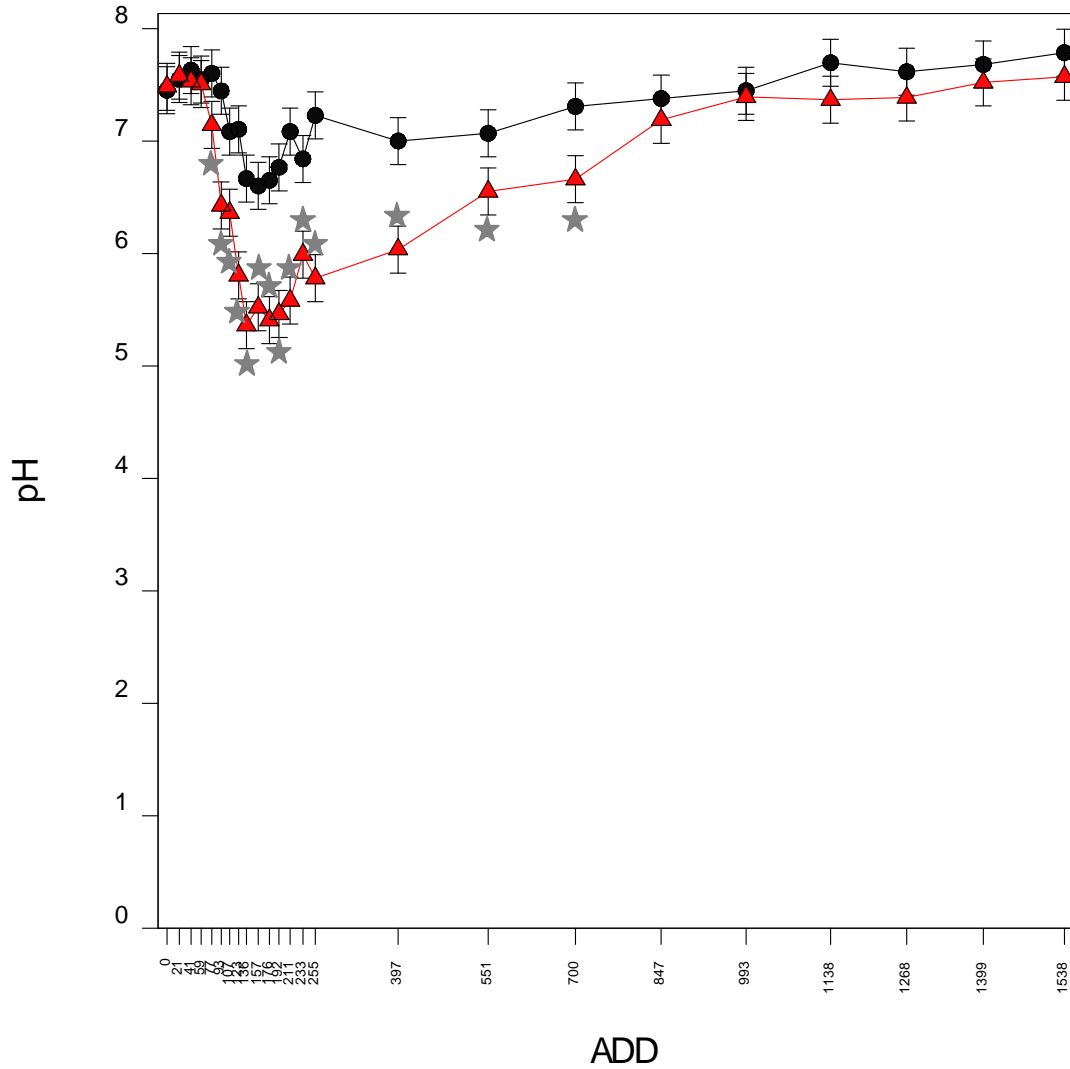


Figure 20. Soil pH of control (●) and experimental (▲) soil collected within the cadaver decomposition island at the Technical and Protective Operations Facility in Ottawa, Ontario, Canada during the 2008 summer trial. ★ = significant difference $p < 0.05$ (ANOVA, $F_{\text{Treatment}(1, 384)} = 116.29$, $p < 0.001$, $F_{\text{ADD}(23, 384)} = 16.04$, $p < 0.001$, $F_{\text{Int}(23, 384)} = 3.18$, $p < 0.001$, bars = s.e. of differences of means).

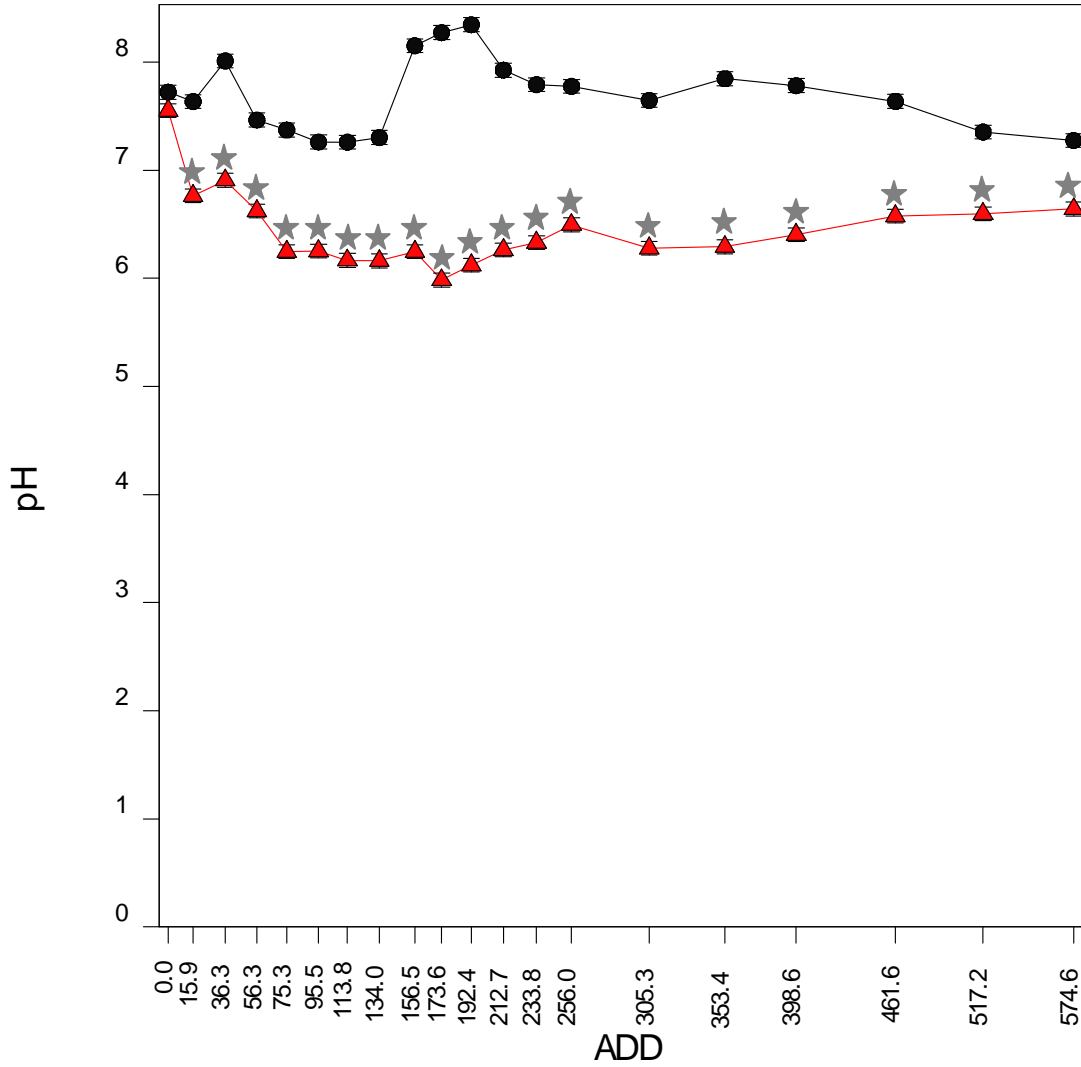


Figure 21. Soil pH of control (●) and experimental (▲) soil collected within the cadaver decomposition island at the Technical and Protective Operations Facility in Ottawa, Ontario, Canada during the 2009 summer trial. ★ = significant difference $p < 0.05$ (ANOVA, $F_{\text{Treatment}(1, 2120)} = 3781.86$, $p < 0.001$, $F_{\text{ADD}(19, 2120)} = 25.21$, $p < 0.001$, $F_{\text{Int}(19, 2120)} = 32.41$, $p < 0.001$, bars = s.e. of differences of means).

4.3.2 Discussion

The effect of soil pH on the decomposition process is relatively unknown (Carter and Tibbett, 2008). Research has suggested that bacterial growth is favoured in neutral or slightly alkaline conditions whereas acidic conditions promote the growth of fungal species (Rousk et al., 2009). Vass (1992) maintained that acidic soils can inhibit bacterial activity and thus impede the decomposition process. Naturally, the effect of soil pH on decomposition is most important for buried remains where the remains are in direct contact with the soil environment. As this study was conducted on the soil surface, however, the effect of decomposition on the pH of underlying soil was examined. The pH of experimental soil samples collected during the 2008 and 2009 trials was significantly lower overall than control soil samples (refer to Figures 20 and 21, respectively). Towne (2000) determined that the pH of soil beneath ungulate carcasses on the soil surface was also significantly lower than the surrounding soil. In the 2008 trial, soil pH decreased by a value of 2.1 in the early stages of decomposition. Soil pH increased by a value of approximately 1.5 as decomposition progressed. Soil pH may decrease in the early stages of decomposition as a result of the fermentative processes carried out by anaerobic bacteria in the gastrointestinal (GI) tract and soil (Gill-King, 1997; Forbes and Dadour, 2009) and subsequently increase due to proteolysis (Rodriguez and Bass, 1985). Conversely, many studies have indicated that the decomposition of animal carcasses yields an initial increase in soil pH followed by a decrease in pH (Hopkins et al., 2000; Melis et al., 2007; Wilson et al., 2007; Benninger et al., 2008; Haslam and Tibbett, 2009). The increase in soil pH has been attributed to the release of nitrogen mineralization by-products (e.g. ammonium ions) from the degradation of macromolecules (Hopkins et al., 2000). Hopkins et al. (2000) established that an increase in soil pH corresponded to an increase in ammonium ion concentrations. A subsequent decrease in soil pH is typically observed with continued soft tissue degradation due to the presence of by-products, i.e. acetic acid, phenolic compounds and fatty acids (Vass et al., 1992; Haslam and Tibbett, 2009). Haslam and Tibbett (2009) and Towne (2000) suggested that the decrease in soil pH could also be related to the nitrification of ammonia to nitrate, which is an acidifying reaction.

The decreased pH values observed in this study could be related to the leaching of decomposition fluid which contains acidic by-products, such as volatile and long-chain fatty acids (Vass et al., 1992; Swann et al., 2010a; Swann et al., 2010b). Furthermore, the elevated concentrations of nitrogen-containing compounds that are typically associated with an initial increase in soil pH can be short-lived as soil nitrogen is often lost to the environment as a result of volatilization and denitrification (Towne, 2000; Carter et al., 2007). The evaporative losses would be more extensive in this study due to the carcasses being deposited on the soil surface as opposed to buried beneath the soil where compounds can be retained within the soil matrix.

Soil pH measurements cannot be used in PMI estimations due to the lack of a distinct pattern in relation to individual decomposition stages. However, soil pH could potentially be used as supporting evidence for the detection of a decomposition site, especially in cases where remains have been relocated. Variation in soil pH in an area suspected of having contained decomposing remains can support the notion that remains in an early stage of decomposition had been present in the area in the recent past. The initial decrease in soil pH observed in early stages followed by an increase in pH in more advanced stages was contrary to some published literature on the pH of decomposition soil with respect to both surface decomposition trials and buried remains. The basis for this discrepancy is currently unknown. However, this research can only be applied to the particular soil type used in this study (i.e. fine sand) and the analysis of pH of decomposition soil in other soil types should be conducted.

4.4 Fatty Acid Analysis

Fatty acid analysis was conducted on control and experimental soil samples of the 2008 and 2009 trials. Fatty acids were extracted from the soil matrix, derivatized and analyzed by Gas Chromatography-Mass Spectrometry (GC-MS). The fatty acids identified were eluted from the gas chromatograph at the following retention times: 10.528 minutes for myristic acid (C14:0), 11.947 minutes for palmitic acid (C16:0), 12.243 minutes for palmitoleic acid (C16:1), 13.287 minutes for stearic acid (C18:0) and 13.519 minutes for oleic acid (C18:1) (Figure 22a-b). The internal standard (IS) used in this study was nonadecanoic acid (C19:0); it had a retention time of 13.905 minutes. Other peaks were visible on the chromatogram; they were identified as siloxane-containing compounds by the mass spectral library.

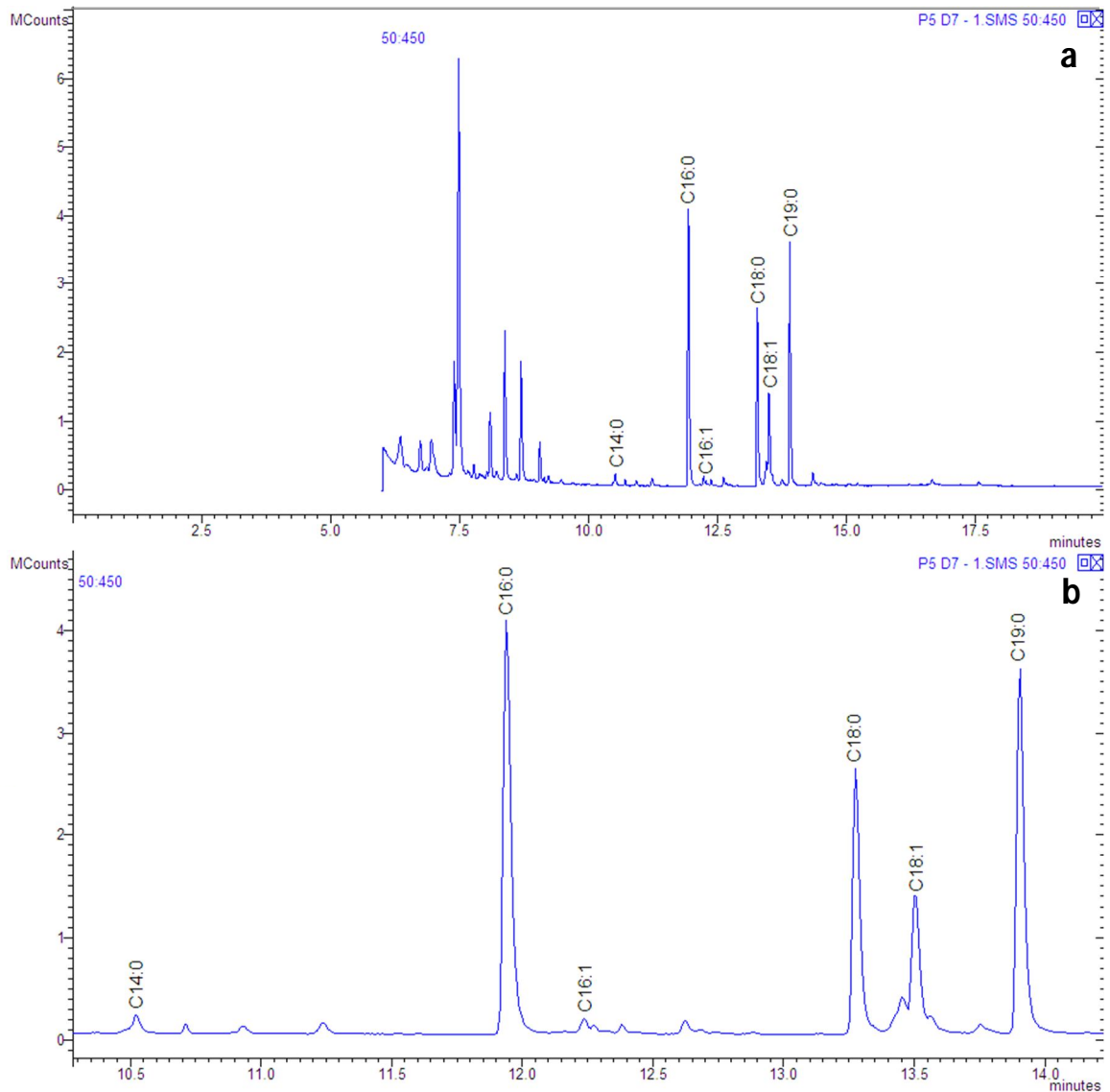


Figure 22a-b. Sample chromatogram of an experimental soil sample collected at 123.0 ADD of the 2008 trial within the cadaver decomposition island at the Technical and Protective Operations Facility in Ottawa, Ontario, Canada. The trimethylsilyl fatty acid esters identified were: myristic acid (C14:0), palmitic acid (C16:0), palmitoleic acid (C16:1), stearic acid (C18:0) and oleic acid (C18:1). Nonadecanoic acid (C19:0) was the internal standard used in this study. (A) Complete chromatogram (B) Chromatogram focused on target compounds.

4.4.1 2008 Summer Trial

Myristic Acid (C14:0)

The myristic acid (C14:0) content of experimental soil was determined to be significantly higher ($p < 0.05$) overall than control soil for the 2008 trial (Figure 23). Specifically, the C14:0 content of experimental soil samples was significantly higher than control samples from 123.0 ADD up to and including 550.8 ADD. During this time frame, the carcasses had reached the ‘first sign of bone’ [6] and ‘more than half of bone exposed’ [7] stages of decomposition. There appears to be a three peak cycle in experimental samples over the course of the trial. Initially, the C14:0 content increases from basal levels at 136.1 ADD. There was a slight drop in levels prior to a second increase in C14:0 content at 176.0 ADD, whereupon the level of C14:0 was highest for the duration of the trial (mean Peak Area Ratio (PAR) of 8.2). Subsequently, C14:0 levels decreased until 254.5 ADD. A third peak in C14:0 content occurred at 396.6 ADD with a continued decrease to basal levels thereafter (Figure 23).

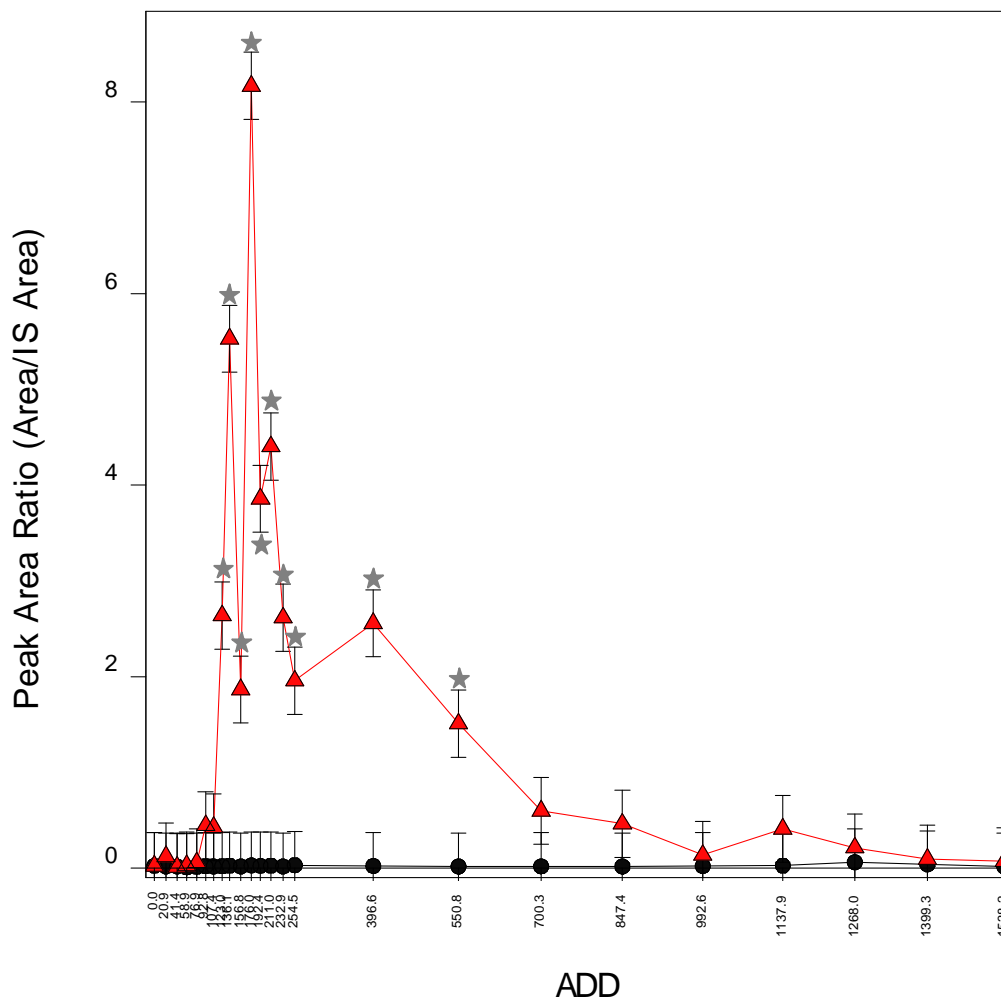


Figure 23. Myristic acid content of control (—●—) and experimental (—▲—) soil collected within the cadaver decomposition island at the Technical and Protective Operations Facility in Ottawa, Ontario, Canada during the 2008 summer trial. ★ = significant difference $p < 0.05$ (ANOVA, $F_{\text{Treatment}(1, 384)} = 241.31$, $p < 0.001$, $F_{\text{ADD}(23, 384)} = 18.10$, $p < 0.001$, $F_{\text{Int}(23, 384)} = 18.07$, $p < 0.001$, bars = s.e. of differences of means).

Palmitic Acid (C16:0)

Overall, the palmitic acid (C16:0) content of experimental soil samples was significantly greater ($p < 0.05$) than control samples for the 2008 trial (Figure 24). Similar to C14:0 content, experimental samples were significantly higher than control samples from 123.0 ADD up to and including 550.8 ADD and there was an apparent three peak cycle that emerged throughout the trial. Carcasses had reached the ‘first sign of bone’ [6] and ‘more than half of bone exposed’ [7] stages when C16:0 levels were significantly

greater in experimental samples. A pattern analogous to that of C14:0 content of experimental samples was observed for C16:0 content. There was an initial increase in C16:0 levels from basal levels until 136.1 ADD. The high point of the three peaks occurred at 136.1, 176.0 and 396.6 ADD where the highest levels of C16:0 were detected at 176.0 ADD with a mean PAR of 197.2. The intermediate points between the peaks demonstrated a decrease in C16:0 content. C16:0 content returned to basal levels by 700.3 ADD (Figure 24).

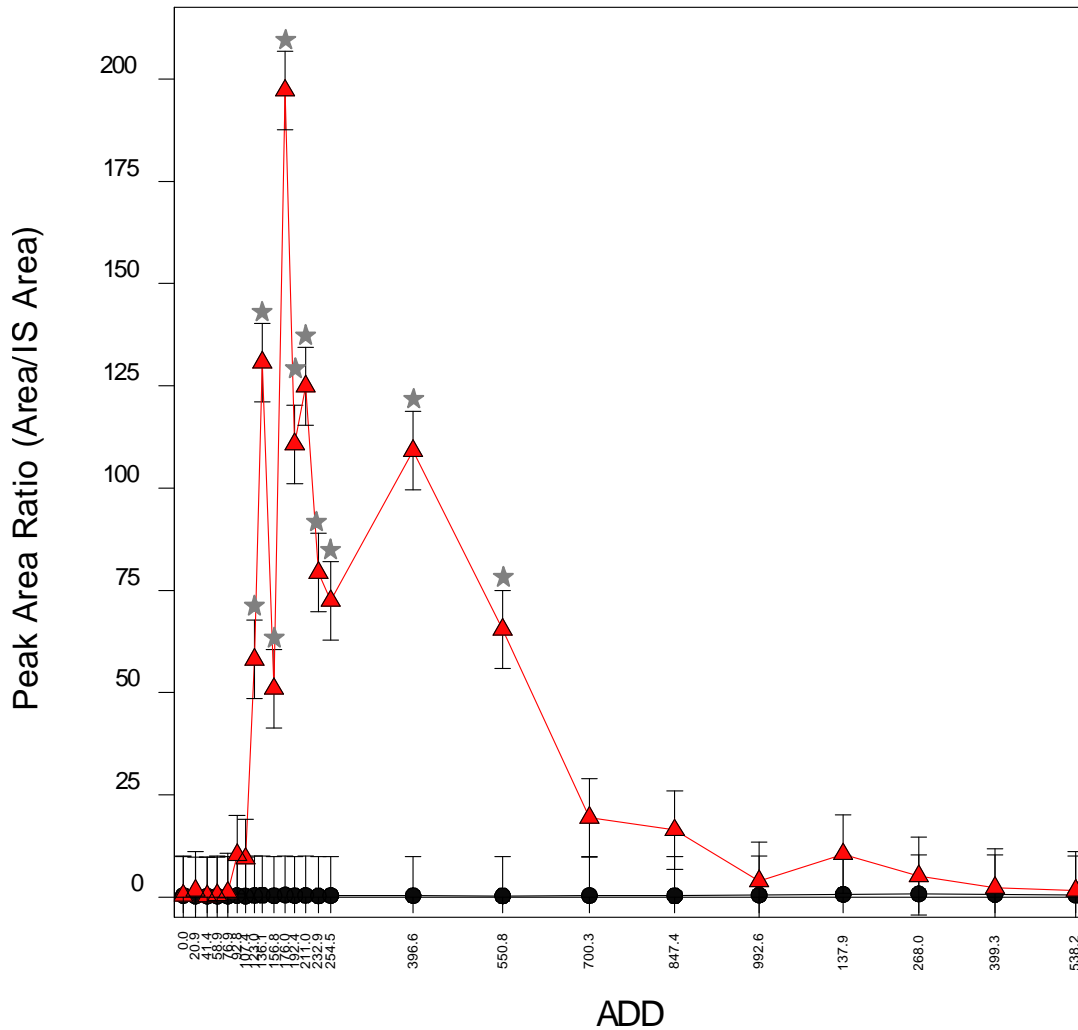


Figure 24. Palmitic acid content of control (—●—) and experimental (—▲—) soil collected within the cadaver decomposition island at the Technical and Protective Operations Facility in Ottawa, Ontario, Canada during the 2008 summer trial. ★ = significant difference $p < 0.05$ (ANOVA, $F_{\text{Treatment}(1, 384)} = 261.08$, $p < 0.001$, $F_{\text{ADD}(23, 384)} = 16.54$, $p < 0.001$, $F_{\text{Int}(23, 384)} = 16.54$, $p < 0.001$, bars = s.e. of differences of means).

Palmitoleic Acid (C16:1)

Overall, there was a significantly greater ($p < 0.05$) palmitoleic acid (C16:1) content in experimental soil samples compared to control soil samples (Figure 25). In particular, experimental samples were significantly higher than control samples from 123.0 ADD up to and including 396.6 ADD, except at 156.8 and 254.5 ADD. During this period, the carcasses had reached decomposition stages [6] and [7]. The three peak fatty acid cycle was also apparent for C16:1 levels of experimental samples with high points at 136.1, 176.0 and 396.6 ADD while intermediate points approach basal levels. C16:1 content returned to levels comparable to those of control samples by 550.8 ADD (Figure 25).

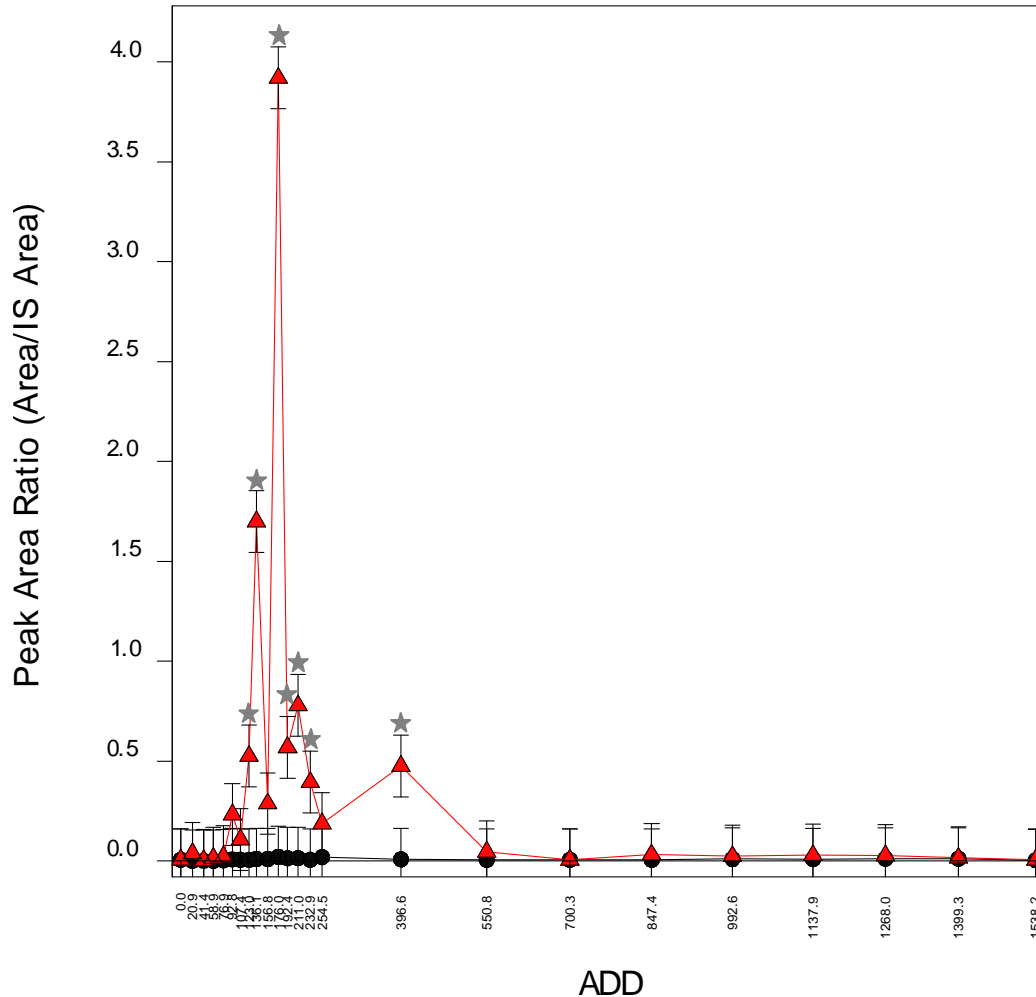


Figure 25. Palmitoleic acid content of control (—●—) and experimental (—▲—) soil collected within the cadaver decomposition island at the Technical and Protective Operations Facility in Ottawa, Ontario, Canada during the 2008 summer trial. ★ = significant difference $p < 0.05$ (ANOVA, $F_{\text{Treatment}(1, 384)} = 74.66$, $p < 0.001$, $F_{\text{ADD}(23, 384)} = 14.96$, $p < 0.001$, $F_{\text{Int}(23, 384)} = 14.74$, $p < 0.001$, bars = s.e. of differences of means).

Stearic Acid (C18:0)

The stearic acid (C18:0) content was significantly higher ($p < 0.05$) overall in experimental samples than control samples (Figure 26). C18:0 levels of experimental samples were significantly higher than control samples from 123.0 ADD up to and including 700.3 ADD during which time the carcasses reached the ‘first sign of bone’ [6] and ‘more than half of bone exposed’ [7] stages. The three peak cycle was evident in experimental samples over the course of the trial. Initially, C18:0 levels increased from

basal levels and peaked at 136.1 ADD. There was a subsequent decrease in C18:0 content at 156.8 ADD followed by a substantial increase in C18:0 content at 176.0 ADD where the highest level was observed (mean PAR of 99.7). C18:0 levels in successive samples decreased until 254.5 ADD. Again, levels increased at 396.6 ADD before continuing to decrease towards basal levels which were ultimately achieved by 847.4 ADD (Figure 26).

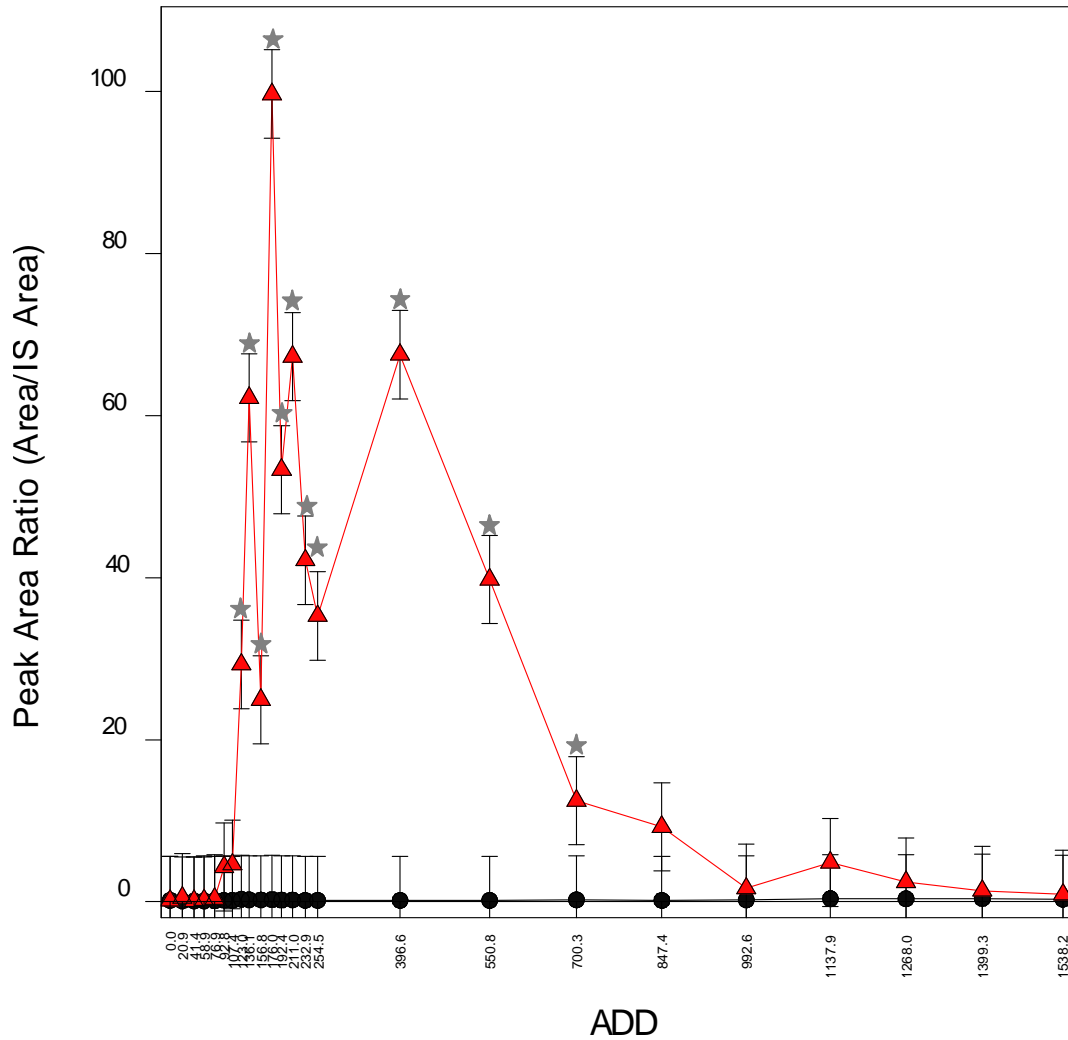


Figure 26. Stearic acid content of control (●) and experimental (▲) soil collected within the cadaver decomposition island at the Technical and Protective Operations Facility in Ottawa, Ontario, Canada during the 2008 summer trial. ★ = significant difference $p < 0.05$ (ANOVA, $F_{\text{Treatment}(1, 384)} = 219.54$, $p < 0.001$, $F_{\text{ADD}(23, 384)} = 13.81$, $p < 0.001$, $F_{\text{Int}(23, 384)} = 13.80$, $p < 0.001$, bars = s.e. of differences of means).

Oleic Acid (18:1)

Overall, oleic acid (C18:1) content of experimental soil samples was significantly higher ($p < 0.05$) than control samples (Figure 27). All experimental samples ranging from 123.0 ADD up to and including 550.8 ADD were significantly greater than control samples. The carcasses had reached decomposition stages [6] and [7] during this period. The three peak fatty acid cycle was apparent for C18:1 content. The high points of the three peaks occurred at 136.1, 176.0 and 396.6 ADD. Intermediate points of the peaks exhibited decreasing levels of C18:1. The highest level of C18:1 was detected at 176.0 ADD with a mean PAR of 68.6. C18:1 content returned to control sample levels by 700.3 ADD (Figure 27).

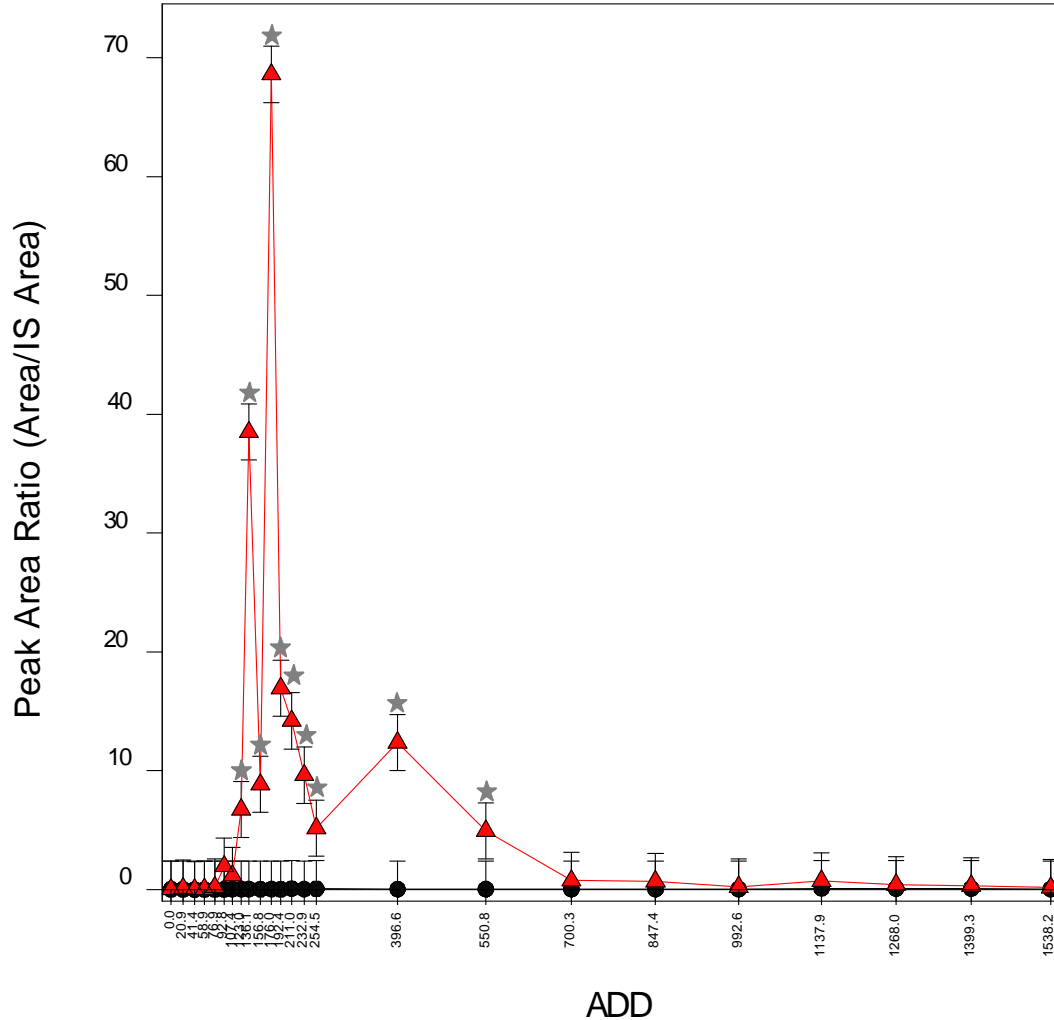


Figure 27. Oleic acid content of control (—●—) and experimental (—▲—) soil collected within the cadaver decomposition island at the Technical and Protective Operations Facility in Ottawa, Ontario, Canada during the 2008 summer trial. ★ = significant difference $p < 0.05$ (ANOVA, $F_{\text{Treatment}(1, 384)} = 137.11$, $p < 0.001$, $F_{\text{ADD}(23, 384)} = 21.59$, $p < 0.001$, $F_{\text{Int}(23, 384)} = 21.58$, $p < 0.001$, bars = s.e. of differences of means).

Relative Fatty Acid Content

The data for the fatty acid content of experimental soil samples for each fatty acid identified were compiled in order to ascertain relative levels with respect to each fatty acid (Figure 28). The three peak fatty acid cycle was apparent for each fatty acid and the high points of the peaks occurred at the same ADD (136.1, 176.0 and 396.6 ADD) and during the same decomposition stages ([6] and [7]). In addition, the highest level of fatty acid detected over the duration of the trial occurred at 176.0 ADD for each fatty acid.

Saturated fatty acids (i.e. C16:0 and C18:0) were the most abundant fatty acids detected over the course of the trial while C16:0 was the highest. The level of C16:0 was significantly higher ($p < 0.05$) than all other fatty acids from 92.8 ADD up to and including 847.4 ADD and at 1137.9 ADD. The second most abundant fatty acid was C18:0. Apart from C16:0, the level of C18:0 was significantly greater than all other fatty acids from 123.0 ADD up to and including 847.4 ADD and at 1137.9 ADD. C18:1 content was significantly greater than C14:0 and C16:1 content from 123.0 ADD up to and including 232.9 ADD and at 396.6 ADD. Conversely, the relative abundance of C14:0 and C16:1 detected was negligible in comparison to C16:0, C18:0 and C18:1 (Figure 28).

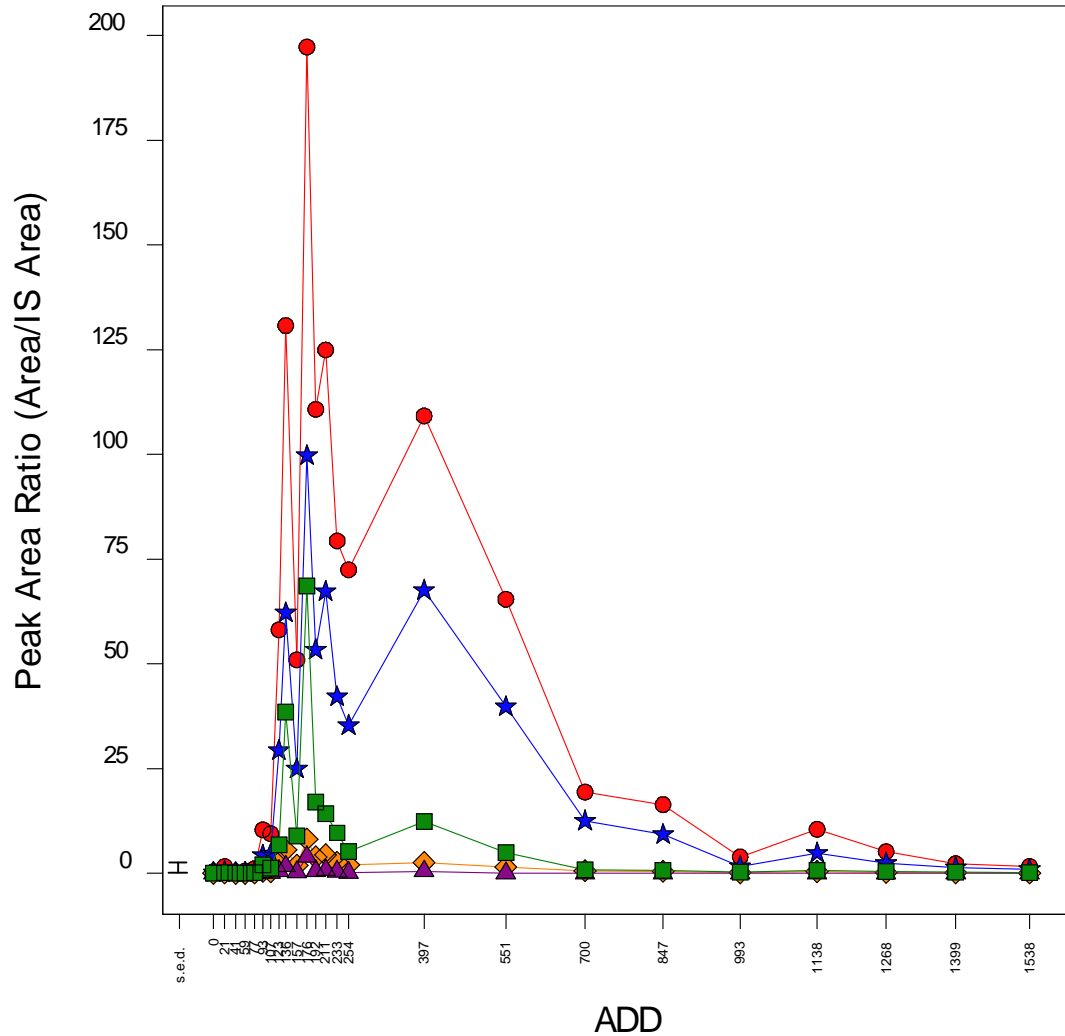


Figure 28. Fatty acid content of experimental soil collected within the cadaver decomposition island at the Technical and Protective Operations Facility in Ottawa, Ontario, Canada during the 2008 summer trial. The fatty acids identified were C14:0 (◇), C16:0 (●), C16:1 (▲), C18:0 (★) and C18:1 (■). (ANOVA, $F_{\text{Fatty acid}(4, 960)} = 167.00$, $p < 0.001$, $F_{\text{ADD}(23, 960)} = 39.44$, $p < 0.001$, $F_{\text{Int}(92, 960)} = 10.29$, $p < 0.001$, bar = s.e. of differences of means).

Table 4 shows the relative percent composition of fatty acids detected over the course of the 2008 trial. The relative percent composition of each fatty acid remained relatively constant throughout the trial. The saturated fatty acids C16:0 and C18:0 were the most abundant fatty acids detected with a mean percent composition of 60.5% and 29.2%, respectively. C18:1 was the third most abundant fatty acid with a mean percent composition of 7.1%. C14:0 and C16:1 were the least abundant fatty acids detected with a mean percent composition of 2.6% and 0.6%.

Table 4. Relative percent (%) composition of fatty acids detected in the 2008 trial.

ADD	Decomposition Stage Onset	C14:0	C16:0	C16:1	C18:0	C18:1
0	No visible changes [0]	4.4	66.5	1.1	24.6	3.3
20.9	First colour change [3]	5.2	67.3	1.6	20.9	5.0
41.4		4.3	64.7	1.1	25.6	4.3
58.9		4.0	63.5	1.9	24.9	5.7
76.9	Full bloat [4]	3.3	63.8	1.3	20.3	11.3
92.8		2.6	59.9	1.4	24.9	11.3
107.4		2.7	59.9	0.7	29.2	7.5
123.0	First sign of bone [6]	2.7	59.7	0.5	30.1	6.9
136.1		2.3	54.8	0.7	26.1	16.1
156.8		2.1	58.7	0.3	28.7	10.2
176.0	More than half of bone exposed [7]	2.2	52.2	1.0	26.4	18.2
192.4		2.1	59.7	0.3	28.8	9.1
211		2.1	59.0	0.4	31.8	6.7
232.9		2.0	59.2	0.3	31.4	7.2
254.5		1.7	63.0	0.2	30.7	4.5
396.6		1.3	56.8	0.2	35.2	6.4
550.8		1.4	58.6	0.0	35.6	4.4
700.3		1.8	58.4	0.0	37.5	2.3
847.4		1.7	61.1	0.1	34.5	2.6
992.6		2.3	65.7	0.4	27.8	3.8
1137.9		2.5	63.7	0.2	29.3	4.4
1268.0		2.6	62.5	0.3	29.7	4.9
1399.3		2.4	55.6	0.4	33.6	8.0
1538.2		2.6	58.4	0.3	32.8	5.9
Mean		2.6	60.5	0.6	29.2	7.1

4.4.2 2009 Summer Trial

Soil samples collected at 10 cm intervals commencing at the soil-carcass boundary (0 cm) up to 50 cm were analyzed. The top two centimetres of the core samples were separated from the bottom two to five centimetres to determine the extent at which decomposition fluid leached into the soil vertically. Preliminary GC-MS analysis indicated that levels of fatty acids detected in the bottom portion of the core samples were negligible in comparison to the top portion. As such, only analysis of the top portion was conducted.

Relative Myristic Acid (C14:0) Content

The relative myristic acid (C14:0) content with respect to the distances at which experimental samples were collected from the carcasses (0 cm, 10 cm, 20 cm, 30 cm, 40 cm and 50 cm) is shown in Figure 29. The most abundant levels of C14:0 were detected at 0 cm and decreased successively until 50 cm. C14:0 levels were significantly greater ($p < 0.05$) at 0 cm than all other distances from 75.3 ADD up to and including 212.7 ADD and at 305.3, 517.2 and 574.6 ADD. However, C14:0 content detected at 10 cm was significantly greater at 233.8 ADD than all other distances. Furthermore, the level of C14:0 detected at 30 cm was significantly higher than levels at 10 cm and 20 cm at 156.5 ADD (Figure 29).

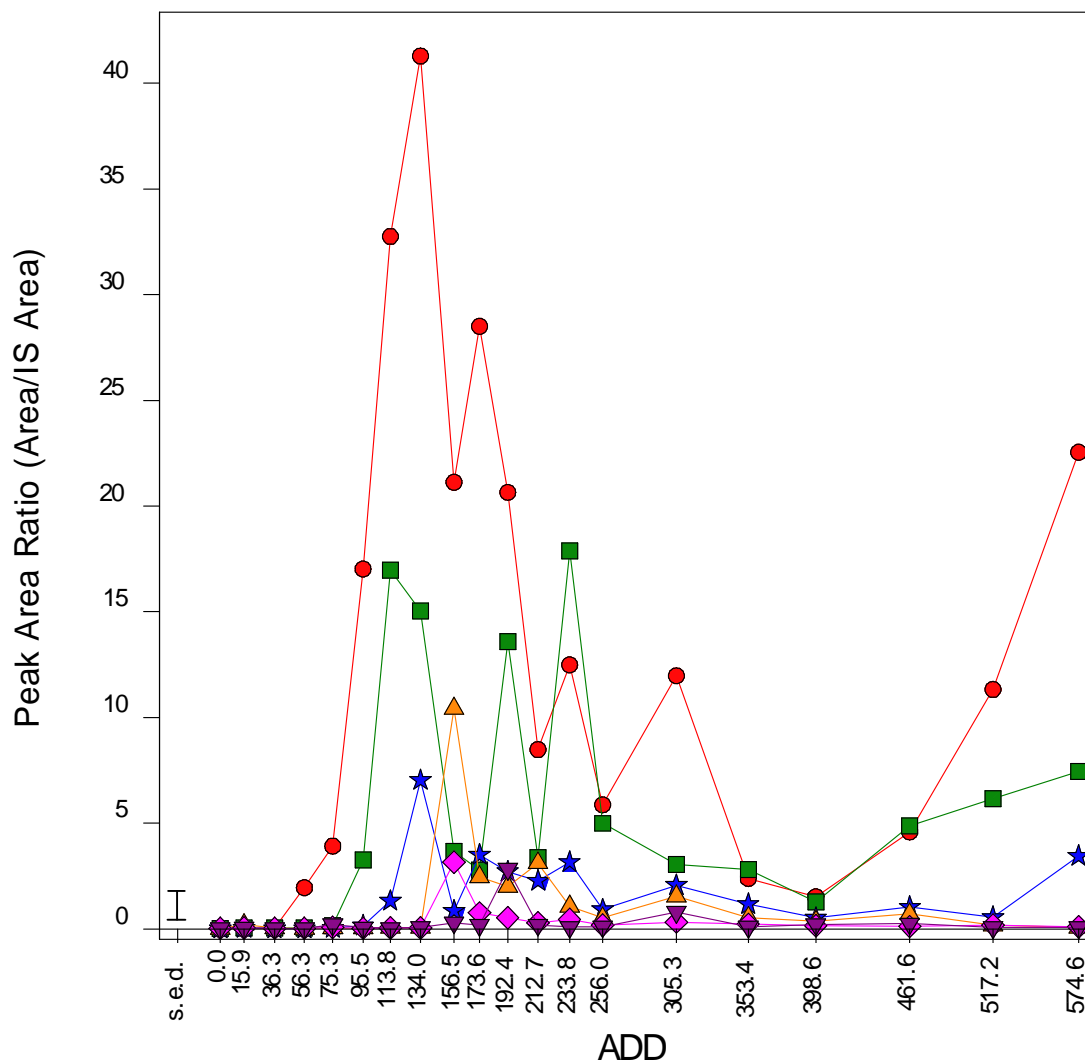


Figure 29. Myristic acid content of experimental soil collected 0 cm (—●—), 10 cm (—■—), 20 cm (—★—), 30 cm (—▲—), 40 cm (—◆—) and 50 cm (—▼—) away from the pig carcasses at the Technical and Protective Operations Facility in Ottawa, Ontario, Canada during the 2009 summer trial. (ANOVA, $F_{\text{Distance}(5, 240)} = 23.03$, $p < 0.001$, $F_{\text{ADD}(19, 240)} = 3.02$, $p < 0.001$, $F_{\text{Int}(95, 240)} = 1.32$, $p = 0.047$, bar = s.e. of differences of means).

Relative Palmitic Acid (C16:0) Content

Figure 30 depicts the relative palmitic acid (C16:0) content with respect to the distances at which experimental soil samples were collected from the carcasses (0 cm, 10 cm, 20 cm, 30 cm, 40 cm and 50 cm). A similar pattern was observed for the relative C16:0 content as previously described for C14:0. In general, the level of C16:0 was most abundant at 0 cm followed successively by 10 cm, 20 cm, 30 cm, 40 cm and 50 cm. The

level of C16:0 was significantly greater ($p < 0.05$) at 0 cm than all other distances from 75.3 ADD up to and including 212.7 ADD and at 305.3 517.2 and 574.6 ADD. However, at 233.8 ADD the level of C16:0 was significantly higher at 10 cm than all other distances. Furthermore, the level of C16:0 detected at 156.5 ADD was significantly greater at 30 cm than at 10 cm and 20 cm (Figure 30).

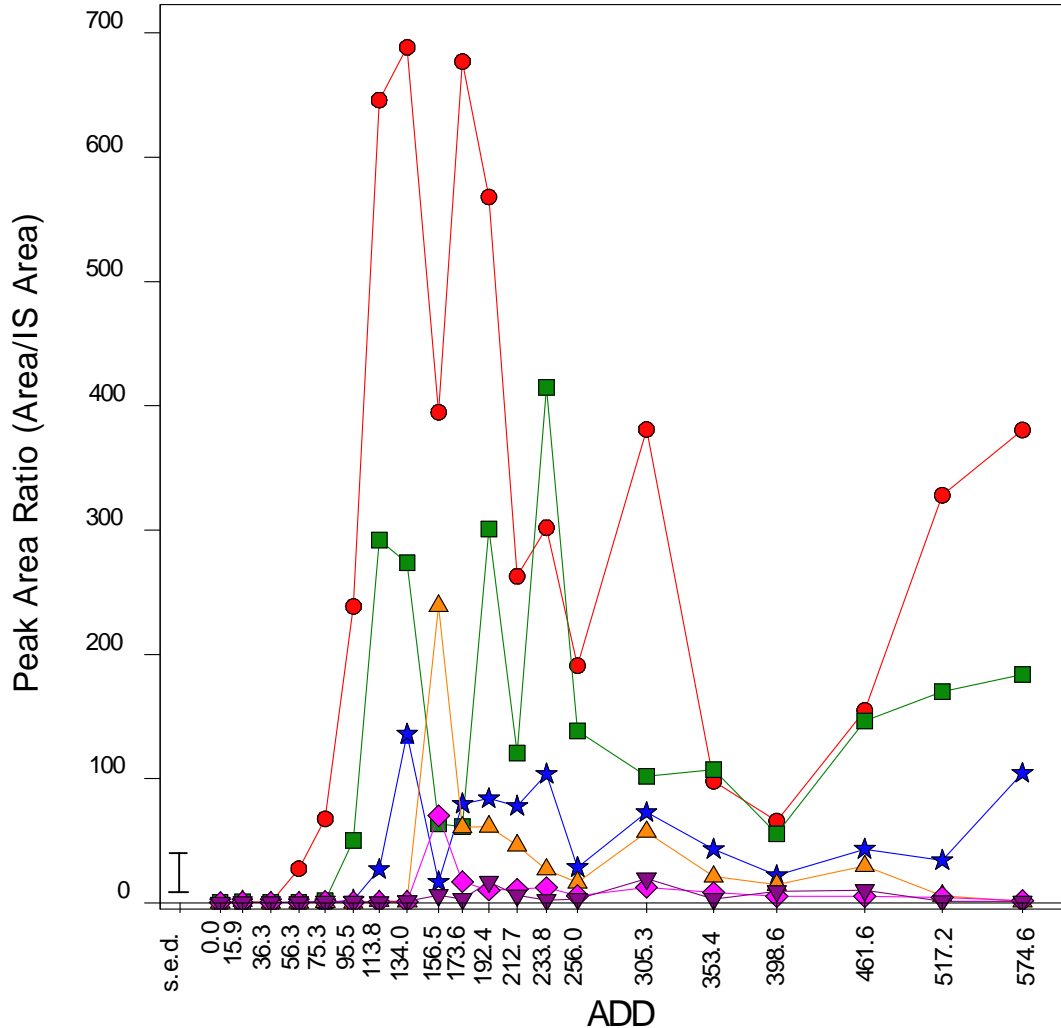


Figure 30. Palmitic acid content of experimental soil collected 0 cm (●), 10 cm (■), 20 cm (★), 30 cm (▲), 40 cm (◆) and 50 cm (▼) away from the pig carcasses at the Technical and Protective Operations Facility in Ottawa, Ontario, Canada during the 2009 summer trial. (ANOVA, $F_{\text{Distance}(5, 240)} = 23.45$, $p < 0.001$, $F_{\text{ADD}(19, 240)} = 2.53$, $p < 0.001$, $F_{\text{Int}(95, 240)} = 1.07$, $p = 0.331$, bar = s.e. of differences of means).

Relative Palmitoleic Acid (C16:1) Content

Figure 31 displays the relative palmitoleic acid (C16:1) content with respect to the distances at which experimental samples were collected from the carcasses (0 cm, 10 cm, 20 cm, 30 cm, 40 cm and 50 cm). A pattern similar to that observed in C14:0 and C16:0 was also observed for C16:1. The sequential order of fatty acid abundance by distance was: 0 cm, 10 cm, 20 cm, 30 cm, 40 cm and 50 cm. The C16:1 content of experimental samples detected at 0 cm was significantly greater ($p < 0.05$) than all other distances from 75.3 ADD up to and including 212.7 ADD and at 305.3 and 517.2 ADD. At 233.8 and 256.0 ADD, however, the level of C16:1 was significantly higher at 10 cm than at 0 cm. Moreover, at 156.5 ADD, C16:1 content was significantly greater at 30 cm than at 10 cm and 20 cm. Similarly, the level of C16:1 detected at 40 cm was significantly greater than that detected at 20 cm at 156.5 ADD (Figure 31).

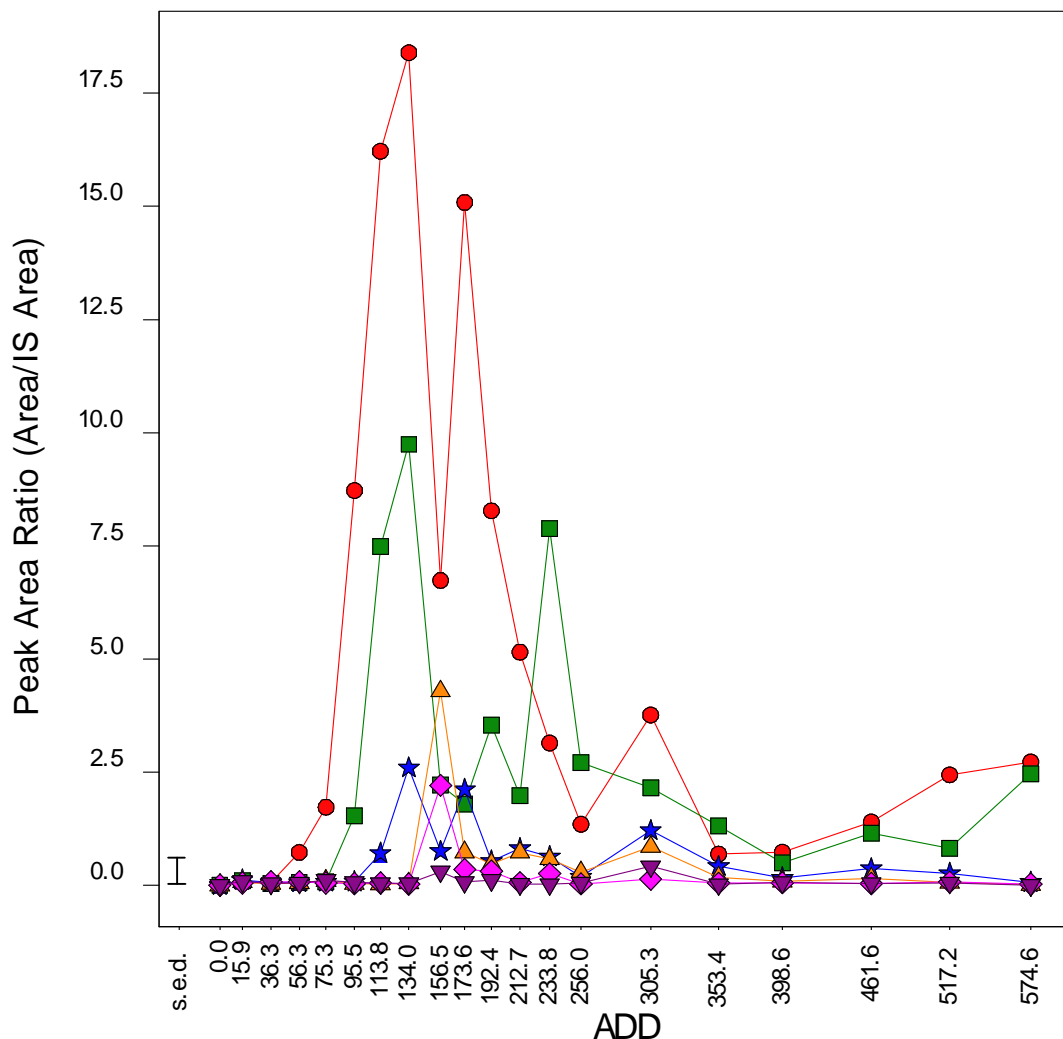


Figure 31. Palmitoleic acid content of experimental soil collected 0 cm (—●—), 10 cm (—■—), 20 cm (—★—), 30 cm (—▲—), 40 cm (—◆—) and 50 cm (—▼—) away from the pig carcasses at the Technical and Protective Operations Facility in Ottawa, Ontario, Canada during the 2009 summer trial. (ANOVA, $F_{\text{Distance}(5, 240)} = 18.56, p < 0.001$, $F_{\text{ADD}(19, 240)} = 3.33, p < 0.001$, $F_{\text{Int}(95, 240)} = 1.52, p = 0.006$, bar = s.e. of differences of means).

Relative Stearic Acid (C18:0) Content

The relative stearic acid (C18:0) content with respect to the distance at which experimental samples were collected from the carcasses (0 cm, 10 cm, 20 cm, 30 cm, 40 cm and 50 cm) is represented in Figure 32. A pattern similar to that described for C14:0, C16:0 and C16:1 was apparent for C18:0. In general, the most abundant level of C18:0 was detected at 0 cm and continued to decrease until 50 cm. C18:0 content of experimental samples at 0 cm was significantly higher ($p < 0.05$) than all other distances

from 95.5 ADD up to and including 212.7 ADD and at 305.3, 517.2 and 574.6 ADD. However, C18:0 content was significantly greater at 10 cm than 0 cm at 233.8 ADD. Furthermore, the level of C18:0 detected at 30 cm at 156.5 ADD was significantly higher than that detected at 10 cm and 20 cm (Figure 32).

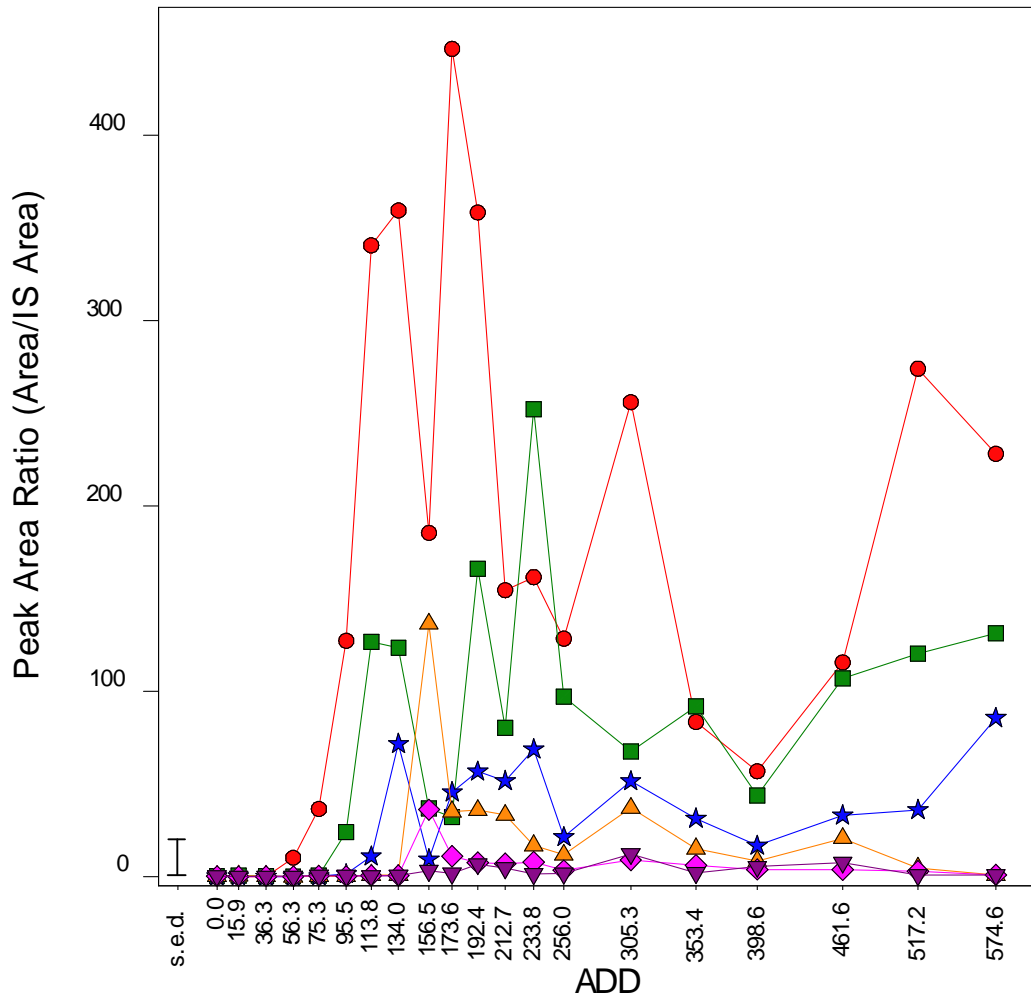


Figure 32. Stearic acid content of experimental soil collected 0 cm (●), 10 cm (■), 20 cm (★), 30 cm (▲), 40 cm (◆) and 50 cm (▼) away from the pig carcasses at the Technical and Protective Operations Facility in Ottawa, Ontario, Canada during the 2009 summer trial. (ANOVA, $F_{\text{Distance}(5, 240)} = 21.94$, $p < 0.001$, $F_{\text{ADD}(19, 240)} = 2.11$, $p = 0.005$, $F_{\text{Int}(95, 240)} = 0.96$, $p = 0.575$, bar = s.e. of differences of means).

Relative Oleic Acid (C18:1) Content

Figure 33 depicts the relative oleic acid (C18:1) content with respect to the distance at which experimental samples were collected from the carcasses (0 cm, 10 cm, 20 cm, 30 cm, 40 cm and 50 cm). A similar pattern was noted for C18:1 content as that previously described for the relative content of each fatty acid. In general, the most abundant level of C18:1 was detected at 0 cm followed by 10 cm, 20 cm, 30 cm, 40 cm and 50 cm. The C18:1 content of experimental samples at 0 cm was significantly greater ($p < 0.05$) than that at all other distances from 95.5 ADD up to and including 212.7 ADD and at 256.0, 305.3 and 517.2 ADD. However, the level of C18:1 at 233.8 ADD was significantly higher at 10 cm than all other distances. Furthermore, the C18:1 content detected at 156.5 ADD was significantly greater at 30 cm than at 10 cm and 20 cm. The level of C18:1 at 156.5 ADD was also significantly higher at 40 cm than at 20 cm (Figure 33).

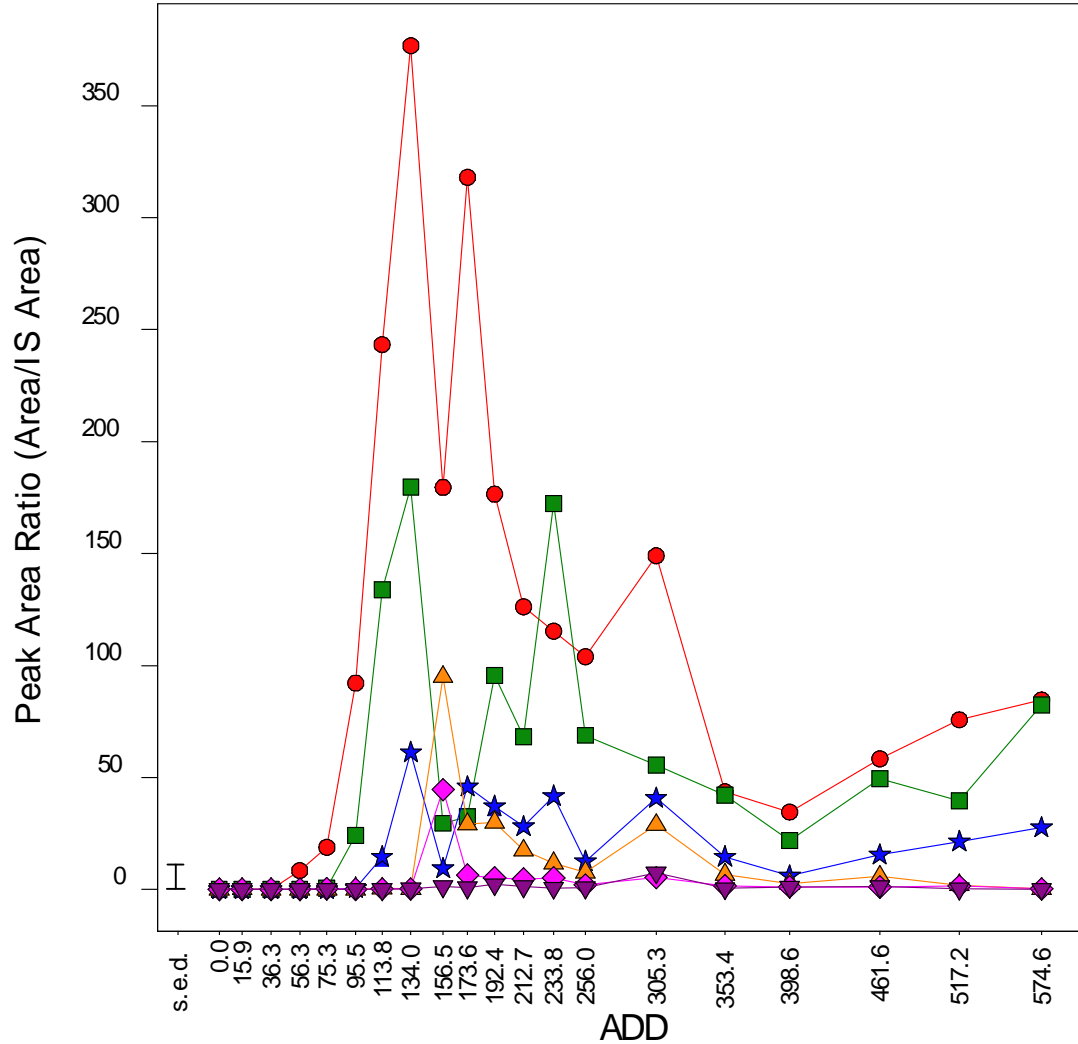


Figure 33. Oleic acid content of experimental soil collected 0 cm (●), 10 cm (■), 20 cm (★), 30 cm (▲), 40 cm (◆) and 50 cm (▼) away from the pig carcasses at the Technical and Protective Operations Facility in Ottawa, Ontario, Canada during the 2009 summer trial. (ANOVA, $F_{\text{Distance}(5, 240)} = 24.11$, $p < 0.001$, $F_{\text{ADD}(19, 240)} = 3.39$, $p < 0.001$, $F_{\text{Int}(95, 240)} = 1.36$, $p = 0.032$, bar = s.e. of differences of means).

Relative Fatty Acid Content

The fatty acid content of experimental soil for each fatty acid was compiled to establish the relative abundance of fatty acid content (Figure 34). Saturated fatty acids (i.e. C16:0 and C18:0) were most abundant over the course of the trial. Specifically, C16:0 was the most abundant fatty acid detected. The level of C16:0 was significantly higher ($p < 0.05$) than all other fatty acids from 95.5 ADD up to and including 305.3 ADD

and from 461.6 to 574.6 ADD. Moreover, C18:0 content was significantly greater than all fatty acids apart from C16:0 at 173.6, 192.4, 233.8, 305.3 and 353.4 ADD and from 461.6 ADD up to and including 574.6 ADD. The unsaturated fatty acid C18:1 was the third most abundant fatty acid with a level significantly greater than C14:0 and C16:1 from 95.5 ADD up to and including 353.4 ADD and from 461.6 to 574.6 ADD. During the period in which increased levels of fatty acids were detected, the carcasses were predominantly in the 'first sign of bone' [6] and 'more than half of bone exposed' [7] stages of decomposition. The levels of C14:0 and C16:1 were negligible in comparison to C16:0, C18:0 and C18:1 (Figure 34).

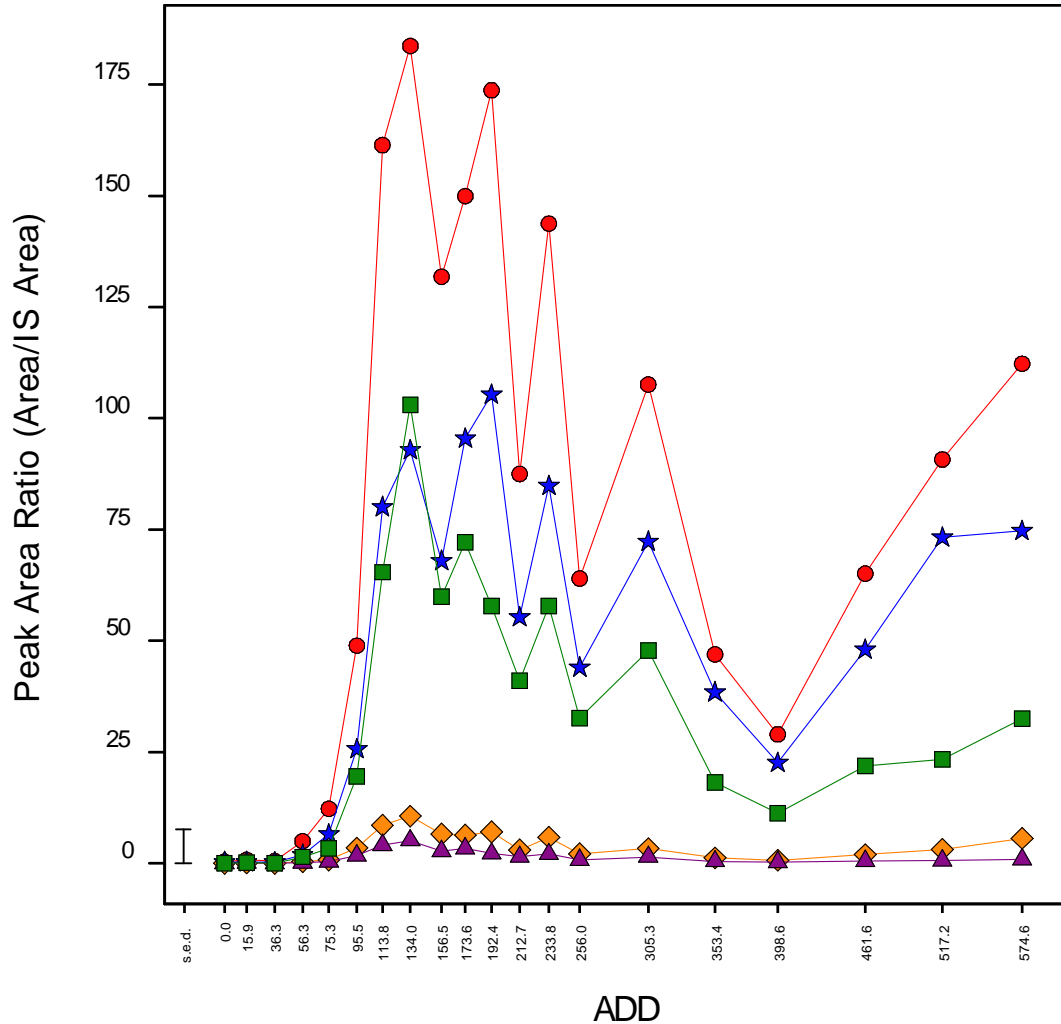


Figure 34. Fatty acid content of experimental soil collected within the cadaver decomposition island at the Technical and Protective Operations Facility in Ottawa, Ontario, Canada during the 2009 summer trial. The fatty acids identified were C14:0 (◆), C16:0 (●), C16:1 (▲), C18:0 (★) and C18:1 (■). (ANOVA, $F_{\text{Fatty acid}(4, 1700)} = 34.24$, $p < 0.001$, $F_{\text{ADD}(19, 1700)} = 5.18$, $p < 0.001$, $F_{\text{Int}(76, 1700)} = 1.04$, $p = 0.386$, bar = s.e. of differences of means).

Relative Fatty Acid Content by Distance

Figure 35 depicts the relative fatty acid content of experimental samples with respect to the distances at which the samples were collected. The level of C16:0 was significantly higher ($p < 0.05$) than all other fatty acids at 0 cm, 10 cm and 20 cm. C18:0 was the second most abundant fatty acid detected. With the exception of C16:0, the level of C18:0 was significantly higher than all other fatty acids at 0 cm and 10 cm. The third most abundant fatty acid, C18:1, was significantly greater than C14:0 and C16:1 from

0 cm to 20 cm. The levels of C14:0 and C16:1 were negligible in comparison to the levels of C16:0, C18:0 and C18:1.

In general, there was a successive decrease in the level of each fatty acid with an increase in distance from the pig carcasses. The levels of C16:0, C18:0 and C18:1 were significantly higher at 0 cm and 10 cm than at all distances located further away. Furthermore, C16:0 content was significantly greater at 20 cm and 30 cm than at 40 cm and 50 cm. Moreover, the level of C18:0 was significantly higher at 20 cm than at 40 cm and 50 cm whereas the level of C18:1 at 20 cm was only significantly higher than that at 50 cm. There was no significant difference between the levels of C14:0 and C16:1 at any distance (Figure 35).

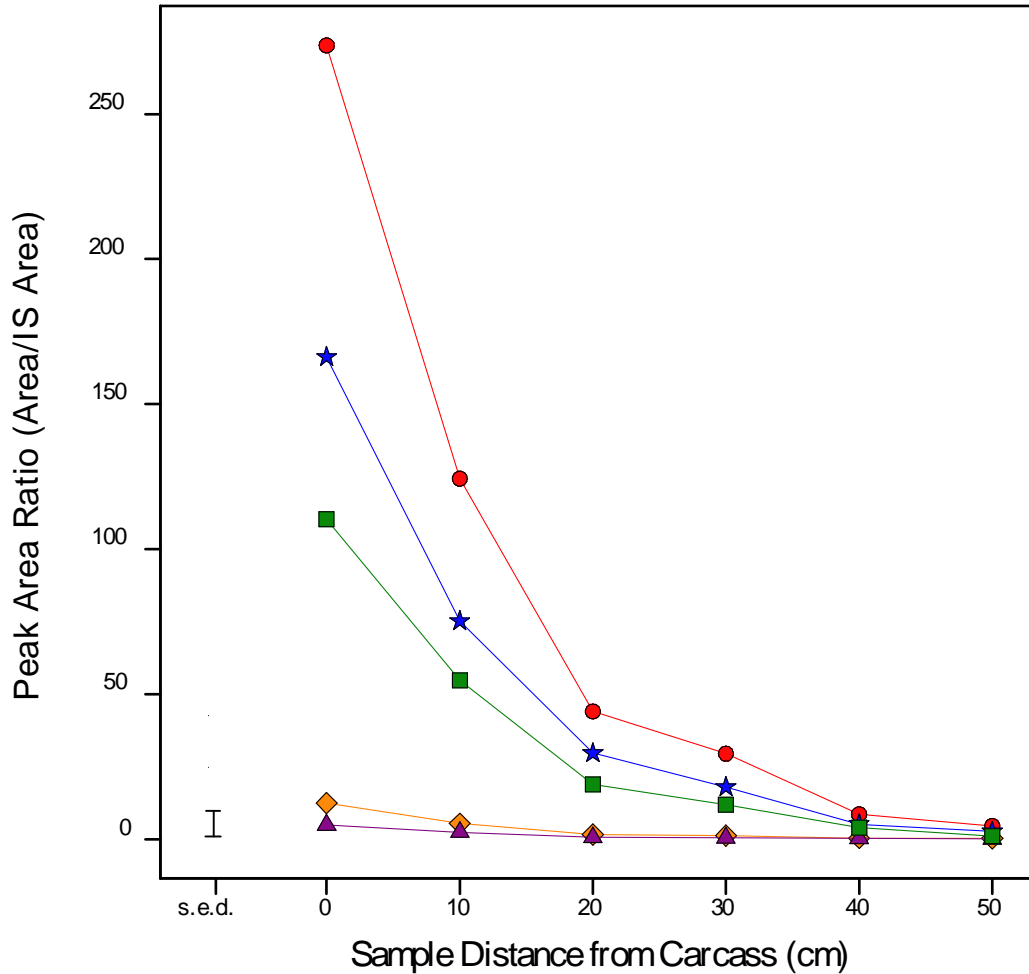


Figure 35. Relative fatty acid content with respect to the distances at which experimental soil samples were collected within the cadaver decomposition island at the Technical and Protective Operations Facility in Ottawa, Ontario, Canada during the 2009 summer trial. The fatty acids identified were C14:0 (—◇—), C16:0 (—●—), C16:1 (—▲—), C18:0 (—★—) and C18:1 (—■—). (ANOVA, $F_{\text{Distance}(5, 1770)} = 58.95$, $p < 0.001$, $F_{\text{Fatty acid}(4, 1770)} = 41.85$, $p < 0.001$, $F_{\text{Int}(20, 1770)} = 11.51$, $p < 0.001$, bar = s.e. of differences of means).

The relative percent composition of fatty acids detected at each distance from the carcasses in the 2009 trial is displayed in Table 5. The percent composition of each fatty acid remained relatively constant at each distance. The saturated fatty acids C16:0 and C18:0 were the most abundant fatty acids detected at each distance with a mean percent composition of 48.5% and 29.7%, respectively. The unsaturated fatty acid C18:1 was the third most abundant fatty acid detected with a mean percent composition of 18.8%. C14:0 and C16:1 were the least abundant fatty acids detected with a mean percent

composition of 2.2% and 0.9%, respectively. These results were similar to those observed over the course of the 2008 trial (refer to Table 4).

Table 5. Relative percent (%) composition of fatty acids detected at each distance from the carcasses in the 2009 trial.

Fatty Acid	Distance From Carcasses (cm)						Mean
	0	10	20	30	40	50	
C14:0	2.2	2.1	1.6	2.0	1.7	3.6	2.2
C16:0	48.2	47.4	46.5	48.4	47.0	53.6	48.5
C16:1	0.9	0.9	0.6	0.7	1.1	1.2	0.9
C18:0	29.3	28.7	31.4	29.5	28.2	31.0	29.7
C18:1	19.4	20.9	19.9	19.5	22.1	10.7	18.8

Cadaver Decomposition Island (CDI) Perimeter

The ‘Observed CDI Perimeter’ was measured as described in *Chapter 2: Materials and Methods*. Furthermore, the ‘Detected CDI Perimeter’ was determined to be the furthest distance from the carcasses at which fatty acids were detected above basal levels in the soil by GC-MS analysis. Table 6 demonstrates the ‘Observed’ and ‘Detected’ CDI perimeters at each ADD for the 2009 trial. The perimeter measurements were dissimilar across most ADD. The ‘Observed CDI Perimeter’ increased from 0 cm until 156.5 ADD where the maximum CDI perimeter was observed at 50 cm from the carcasses. The ‘Observed CDI Perimeter’ remained at 50 cm until 517.2 ADD when it was observed at 30 cm. Conversely, no distinct pattern was apparent for the ‘Detected CDI Perimeter’ measurements. The CDI perimeter was detected at 0 cm, 10 cm, 20 cm, 30 cm and 50 cm across varying ADD.

Table 6. Perimeter measurements of the cadaver decomposition island (CDI).

ADD	Observed CDI Perimeter (cm)	Detected CDI Perimeter (cm)
0	-	-
15.9	-	-
36.3	-	-
56.3	0	-
75.3	0	-
95.5	10	0
113.8	20	10
134.0	20	20
156.5	50	50
173.6	50	30
192.4	50	50
212.7	50	50
233.8	50	20
256.0	50	10
305.3	50	50
353.4	50	10
398.6	50	50
461.6	50	50
517.2	30	10
574.6	30	20

4.4.3 Discussion

Fatty Acid Content of Decomposition Soil

The analysis of fatty acids in decomposition soil was carried out to determine its usefulness for estimating the PMI. Fatty acids are released from adipose tissue during the decomposition process (Dent et al., 2004). Adipose tissue is mainly composed of lipids (60-85% by weight) of which 90-99% are triglycerides (Hirsch et al., 1960; Dent et al., 2004). Each triglyceride molecule is comprised of one glycerol molecule attached to three fatty acid molecules of varying carbon chain length (Dent et al., 2004). In humans, the most common fatty acid in adipose tissue is the unsaturated fatty acid, oleic acid (C18:1) (Hirsch et al., 1960; Pfeiffer et al., 1998; Dent et al., 2004; Janaway et al., 2009). Similarly, lipid content and fatty acid composition studies on adipose tissue indicated that oleic acid (C18:1) is the most abundant fatty acid in pigs (Davenel et al., 1999; Monziols et al., 2007). The unsaturated fatty acids, linoleic acid (C18:2) and palmitoleic acid (C16:1), as well as the saturated fatty acids, palmitic acid (C16:0) and stearic acid (C18:0), are also widespread in human and pig adipose tissues (Hirsch et al., 1960; Pfeiffer et al., 1998; Davenel et al., 1999; Dent et al., 2004; Monziols et al., 2007). Myristic acid (C14:0) has been detected in adipose tissue, however to a lesser extent (Hirsch et al., 1960; Monziols et al., 2007).

After death, triglycerides are hydrolyzed by intrinsic lipases to yield a mixture of free fatty acids (Dent et al., 2004; Mohan Kumar et al., 2009; Notter et al., 2009). Depending on oxygen availability, fatty acids can undergo oxidation or hydrogenation. In aerobic conditions microorganisms (bacteria and fungi) can carry out oxidation reactions to produce aldehydes and ketones (Fiedler and Graw, 2003; Dent et al., 2004; Mohan Kumar et al., 2009; Notter et al., 2009). Conversely, in an anaerobic environment unsaturated fatty acids can undergo hydrogenation by bacterial enzymes to yield saturated fatty acids (Fiedler and Graw, 2003; Dent et al., 2004; Mohan Kumar et al., 2009; Notter et al., 2009). Furthermore, a single step β -oxidation, in which a two-carbon (C₂) unit is lost from the fatty acid chain, can also be carried out by bacterial enzymes (Bereuter et al., 1996; Fiedler and Graw, 2003).

At end-stage autolysis, an anaerobic environment ensues within the decomposing remains which initiates the putrefactive process (Gill-King, 1997). Throughout the putrefactive process intrinsic microorganisms degrade macromolecules (Gill-King, 1997). In the case of adipose tissue degradation, unsaturated fatty acids are hydrogenated to saturated fatty acids due to the anaerobic conditions. As a result, C18:1 and C18:2 can be converted to C18:0 while C16:1 can be converted to C16:0 (Dent et al., 2004; Forbes et al., 2004). A single step β -oxidation can further degrade C18:0 to C16:0 (Bereuter et al., 1996; Notter et al., 2009). Although, no known literature has cited the conversion of C16:0 to C14:0, it may be considered as a possible degradative pathway.

The analysis of fatty acids extracted from the soil of buried remains is often studied with respect to adipocere formation. Adipocere is a soap-like substance that can develop following the postmortem conversion of adipose tissue from decomposing remains into a lipid mixture under anaerobic conditions (Forbes et al., 2003). Adipocere may take weeks or years to develop (Forbes et al., 2003) as anaerobic processes occur at a slower rate than aerobic processes (Janaway et al., 2009). The analysis of fatty acids can be conducted over long time periods, as fatty acids have been detected in 12 year old gravesoil samples collected from exhumations carried out in Australian cemeteries (Forbes et al., 2003). Furthermore, Vane and Trick (2005) detected fatty acids in soil samples recovered from burial sites of cattle and pig carcasses from the Foot and Mouth epidemic of 1967. The generation of a fatty acid profile may provide information regarding the extent of adipocere formation which, when all factors considered, may aid in the estimation of the decomposition interval (Forbes et al., 2004). Although the formation of adipocere was not observed in this study, analyzing the fatty acid content of decomposition soil from pig carcasses decomposing on a soil surface may provide information on the extent of decomposition thus aiding in PMI estimations.

The analysis of free fatty acids extracted from control and decomposition soil collected during the 2008 and 2009 trials was conducted using Gas Chromatography-Mass Spectrometry (GC-MS). The trimethylsilyl (TMS) fatty acid esters identified in soil samples were myristic acid (C14:0), palmitic acid (C16:0), palmitoleic acid (C16:1), stearic acid (C18:0) and oleic acid (C18:1) (refer to Figure 22a-b). Contrary to results

obtained in other studies (Forbes et al., 2003; Notter et al., 2008), the saturated fatty acids C16:0 and C18:0 eluted from the gas chromatograph (GC) prior to their corresponding unsaturated fatty acids C16:1 and C18:1, respectively. The elution order is dependent on the boiling point of compounds and the polarity of the GC column (Christie, 2008). Christie (2008) indicated that saturated fatty acids elute before their corresponding unsaturated fatty acids in high polarity columns, such as the column used in this study (VF-23ms column, Varian Inc. Canada, Mississauga, Canada). Furthermore, the chromatogram displayed other peaks that could not be identified with a high degree of certainty using the mass spectral library. The library indicated, however, that the unidentified compounds were siloxane-containing compounds suggesting the peaks were most likely generated by excess derivatizing agent (BSTFA), artefacts produced by the derivatizing agent and/or derivatization of nonspecific compounds extracted from the soil matrix (Little, 1999).

For each fatty acid detected (C14:0, C16:0, C16:1, C18:0 and C18:1) in the 2008 (refer to Figures 23-27) and 2009 trials (refer to Figures 29-33 and Appendices B-F), the fatty acid content of experimental soil was significantly higher than control soil predominantly during the ‘first sign of bone’ [6] and ‘more than half of bone exposed’ [7] stages of decomposition. It was during stage [6] that the majority of decomposition fluid leached from the pig carcasses into the surrounding soil environment. The increase in fatty acid levels over this period can therefore be attributed to the leaching of decomposition fluid into the surrounding soil environment. Furthermore, fatty acids have been detected in studies that analyzed the composition of decomposition fluid (Cabirol et al., 1998; Swann et al., 2010a; Swann et al., 2010b). However, the leaching of decomposition fluid from remains is typically associated with the putrefactive process (Gill-King, 1997; Vass et al., 2002; Dent et al., 2004). This apparent discrepancy is due to the designation of decomposition stages which was based on the most advanced stage observed in the carcasses. Differential decomposition occurs when one area of the carcass is in a different decomposition stage than other areas (Wilson et al., 2007). This phenomenon was observed in the carcasses as skeletonization of the skull (‘first sign of bone’ [6]) typically occurred while the torso of the carcass was in the ‘post bloat’ [5] stage.

It should be noted that the 2008 trial ended at a higher ADD value (1538.2 ADD) than the 2009 trial (574.6 ADD) due to the fact that the 2008 trial was carried out for a longer period of time. This may explain the increased levels of C16:0, C18:0 and C18:1 observed towards the end of the 2009 trial (refer to Figure 34). It is likely that insufficient time elapsed for fatty acid levels to return to basal levels in the 2009 trial.

In the 2008 and 2009 trials, C16:0 was the most abundant fatty acid detected overall. The level of C16:0 of experimental soil samples was significantly higher than all other fatty acids detected from 92.8 to 847.4 ADD and at 1137.9 ADD in 2008 (refer to Figure 28). In 2009, C16:0 was higher than all other fatty acids from 95.5 ADD up to and including 305.3 ADD and from 461.6 to 574.6 ADD (refer to Figure 34). Furthermore, the mean percent composition of C16:0 over the course of the trials was 60.5% in 2008 (refer to Table 4) and 48.5% in 2009 (refer to Table 5). Similar results were obtained by researchers that analyzed the fatty acid content of soil from buried remains (Forbes et al., 2002; Forbes et al., 2003; Forbes et al., 2004; Vane and Trick, 2005). These researchers examined the fatty acid content of soil with respect to adipocere formation. Similar to this study, fatty acids were converted to TMS fatty acid esters prior to GC-MS analysis. C16:0 was determined to be the most abundant fatty acid detected in each study. For example, Forbes et al. (2002) determined that C16:0 comprised 71.0% of the fatty acid content of soil recovered from 13 and 26 year old graves in a wet environment. Similar results were also observed in studies where decomposing tissue samples were analyzed in burial environments (Takatori, 2001; Forbes et al., 2005a; Forbes et al., 2005c; Forbes et al., 2005d; Notter et al., 2008). Again, fatty acids were converted to TMS fatty acid esters in each study, except for the study conducted by Takatori (2001) in which fatty acids were converted to fatty acid methyl esters (FAMES) prior to GC-MS analysis. C16:0 was also the most abundant fatty acid detected in each study. For instance, Takatori (2001) determined that the relative concentration of C16:0 was 55.9% in human adipocere samples at a burial interval of 6 months.

C18:0 was the second most abundant fatty acid detected over the course of the 2008 and 2009 studies (refer to Figure 28 and Figure 34, respectively). In 2008, the

C18:0 content of experimental samples was significantly higher than all other fatty acids, except for C16:0, from 123.0 ADD up to and including 847.4 ADD and at 1137.9 ADD. The level of C18:0 was higher than all fatty acids except C16:0 at 173.6, 192.4, 233.8, 305.3 and 353.4 ADD in the 2009 trial. Furthermore, the mean percent composition of C18:0 was determined to be 29.2% in 2008 (refer to Table 4) and 29.7% in 2009 (refer to Table 5). Similar results were obtained in previous soil analysis studies (Forbes et al., 2002; Forbes et al., 2003; Forbes et al., 2004; Vane and Trick, 2005). Forbes et al. (2002) demonstrated that the level of C18:0 was the second most abundant fatty acid detected. Specifically, the relative percent composition of C18:0 ranged from 21.0% to 35.0% in soil collected from graves ranging from 5.5 to 50 years old. Studies conducted on adipocere tissue samples (Takatori, 2001; Forbes et al., 2005a; Forbes et al., 2005c; Forbes et al., 2005d; Notter et al., 2008) exhibited results comparable to those obtained through soil analysis. It was determined that the percent composition of C18:0 of adipocere samples from animal carcasses (pig, cattle, sheep and rabbit) ranged from 17.0% to 36.0% at a burial interval of 0, 6, 9 and 12 months (Forbes et al., 2005a).

The third most abundant fatty acid detected in the 2008 and 2009 trials was C18:1 (refer to Figures 28 and 34, respectively). The C18:1 content of 2008 experimental soil samples was higher than C14:0 and C16:1 content from 123.0 ADD up to and including 232.9 ADD and at 396.6 ADD. In 2009, C18:1 content was significantly greater than C14:0 and C16:1 from 95.5 ADD up to and including 353.4 ADD and from 461.6 to 574.6 ADD. The mean percent composition of C18:1 was 7.1% and 18.8% in 2008 and 2009, respectively. Comparable results were obtained in other soil and tissue analysis studies (Forbes et al., 2004; Forbes et al., 2005a). The relative percent composition of C18:1 was determined to be 5.8% in soil samples collected beneath a cadaver that was demonstrating an intermediate stage of adipocere formation (Forbes et al., 2004). In addition, the relative percent composition of C18:1 was determined to be 6.0% and 5.0% in pig adipocere samples at a burial interval of 9 and 12 months, respectively (Forbes et al., 2005a).

C14:0 and C16:1 were the least abundant fatty acids detected over the course of the 2008 (refer to Figure 28) and 2009 (refer to Figure 34) trials. The relative abundance

of C14:0 and C16:1 was almost negligible in comparison to the other fatty acids detected. In particular, the mean percent composition of C14:0 was 2.6% in 2008 and 2.2% in 2009. Furthermore, the mean percent composition of C16:1 was 0.6% and 0.9% in 2008 and 2009, respectively. Similar results were obtained in studies on adipocere formation (Vane and Trick, 2005; Forbes et al., 2005a). Soil and tissue analysis of pig and cattle adipocere samples collected from burial pits at various depths indicated that the percent compositions of C14:0 and C16:1 were approximately 3.6% and 0.9%, respectively (Vane and Trick, 2005). In a study conducted by Forbes et al. (2005a), the percent composition of C14:0 in pig adipocere samples was determined to be 2.0% at a burial interval of six months. Over this period, C16:1 went undetected in the same pig adipocere samples (Forbes et al., 2005a).

Fatty acids became detectable in the soil upon the leaching of decomposition fluid from the carcasses into the surrounding environment. Even though C18:1 is the most abundant fatty acid in adipose tissue (Pfeiffer et al., 1998; Davenel et al., 1999; Dent et al., 2004; Monziols et al., 2007; Janaway et al., 2009), it was not the most abundant fatty acid detected over the course of the 2008 and 2009 trials. Furthermore, C18:2, another widespread fatty acid in adipose tissue, was not detected in any of the decomposition soil samples. In this study, C16:0 and C18:0 were the most abundant fatty acids detected in decomposition soil overall. The increased levels of these fatty acids can be attributed to the anaerobic putrefactive processes that occurred within the carcasses. As previously mentioned, C18:1 and C18:2 were most likely converted to C18:0 while C16:1 was converted to C16:0 through the process of hydrogenation. A single step β -oxidation of C18:0 to C16:0 may have also contributed to the increased levels of C16:0. Furthermore, the leaching of decomposition fluid provided an environment for oxidative processes to occur as the anaerobic degradative products were exposed to an aerobic environment. The return of fatty acid levels to basal levels prior to the end of the 2008 trial can be attributed to the oxidation of fatty acids following the exposure of anaerobic degradative products to an aerobic environment.

The relative percent composition determined for each fatty acid in the 2008 and 2009 trials was comparable to the results of fatty acid analysis studies conducted on soil

(Forbes et al., 2002; Forbes et al., 2003; Forbes et al., 2004; Vane and Trick, 2005) and adipocere samples (Takatori, 2001; Forbes et al., 2005a; Forbes et al., 2005c; Forbes et al., 2005d; Notter et al., 2008) from human and animal decomposition trials. However, there was a discrepancy between the decomposition interval of this study and the comparative studies. This study was conducted over weeks (represented in terms of ADD) whereas the comparative studies were conducted over several months or years. The discrepancy was due to the fact that the comparative studies examined the formation of adipocere which is an anaerobic process that can take several weeks to years to develop (Forbes et al., 2003). According to Casper's rule as described by Fiedler and Graw (2003), the degree of degradation of decomposing remains on a soil surface occurs at a rate eight times faster than the rate of degradation beneath the soil surface. Furthermore, adipocere is resistant to degradation and can be stable for several years (Forbes et al., 2002). Conversely, due to the aerobic conditions of this study the levels of fatty acids returned to basal levels prior to the end of the 2008 trial. In addition, there was a discrepancy in the time scale units between this study and the comparative studies. This study expressed time in terms of ADD whereas calendar days (i.e. weeks, months and years) were used in the comparative studies. ADD is based on the accumulation of temperature within a given period allowing for cross-seasonal comparisons. It is probable that temperature data beneath the soil surface was not available for most of the comparative studies; ADD could therefore not be calculated. This discrepancy limits the extent to which comparisons can be made with these studies with respect to the decomposition interval.

Another important difference between the comparative studies (Takatori, 2001; Forbes et al., 2002; Forbes et al., 2003; Forbes et al., 2004; Vane and Trick, 2005; Forbes et al., 2005a; Forbes et al., 2005c; Forbes et al., 2005d; Notter et al., 2008) and this study was the variation in the lipid degradation profile over time. The degree of adipocere formation can be categorized into early, intermediate and advanced stages of adipocere formation (Forbes et al., 2004). In general, these stages are classified by the level of saturated fatty acids in relation to unsaturated fatty acids (Forbes et al., 2004). Each successive stage is associated with an increase in saturated fatty acids and a corresponding decrease in unsaturated fatty acids (Forbes et al., 2004). Conversely, in

this study the relative proportion of each fatty acid remained relatively constant throughout the trials. In effect, neither the decomposition stages nor the lipid degradation profile could be differentiated based on relative proportion of fatty acid content in soil. A drawback to this research is the lack of comparable studies that analyze the fatty acid content in soil from surface decomposition trials.

This research was unique to other fatty acid analysis studies in that decomposition soil was analyzed from pig carcasses decomposing on a soil surface as opposed to buried beneath the soil surface. The effect of decomposition on the surrounding soil environment has been largely unexplored (Benninger et al., 2008), particularly with respect to the fatty acid content of soil from surface decomposition trials. The detection of fatty acids in decomposition soil currently cannot be used for the estimation of the PMI as the relative percent composition of fatty acids is relatively constant throughout the decomposition process. However, the detection of increased fatty acid levels in suspected decomposition soil compared to control soil can potentially be used as evidence to indicate the presence of a decomposition site in cases regarding the relocation or scavenging of remains.

Fatty Acid Cycle

A three peak fatty acid cycle was observed for each fatty acid in the 2008 (refer to Figures 23-27) study. Although the basis for the cycles was not examined, it can be speculated that the cycles were related to a shift in microbial populations. In forensic taphonomy, it is generally accepted that initial decomposition stages are dominated by enteric anaerobic microorganisms whereas soil-bearing and non-enteric microorganisms partake in later stages of decomposition (Carter et al., 2010). Furthermore, microbial communities in soil are affected by factors such as nutrient availability, changes to nutrient input, soil pH and the water content of soil (Rousk et al., 2009). The presence of decomposing remains can alter the status of these factors thereby affecting the microbial communities. These communities have the ability to adapt to the changing environment through functional and/or efficiency changes (Haslam and Tibbett, 2009). Furthermore, the altered environment may provide a competitive advantage to particular populations thus promoting their growth (Rousk et al., 2009). It is possible that altered and/or novel

microbial communities utilize diverse degradative pathways leading to a resurgence in fatty acid levels. It can also be hypothesized that microorganisms produce and release fatty acids through metabolic processes thereby contributing to the levels of fatty acids detected.

Swann et al. (2010b) reported a similar three peak fatty acid cycle in their study of decomposition fluids in the absence of soil. The authors hypothesized that the cycles were related to the level of fly activity, the feeding cycle of fly larvae (maggots) and the adipose tissue of the remains (Swann et al., 2010b). The cycles were attributed to the apparent increase in fatty acid levels during the initial growth and feeding stage of the maggots followed by a decrease in fatty acid production during the pupation period (Swann et al., 2010b). The successive increases in fatty acid levels were attributed to successive waves of fly colonization (Swann et al., 2010b). The relationship of the fly cycle to fatty acid levels was not tested by Swann et al. (2010b) nor during this study and further research is therefore required to test this hypothesis. The three peak fatty acid cycle was observed for each fatty acid during the 2008 trial. The basis of the three peak fatty acid cycle may reveal information about other decomposition processes e.g. the succession of microorganisms and the maggot feeding cycle. By discerning an interaction of seemingly independent processes, the decomposition process as a whole can be more thoroughly understood. This distinct pattern has the potential to aid in PMI estimations upon further research.

Fatty Acid Content by Distance from the Carcasses

A different sampling method was used in the 2009 trial as compared to the 2008 trial. Soil samples were collected at 10 cm intervals from the soil-carcass boundary (0 cm) up to 50 cm. This sampling method was designed to characterize the CDI at regular intervals throughout the decomposition process. Control and experimental soil samples were analyzed for the content of each identified fatty acid (C14:0, C16:0, C16:1, C18:0 and C18:1) at each distance.

In general, the most abundant levels of each fatty acid were detected at 0 cm and successively decreased until 50 cm (refer to Figures 29-33). The increased levels of fatty

acids at 0 cm were expected as the carcasses were in direct contact with the soil at this distance. Also, a decrease in fatty acid levels was expected to coincide with an increase in sample distance from the carcasses. It can be speculated that the soil matrix played a diluting role with respect to the fatty acid levels; the highest abundance of fatty acids entering the soil would be found closest to their source (i.e. the carcass) and as decomposition fluid dispersed outwards fewer fatty acids would be available to enter the soil matrix with increasing distance from the carcass. The anomalies observed at 156.5 and 233.8 ADD could be attributed to CDI irregularities. Although the sampling method was highly standardized for the 2009 trial, the area from which samples were collected was different each sampling day and the decomposition fluid did not necessarily leach from the remains in a uniform manner. For example, it was observed that more fluid leached from the abdominal area as compared to the dorsal side of the carcasses. Furthermore, it is possible that irregularities in the topographic features of the soil and/or micro-environmental differences in the soil can promote the retention of decomposition fluid, and therefore fatty acids, over other areas of the soil landscape.

The 'Observed CDI Perimeter' was measured at the research site whereas the 'Detected CDI Perimeter' was determined through GC-MS analysis (refer to Table 6). The measurements of the 'Observed CDI Perimeter' did not correspond with the 'Detected CDI Perimeter'. The CDI is noted visually as a dark stain surrounding the decomposing remains (Carter et al., 2007). However, the exact nature of the CDI has yet to be elucidated. The discrepancy between the measurements of the perimeters indicates that determining the fatty acid content of soil collected from anywhere within the CDI is not necessarily an appropriate method of sampling. The highest fatty acid levels were detected at the soil-carcass boundary (0 cm), therefore soil sample collection should be carried out closest to the decomposing remains to detect the highest levels of fatty acids. In cases where remains have been relocated, for example, soil samples should be collected at the site where the remains are suspected to have been placed. Furthermore, control sites for soil analysis should be established several metres from the remains as there is evidence that fatty acids can be detected 50 cm away from the remains.

4.5 Limitations

A limitation to this study was the use of different sampling methods during the two research trials. A more standardized sampling method was utilized during the 2009 trial as compared to the 2008 trial. As such, soil samples collected at regular intervals aimed at characterizing the CDI with respect to fatty acid content were not collected during the 2008 trial. The use of a similar sampling regime throughout the two trials would have facilitated inter-year comparisons. Furthermore, in order to facilitate inter-study comparisons a Standard Operating Procedure (SOP) for soil sampling should be developed. This would provide standard sampling procedures for all researchers performing soil analysis thereby, allowing for comparisons to be made across studies conducted in varying soil types and across geographic regions, seasons and years.

Furthermore, the 2008 trial was carried out for a longer period of time than the 2009 trial. The 2009 trial was ended at 574.6 ADD (experimental day 28) due to the fact that soft tissue had been completely removed from the carcasses with only dry skin and bones remaining. However, not all fatty acid levels returned to basal levels by the end of the 2009 trial. It is possible that an incomplete fatty acid profile was obtained in 2009. The generation of a complete fatty acid profile is essential to understanding the lipid degradative process. Moreover, a complete fatty acid profile may provide information that can be linked to other decomposition processes, such as the maggot feeding cycle as postulated by Swann et al. (2010b).

The delayed arrival of the GC-MS instrument proved to be another drawback of this study. The delivery of the instrument was postponed for several months. Subsequent to the arrival of the instrument several days of technical training were required. Due to the time constraints the delay imposed, soil analysis of 2008 samples collected in the forested area at the research site could not be conducted. The analysis of these soil samples could have revealed or alluded to the effect of sun exposure on the chemical properties and composition of decomposition soil. This research is important as remains can be exposed to various levels of sun exposure (e.g. full or partial sun exposure).

4.6 Relevance to Forensic Science

An important aspect of forensic science research is to develop accurate methods for estimating the PMI. Current methods used in PMI estimation typically involve the characteristic chemical or physical changes that occur in the body after death and throughout the decomposition process (Perry et al., 1988; Babapulle and Jayasundera, 1993; Munoz et al., 2001; Vass et al., 2002). However, the use of soil-based methods for aiding in PMI estimations has been deemed plausible (Benninger et al., 2008). The results of this study indicated that the water content, pH and fatty acid content of soil cannot be used to estimate the PMI at this time. The analysis of soil properties (i.e. soil pH and fatty acid content of soil), however, can be considered for use in cases where remains have been relocated to determine the initial deposition site.

In this study, variation in soil pH and increased levels of fatty acids were detected in decomposition soil as compared to control soil. In cases where the relocation of remains is suspected, soil pH measurements and the fatty acid content of soil can provide supporting or opposing evidence for law enforcement agencies. These soil properties are also especially important in forensic science for cases in which remains have not been recovered. Variation in soil pH measurements and increased fatty acid levels detected in an area suspected of having contained decomposing remains can be used to support the premise that remains had been present in the area at one time in the recent past. Furthermore, if soil collected beneath decomposing remains do not demonstrate differences in pH and fatty acid content from control soil samples it can be speculated that the location of the remains was not the initial site of decomposition or a significant amount of time has passed since decomposition occurred. It should be reiterated that the results presented herein can only be applied to environments comprised of fine sand. Soil-based methods, such as those utilized in this study, would not require extensive training for law enforcement agents as far as evidence collection is concerned, though standardization would be required. Soil samples could then be sent to an appropriate laboratory for soil analysis. The methods employed in this study could be easily implemented by law enforcement officials.

Chapter 5 – Diffusion Model

5.1 Results

A diffusion model was developed to predict the development of the cadaver decomposition island (CDI) in soil over time (refer to 2.7.2 *Derivation of the Diffusion Model*). The CDI forms as decomposition fluid leaches from decomposing remains into the surrounding soil.

5.1.1 Diffusion Model Test

The diffusion model test was carried out to determine if the soil properties required for the diffusion model could be ascertained by determining the rate at which a set amount of fluid diffused through the soil. It was determined that the diffusion model test was inappropriate for measuring soil properties for the diffusion model developed in this study and, therefore, was not considered in the development of the diffusion model. In order to determine the soil properties to be used in the diffusion model, the test must be able to accurately represent the physical mechanisms that are present during the diffusion process. This would ensure that the cadaver regime in Figure 2 is being considered in the determination of the soil properties. Other tests (e.g. evaporative test) have recently been developed to measure these properties.

5.1.2 Simulation of the Diffusion Model

The derivation of the diffusion model was performed using soil and fluid parameters including, permeability, soil and fluid density, viscosity and moisture content. The result is a classical expression for flow through a porous medium. The behaviour of the spreading of the moisture (representative of decomposition fluid) with respect to the moisture content of the soil and the radius (distance to which the front of the CDI evolved) is illustrated in Figure 36. A time period of $T = 1$ corresponds to 23 hours. This simulation was based on the assumptions that the fluid is released from a point source (not from the remains as a whole entity) and that there was a boundary condition of zero residual moisture in the soil. As seen in Figure 36, the moisture content decreases successively from $T = 1$ to $T = 10$ while, the radius at which the front of the fluid (the CDI) spread through the soil increased successively from $T = 1$ to $T = 10$. The values for the moisture content used in this simulation were similar to the values determined for the

gravimetric water content of experimental soil (soil containing decomposition fluid) in the 2009 trial (refer to Figure 19). The change in radius from $T = 1$ to $T = 10$ is approximately 0.3 m (30 cm). This value is also similar to the maximum value of the ‘Observed CDI Perimeter’ (50 cm) which was initially observed on experimental day 8 (156.5 ADD) (refer to Table 6). The ‘Observed CDI Perimeter’ is comparable to the radius predicted by the simulated model. The degree by which the radius increases sequentially decreases at each time point; the difference in radius from $T = 1$ to $T = 2$ is approximately 7.6 cm whereas the difference from $T = 9$ to $T = 10$ is approximately 1.7 cm.

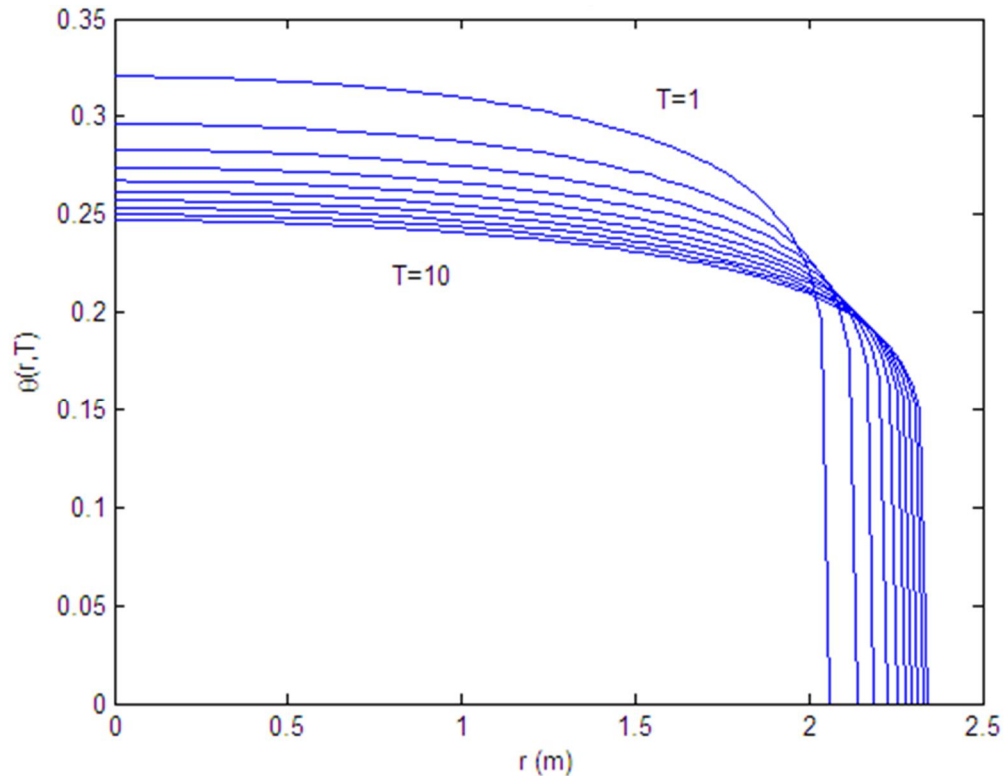


Figure 36. The behaviour of moisture content, representative of decomposition fluid, as a function of radius, r , and time, T , for Rubicon sandy loam soil. $T = 1$ corresponds to 23 hours.

The evolution of the liquid front in Rubicon sandy loam soil (this study) and Isere sand is represented in Figure 37. It should be noted that the soil types considered here were not named based on characterization of the soil but rather were taken from the

literature (refer to Tzimopoulos and Sakellariou-Makrantonaki, 1996). The properties of Rubicon sandy loam soil were determined to best represent the soil type used in this study (fine sand as determined by the Agriculture and Food Laboratory at the University of Guelph). The change in the front radius (vertical difference) over time should be considered and not the exact radius at which each curve was generated. The difference in the front radius from $T = 1$ to $T = 10$ is approximately 0.3 m (30 cm) in Rubicon sandy loam and approximately 0.2 m (20 cm) in Iserre sand. This simulation was also based on the assumption that the fluid was released from a point source.

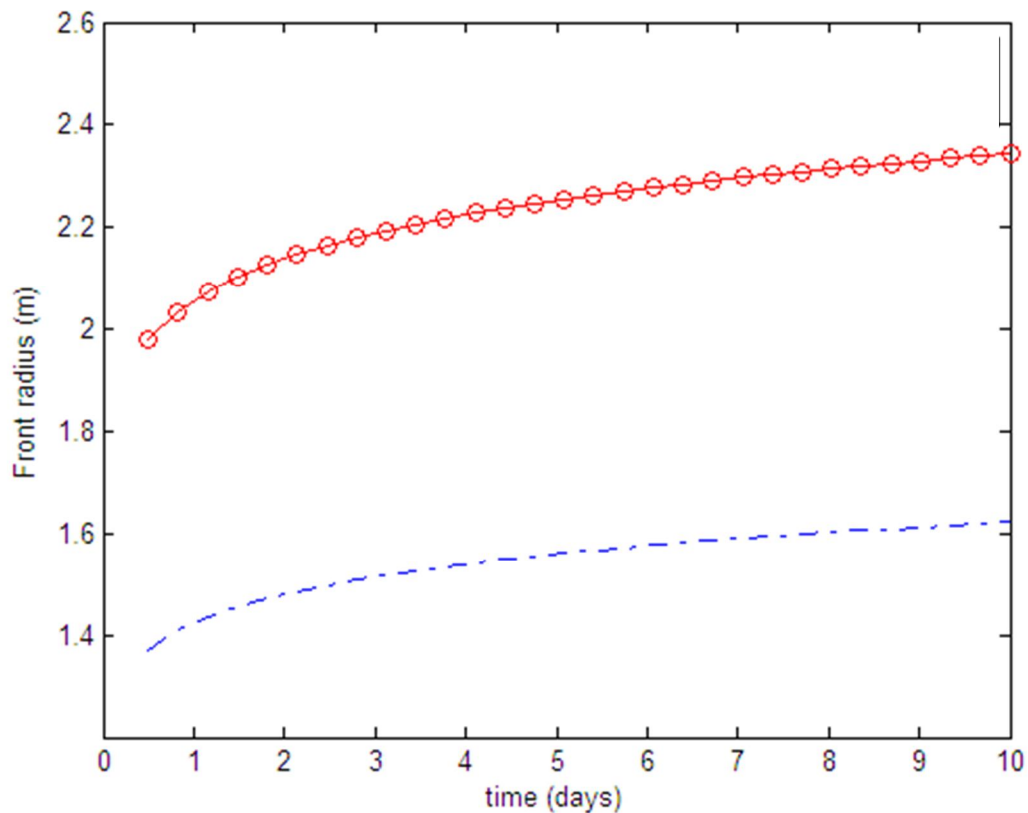


Figure 37. Evolution of the liquid front in (—○—) Rubicon sandy loam and (---) Iserre sand. For Rubicon sandy loam $m = 7.84$ and for Iserre sand $m = 3.25$ (Tzimopoulos and Sakellariou-Makrantonaki, 1996).

5.2 Discussion

A diffusion model was successfully developed to model the development of the cadaver decomposition island (CDI) in soil over time. The soil texture was determined to

be fine sand as per the Agriculture and Food Laboratory at the University of Guelph in Guelph, Ontario. However, the parameters for the soil used in this model are better represented by Rubicon sandy loam soil described by Tzimopoulos and Sakellarios-Makrantonaki (1996). It can be assumed that although named differently the parameters for each soil type are similar.

It was determined that the diffusion model test conducted was inappropriate for measuring soil properties for the diffusion model developed in this study due to the nature of the test. This model assumes that the decomposing remains act as a hub from which decomposition fluid is released. The leaching of decomposition fluid into the surrounding soil moistens the soil but does not cause it to become saturated. This notion implies that the cadaver regime illustrated in Figure 4 is more representative of the parameters considered in the development of this model and that capillary pressure, P_c , has a substantial effect on the diffusion of the fluid through the soil. The diffusion model test is more representative of the saturated soil regime illustrated in Figure 4. This regime implies that the soil is saturated and consequently, that the effect of the capillary pressure is low (refer to Figure 4). The results of this test were, therefore, not considered in the diffusion model. An evaporative test may prove to be more appropriate for the determination of soil properties as opposed to the infiltration test used in this study since it records soil properties in unsaturated conditions (Schindler et al., 2010).

The simulation of the diffusion model demonstrated that there was a successive decrease in moisture content and increase in radius of the fluid front from $T = 1$ to $T = 10$ (refer to Figure 36). Since the model assumes that the fluid is released from a point source, the moisture content at the source decreases with time as the fluid diffuses through the soil and away from the source. Furthermore, as the fluid is propagating through the soil the radius of the fluid front increases with time, however, the speed at which the fluid front moves decreases. The change in radius from $T = 1$ to $T = 10$ was approximately 30 cm as depicted in Figure 36. Although the maximum radius was not predicted by the simulation, it can be assumed that the predicted radius will not extend much beyond 30 cm due to the decrease in the degree by which the radius increases with each time point. This value is similar to the maximum value measured for the 'Observed

CDI Perimeter' (fluid front) at the research site in the 2009 trial (50 cm). This perimeter was initially observed on experimental day 8 which also corresponds well with $T = 10$ (approximately 10 days). In this study, the radius of the CDI ('Observed CDI Perimeter') was measured as if the fluid was released from a point source as one measurement of the perimeter was taken with a metre stick each sampling day (a measurement was taken at the soil-carcass boundary (0 cm) up to the perimeter). However, due to potential irregularities in the perimeter of the CDI around the remains an effective radius should be calculated from the area of the CDI.

The results of the simulation indicate that there is a potential to generate PMI estimations for early stages of decomposition if soil parameters can be determined. The CDI radius can be measured and checked against the model to determine the estimated PMI. PMI estimations become difficult to predict for more advanced stages of decomposition due to the fact that the fluid will diffuse through the soil to a maximum radius (i.e. once the decomposition fluid has ceased to leach from the remains). The maximum radius may be observed for extended periods of time (refer to Table 6). For more advanced stages, minimum PMI estimations can be provided. However, more accuracy between the observed data ('Observed CDI Perimeter') and the simulated model may be required to generate postmortem interval (PMI) estimations that can be applied to actual forensic cases i.e. calculation of the effective radius. The discrepancy between the 'Observed CDI Perimeter' and the radius predicted by the model (approximately 20 cm) may possibly cause PMI estimations to be miscalculated by several days. Further studies may reveal more accurate soil and fluid parameters to be used in the model. The inclusion of more complex parameters may also be required for cases involving complex soil topography and for cases in which violations of assumptions occur.

The extent of the evolution of the liquid front was predicted to be more extensive in Rubicon sandy loam soil than in Isere sand. The parameters described for Isere sand indicated that this soil type is less conducive to the propagation of fluid through pore spaces than Rubicon sandy loam soil (Tzimopoulos and Sakellarios-Makrantonaki, 1996). This difference was predicted when the model was simulated using the soil parameters specific for each soil type i.e. the difference in the front radius was

approximately 30 cm in Rubicon sandy loam soil whereas the difference was only 20 cm in Isere sand. Given appropriate soil parameters can be determined for a particular soil type, this model has the ability to predict differences in the evolution of the liquid front and, with further research, potentially generate PMI estimations in various soil types.

5.3 Limitations

An important limitation to this study was the need to make assumptions regarding the soil matrix and fluid properties. For example, it was assumed that the soil matrix does not deform when fluid passes through it and that the fluid that leaches into the soil is not affected by evaporation or precipitation. These assumptions provide ideal situations for the ease of deriving and simulating the diffusion model. There is a possibility, however, that these assumptions will not be accurate in certain environmental conditions. Excessive precipitation, for instance, could skew the radius of the liquid front thereby inhibiting the measurement of the front by visual means. The diffusion model is sensitive to minor changes in the parameters of the model and thus violation of any of the assumptions could lead to inaccurate PMI estimations.

The diffusion model assumes that the decomposition fluid is released from a point source. In this study, the radius of the CDI ('Observed CDI Perimeter') was measured as if fluid was released from a point source. However, due to potential irregularities in the perimeter of the CDI around the remains an effective radius should be calculated from the area of the CDI (A) where,

$$A(t) = \pi(r(t))^2 \quad (5.1)$$

and r is equal to radius and t is equal to time. As an effective radius was not measured, the radius of the CDI may have been over- or underestimated in this study. Measurements of the effective radius should be compared to the predicted radius to determine if better accuracy can be achieved.

5.4 Relevance to Forensic Science

The simulation of the nonlinear diffusion model is a newly developed method that has the potential to provide PMI estimations for early stages of decomposition. For more advanced stages of decomposition minimum PMI estimations can be generated. The diffusion model can be simulated for different soil types using determined soil parameters although sufficient background in mathematical modelling may be required to simulate the model. Effects of precipitation and evaporation can also be routinely added to the model. By determining parameters of the soil required for the diffusion model from the area in which the decomposing remains were found, simulations of the diffusion model can be carried out. The effective radius of the CDI (as determined from the area of the ‘Observed CDI Perimeter’) can be compared with the model to estimate the PMI.

***Chapter 6 –
Conclusions and Future
Considerations***

6.1 Conclusions

The physical and chemical analysis of pig decomposition using conventional and newly developed methods was successfully carried out in this study. The aims of this study were to determine a relationship of the visible characteristics of human and pig decomposition using a decomposition scoring system to determine whether there is a difference, to generate a fatty acid profile from decomposition soil using GC-MS analysis and to develop a diffusion model to predict the development of the CDI. Although the PMI cannot be estimated from the methods used at this time, further studies have the potential to aid in PMI estimations.

Photographs of pig carcasses decomposing on forested and open land were scored using a decomposition scoring system developed for human decomposition. It was determined that a decomposition scoring system that accounts for the differential decomposition of pig carcasses is required to better represent pig decomposition. The decomposition scores for both sets of carcasses were related to ADD and ADD values were compared. In general, the ADD values for each decomposition score obtained for the shaded and sun exposed carcasses were significantly different; however, there was more similarity between the ADD values for the onset of each score. These results indicated that the characterization of the end of each decomposition score (stage) was required and that the effect of solar radiation on temperature variations should be considered in the calculation of ADD. The development of improved decomposing scoring systems and methods for calculating ADD has the potential to aid in the estimation of the PMI in pig carcass decomposition. This study also indicated that the calculation of ADD must be modified to allow for a meaningful comparison of pig and human decomposition.

The decomposition of pig carcasses was found to alter the underlying soil environment. The water content, pH and fatty acid content of soil was altered in response to the presence of decomposing pig carcasses. Palmitic (C16:0), stearic (C18:0) and oleic (C18:1) acids were the most abundant fatty acids detected in decomposition soil whereas the levels of myristic (C14:0) and palmitoleic (C16:1) acids were negligible in comparison. The most abundant levels of fatty acids were also detected at the soil-

carcass boundary (0 cm) and successively decreased at further distances. The chemical changes in soil associated with pig decomposition in particular, variations in soil pH and increased fatty acid content of decomposition soil, has the potential to be used in forensic science as a means of identifying a decomposition site. Furthermore, a distinct three peak fatty acid cycle was observed which has the potential to aid in PMI estimations upon further research.

A nonlinear diffusion model was developed to predict the development of the CDI in soil over time. The simulation of the model using soil and fluid parameters indicated that the diffusion model has the potential to be used in estimating the PMI for early stages of decomposition, although means for calculating the effective radius must first be established. Moreover, a minimum PMI estimation can potentially be provided for advanced stages of decomposition. The measurement of the effective radius of the CDI should correspond to a radius predicted by the simulated model and thus to a particular time point or the estimated PMI.

6.2 Future Considerations

In this study, it was determined that the scoring of photographs of pig carcasses using the system developed for human remains may not be appropriate to qualify pig decomposition due to differential decomposition observed in the carcasses. A scoring system that considers the differential decomposition of remains as well as the recovery of partial remains is required to improve the representation of decomposition processes. Furthermore, the comparison of ADD values for shaded and sun exposed pig carcasses indicated that the characterization of the end of each decomposition score, with the goal of providing similar ADD values for remains decomposing in varying environmental conditions, would be ideal. However, this task could prove to be very difficult as physical characteristics of decomposition are associated with the onset of a decomposition score (stage) and not the end given that decomposition is a continuum. In order to decrease the variability of the ADD values for the decomposition scores between the two groups of carcasses studies should focus on improving the calculation of ADD as

opposed to further characterizing decomposition scores. The effect of solar radiation on sun exposed remains must be examined especially with respect to temperature effects and the calculation of ADD. Although the decomposition scoring system used in this study cannot aid in estimating the PMI at this time, the development of improved scoring systems and methods for calculating ADD that account for temperature differences in varying environments (e.g. no sun versus full sun exposure) have the potential to aid in PMI estimations. Improved methods for calculating ADD may, also, allow for a meaningful comparison of pig and human decomposition which may elucidate whether pig decomposition is an appropriate model for human decomposition.

The gravimetric water content, pH and fatty acid analysis of control and experimental soil were successfully carried out in this study. The results indicated that soil pH and fatty acid content of soil have the potential to indicate the presence of a decomposition site in cases of the relocation and scavenging of remains. PMI estimations could not be formulated from the current results; however, there is potential for further research in this area to aid in PMI estimations. The three peak fatty acid cycle was a distinct feature observed for each fatty acid in the 2008 trial. Additional surface decomposition trials need to be conducted in varying soil types in an attempt to replicate the results herein and to provide comparative surface decomposition studies. Studies should also be performed to determine the concentration of fatty acids extracted from decomposition soil throughout the decomposition process to further characterize the three peak cycle and potentially aid in PMI estimations. These studies should be conducted using a standardized sampling method to provide comparable results. A Standard Operating Procedure (SOP) should be developed to standardize techniques for collecting samples for soil analysis thus facilitating inter-study comparisons. Furthermore, an analysis of tissue and soil collected simultaneously from remains decomposing on the soil surface should be conducted in an attempt to relate the fatty acid content of tissue to the fatty acid content of decomposition soil. This research may elucidate more information about the degradation of lipids and how this corresponds to the fatty acids detected in decomposition soil. The analysis of soil collected from remains decomposing in a forested (shaded) area should also be conducted to elucidate the effects of sun exposure on the decomposition process with respect to the chemical properties and composition of

decomposition soil. Furthermore, studies need to be carried out on the feeding cycle of maggots in relation to the fatty acid content of soil. A positive relationship could lead to the development of more accurate PMI estimations given that forensic entomology is currently used to estimate the PMI.

The simulation of the diffusion model provided an indication that further studies have the potential to provide more accurate PMI estimations. Studies should be conducted on methods for determining or calculating the effective radius of the CDI. Another consideration for the model should be the release of fluid as a function of time. Fluid is released from the remains as a whole (not from a point source as assumed in this model) and is released over several time points. As such, an effective radius must be calculated over time to more accurately represent the development of the CDI over time and thus provide more accurate PMI estimations. Furthermore, parameters in the diffusion model should be included to better represent situations where assumptions of the model have been violated such as cases where excessive precipitation or evaporation interfere with the normal development of the CDI. A model should also be developed to characterize situations in which remains are recovered on soil surfaces with complex topographies such as an inclination.

Chapter 7 – References

- Adlam, R.E. and T. Simmons (2007). The effect of repeated physical disturbance on soft tissue decomposition--are taphonomic studies an accurate reflection of decomposition? *Journal of Forensic Sciences*, **52**(5): 1007-1014.
- Amendt, J., R. Krettek and R. Zehner (2004). Forensic entomology. *Naturwissenschaften*, **91**(2): 51-65.
- Anderson, G.S. and S.L. VanLaerhoven (1996). Initial studies on insect succession on carrion in southwestern British Columbia. *Journal of Forensic Sciences*, **41**(4): 617-625.
- Archer, M.S. (2004). Rainfall and temperature effects on the decomposition rate of exposed neonatal remains. *Science and Justice*, **44**(1): 35-41.
- Assouline, S. and D.M. Tartakovsky (2001). Unsaturated hydraulic conductivity function based on a soil fragmentation process. *Water Resources Research*, **35**(5): 1309-1312.
- Aturaliya, S. and A. Lukasewycz (1999). Experimental forensic and bioanthropological aspects of soft tissue taphonomy: 1. Factors influencing postmortem tissue desiccation rate. *Journal of Forensic Sciences*, **44**(5): 893-896.
- Babapulle, C.J. and N.P. Jayasundera (1993). Cellular changes and time since death. *Medicine, Science and the Law*, **33**(3): 213-222.
- Bass, W.M. (1997). Outdoor Decomposition Rates in Tennessee. In W.D. Haglund and M.H. Sorg (Eds.), *Forensic Taphonomy: The Postmortem Fate of Human Remains*. New York, CRC Press: 181-186.
- Bear, J. and Y. Bachmat (1990). The Porous Medium. In *Introduction to Modeling of Transport Phenomena in Porous Media*. London, Kluwer Academic: 1-15.
- Benninger, L.A., D.O. Carter and S.L. Forbes (2008). The biochemical alteration of soil beneath a decomposing carcass. *Forensic Science International*, **180**(2-3): 70-75.
- Bereuter, T.L., E. Lorbeer, C. Reiter, H. Seidler and H. Unterdorfer (1996). Post-mortem alterations of human lipids - part I: evaluation of adipocere formation and mummification by desiccation. In K. Spindler, H. Wilfing, E. Rastbichler-Zissernig, D. zur Nedden and H. Nothdurfter (Eds.), *Human Mummies: A Global Survey of their Status and the Techniques of Conservation*. Innsbruck, Springer-Verlag/Wien: 265-274.
- Cabirol, N., M.T. Pommier, M. Gueux and G. Payen (1998). Comparison of lipid composition in two types of human putrefactive liquid. *Forensic Science International*, **94**(1-2): 47-54.

- Campbell, N.A. and J.B. Reece (2002a). Water and the fitness of the environment. In *Biology, Sixth Edition*. San Francisco, Benjamin Cummings: 49.
- Campbell, N.A. and J.B. Reece (2002b). An introduction to metabolism. *Biology, Sixth Edition*. San Francisco, Benjamin Cummings: 94-96.
- Campbell, N.A. and J.B. Reece (2002c). Membrane structure and function. *Biology, Sixth Edition*. San Francisco, Benjamin Cummings: 142-149.
- Campbell, N.A. and J.B. Reece (2002d). Cellular respiration: harvesting chemical energy. *Biology, Sixth Edition*. San Francisco, Benjamin Cummings: 155-175.
- Campobasso, C.P., G. Di Vella and F. Introna (2001). Factors affecting decomposition and Diptera colonization. *Forensic Science International*, **120**(1-2): 18-27.
- Carter, D.O. and M. Tibbett (2008). Cadaver Decomposition and Soil: Processes. In M. Tibbett and D.O. Carter (Eds.), *Soil Analysis in Forensic Taphonomy*. Boca Raton, CRC Press: 29-51.
- Carter, D.O., D. Yellowlees and M. Tibbett (2007). Cadaver decomposition in terrestrial ecosystems. *Naturwissenschaften*, **94**(1): 12-24.
- Carter, D.O., D. Yellowlees and M. Tibbett (2010). Moisture can be the dominant environmental parameter governing cadaver decomposition in soil. *Forensic Science International*, **200**: 60-66.
- Catts, E.P. (1992). Problems in estimating the postmortem interval in death investigations. *Journal of Agricultural Entomology*, **9**(4): 245-255.
- Catts, E.P. and M.L. Goff (1992). Forensic entomology in criminal investigations. *Annual Review of Entomology*, **37**: 253-272.
- Christie, W. (2008). What Column Do I Need for Gas Chromatographic Analysis of Fatty Acids? Retrieved June 23, 2010, from <http://www.lipid.co.uk/>.
- City of Ottawa. (2008). About Ottawa. Retrieved December 19, 2008, from http://www.ottawa.com/about/faq_e.shtml.
- Clark, M.A., M.B. Worrell and J.E. Pless (1997). Postmortem Changes in Soft Tissues. In W.D. Haglund and M.H. Sorg (Eds.), *Forensic Taphonomy: The Postmortem Fate of Human Remains*. New York, CRC Press: 151-164.
- Cockle, D. *Tissue Decomposition Classification System: Instructional Information* (unpublished doctoral thesis, Simon Fraser University, 2008).

- Cosoli, P., M. Fermeglia and M. Ferrone (2010). Molecular simulation of atrazine adhesion and diffusion in a saturated sand model. *Soil and Sediment Contamination: An International Journal*, **19**(1): 72-87.
- Dadour, I.R. and M.L. Harvery (2008). The Role of Invertebrates in Terrestrial Decomposition: Forensic Applications. In M. Tibbett and D.O. Carter (Eds.), *Soil Analysis in Forensic Taphonomy*. Boca Raton, CRC Press: 109-122.
- Davenel, A., A. Riaublanc, P. Marchal and G. Gandemer (1999). Quality of pig adipose tissue: relationship between solid fat content and lipid composition. *Meat Science*, **51**: 73-79.
- Dent, B.B., S.L. Forbes and B.H. Stuart (2004). Review of human decomposition processes in soil. *Environmental Geology*, **45**: 576-585.
- Efremov, J.A. (1940). Taphonomy: new branch of paleontology. *Pan-American Geologist*, **74**: 81-93.
- Environment Canada. (2004). Canadian Climate Normals 1971-2000. Retrieved December 19, 2008, from http://www.climate.weatheroffice.ec.gc.ca/climate_normals/results_e.html.
- Fiedler, S. and M. Graw (2003). Decomposition of buried corpses, with special reference to the formation of adipocere. *Naturwissenschaften*, **90**(7): 291-300.
- Fitzgerald, C.M. and M. Oxenham (2009). Modelling time-since-death in Australian temperate conditions. *Australian Journal of Forensic Sciences*, **41**(1): 27-41.
- Fitzpatrick, R. W. (2008). Nature, Distribution, and Origin of Soil Materials in the Forensic Comparison of Soils. In M. Tibbett and D.O. Carter (Eds.), *Soil Analysis in Forensic Taphonomy*. Boca Raton, CRC Press: 1-28.
- Fleetwood, A. and I. Larsson (1968). Precipitation, soil moisture content and ground water storage in a sandy soil in southern Sweden. *Oikos*, **19**(2): 234-241.
- Forbes, S.L. (2008b). Potential Determinants of Postmortem and Postburial Interval of Buried Remains. In M. Tibbett and D.O. Carter (Eds.), *Soil Analysis in Forensic Taphonomy*. Boca Raton, CRC Press: 225-246.
- Forbes, S.L. and I. Dadour (2009). The Soil Environment and Forensic Entomology. In J.H. Byrd and J.L. Castner (Eds.), *Forensic Entomology: The Utility of Arthropods in Legal Investigations*. Boca Raton, CRC Press: 407-426.
- Forbes, S.L., B.B. Dent and B.H. Stuart (2005b). The effect of soil type on adipocere formation. *Forensic Science International*, **154**(1): 35-43.

- Forbes, S.L., J. Keegan, B.H. Stuart and B.B. Dent (2003). A gas chromatography-mass spectrometry method for the detection of adipocere in grave soils. *European Journal of Lipid Science and Technology*, **105**: 761-768.
- Forbes, S.L., B.H. Stuart, I.R. Dadour and B.B. Dent (2004). A preliminary investigation of the stages of adipocere formation. *Journal of Forensic Sciences*, **49**(3): 566-574.
- Forbes, S.L., B.H. Stuart and B.B. Dent (2002). The identification of adipocere in grave soils. *Forensic Science International*, **127**(3): 225-230.
- Forbes, S.L., B.H. Stuart and B.B. Dent (2005c). The effect of the burial environment on adipocere formation. *Forensic Science International*, **154**(1): 24-34.
- Forbes, S.L., B.H. Stuart and B.B. Dent (2005d). The effect of the method of burial on adipocere formation. *Forensic Science International*, **154**(1): 44-52.
- Forbes, S.L., B.H. Stuart, B.B. Dent and S. Fenwick-Mulcahy (2005a). Characterization of adipocere formation in animal species. *Journal of Forensic Sciences*, **50**(3): 633-640.
- Galloway, A. (1997). The Process of Decomposition: a model from the Arizona-Sonoran Desert. In W.D. Haglund and M.H. Sorg (Eds.), *Forensic Taphonomy: The Postmortem Fate of Human Remains*. New York, CRC Press: 139-150.
- Gill-King, H. (1997). Chemical and Ultrastructural Aspects of Decomposition. In W.D. Haglund and M.H. Sorg (Eds.), *Forensic Taphonomy: The Postmortem Fate of Human Remains*. New York, CRC Press: 93-108.
- Goff, L.M. (2009). Early post-mortem changes and stages of decomposition in exposed cadavers. *Experimental and Applied Acarology*, **49**(1-2): 21-36.
- Haglund, W.D. (1997a). Dogs and Coyotes: Postmortem Involvement with Human Remains. In W.D. Haglund and M.H. Sorg (Eds.), *Forensic Taphonomy: The Postmortem Fate of Human Remains*. New York, CRC Press: 367-381.
- Haglund, W.D. (1997b). Rodents and Human Remains. In W.D. Haglund and M.H. Sorg (Eds.), *Forensic Taphonomy: The Postmortem Fate of Human Remains*. New York, CRC Press: 405-414.
- Haglund, W.D. and M.H. Sorg (1997a). Introduction to Forensic Taphonomy. In W.D. Haglund and M.H. Sorg (Eds.), *Forensic Taphonomy: The Postmortem Fate of Human Remains*. New York, CRC Press: 1-9.

- Haglund, W.D. and M.H. Sorg (1997b). Method and Theory of Forensic Taphonomy Research. In W.D. Haglund and M.H. Sorg (Eds.), *Forensic Taphonomy: The Postmortem Fate of Human Remains*. New York, CRC Press: 13-26.
- Halket, J.M. and V.G. Zaikin (2003). Derivatization in mass spectrometry - 1. Silylation. *European Journal of Mass Spectrometry*, **9**: 1-21.
- Harris, D.C. (2003). Monoprotic Acid-Base Equilibria. *Quantitative Chemical Analysis*. New York, W.H. Freeman and Company: 182.
- Haslam, T.C. and M. Tibbett (2009). Soils of contrasting pH affect the decomposition of buried mammalian (*Ovis aries*) skeletal muscle tissue. *Journal of Forensic Sciences*, **54**(4): 900-904.
- Hirsch, J., J.W. Farquhar, E.H. Ahrens, M.L. Peterson and W. Stoffel (1960). Studies of adipose tissue in man - A microtechnic for sampling and analysis. *American Journal of Clinical Nutrition*, **8**(4): 499-511.
- Hopkins, D.W., P.E.J. Wiltshire and B.D. Turner (2000). Microbial characteristics of soils from graves: an investigation at the interface of soil microbiology and forensic science. *Applied Soil Ecology*, **14**: 283-288.
- Howard, G.T., B. Duos and E.J. Watson-Horzelski (2010). Characterization of the soil microbial community associated with the decomposition of a swine carcass. *International Biodeterioration and Biodegradation*, **64**: 300-304.
- James, R.A., P.A. Hoadley and B.G. Sampson. (1997). Determination of postmortem interval by sampling vitreous humour. *American Journal of Forensic Medicine and Pathology*, **18**(2): 158-162.
- Janaway, R.C., S.L. Percival and A.S. Wilson (2009). Decomposition of Human Remains. In Percival, S.L. (Ed.), *Microbiology and Aging: Clinical Manifestations*. New York, Springer Science + Business Media: 313-334.
- Lay, J.F., O. Scarpati and A. Capriolo (2008). Precipitation variability and soil water content in Pampean Flatlands (Argentina). *Geofisica Internacional*, **47**(4): 341-354.
- Little, J.L. (1999). Artifacts in trimethylsilyl derivatization reactions and ways to avoid them. *Journal of Chromatography A*, **844**(1-2): 1-22.
- Mann, R.W., W.M. Bass and L. Meadows (1990). Time since death and decomposition of the human body: variables and observations in case and experimental field studies. *Journal of Forensic Sciences*, **35**(1): 103-111.

- Matuszewski, S., D. Bajerlein, S. Konwerski and K. Szpila (2010). Insect succession and carrion decomposition in selected forests of Central Europe. Part 1: Pattern and rate of decomposition. *Forensic Science International*, **194**(1-3): 85-93.
- Megyesi, M.S., S.P. Nawrocki and N.H. Haskell (2005). Using accumulated degree-days to estimate the postmortem interval from decomposed human remains. *Journal of Forensic Sciences*, **50**(3): 618-626.
- Melis, C., N. Selva, I. Teurlings, C. Skarpe, J. D.C. Linnell and R. Andersen (2007). Soil and vegetation nutrient response to bison carcasses in Bialowieza Primeval Forest, Poland. *Ecological Research*, **22**: 807-813.
- Mohan Kumar, T.S., F.N. Monteiro, P. Bhagavath and S.M. Bakkannavar (2009). Early adipocere formation: a case report and review of literature. *Journal of Forensic and Legal Medicine*, **16**(8): 475-477.
- Monziols, M., M. Bonneau, A. Davenel and M. Kouba (2007). Comparison of the lipid content and fatty acid composition of intermuscular and subcutaneous adipose tissues in pig carcasses. *Meat Science*, **76**: 54-60.
- Munoz, J.I., J.M. Suarez-Penaranda, X.L. Otero, M.S. Rodriguez-Calvo, E. Costas, X. Miguens and L. Concheiro (2001). A new perspective in the estimation of postmortem interval (PMI) based on vitreous. *Journal of Forensic Sciences*, **46**(2): 209-214.
- Notter, S.J., B.H. Stuart, B.B. Dent and J. Keegan (2008). Solid-phase extraction in combination with GC/MS for the quantification of free fatty acids in adipocere. *European Journal of Lipid Science and Technology*, **110**: 73-80.
- Notter, S.J., B.H. Stuart, R. Rowe and N. Langlois (2009). The initial changes of fat deposits during the decomposition of human and pig remains. *Journal of Forensic Sciences*, **54**(1): 195-201.
- O'Brien, R.C., S.L. Forbes, J. Meyer and I. Dadour (2010). Forensically significant scavenging guilds in the southwest of Western Australia. *Forensic Science International*, **198**(1-3): 85-91.
- O'Brien, R.C., S.L. Forbes, J. Meyer and I.R. Dadour (2007). A preliminary investigation into the scavenging activity on pig carcasses in Western Australia. *Forensic Science, Medicine and Pathology*, **3**(3): 194-199.
- Ontario Ministry of Natural Resources. (2008). Ontario's Forests. Retrieved December 19, 2008, from http://www.mnr.gov.on.ca/en/Business/Forests/2ColumnSubPage/STEL02_163390.html.

- Payne, J.A. (1965). A summer carrion study of the baby *Sus Scrofa* Linnaeus. *Ecology*, **46**(5): 592-602.
- Perry, W.L., 3rd, W.M. Bass, W.S. Riggsby and K. Sirotkin (1988). The autodegradation of deoxyribonucleic acid (DNA) in human rib bone and its relationship to the time interval since death. *Journal of Forensic Sciences*, **33**(1): 144-153.
- Pfeiffer, S., S. Milne and R.M. Stevenson (1998). The natural decomposition of adipocere. *Journal of Forensic Sciences*, **43**(2): 368-370.
- Pinheiro, J. (2006). Decay Process of a Cadaver. In A. Schmitt, E. Cunha and J. Pinheiro (Eds.), *Forensic Anthropology and Medicine: Complementary Sciences From Recovery to Cause of Death*. Totowa, Humana Press: 85-116.
- Prieto, J.L., C. Magana and D.H. Ubelaker (2004). Interpretation of postmortem change in cadavers in Spain. *Journal of Forensic Sciences*, **49**(5): 918-923.
- Ptashnyk, M., T. Roose and G.J.D. Kirk (2010). Diffusion of strongly sorbed solutes in soil: a dual-porosity model allowing for slow access to sorption sites and time-dependent sorption reactions. *European Journal of Soil Science*, **61**: 108-119.
- Ritchie, J.T. (1981). Water dynamics in the soil-plant-atmosphere system. *Plant and Soil*, **58**(1-3): 81-96.
- Rodriguez, W.C. (1997). Decomposition of Buried and Submerged Bodies. In W.D. Haglund and M.H. Sorg (Eds.), *Forensic Taphonomy: The Postmortem Fate of Human Remains*. New York, CRC Press: 459-467.
- Rodriguez, W.C. and W.M. Bass (1985). Decomposition of buried bodies and methods that may aid in their location. *Journal of Forensic Sciences*, **30**(3): 836-852.
- Rousk, J., P.C. Brookes and E. Baath (2009). Contrasting soil pH effects on fungal and bacterial growth suggest functional redundancy in carbon mineralization. *Applied and Environmental Microbiology*, **75**(6): 1589-1596.
- Schindler, U., W. Dumer, G. von Unold and L. Muller (2010). Evaporation method for measuring unsaturated hydraulic properties of soils: extending the measurement range. *Soil Science Society of America Journal*, **74**(4): 1071-1083.
- Schoenly, K.G., N.H. Haskell, D.K. Mills, C. Bieme-Ndi, K. Larsen and Y. Lee (2006). Recreating death's acre in the school yard: using pig carcasses as model corpses. *The American Biology Teacher*, **68**(7): 402-410.
- Sharanowski, B.J., E.G. Walker and G.S. Anderson (2008). Insect succession and decomposition patterns on shaded and sunlit carrion in Saskatchewan in three different seasons. *Forensic Science International*, **179**(2-3): 219-240.

- Shaw, B.D., A. Tuli, J.-B. Wei and J.W. Hopmans (2010). Analytical modeling of soil solution monitoring by diffusion in porous cups. *Transport in Porous Media*, **81**: 341-360.
- Shean, B.S., L. Messinger and M. Papworth (1993). Observations of differential decomposition on sun exposed v. shaded pig carrion in coastal Washington State. *Journal of Forensic Sciences*, **38**(4): 938-949.
- Shieh, L.J., P.K. Halpern, B.A. Clemens, H.H. Wang and F.F. Abraham (1972). Air quality diffusion model; application to New York City. *IBM Journal of Research and Development*, **16**(2): 162-170.
- Simonsen, J., J. Voigt and N. Jeppesen (1977). Determination of the time of death by continuous post-mortem temperature measurements. *Medicine, Science and the Law*, **17**(2): 112-122.
- Swann, L., G.E. Chidlow, S.L. Forbes and S.W. Lewis (2010a). Preliminary studies into the characterization of chemical markers of decomposition for geoforensics. *Journal of Forensic Sciences*, **55**(2): 308-314.
- Swann, L., S.L. Forbes and S.W. Lewis (2010b). Observations of the temporal variation in chemical content of decomposition fluid: A preliminary study using pigs as a model system. *Australian Journal of Forensic Sciences*. Published online March 31, 2010. DOI: 10.1080/00450610903258102.
- Takatori, T. (1996). Investigations on the mechanism of adipocere formation and its relation to other biochemical reactions. *Forensic Science International*, **80**(1-2): 49-61.
- Takatori, T. (2001). The mechanism of human adipocere formation. *Legal Medicine (Tokyo)*, **3**(4): 193-204.
- Taylor, R.V. and T.R. Seastedt (1994). Short- and long-term patterns of soil moisture in alpine tundra. *Arctic and Alpine Research*, **26**(1): 14-20.
- Tirabassi, T. (1989). Analytical air pollution advection and diffusion models. *Water, Air and Soil Pollution*, **47**: 19-24.
- Towne, E.G. (2000). Prairie vegetation and soil nutrient responses to ungulate carcasses. *Oecologia*, **122**: 232-239.
- Tzimopoulos, C.D. and M. Sakellariou-Makrantonaki (1996). A new analytical model to predict the hydraulic conductivity of unsaturated soils. *Water Resources Management*, **10**: 397-414.

- Vane, C.H. and J.K. Trick (2005). Evidence of adipocere in a burial pit from the foot and mouth epidemic of 1967 using gas chromatography-mass spectrometry. *Forensic Science International*, **154**(1): 19-23.
- Vass, A.A., S.A. Barshick, G. Sega, J. Caton, J.T. Skeen, J.C. Love and J.A. Synsteliën (2002). Decomposition chemistry of human remains: a new methodology for determining the postmortem interval. *Journal of Forensic Sciences*, **47**(3): 542-553.
- Vass, A.A., W.M. Bass, J.D. Wolt, J.E. Foss and J.T. Ammons (1992). Time since death determinations of human cadavers using soil solution. *Journal of Forensic Sciences*, **37**(5): 1236-1253.
- Wang, W. and T.E. Daniels (2006). Diffusion and graph spectral methods for network forensic analysis. *New Security Paradigms Workshop*. Germany, Association for Computing Machinery.
- Widdowson, E.M. (1950). Chemical composition of newly born mammals. *Nature*, **166**(4224): 626-628.
- Wilson, A.S., R.C. Janaway, A.D. Holland, H.I. Dodson, E. Baran, A.M. Pollard and D.J. Tobin (2007). Modelling the buried human body environment in upland climes using three contrasting field sites. *Forensic Science International*, **169**(1): 6-18.
- Zwillinger, D. and S. Kokoska (2000). Nonparametric Statistics. *Standard Probability and Statistics Tables and Formulae*. Boca Raton, Chapman & Hall/CRC: 372-381.

Chapter 8 – Appendices

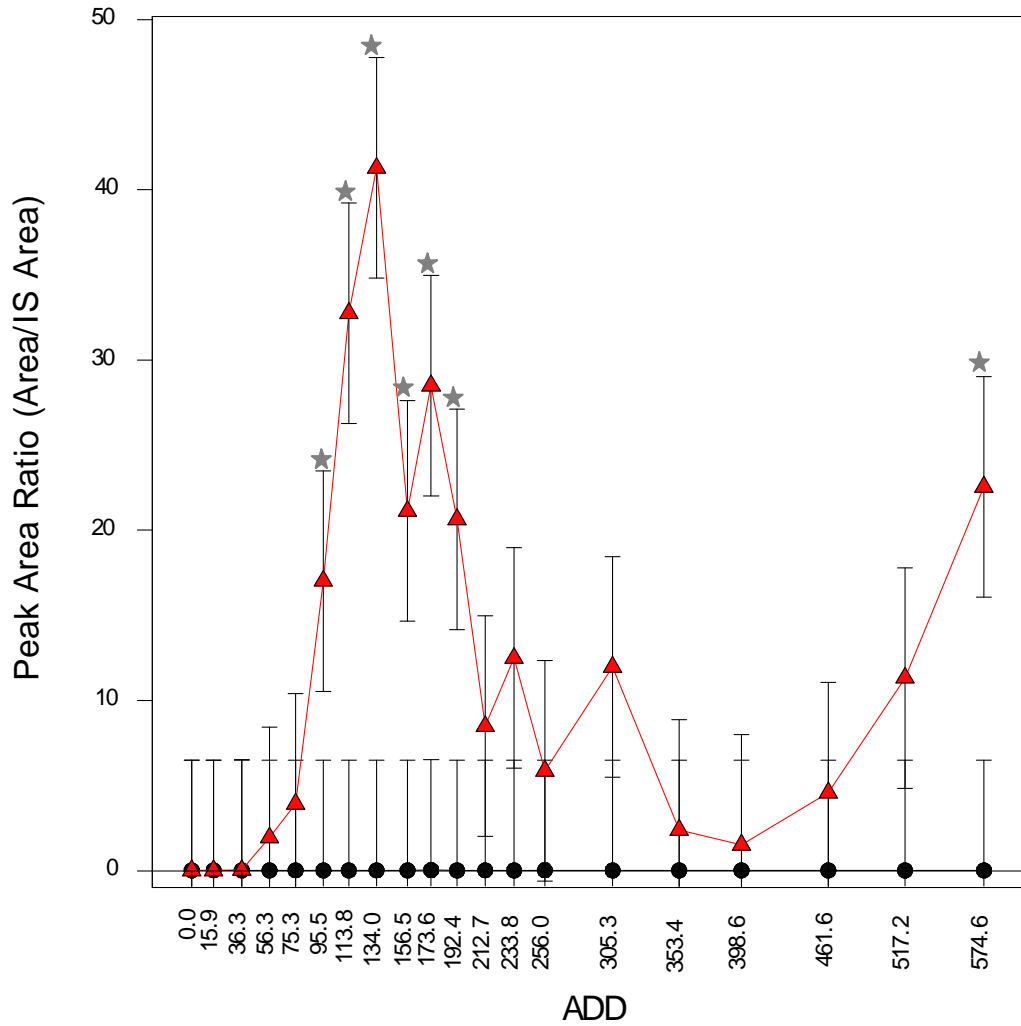
*Appendix A –
Tissue Decomposition
Classification System*

Baseline Decomposition Scoring System*

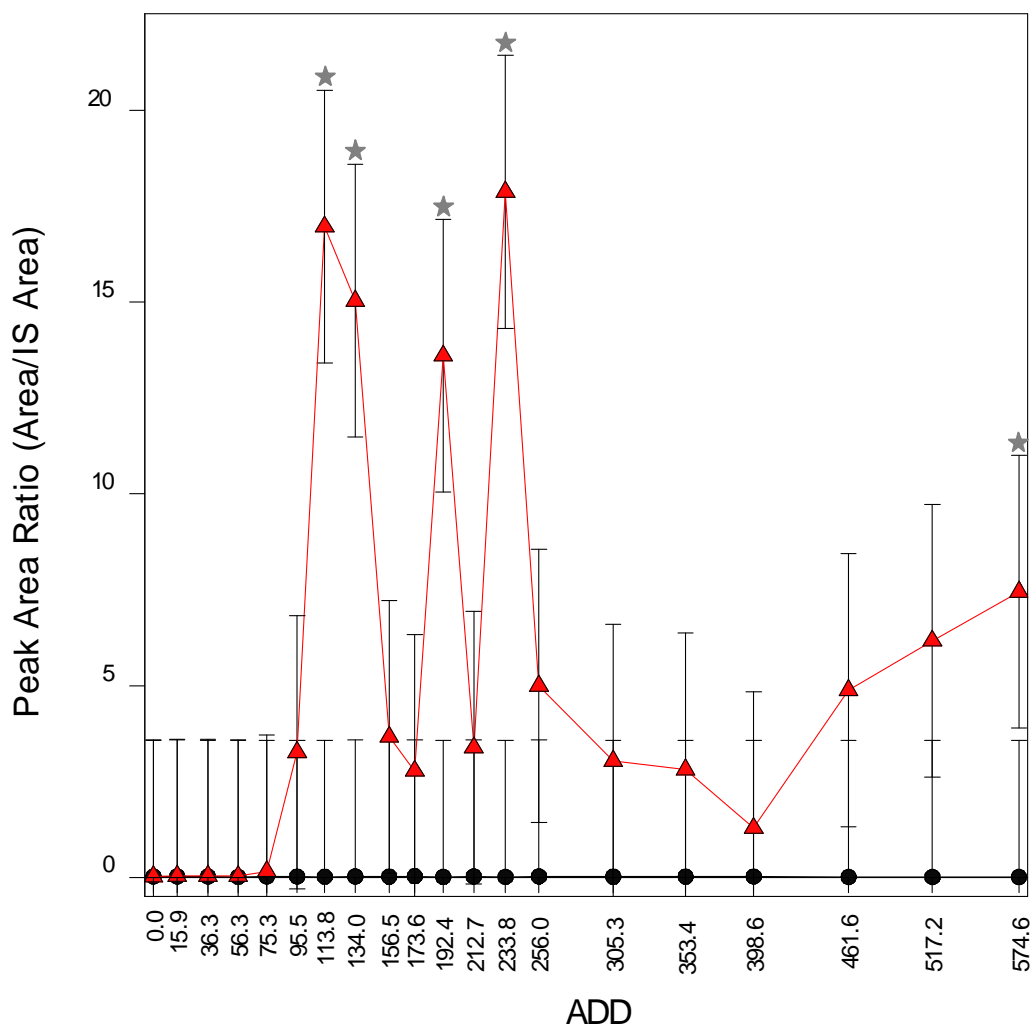
Category	Stage of decomposition	Point value
Autolysis	No visible changes	0
	First visible change	1
	First tissue change	2
Putrefaction	First colour change	3
	Full bloat	4
	Post bloat	5
Skeletonization	First sign of bone	6
	More than ½ of bone exposed	7
	Total skeletonization	8

* Cockle (2008)

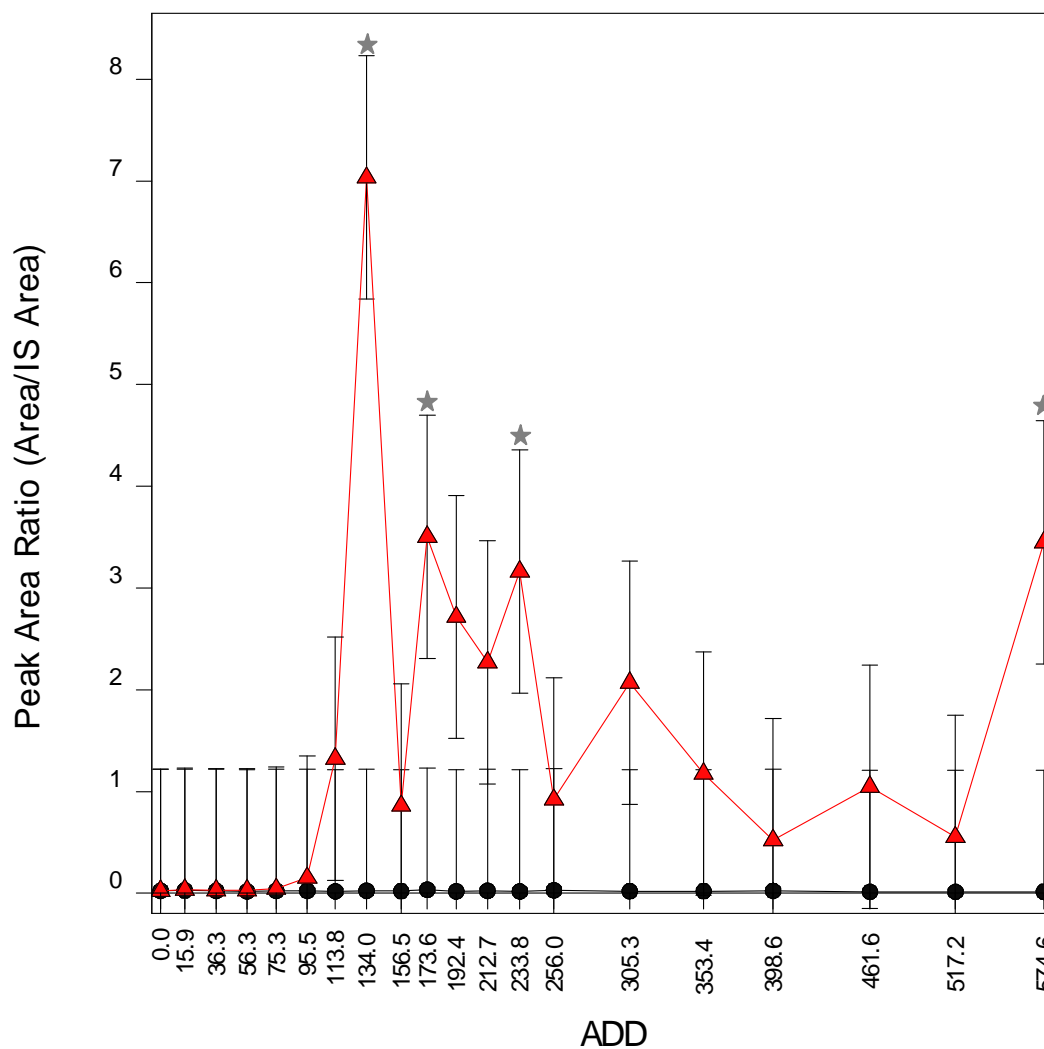
***Appendix B –
Myristic Acid Content of
Soil Samples by Distance***



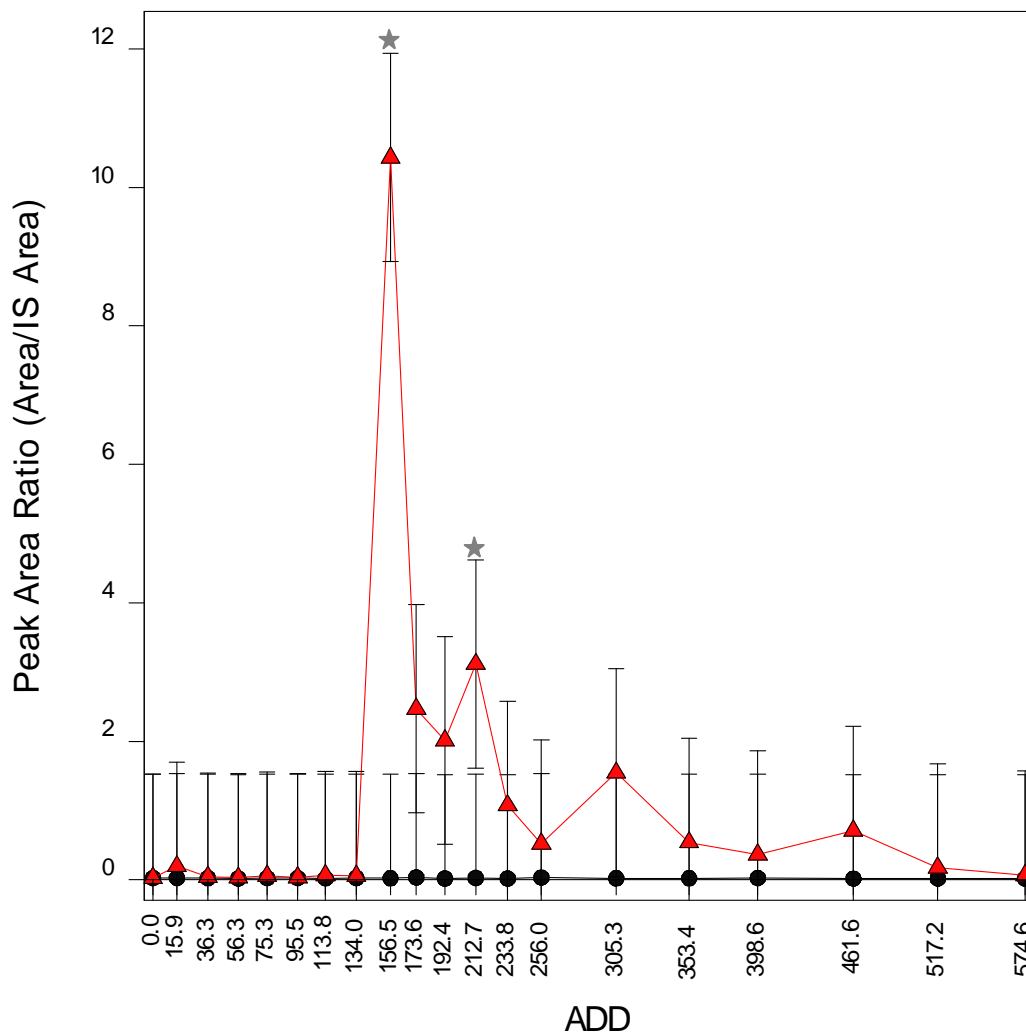
Appendix B-1. Myristic acid content of control (●) and experimental (▲) soil collected 0 cm away from the pig carcasses at the Technical and Protective Operations Facility in Ottawa, Ontario, Canada during the 2009 summer trial. ★ = significant difference $p < 0.05$ (ANOVA, $F_{\text{Treatment}(1, 80)} = 36.65$, $p < 0.001$, $F_{\text{ADD}(19, 80)} = 1.73$, $p = 0.048$, $F_{\text{Int}(19, 80)} = 1.73$, $p = 0.048$, bars = s.e. of differences of means).



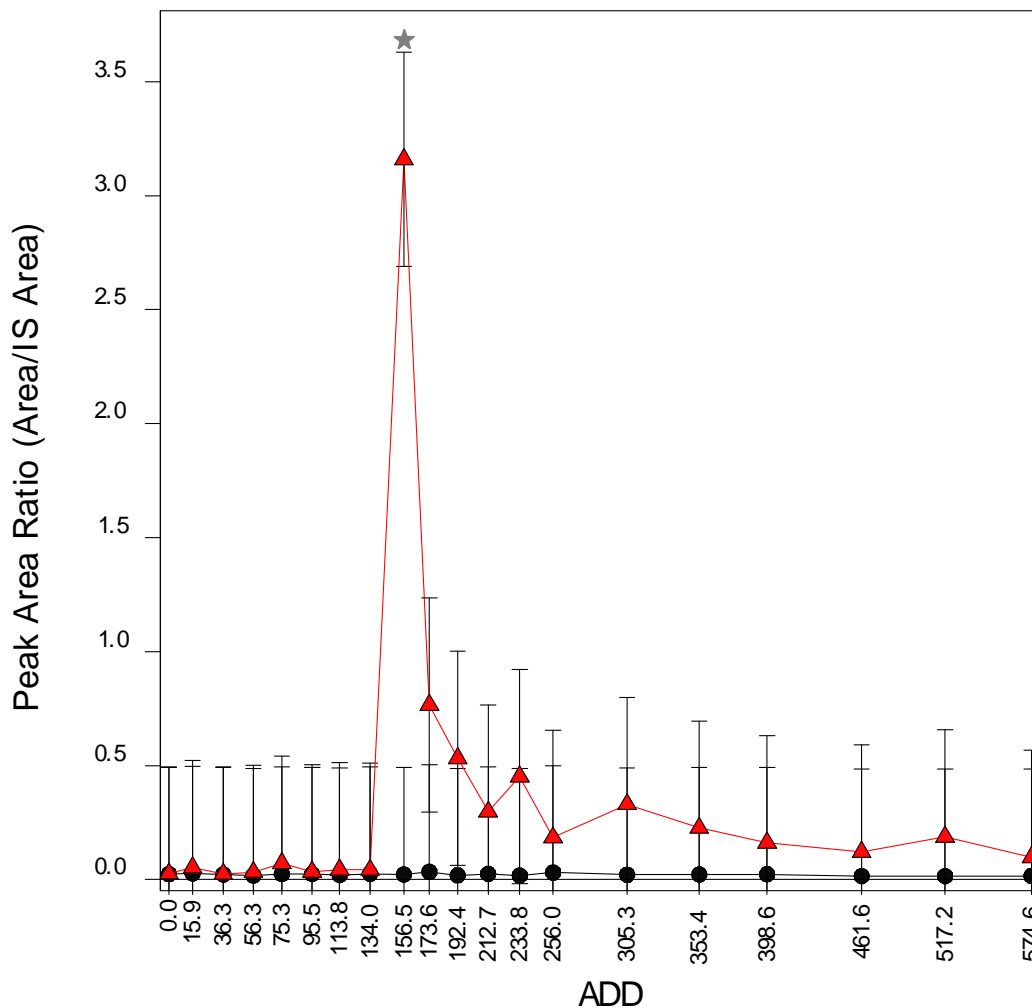
Appendix B-2. Myristic acid content of control (—●—) and experimental (—▲—) soil collected 10 cm away from the pig carcasses at the Technical and Protective Operations Facility in Ottawa, Ontario, Canada during the 2009 summer trial. ★ = significant difference $p < 0.05$ (ANOVA, $F_{\text{Treatment}(1, 80)} = 22.66$, $p < 0.001$, $F_{\text{ADD}(19, 80)} = 1.43$, $p = 0.182$, $F_{\text{Int}(19, 80)} = 1.34$, $p = 0.182$, bars = s.e. of differences of means).



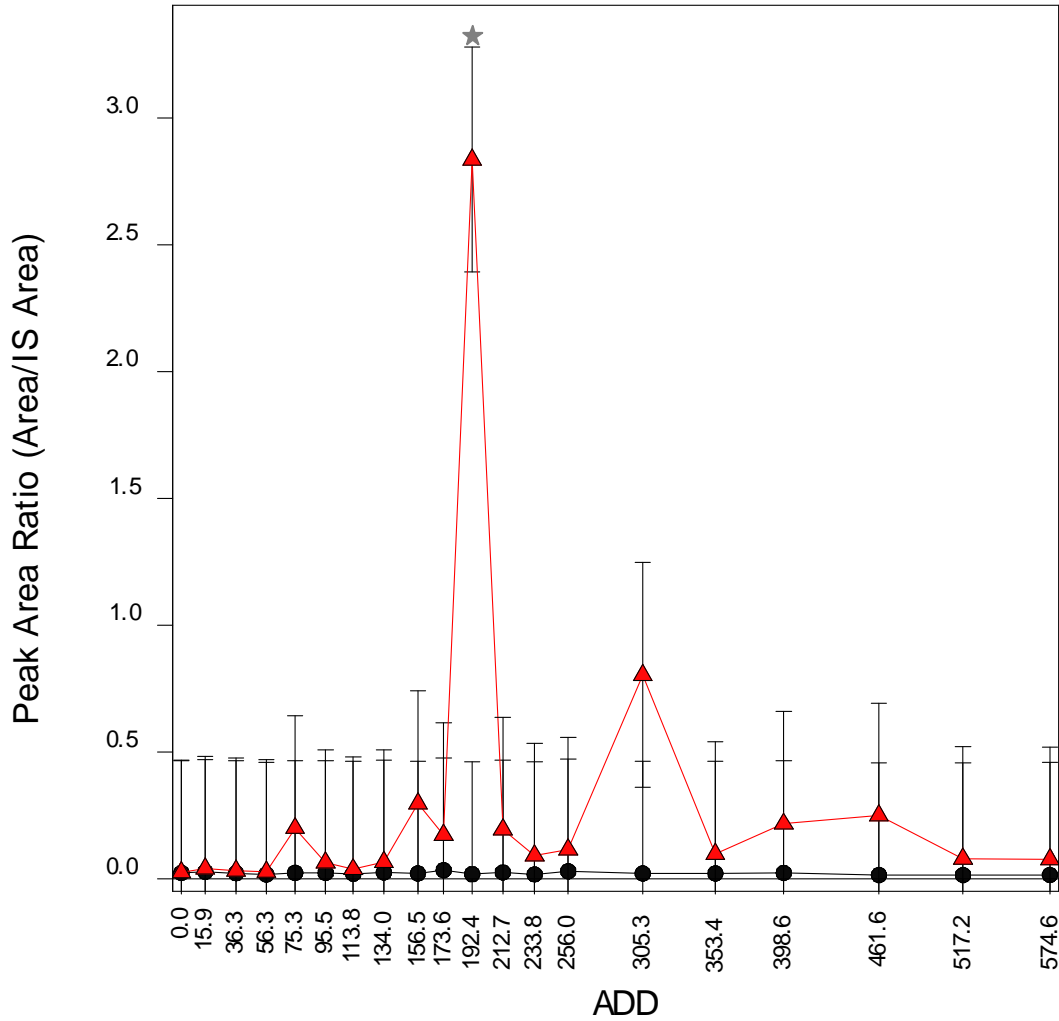
Appendix B-3. Myristic acid content of control (●) and experimental (▲) soil collected 20 cm away from the pig carcasses at the Technical and Protective Operations Facility in Ottawa, Ontario, Canada during the 2009 summer trial. ★ = significant difference $p < 0.05$ (ANOVA, $F_{\text{Treatment}(1, 80)} = 16.26$, $p < 0.001$, $F_{\text{ADD}(19, 80)} = 1.09$, $p = 0.378$, $F_{\text{Int}(19, 80)} = 1.09$, $p = 0.380$, bars = s.e. of differences of means).



Appendix B-4. Myristic acid content of control (—●—) and experimental (—▲—) soil collected 30 cm away from the pig carcasses at the Technical and Protective Operations Facility in Ottawa, Ontario, Canada during the 2009 summer trial. ★ = significant difference $p < 0.05$ (ANOVA, $F_{\text{Treatment}(1, 80)} = 5.90$, $p = 0.017$, $F_{\text{ADD}(19, 80)} = 1.23$, $p = 0.253$, $F_{\text{Int}(19, 80)} = 1.23$, $p = 0.254$, bars = s.e. of differences of means).

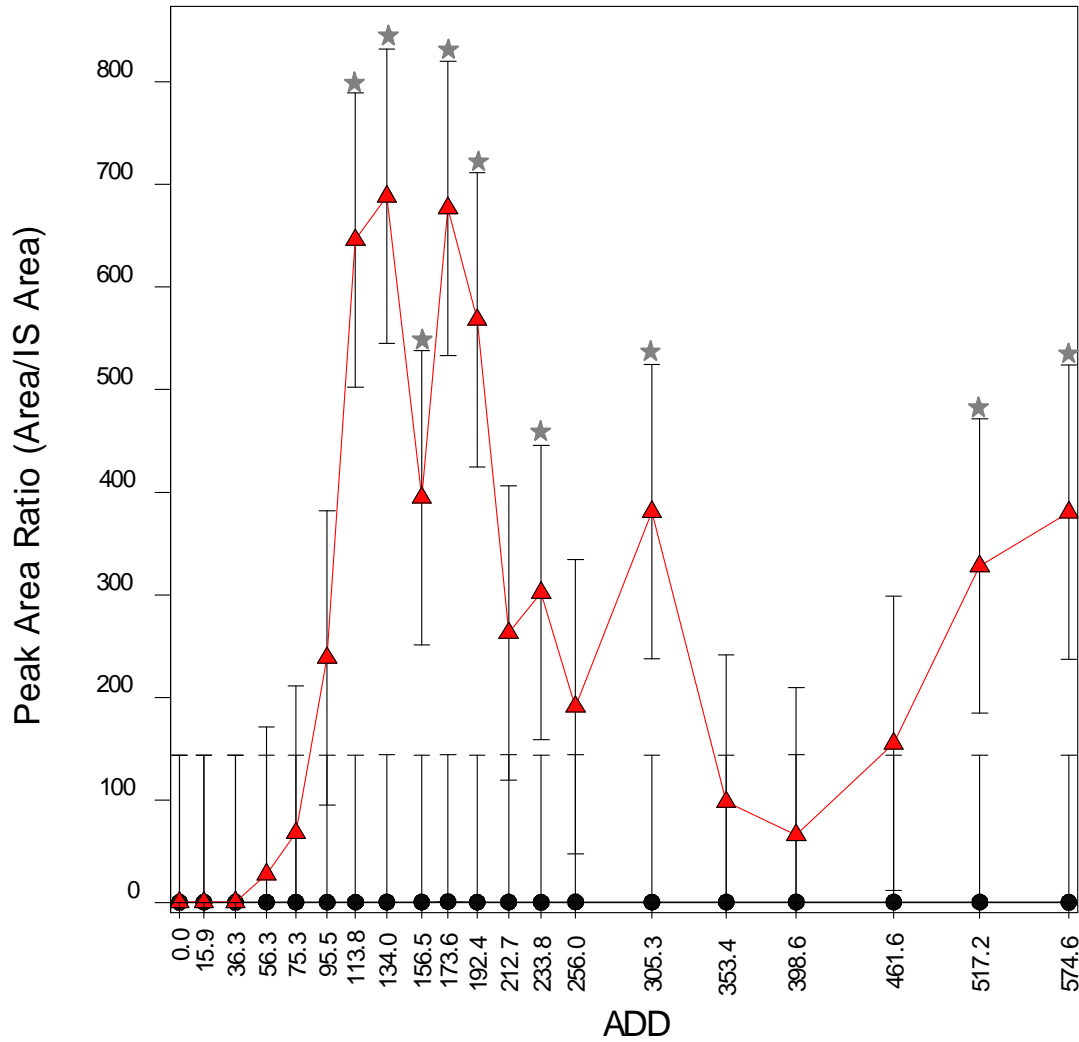


Appendix B-5. Myristic acid content of control (●) and experimental (▲) soil collected 40 cm away from the pig carcasses at the Technical and Protective Operations Facility in Ottawa, Ontario, Canada during the 2009 summer trial. ★ = significant difference $p < 0.05$ (ANOVA, $F_{\text{Treatment}(1, 80)} = 4.64$, $p = 0.034$, $F_{\text{ADD}(19, 80)} = 1.09$, $p = 0.379$, $F_{\text{Int}(19, 80)} = 1.09$, $p = 0.381$, bars = s.e. of differences of means).

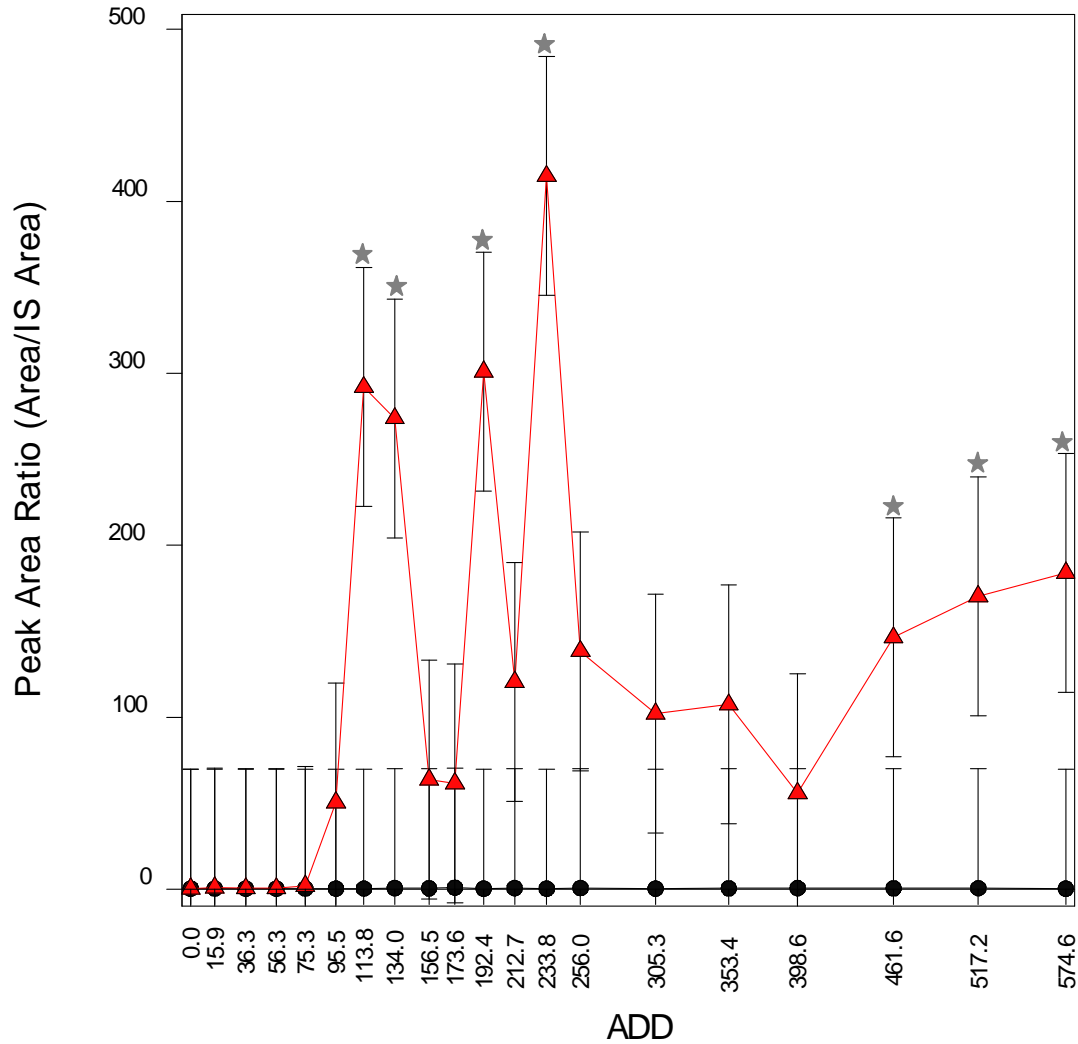


Appendix B-6. Myristic acid content of control (—●—) and experimental (—▲—) soil collected 50 cm away from the pig carcasses at the Technical and Protective Operations Facility in Ottawa, Ontario, Canada during the 2009 summer trial. ★ = significant difference $p < 0.05$ (ANOVA, $F_{\text{Treatment}(1, 80)} = 3.56$, $p = 0.063$, $F_{\text{ADD}(19, 80)} = 0.99$, $p = 0.480$, $F_{\text{Int}(19, 80)} = 1.00$, $p = 0.474$, bars = s.e. of differences of means).

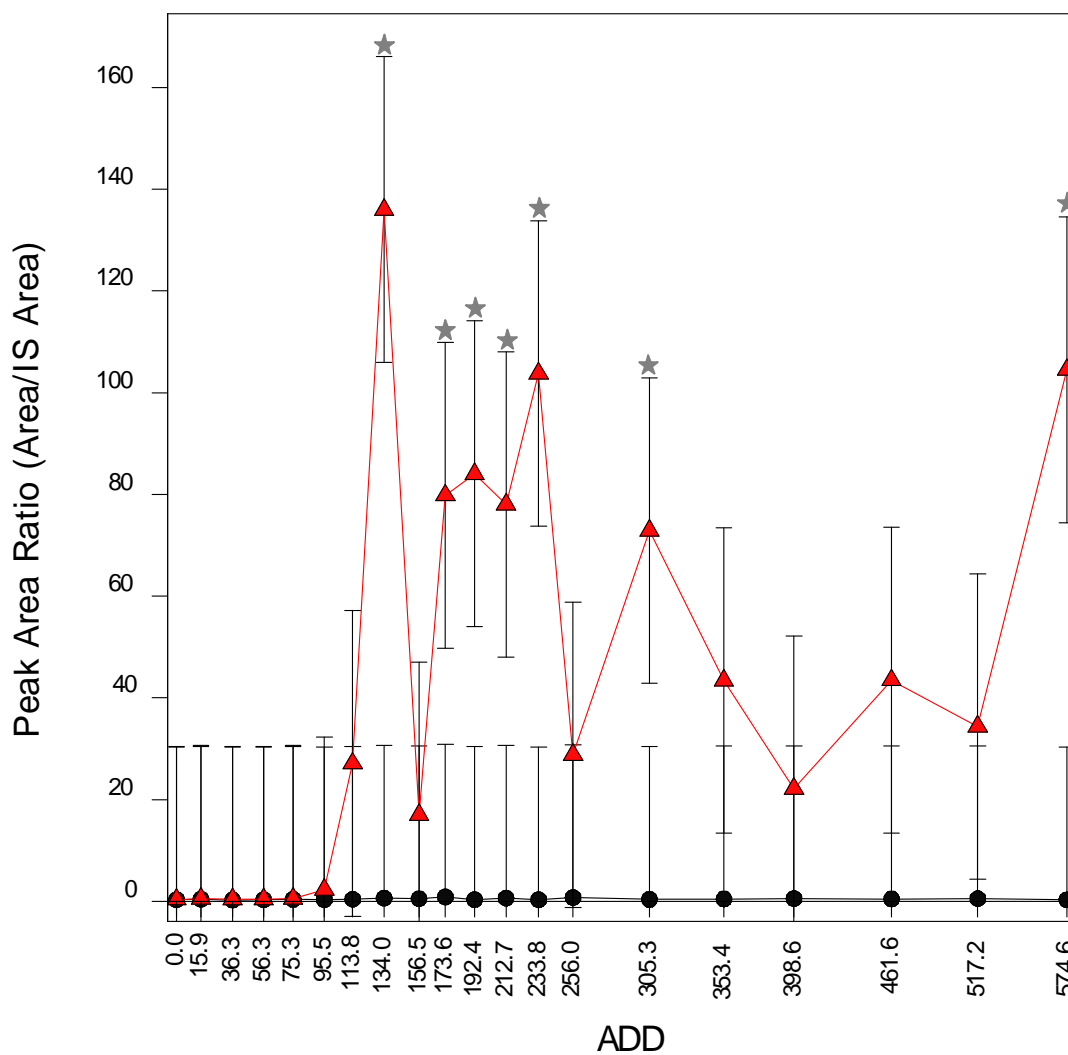
*Appendix C –
Palmitic Acid Content of
Soil Samples by Distance*



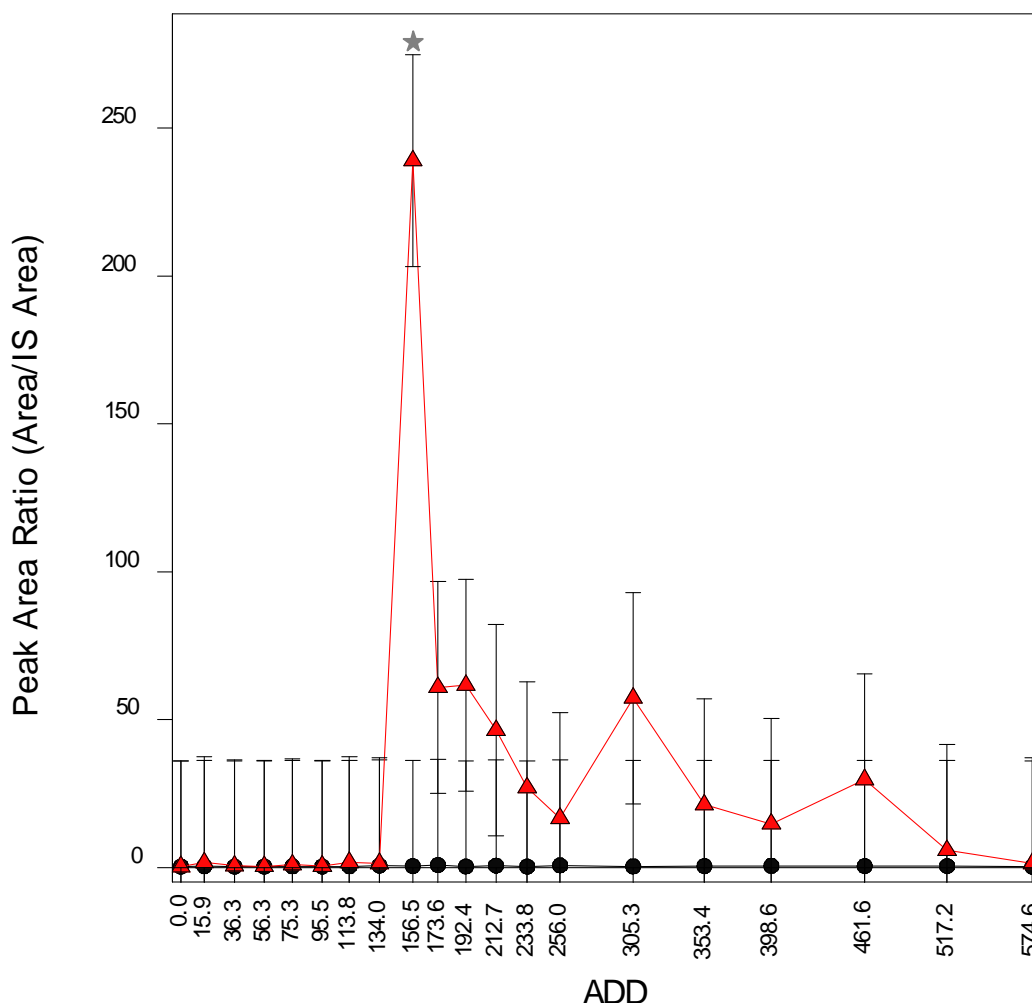
Appendix C-1. Palmitic acid content of control (●) and experimental (▲) soil collected 0 cm away from the pig carcasses at the Technical and Protective Operations Facility in Ottawa, Ontario, Canada during the 2009 summer trial. ★ = significant difference $p < 0.05$ (ANOVA, $F_{\text{Treatment}(1, 80)} = 36.28$, $p < 0.001$, $F_{\text{ADD}(19, 80)} = 1.31$, $p = 0.200$, $F_{\text{Int}(19, 80)} = 1.31$, $p = 0.201$, bars = s.e. of differences of means).



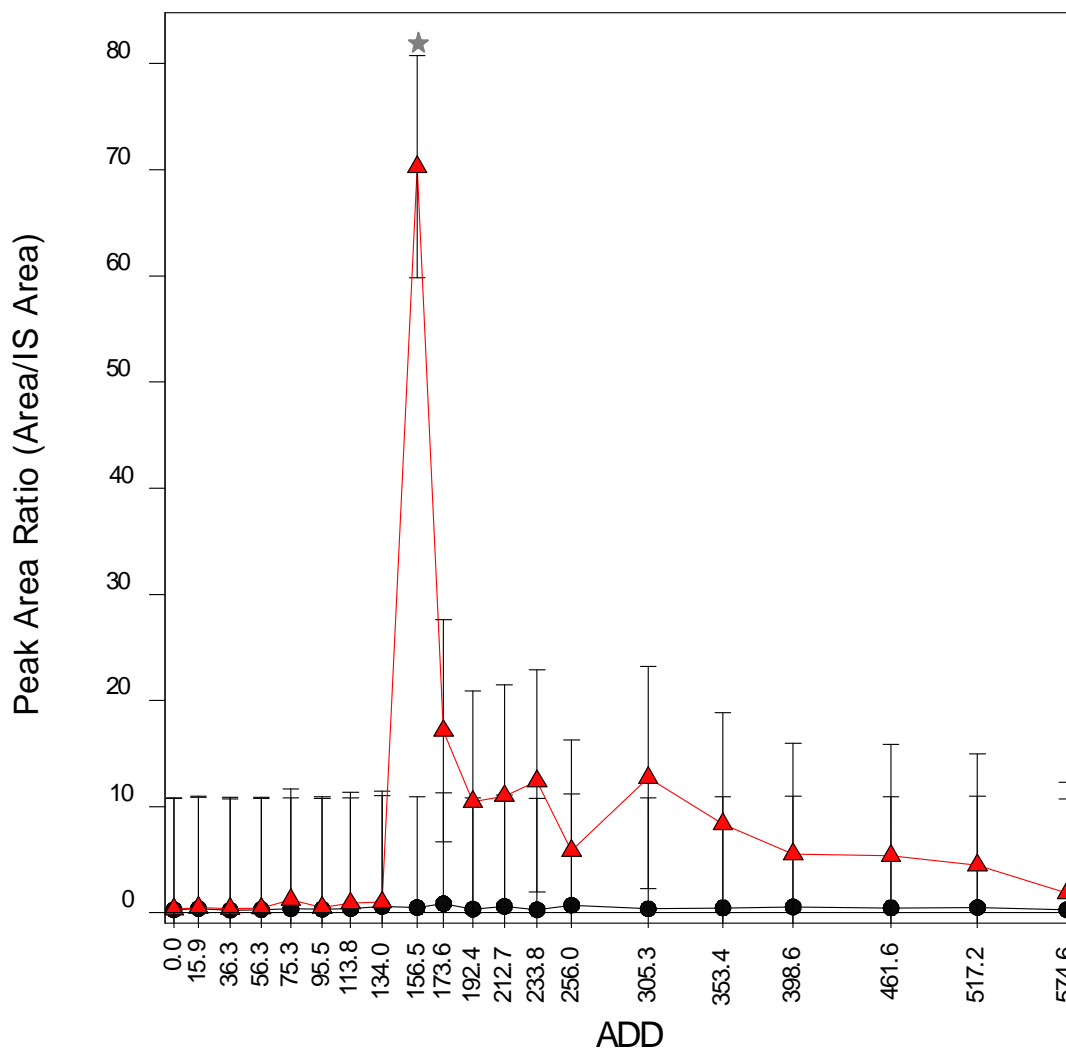
Appendix C-2. Palmitic acid content of control (—●—) and experimental (—▲—) soil collected 10 cm away from the pig carcasses at the Technical and Protective Operations Facility in Ottawa, Ontario, Canada during the 2009 summer trial. ★ = significant difference $p < 0.05$ (ANOVA, $F_{\text{Treatment}(1, 80)} = 31.81$, $p < 0.001$, $F_{\text{ADD}(19, 80)} = 1.46$, $p = 0.125$, $F_{\text{Int}(19, 80)} = 1.46$, $p = 0.125$, bars = s.e. of differences of means).



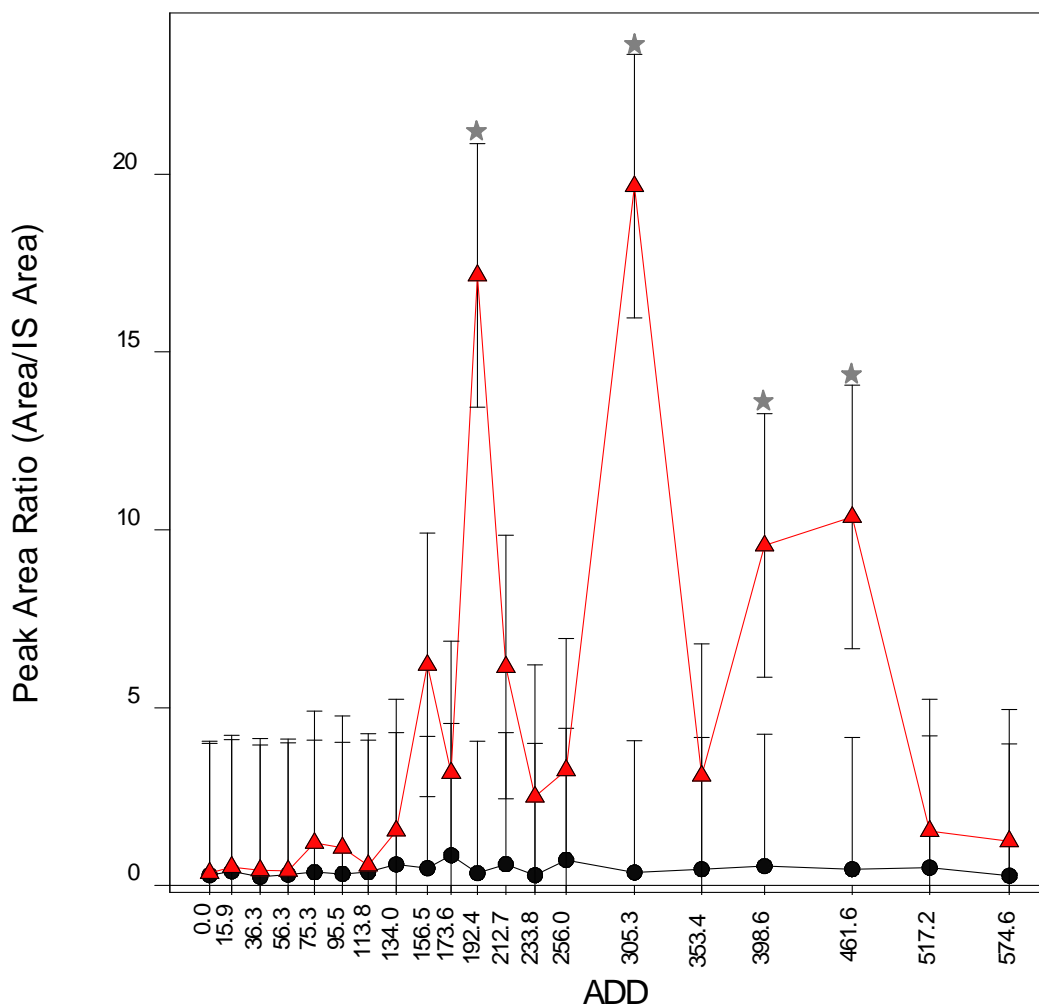
Appendix C-3. Palmitic acid content of control (—●—) and experimental (—▲—) soil collected 20 cm away from the pig carcasses at the Technical and Protective Operations Facility in Ottawa, Ontario, Canada during the 2009 summer trial. ★ = significant difference $p < 0.05$ (ANOVA, $F_{\text{Treatment}(1, 80)} = 21.02$, $p < 0.001$, $F_{\text{ADD}(19, 80)} = 0.98$, $p = 0.490$, $F_{\text{Int}(19, 80)} = 0.98$, $p = 0.495$, bars = s.e. of differences of means).



Appendix C-4. Palmitic acid content of control (—●—) and experimental (—▲—) soil collected 30 cm away from the pig carcasses at the Technical and Protective Operations Facility in Ottawa, Ontario, Canada during the 2009 summer trial. ★ = significant difference $p < 0.05$ (ANOVA, $F_{\text{Treatment}(1, 80)} = 6.59$, $p = 0.012$, $F_{\text{ADD}(19, 80)} = 1.14$, $p = 0.329$, $F_{\text{Int}(19, 80)} = 1.14$, $p = 0.332$, bars = s.e. of differences of means).

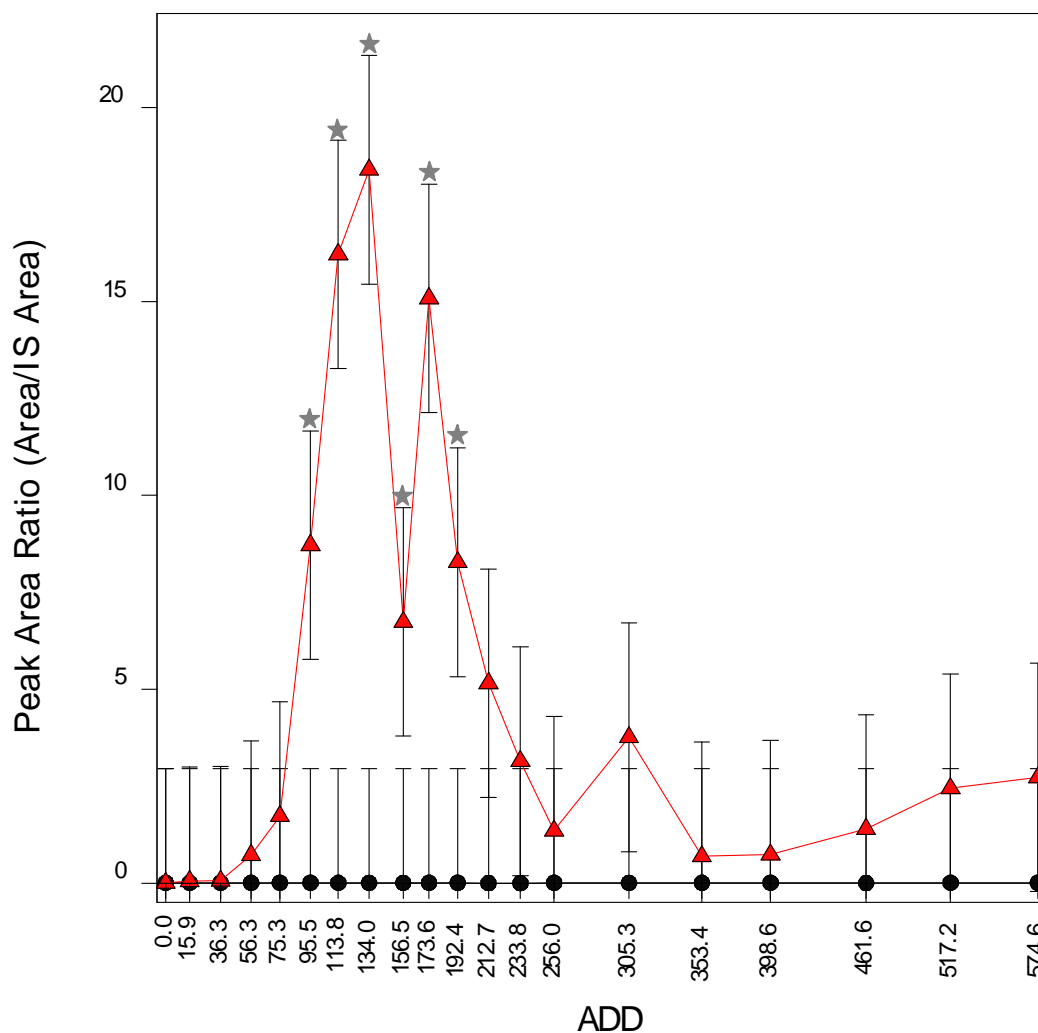


Appendix C-5. Palmitic acid content of control (●) and experimental (▲) soil collected 40 cm away from the pig carcasses at the Technical and Protective Operations Facility in Ottawa, Ontario, Canada during the 2009 summer trial. ★ = significant difference $p < 0.05$ (ANOVA, $F_{\text{Treatment}(1, 80)} = 5.98$, $p = 0.017$, $F_{\text{ADD}(19, 80)} = 1.09$, $p = 0.377$, $F_{\text{Int}(19, 80)} = 1.08$, $p = 0.387$, bars = s.e. of differences of means).

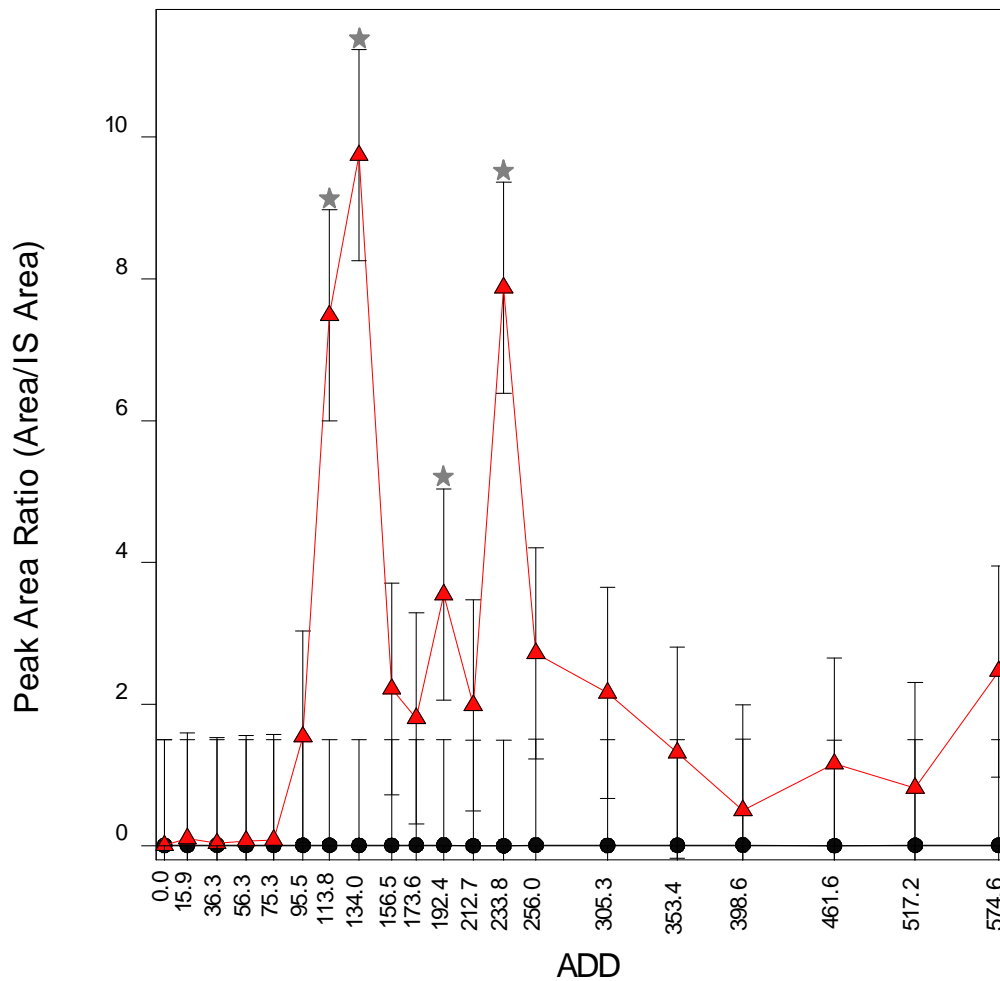


Appendix C-6. Palmitic acid content of control (—●—) and experimental (—▲—) soil collected 50 cm away from the pig carcasses at the Technical and Protective Operations Facility in Ottawa, Ontario, Canada during the 2009 summer trial. ★ = significant difference $p < 0.05$ (ANOVA, $F_{\text{Treatment}(1, 80)} = 11.97$, $p < 0.001$, $F_{\text{ADD}(19, 80)} = 1.15$, $p = 0.321$, $F_{\text{Int}(19, 80)} = 1.14$, $p = 0.328$, bars = s.e. of differences of means).

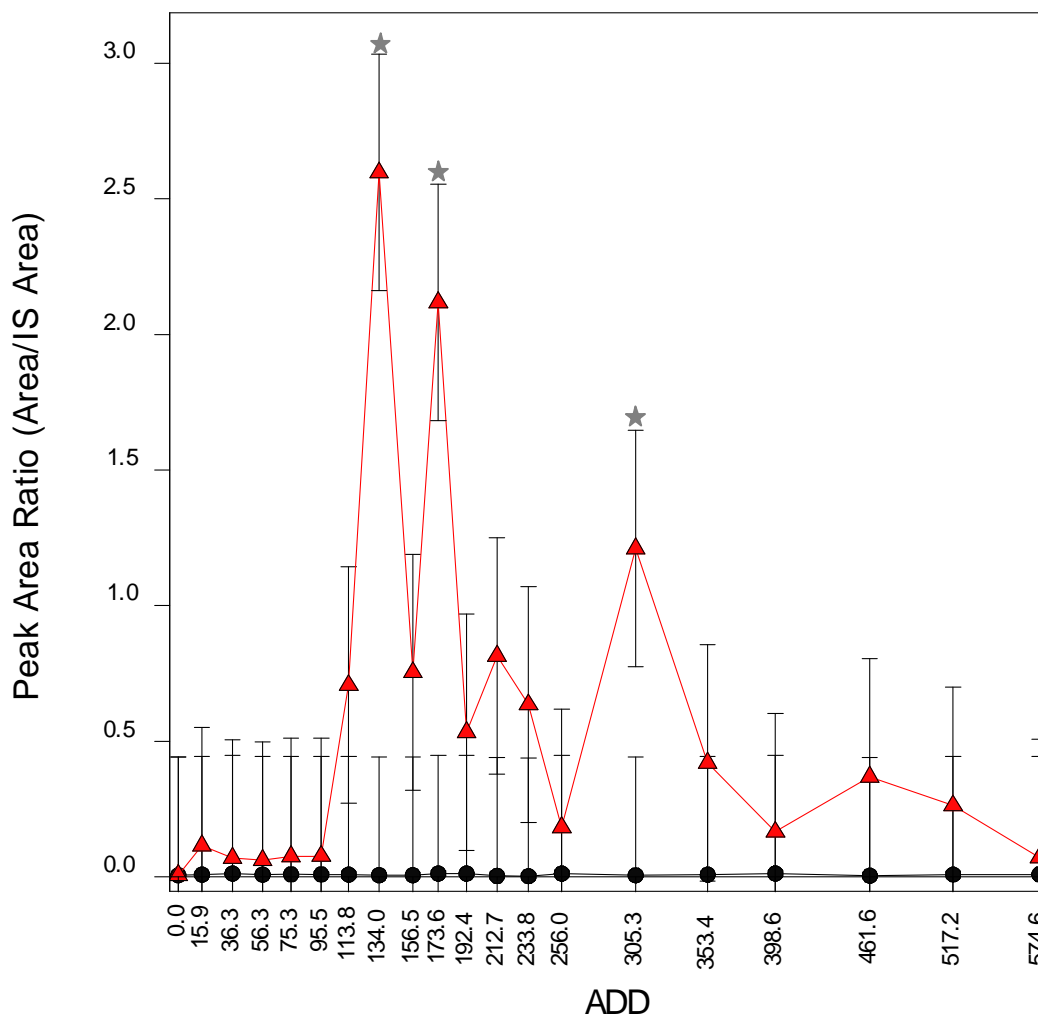
*Appendix D –
Palmitoleic Acid Content
of Soil Samples by
Distance*



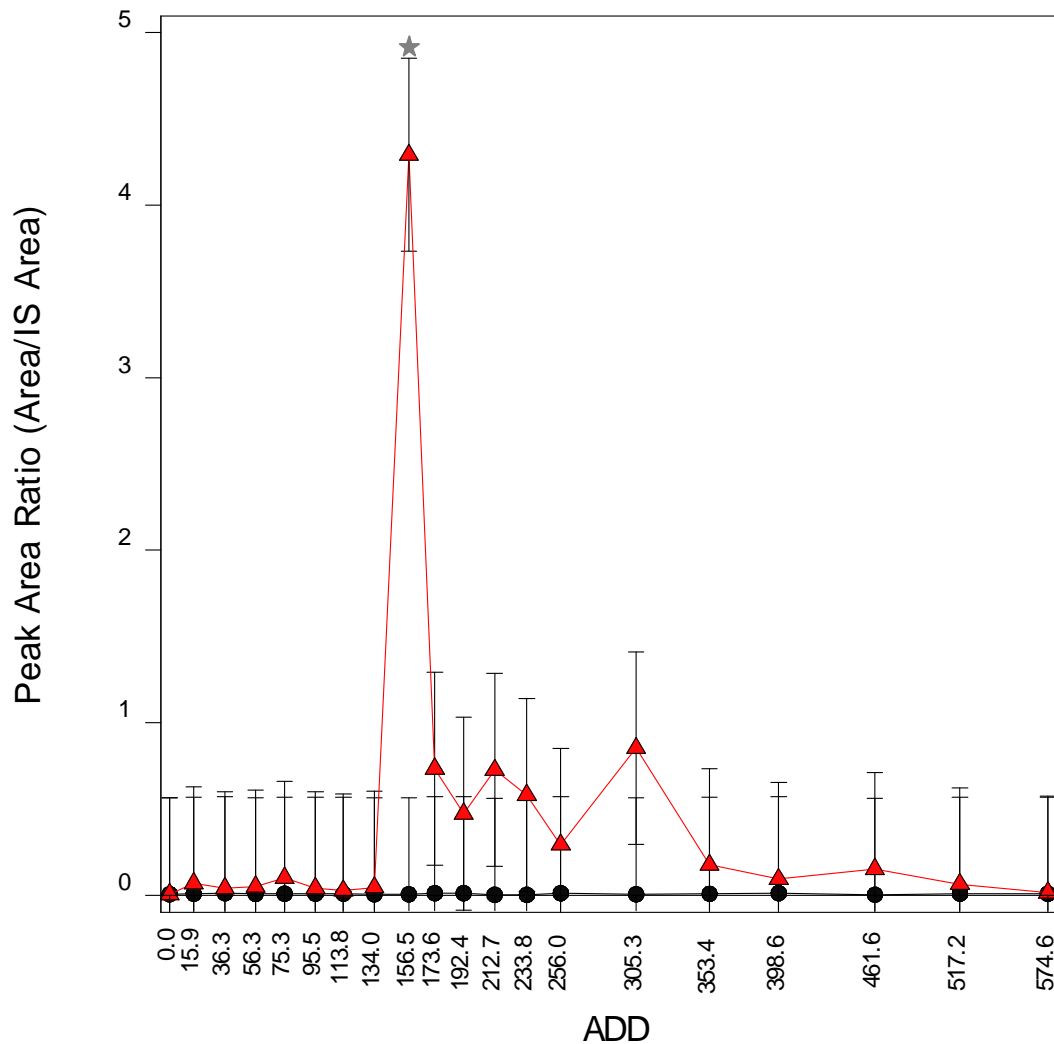
Appendix D-1. Palmitoleic acid content of control (●) and experimental (▲) soil collected 0 cm away from the pig carcasses at the Technical and Protective Operations Facility in Ottawa, Ontario, Canada during the 2009 summer trial. ★ = significant difference $p < 0.05$ (ANOVA, $F_{\text{Treatment}(1, 80)} = 27.25$, $p < 0.001$, $F_{\text{ADD}(19, 80)} = 1.87$, $p = 0.028$, $F_{\text{Int}(19, 80)} = 1.87$, $p = 0.028$, bars = s.e. of differences of means).



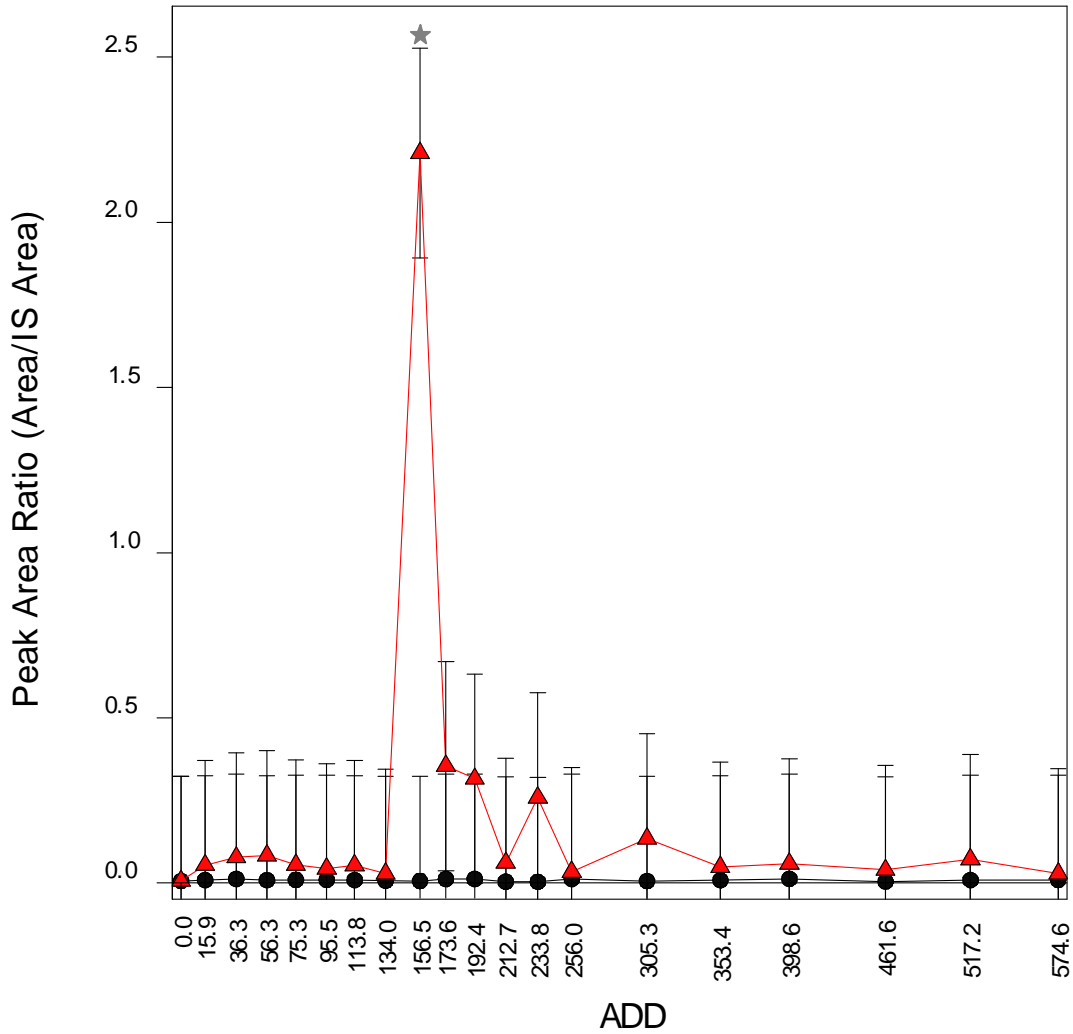
Appendix D-2. Palmitoleic acid content of control (●) and experimental (▲) soil collected 10 cm away from the pig carcasses at the Technical and Protective Operations Facility in Ottawa, Ontario, Canada during the 2009 summer trial. ★ = significant difference $p < 0.05$ (ANOVA, $F_{\text{Treatment}(1, 80)} = 25.35$, $p < 0.001$, $F_{\text{ADD}(19, 80)} = 1.76$, $p = 0.042$, $F_{\text{Int}(19, 80)} = 1.76$, $p = 0.042$, bars = s.e. of differences of means).



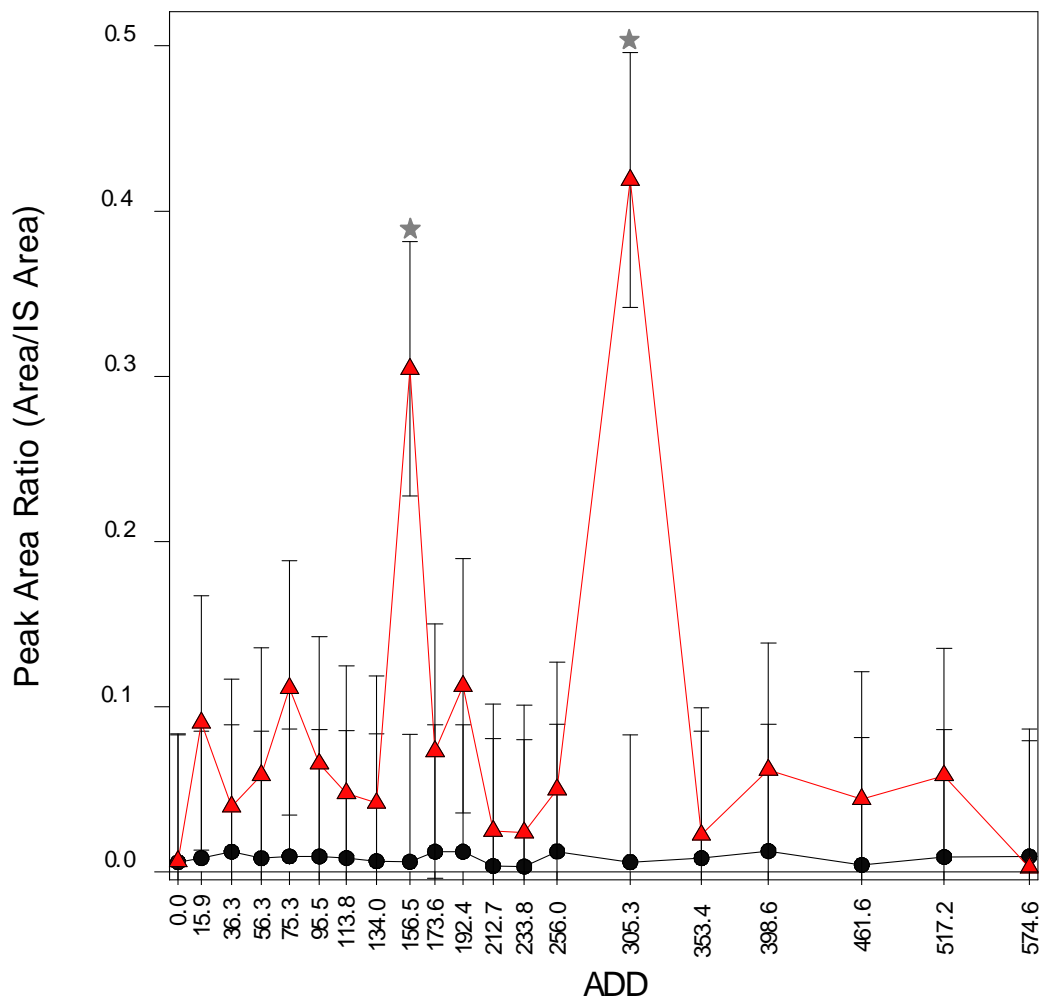
Appendix D-3. Palmitoleic acid content of control (●) and experimental (▲) soil collected 20 cm away from the pig carcasses at the Technical and Protective Operations Facility in Ottawa, Ontario, Canada during the 2009 summer trial. ★ = significant difference $p < 0.05$ (ANOVA, $F_{\text{Treatment}(1, 80)} = 16.18$, $p < 0.001$, $F_{\text{ADD}(19, 80)} = 1.28$, $p = 0.218$, $F_{\text{Int}(19, 80)} = 1.29$, $p = 0.216$, bars = s.e. of differences of means).



Appendix D-4. Palmitoleic acid content of control (●) and experimental (▲) soil collected 30 cm away from the pig carcasses at the Technical and Protective Operations Facility in Ottawa, Ontario, Canada during the 2009 summer trial. ★ = significant difference $p < 0.05$ (ANOVA, $F_{\text{Treatment}(1, 80)} = 6.02$, $p = 0.016$, $F_{\text{ADD}(19, 80)} = 1.43$, $p = 0.135$, $F_{\text{Int}(19, 80)} = 1.44$, $p = 0.133$, bars = s.e. of differences of means).

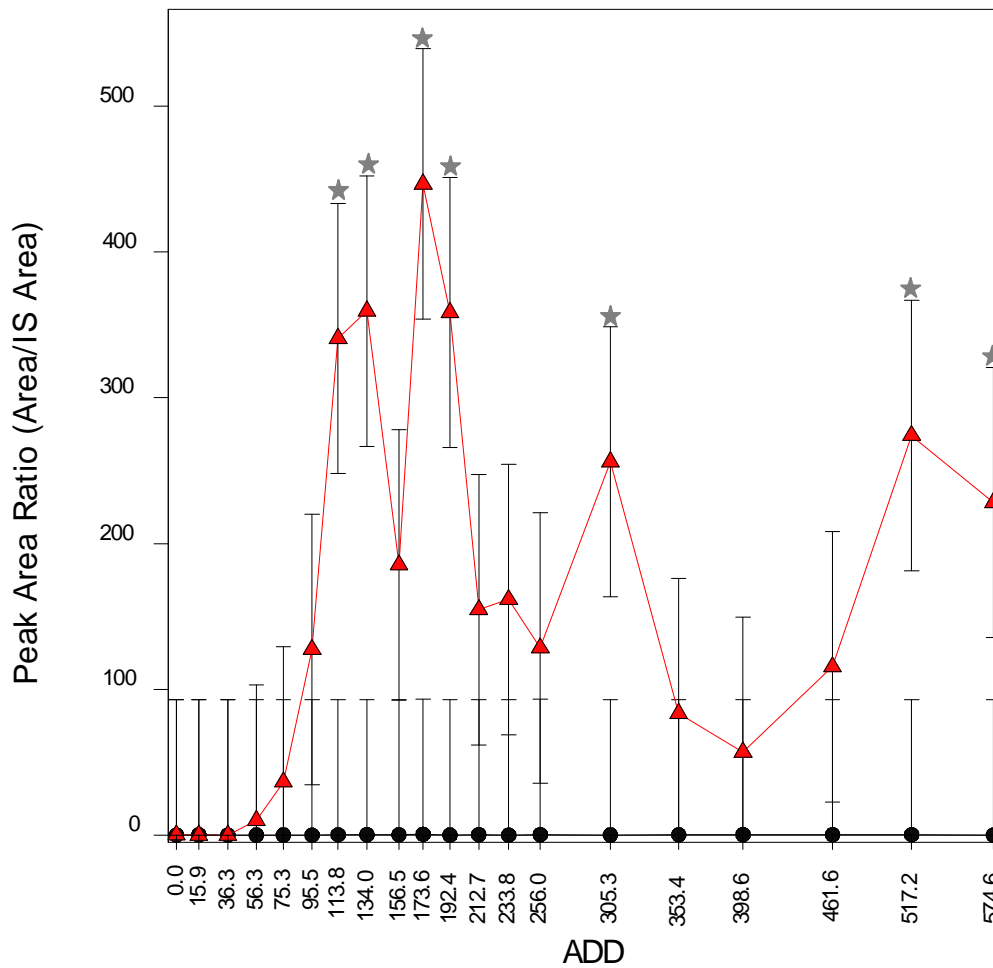


Appendix D-5. Palmitoleic acid content of control (●) and experimental (▲) soil collected 40 cm away from the pig carcasses at the Technical and Protective Operations Facility in Ottawa, Ontario, Canada during the 2009 summer trial. ★ = significant difference $p < 0.05$ (ANOVA, $F_{\text{Treatment}(1, 80)} = 3.68$, $p = 0.058$, $F_{\text{ADD}(19, 80)} = 1.16$, $p = 0.314$, $F_{\text{Int}(19, 80)} = 1.16$, $p = 0.310$, bars = s.e. of differences of means).

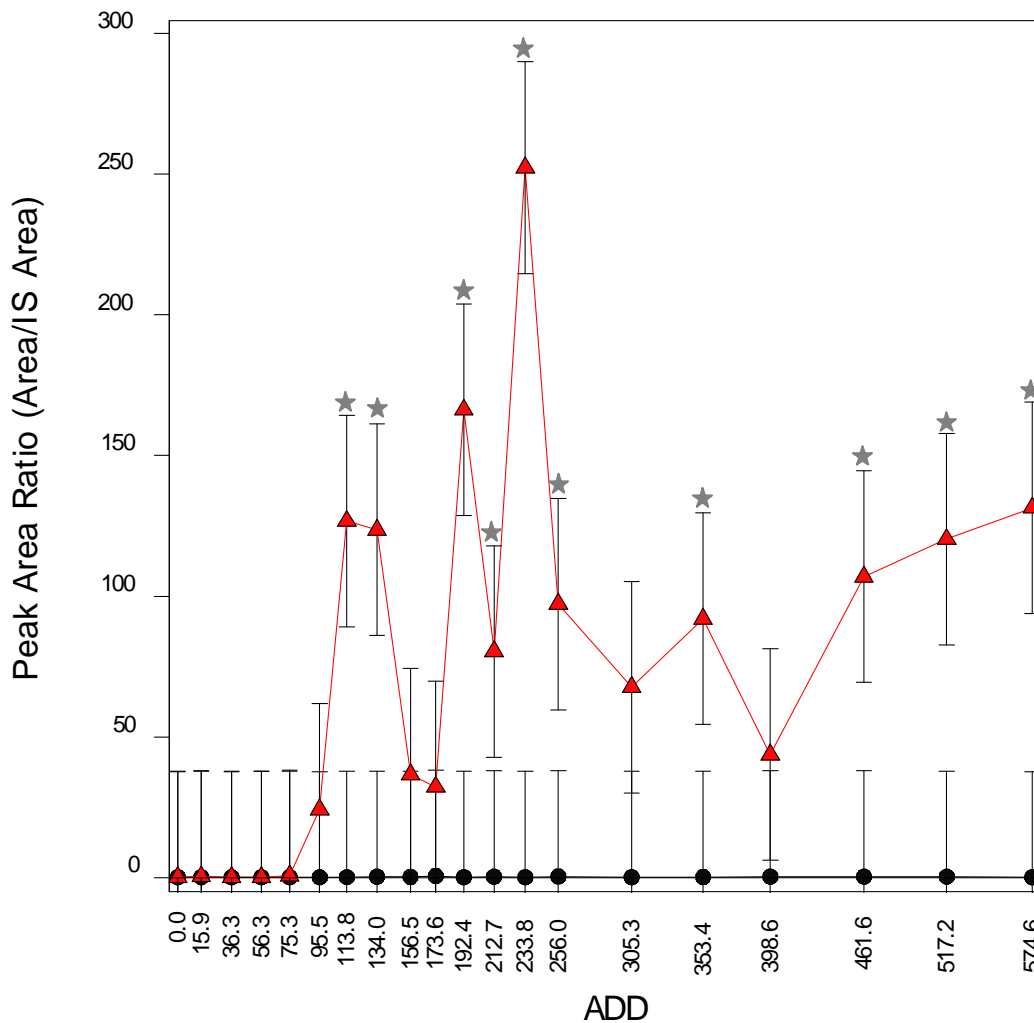


Appendix D-6. Palmitoleic acid content of control (—●—) and experimental (—▲—) soil collected 50 cm away from the pig carcasses at the Technical and Protective Operations Facility in Ottawa, Ontario, Canada during the 2009 summer trial. ★ = significant difference $p < 0.05$ (ANOVA, $F_{\text{Treatment}(1, 80)} = 9.36$, $p = 0.003$, $F_{\text{ADD}(19, 80)} = 0.86$, $p = 0.626$, $F_{\text{Int}(19, 80)} = 0.88$, $p = 0.611$, bars = s.e. of differences of means).

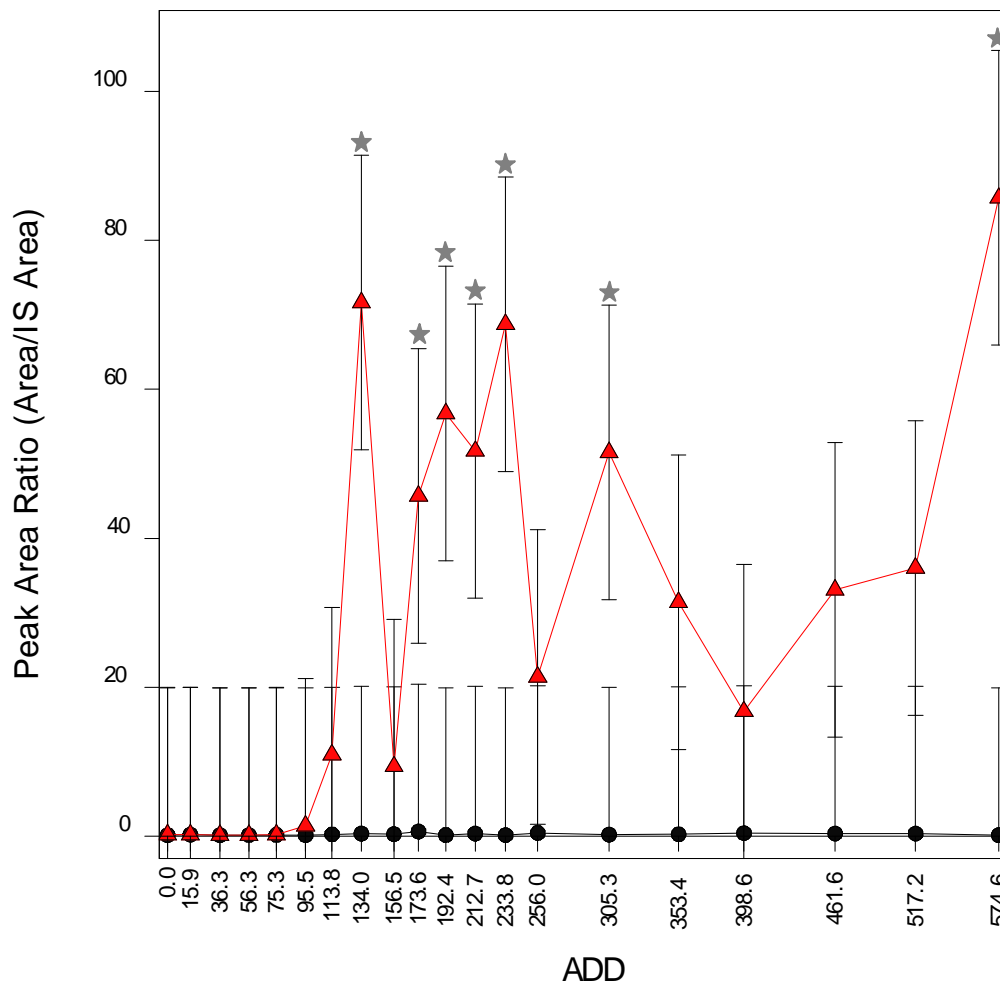
*Appendix E –
Stearic Acid Content of
Soil Samples by Distance*



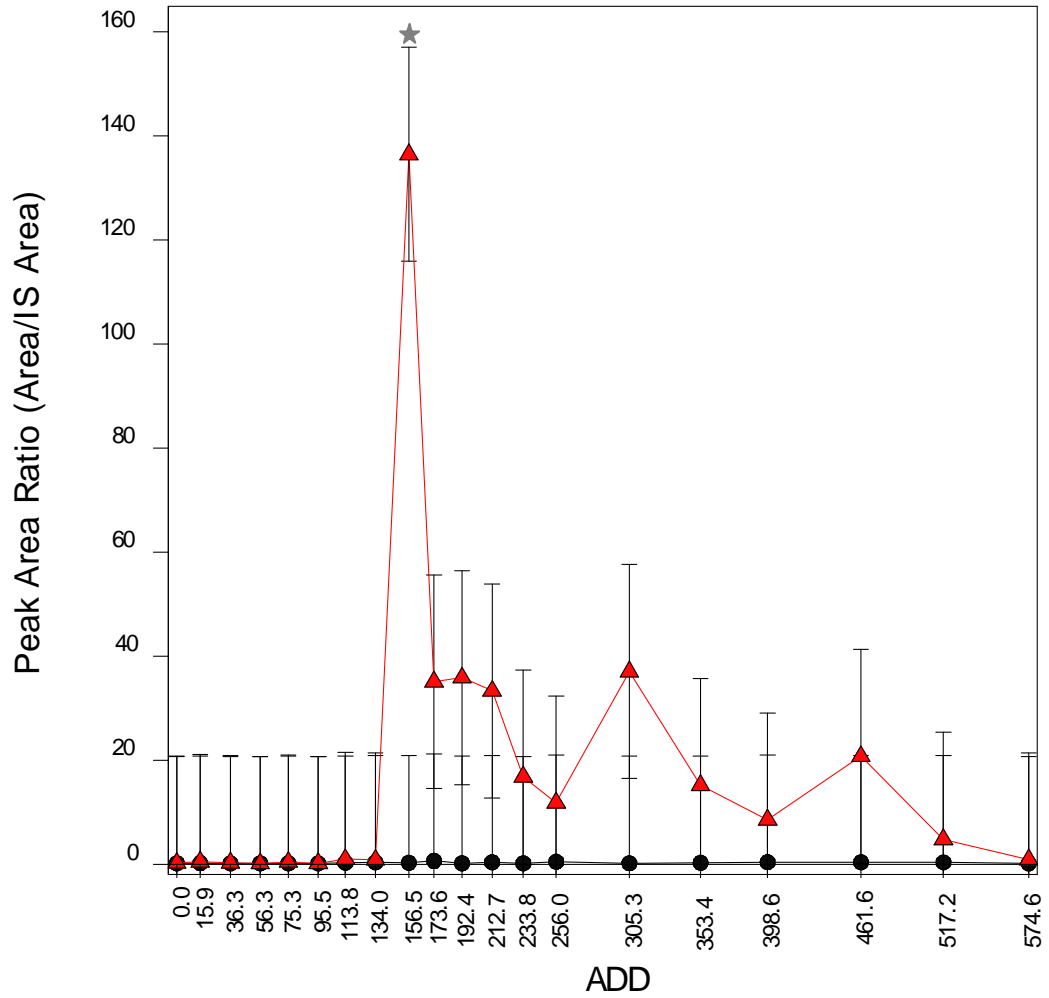
Appendix E-1. Stearic acid content of control (●) and experimental (▲) soil collected 0 cm away from the pig carcasses at the Technical and Protective Operations Facility in Ottawa, Ontario, Canada during the 2009 summer trial. ★ = significant difference $p < 0.05$ (ANOVA, $F_{\text{Treatment}(1, 80)} = 32.06, p < 0.001, F_{\text{ADD}(19, 80)} = 1.09, p = 0.377, F_{\text{Int}(19, 80)} = 1.09, p = 0.378$, bars = s.e. of differences of means).



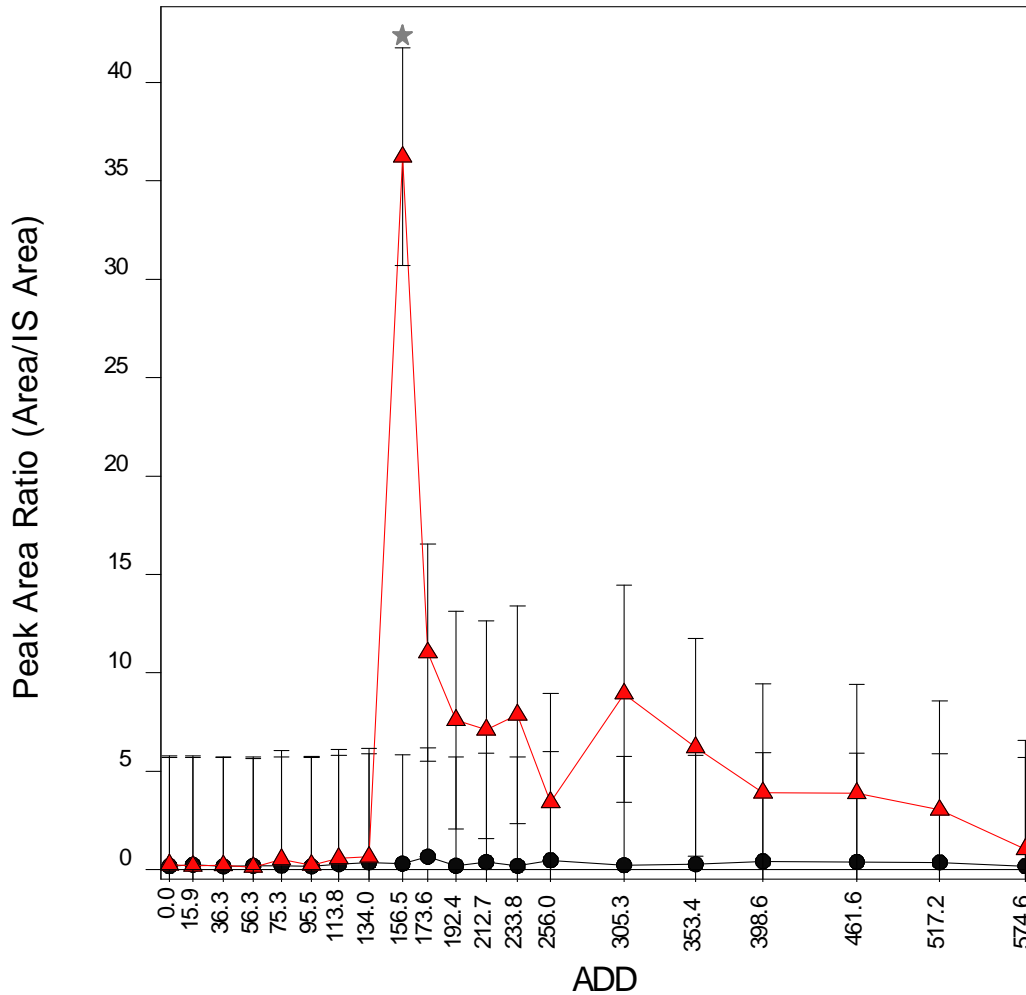
Appendix E-2. Stearic acid content of control (●) and experimental (▲) soil collected 10 cm away from the pig carcasses at the Technical and Protective Operations Facility in Ottawa, Ontario, Canada during the 2009 summer trial. ★ = significant difference $p < 0.05$ (ANOVA, $F_{\text{Treatment}(1, 80)} = 39.73$, $p < 0.001$, $F_{\text{ADD}(19, 80)} = 1.61$, $p = 0.073$, $F_{\text{Int}(19, 80)} = 1.61$, $p = 0.073$, bars = s.e. of differences of means).



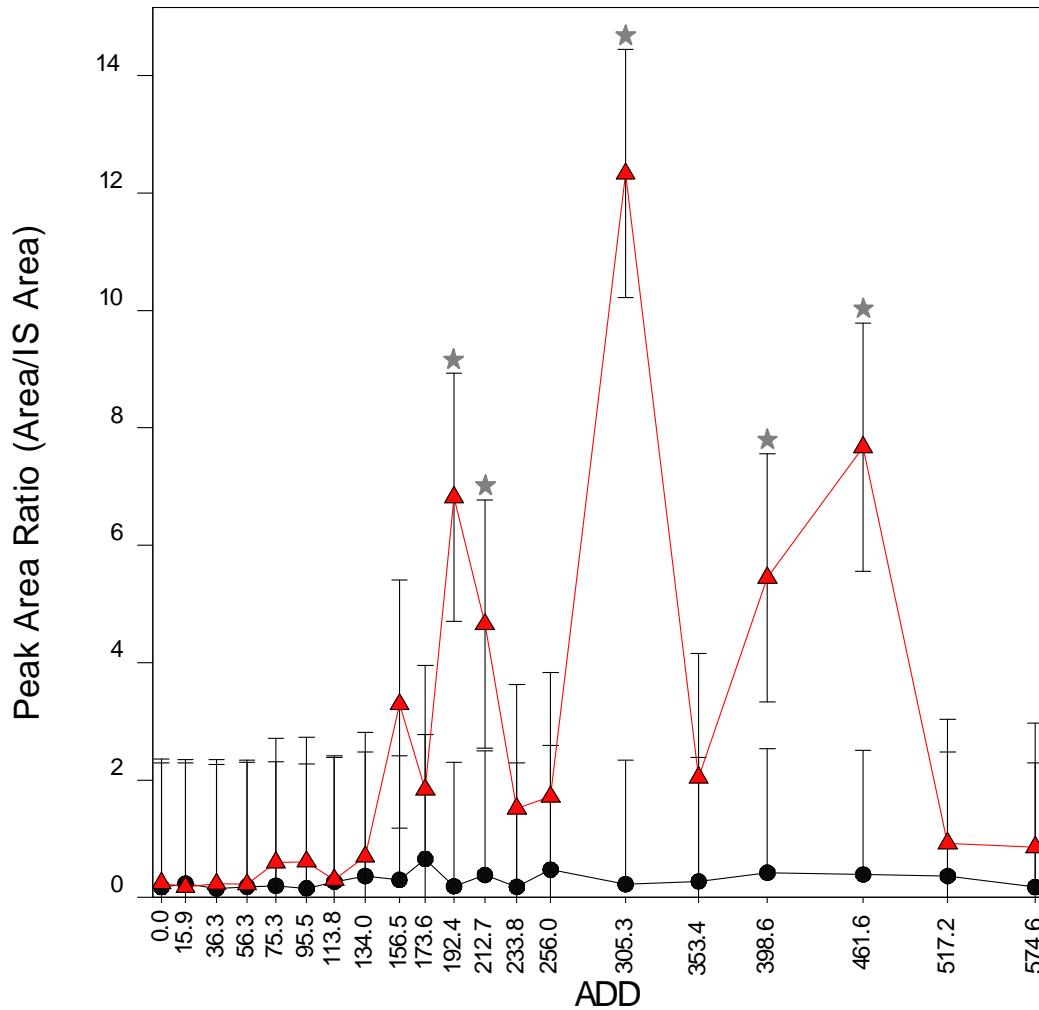
Appendix E-3. Stearic acid content of control (●) and experimental (▲) soil collected 20 cm away from the pig carcasses at the Technical and Protective Operations Facility in Ottawa, Ontario, Canada during the 2009 summer trial. ★ = significant difference $p < 0.05$ (ANOVA, $F_{\text{Treatment}(1, 80)} = 22.10$, $p < 0.001$, $F_{\text{ADD}(19, 80)} = 0.98$, $p = 0.489$, $F_{\text{Int}(19, 80)} = 0.98$, $p = 0.492$, bars = s.e. of differences of means).



Appendix E-4. Stearic acid content of control (—●—) and experimental (—▲—) soil collected 30 cm away from the pig carcasses at the Technical and Protective Operations Facility in Ottawa, Ontario, Canada during the 2009 summer trial. ★ = significant difference $p < 0.05$ (ANOVA, $F_{\text{Treatment}(1, 80)} = 7.43$, $p = 0.008$, $F_{\text{ADD}(19, 80)} = 1.14$, $p = 0.328$, $F_{\text{Int}(19, 80)} = 1.14$, $p = 0.332$, bars = s.e. of differences of means).

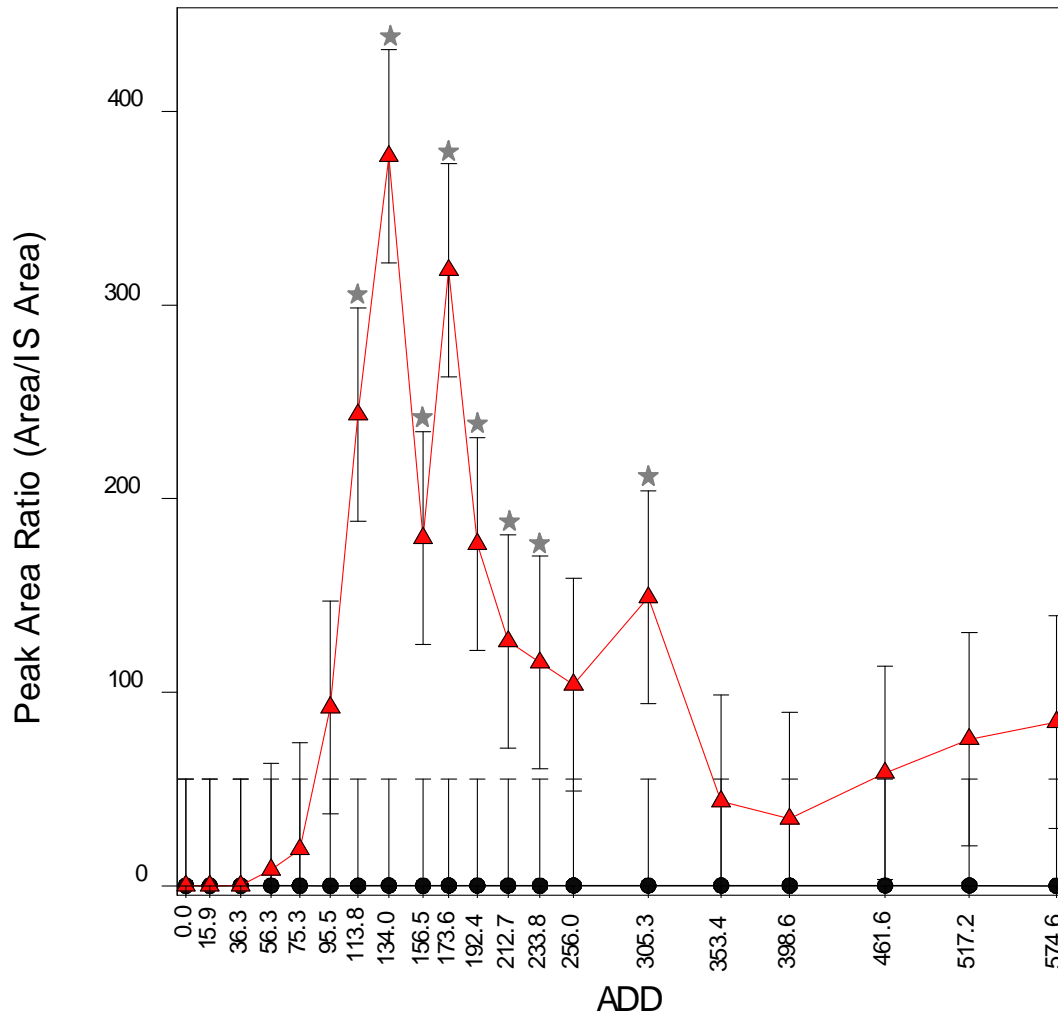


Appendix E-5. Stearic acid content of control (—●—) and experimental (—▲—) soil collected 40 cm away from the pig carcasses at the Technical and Protective Operations Facility in Ottawa, Ontario, Canada during the 2009 summer trial. ★ = significant difference $p < 0.05$ (ANOVA, $F_{\text{Treatment}(1, 80)} = 7.72$, $p = 0.007$, $F_{\text{ADD}(19, 80)} = 1.08$, $p = 0.386$, $F_{\text{Int}(19, 80)} = 1.07$, $p = 0.402$, bars = s.e. of differences of means).

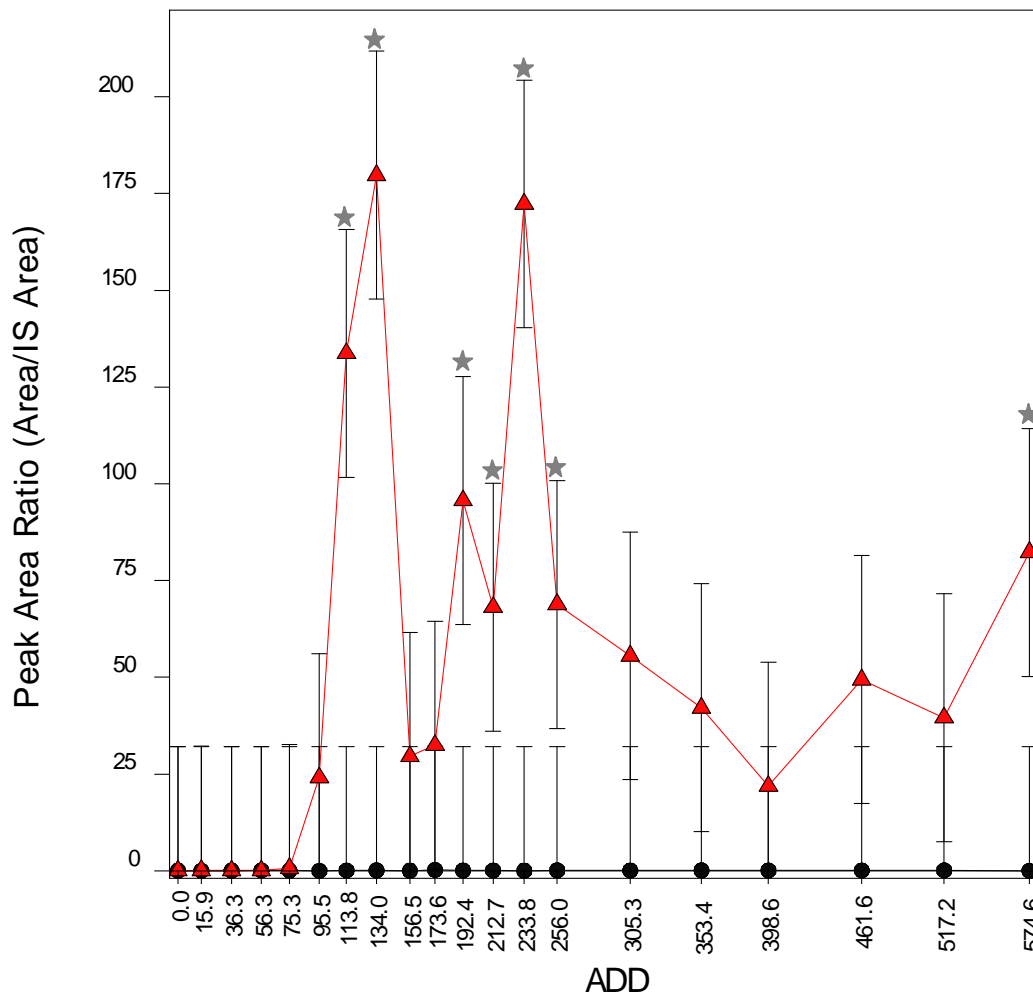


Appendix E-6. Stearic acid content of control (●) and experimental (▲) soil collected 50 cm away from the pig carcasses at the Technical and Protective Operations Facility in Ottawa, Ontario, Canada during the 2009 summer trial. ★ = significant difference $p < 0.05$ (ANOVA, $F_{\text{Treatment}(1, 80)} = 12.05$, $p < 0.001$, $F_{\text{ADD}(19, 80)} = 1.19$, $p = 0.289$, $F_{\text{Int}(19, 80)} = 1.16$, $p = 0.311$, bars = s.e. of differences of means).

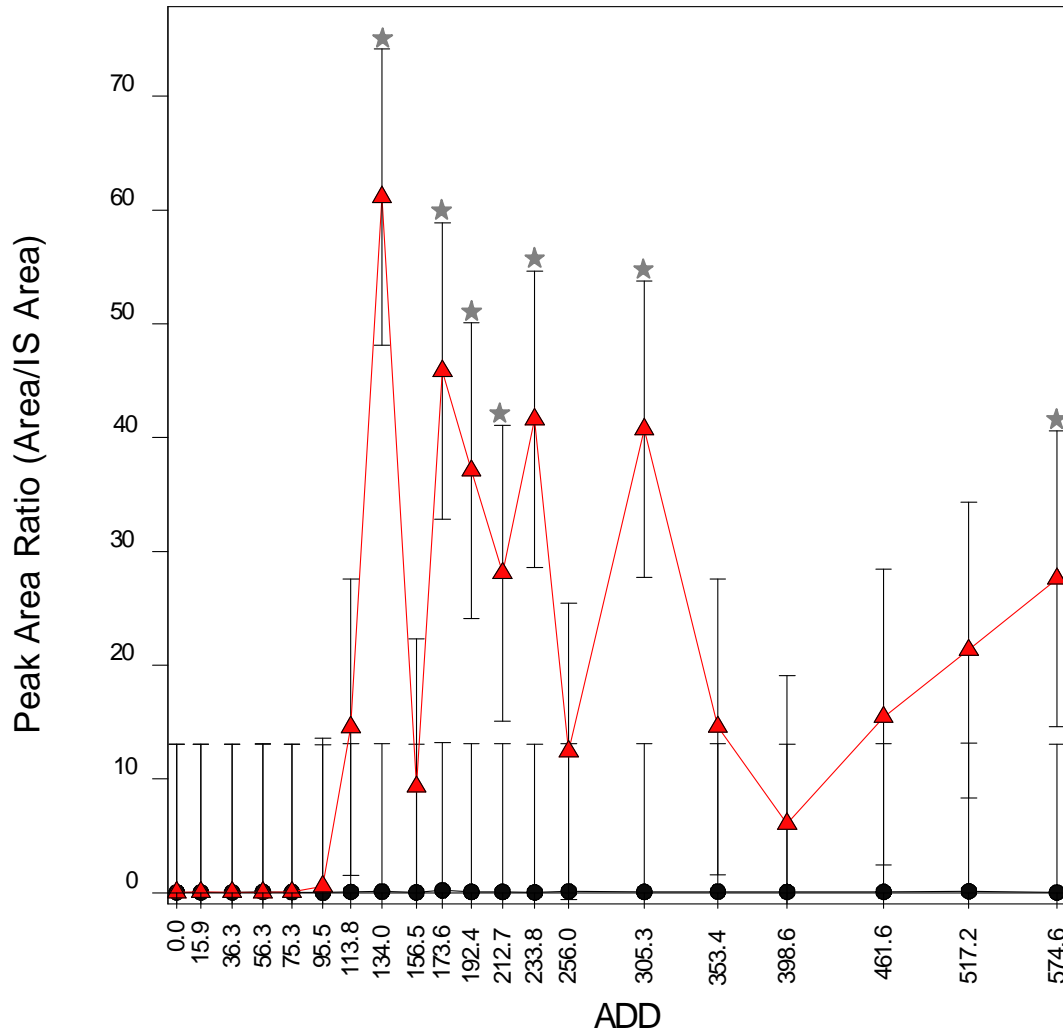
*Appendix F –
Oleic Acid Content of Soil
Samples by Distance*



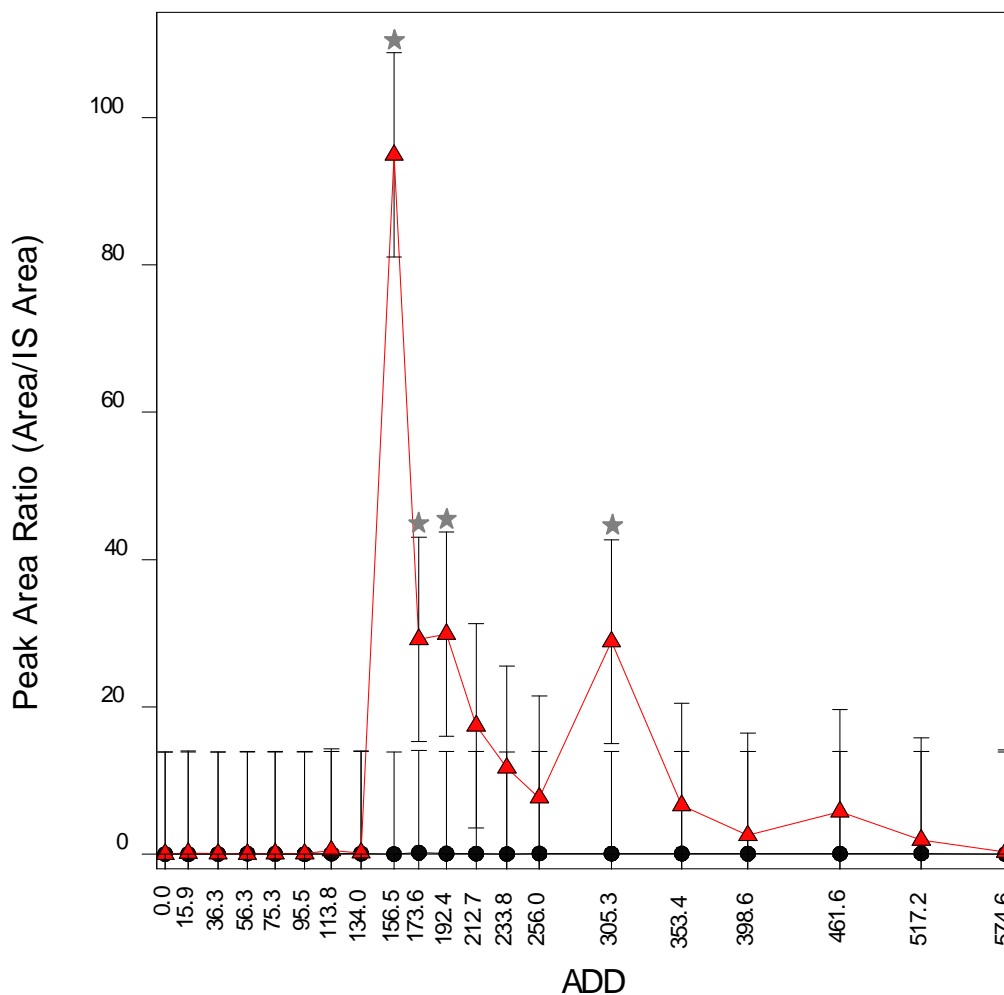
Appendix F-1. Oleic acid content of control (●) and experimental (▲) soil collected 0 cm away from the pig carcasses at the Technical and Protective Operations Facility in Ottawa, Ontario, Canada during the 2009 summer trial. ★ = significant difference $p < 0.05$ (ANOVA, $F_{\text{Treatment}(1, 80)} = 40.15$, $p < 0.001$, $F_{\text{ADD}(19, 80)} = 1.86$, $p = 0.030$, $F_{\text{Int}(19, 80)} = 1.85$, $p = 0.030$, bars = s.e. of differences of means).



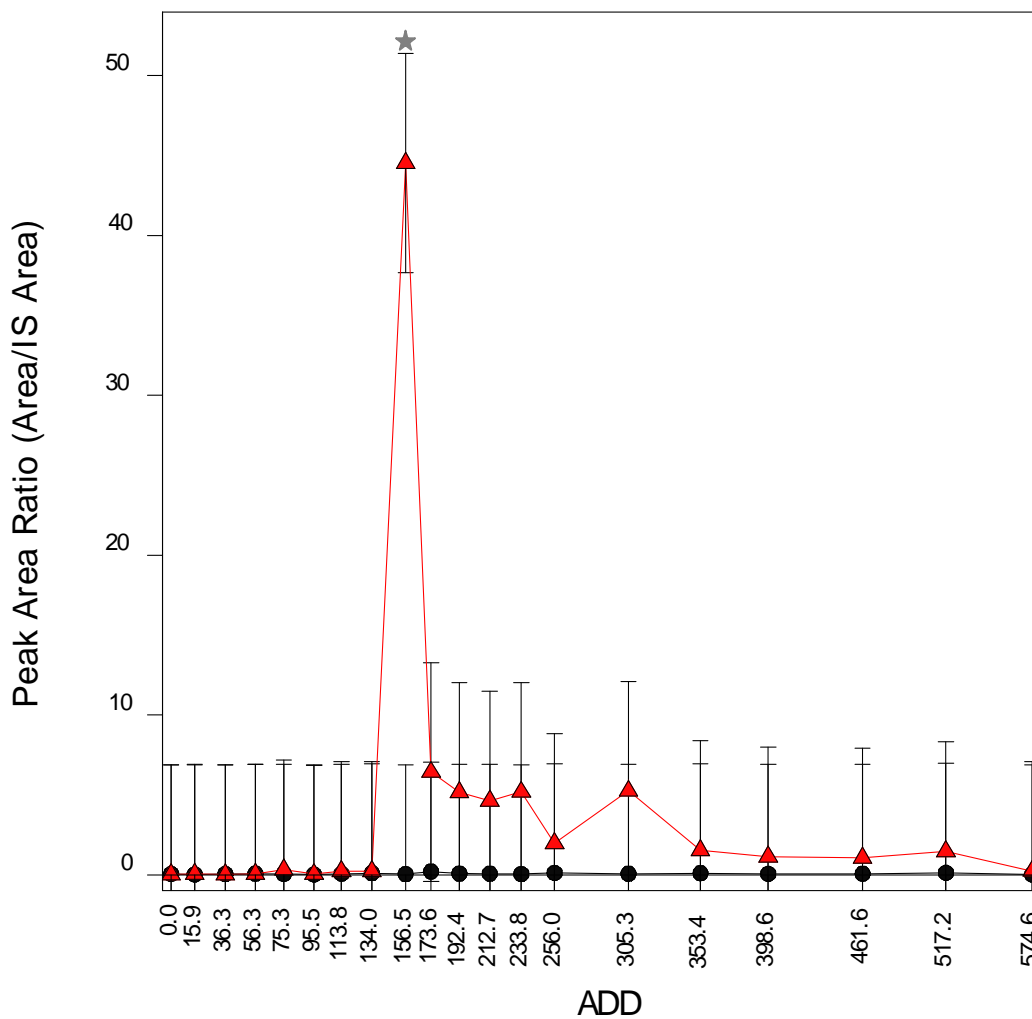
Appendix F-2. Oleic acid content of control (●) and experimental (▲) soil collected 10 cm away from the pig carcasses at the Technical and Protective Operations Facility in Ottawa, Ontario, Canada during the 2009 summer trial. ★ = significant difference $p < 0.05$ (ANOVA, $F_{\text{Treatment}(1, 80)} = 29.23, p < 0.001, F_{\text{ADD}(19, 80)} = 1.46, p = 0.123, F_{\text{Int}(19, 80)} = 1.46, p = 0.123$, bars = s.e. of differences of means).



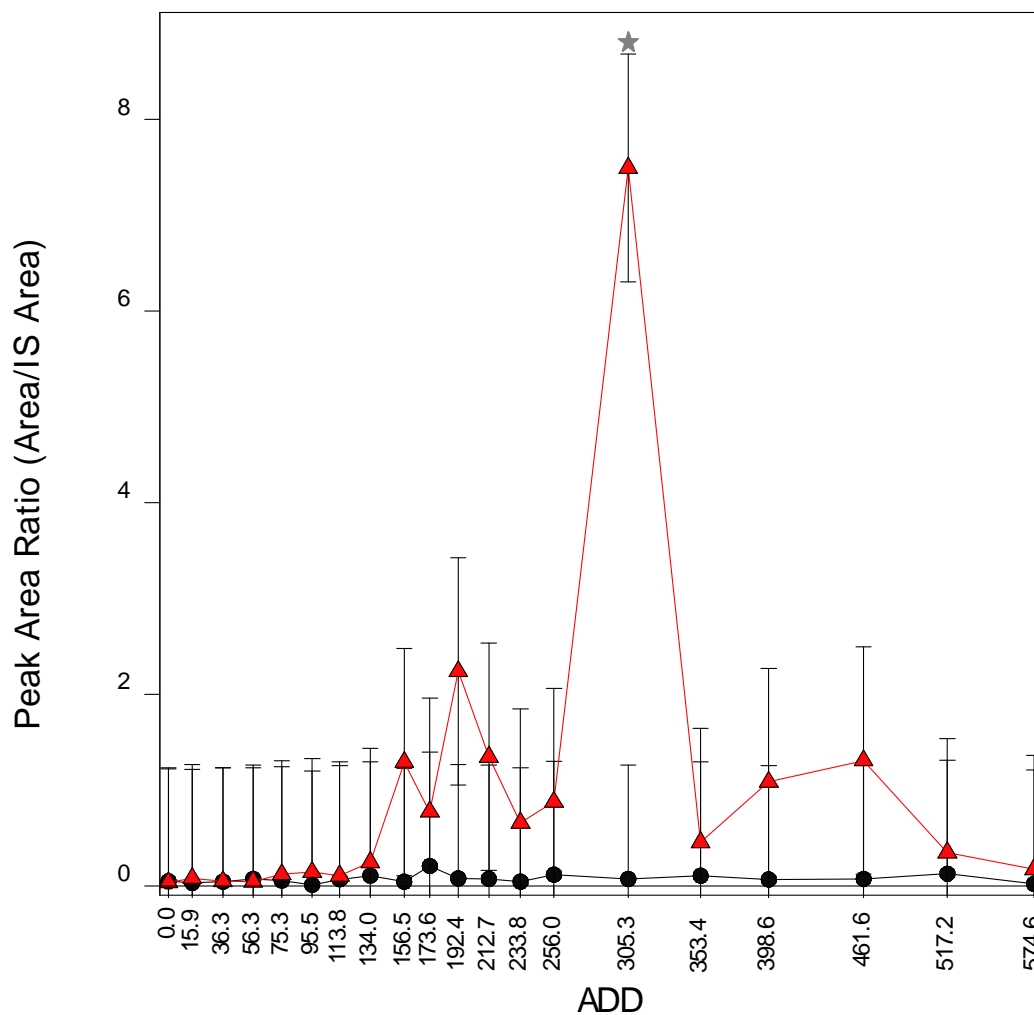
Appendix F-3. Oleic acid content of control (—●—) and experimental (—▲—) soil collected 20 cm away from the pig carcasses at the Technical and Protective Operations Facility in Ottawa, Ontario, Canada during the 2009 summer trial. ★ = significant difference $p < 0.05$ (ANOVA, $F_{\text{Treatment}(1, 80)} = 20.78$, $p < 0.001$, $F_{\text{ADD}(19, 80)} = 1.01$, $p = 0.464$, $F_{\text{Int}(19, 80)} = 1.00$, $p = 0.469$, bars = s.e. of differences of means).



Appendix F-4. Oleic acid content of control (●) and experimental (▲) soil collected 30 cm away from the pig carcasses at the Technical and Protective Operations Facility in Ottawa, Ontario, Canada during the 2009 summer trial. ★ = significant difference $p < 0.05$ (ANOVA, $F_{\text{Treatment}(1, 80)} = 7.29$, $p = 0.008$, $F_{\text{ADD}(19, 80)} = 1.28$, $p = 0.220$, $F_{\text{Int}(19, 80)} = 1.28$, $p = 0.220$, bars = s.e. of differences of means).



Appendix F-5. Oleic acid content of control (●) and experimental (▲) soil collected 40 cm away from the pig carcasses at the Technical and Protective Operations Facility in Ottawa, Ontario, Canada during the 2009 summer trial. ★ = significant difference $p < 0.05$ (ANOVA, $F_{\text{Treatment}(1, 80)} = 3.26$, $p = 0.075$, $F_{\text{ADD}(19, 80)} = 1.02$, $p = 0.448$, $F_{\text{Int}(19, 80)} = 1.02$, $p = 0.447$, bars = s.e. of differences of means).



Appendix F-6. Oleic acid content of control (●) and experimental (▲) soil collected 50 cm away from the pig carcasses at the Technical and Protective Operations Facility in Ottawa, Ontario, Canada during the 2009 summer trial. ★ = significant difference $p < 0.05$ (ANOVA, $F_{\text{Treatment}(1, 80)} = 5.38$, $p = 0.023$, $F_{\text{ADD}(19, 80)} = 0.98$, $p = 0.497$, $F_{\text{Int}(19, 80)} = 0.97$, $p = 0.505$, bars = s.e. of differences of means).